Geology of the Apollo 16 Area, Central Lunar Highlands

Edited by GEORGE E. ULRICH, CARROLL ANN HODGES, and WILLIAM R. MUEHLBERGER

GEOLOGICAL SURVEY PROFESSIONAL PAPER 1048

Prepared on behalf of the National Aeronautics and Space Administration

UNITED STATES GOVERNMENT PRINTING OFFICE, WASHINGTON : 1981

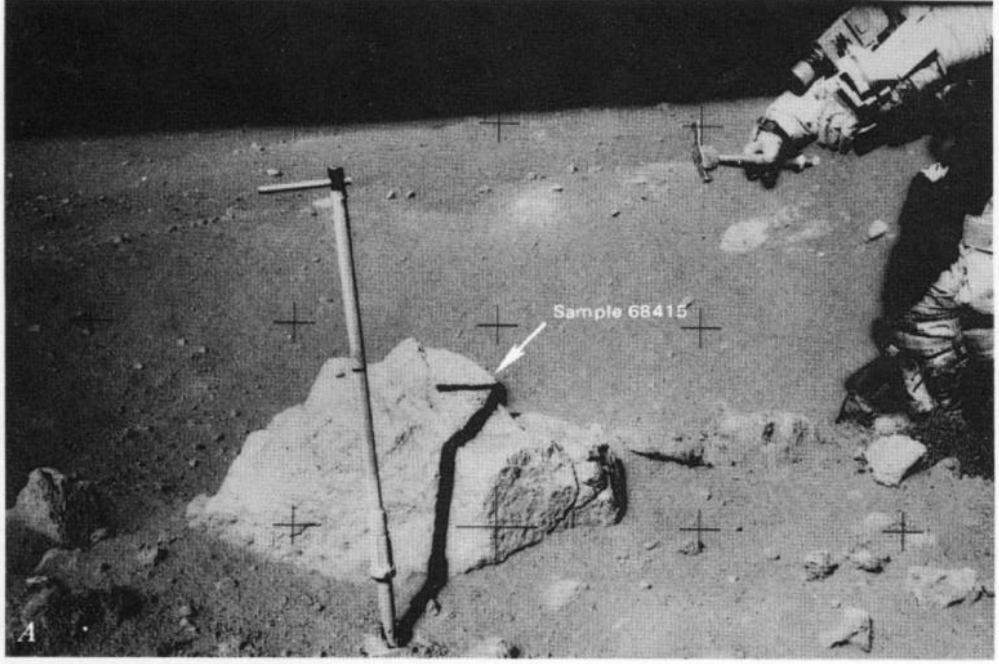

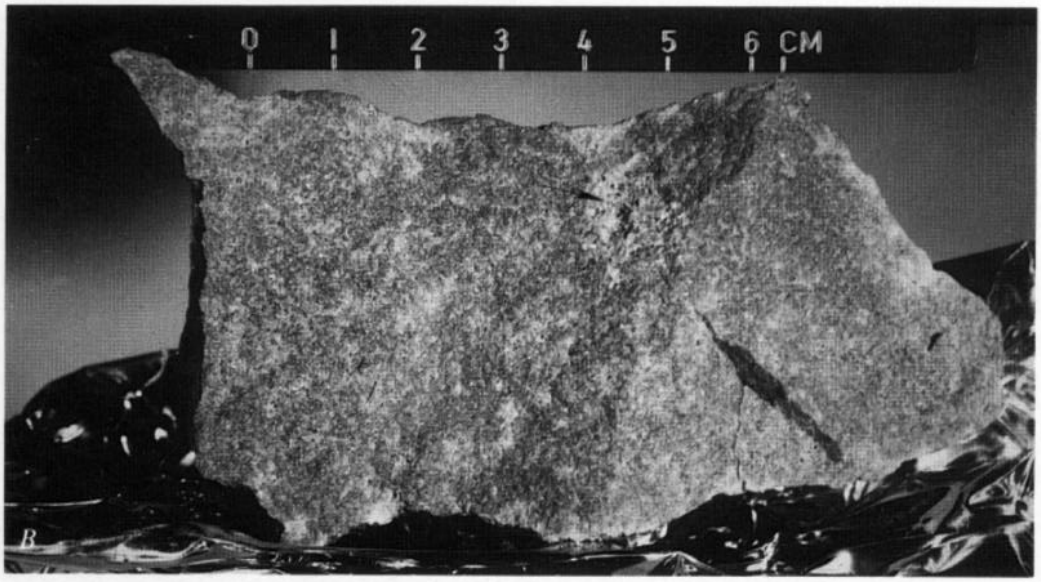

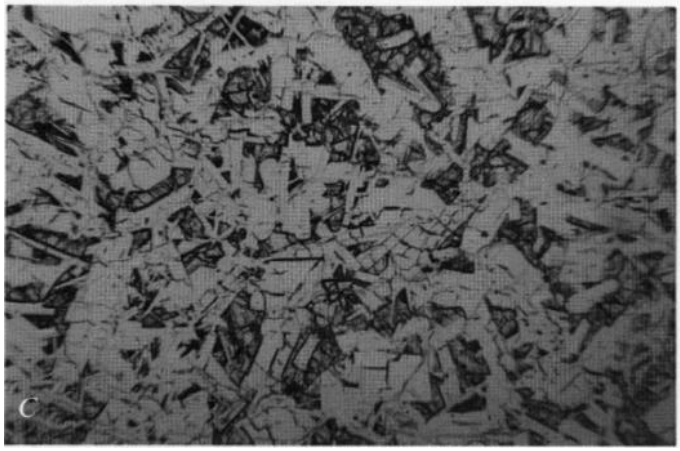

Crystalline rock 68415 ***A.*** White angular boulder at Station 8, 3.4 km northeast of South Ray crater, source of samples 66415 and 66416. Long-handled scoop casts shadow westward across boulder Hasselblad frame No AS16-108-17697.B Fresh broken surface of rock 66415 showing fine-grained crystalline texture with local vug-filling plagioclase (arrow) Lunar Receiving Laboratory No. S-73-39590. C, Photomicrograph of typical texture in 68415 and 66416 showing twinned plagioclane (gray and white) an clinopyroxene (bright colors). Cross-polarized light. Long side is 2.75 mm ***D,*** Same as ***C*** in plane-polarized light showing subophitic texture of plagioclane and darker high-relief pyroxene.

UNITED STATES DEPARTMENT OF THE INTERIOR

JAMES G. WATT, ***Secretary***

GEOLOGICAL SURVEY

Doyle G. Frederick, ***Acting Director***

Library of Congress Cataloging in Publication Data

Geology of the Apollo 16 area, central lunar highlands

Contributions to astrogeology. Geological Survey Professional Paper 1048
Bibliography; p. 534-539.
Supt. of Docs. No.: I 19.16:1048
1. Lunar geology. 2. Project Apollo. I. Ulrich, George E. II. Hodges, Carroll Ann. III. Muehlberger, William R. IV. United States. National Aeronautics and Space Administration. V. Series. VI. Series: United States. Geological Survey. Professional Paper 1048.
QB592.G47 559.9'1 80-607170

For sale by the Superintendent of Documents, U.S. Government Printing Office
Washington, D.C. 20402

CONTENTS

ILLUSTRATIONS

[Plates are in separate case]

ABBREVIATIONS AND ACRONYMS

AET	Apollo Elapsed Time, time after launch of mission from Kennedy Space Center
AFGIT, ALGIT	Apollo Field (Lunar) Geology Investigation Team
ALSEP	Apollo Lunar Surface Experiment Package
ANT	Anorthosite-norite-troctolite rock suite
AP/C	Analytical plotter, model C
ASE	Active Seismic Experiment
c c	Capsule communicator at Mission Control in Houston, A. W. England
CDR	Commander, John W. Young
C/S	Central Station controlling the ALSEP
CSM	Command Service Module, spacecraft that orbited Moon during EVA's.
csvc	Core Sample Vacuum Container
CSSD	Contact Soil Sampling Device (Surface Sampler)
CTR	Crater
DC	Dark-haloed crater
DMB	Dark-matrix breccia
DPS	Descent Propulsion System on LM
DS	Down-sun sampling, photograph
DSB	Down-sun before sampling, photograph
DT	Drive tube, also core tube
END CTR	End crater
EVA	Extravehicular activity; astronaut activity outside the LM
EXP	Experiment
FIIR	Fine-grained intersertal igneous rock
HFE	Heat-Flow Experiment
IR	Interagency Report, U.S. Geological Survey
KREEP	Lunar rock or soil with high concentrations of potassium, rare-earth elements, and phosphorus
LAC	Lunar Aeronautical Chart
LM	Lunar Module
LMB	Light-matrix breccia
LMP	Lunar Module Pilot, Charles M. Duke, Jr.
LOC	Photograph of sample showing location with respect to LRV or LM
LPM	Lunar Portable Magnetometer
LRL	Lunar Receiving Laboratory
LRV	Lunar Roving Vehicle
LSM	Lunar Surface Magnetometer
LSPET	Lunar Sample Preliminary Examination Team
META-ANT	Metamorphosed anorthosite-norite-troctolite
MISC	Miscellaneous
MPA	Mortar Package Assembly
N RAY CTR	North Ray crater
PAN	Photographic panorama, normally 360
PEN-2	Location of second penetrometer reading
PPAN	Partial panorama
POIK	Poikiloblastic or poikilitic
PSE	Passive Seismic Experiment
REE	Rare-earth elements
ROVER	Lunar Roving Vehicle
RTG	Radioisotopic Thermoelectric Generator
SCB	Sample collection bag
SEQ	Scientific equipment bay, in LM
SPL	Sample
S RAY CTR	South Ray crater
SRC	Sample return container
STA	Station, sampling location on traverse
STEREO	Stereoscopic sequence or offset in photographs
STEREOPAIR	Overlapping pair of photographs that give a three-dimensional view
SURF SPLR	Surface sampler (also
s w c	Solar Wind Composition device
USA	Up-sun, after sampling, photograph
USB	Up-sun, before sampling, photograph
USD	Up-sun, during sampling, photograph
UV CAMERA	Far-ultraviolet camera, positioned in shade of the LM
XS, XSUN	Cross-sun, sampling photograph
XSA	Cross-sun, after sampling, photograph
XSB	Cross-sun, before sampling, photograph
XSD	Cross-sun, during sampling, photograph
+ , -Y FOOTPAD	Front and rear footpads, respectively, of LM
+,-Z FOOTPAD	Left and right footpads, respectively, of LM

There you are, our mysterious and unknown Descartes highland plains, Apollo 16 is going to change your image."

John Young could hardly have known the truth of his prediction when he first set foot on the lunar surface at the Apollo 16 landing site. His mission was the most surprising geologically and has generated the most controversy of all six Apollo landings. The Descartes region of the central lunar highlands, since its first serious consideration as a site for manned exploration 4 years earlier, had been strongly supported as a place to sample volcanic rocks much different from those of the maria and the basin margins. Three days of field exploration ranging 4 to 5 km from the lunar module failed to turn up a single recognizable volcanic rock. Instead, a variety of breccias, complicated beyond belief, were collected from every location. Crystalline rocks were found whose textures were clearly igneous (see frontispiece), but they were not volcanic. And therein lies the heart of the geologic mystery of Descartes.

"Well it's back to the drawing boards, or wherever geologists go" (T. K. Mattingly, Apollo 16 Command Module Pilot from lunar orbit).

PREFACE

This volume contains the final results compiled by the Apollo Field Geology Investigations Team for the Apollo 16 mission. Some of the data presented here were reported in preliminary form shortly after the mission (ALGIT, 1972a. 1972b; AFGIT, 1973; Batson and others, 1972; Muehlberger and other?. 1972), hut most of the discussion and interpretations that follow are products of individual efforts which have incorporated much of the large body of data available from postmission studies of the rocks, the geophysical and geochemical data, and the extensive collection of photographs taken by the Apollo I6 astronaut crew on the lunar surface and from orbit. The chapter format was chosen to permit individual authors to develop their ideas independently, and we trust this approach will serve to stimulate rather than confuse the reader.

Our purpose in this volume is to summarize the field observations at the Apollo I6 site and to hring together the various interpretations placed upon these observations by the astronauts and the Field Geology Team. Much of the extensive geochemical and geophysical data puhlished since 1974 on the Apollo I6 site has not been incorporated or referred to here. The intent is not to provide a grand synthesis hut rather to document the local and regional geologic relations and to summarize what inferences can be made from them. Our expectation is that the volume will be used as a reference for researchers desiring tnore complete information on the geologic context of the Apollo 16 samples and on the interpretations of those intimately involved with the planning, execution, and analysis of the geologic exploration.

John Young, Charles Duke, and Kenneth Mattingly deserve special credit for the quality of their performance while exploring this complex area on the surface, from lunar orbit, and later in discourse with the lunar science community. Their continuing interest in the developing story of Descartes began with an unwavering enthusiasm for geologic training exercises in the field. With the able help of Anthony England, mission scientist and communicator during the EVA's. and Friedrich Horz, their geologic trainer in Houston, their competence as scientific investigators reached the high level shown by their ready adaptation to the unexpected conditions encountered on the mission.

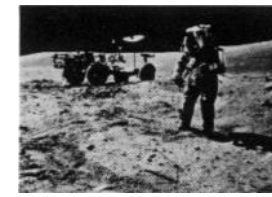

A significant stimulus to the exceptional performance on the Moon was provided by the outstanding backup crew, Fred Haise. Edgar Mitchell, and Stuart Roosa, whose high scientific standards the prime crew was continuously challenged to surpass. We hope that the monthly mission-oriented field exercises planned and executed by members of the Field Geology Teatn prior to the Apollo I6 flight provided the variety of experience in field situations that enabled the crew to make the appropriate observations and geologic judgments required during the mission.

We received valuable assistance before, during. and after the mission from the following associates of the U.S. Geological Survey who are not credited elsewhere hut who nonetheless made significant contributions directly or indirectly to the preparation of this volume: N. G. Bailey, F. E. Beeson. B. M. Bradley. V. J. Fisher, M. H. Hait. E. D. Jackson, R. H. Jahns, D. F. .Johnson, J. S. Loman, R. S. Madden, R. Carroll, W'. E. Miller, R. A. Mills, J. C. Nuttall, D. L. Peck. R. F.. Sabala, 1.. T. Silver, R. B. Skinner. L. B. Sowers, G. A. Swann, H. F. Thomas.J. W. VanDivicr. and D. E. Wilhelms. Immensely helpful editing by James Pinkerton in preparing the manuscripts for publication was a monumental rask and is greatly appreciated.

M. B. Duke, Curator, and R. B. Laughon, Assistant Curator, Lunar Receiving Laboratory. Johnson Space Center, Houston. very kindly made arrangements for mrmbcrs of the Field Geology Team to study the Apollo I6 and I7 thin-section collections and to use their photographic equipment for illustrating some of the discussions in the field geology chapters of this report.

A. SUMMARY OF GEOLOGIC RESULTS FROM APOLLO 16

By WILLIAM R. MUEHLBERGER and GEORGE E. ULRICH

INTRODUCTION

The Apollo 16 mission to the central lunar highlands has provoked a variety of stimulating debates concerning the nature of the original lunar crust, the effects of impact processes on this crust, and the interpretation of lunar landforms from photographic evidence. Considerable disagreement remains about ultimate sources of the samples returned from the Cayley plains and the Descartes mountains. Although the major problems of origin and lunar processes may not be resolved in this volume, it is hoped that subsequent research will take into account the facts of field relations as recorded by the cameras and first-hand observations of the astronauts.

The arrangement of topics in this volume is partly chronologic in that discussions of geologic setting and mission planning are followed by sections on the field geology of four geographic areas sampled by the astronauts: central Cayley plains, North Ray crater, vicinity of South Ray and Baby Ray craters, and Stone mountain. These observation sections are followed by topical discussions on the petrology, regolith, South Ray ejecta distribution, optical properties, morphology, and stratigraphy of the landing site. A summary discussion of the source materials for the Cayley plains and Descartes mountains in the light of available data concludes the interpretive part of the volume. Supplementary sections on the surface photography and the documentation of samples collected by Apollo 16 are updated revisions of U.S. Geological Survey Interagency Reports, Astrogeology 48, 50, 51, 54, prepared immediately after the mission. Twelve folded plates in the separate case include nine plates of lunar surface panoramas mosaicked from 70-mm photographs and annotated with respect to geographic features and geologic data, a premission photomosaic map of the landing site (scale 1:25,000), a postmission geologic map of the landing-site region (1:200,000), and a postmission map of Imbrium-basin-related geology (1:5 million) for the near side of the Moon.

Some geographic names not yet approved by the International Astronomical Union are used informally in the text and figures where identification or reference to their location is considered essential to the discussion for purposes of context or clarification.

A glossary of abbreviations and acronyms used in the texts, illustrations; photographic and sample catalogs, and the photographic panoramas is appended to the volume.

The paragraphs that follow in this chapter are essentially abstracts of each of the succeeding separately authored chapters. Thus this section serves as an overview or extended abstract of the volume that incorporates the major conclusions reached in the independent chapters in the order in which they occur, beginning with the regional geologic setting and ending with the summary of geologic hypotheses.

Chapter A.-The Apollo 16 landing site permitted investigation of two geologic units that are widespread in the lunar highlands: light plains and mountainous "hilly and furrowed" terra, both superposed on old cratered terrain. Outside the landing area, they are embayed by, and are therefore older than, the maria. A volcanic origin for these units, generally accepted prior to the mission, was not supported by the mission results. Various hypotheses of impact-related origins have been proposed to explain the crudely stratified, impact-generated breccias found at the site.

Chapter B.-Apollo 16 was the only site within the central lunar highlands to be explored by astronauts on the surface. It is on the Cayley plains, which are relatively level as compared with the adjacent rugged Descartes mountains. The site is about 70 km west of the Kant plateau, which marks part of the third ring of the Nectaris basin, and about 600 km west of the center of that basin. Other multiringed basins that probably influenced the geology of the landing site are Imbrium, centered about 1,600 km to the northwest, and Orientale, centered 3,500 km to the west-southwest.

A geologic map of the landing site and vicinity (pl. 1) prepared after the mission illustrates a current interpretation of the distribution of geologic materials.

The geologic aspects of the Cayley plains and Descartes mountains can be summarized as follows: (1) The surface units are Imbrian in age; the plains surface has a cratering age that is similar to, if not identical with, that of Orientale basin ejecta cratering ages of the Descartes materials are not so well defined because of their rugged topography, but they are at least as old as Imbrian. (2) The site is within the "sphere of influence" of the Imbrium basin, as evidenced by the radial sculpturing of highlands northwest of the site and by the ridgy morphologic aspect of the Descartes mountains that appears nearly continuous with the Imbrium sculpture. Thus Imbrium ejecta and local material disrupted by the ejecta produced both the mountains and the plains. (3) Because of proximity to the Nectaris basin, the Apollo 16 stratigraphic column probably includes Nectaris basin ejecta at depth, but the basin is so old that these materials are no longer exposed, except perhaps in the lowest walls of the largest craters.

Chapter C.-The three lunar-surface traverses of the Apollo 16 mission were designed to insure maximum return of useful data for a community of scientists and engineers with widely varying objectives. Because the time available for geologic investigations and other experiments was limited, an intricate system of priorities was established for both station locations on each traverse and tasks to be performed at each station. The astronaut crew, John Young and Charles Duke, kept abreast of the planning and the constantly changing priorities, in addition to learning how to travel to and from the Moon. Their terrestrial field training for 18 months before the mission was designed to simulate the lunar traverses and to develop their skills in identifying and describing significant geologic features while photographically documenting and sampling the rocks and soils representing these features.

As a result, all primary geologic objectives were essentially achieved. Well-documented samples were returned from Cayley plains, North and South Ray crater ejecta and Stone mountain materials that may be representative of the Descartes mountains in this part of the lunar highlands. Photographic coverage of all sampling areas and the entire traverse route and telephoto views of all important points remote from the traverse area were obtained.

Chapter D1-D4 .-The central region of the Apollo 16 landing site was investigated at three locations, LM/ALSEP, station 1, and station 2. The samples documented probably represent materials of the underlying Cayley plains down to depths of 70 m or more and ejecta from more distant regions (specifically North and South Ray craters). The percentage of rock types collected from each station was clearly affected by time constraints and may therefore not be representative of the stratigraphic sequence. The most intensively sampled area, LM/ALSEP, probably yielded the most representative collection of the Cayley plains materials. The rock types are similar in all respects to those collected at other stations during the mission. They include fine- to medium-grained, moderately homogeneous crystalline rocks rocks composed primarily of glass; and breccias, by far the dominant type. The variety of rock types collected indicates that the Cayley plains breccias are heterogeneous and suggests that they are composed of isolated pockets of both light and dark breccias deposited by a turbulent process.

Extensive sampling and photography on the rim (station 11) and near the outer edge of the continuous ejecta blanket (station 13) of North Ray crater provide a basis for stratigraphic interpretations in the northern part of Apollo 16 traverse area. Breccias on the rim and walls are of two main types, light matrix and dark matrix. The area1 distribution and petrographic relations of the boulders sampled or photographed suggest a generalized stratigraphic sequence within the crater and, by extrapolation, in the northern part of the landing site. The light-matrix boulders are friable, rounded, and heavily filleted. Their abundance on the rim and upper-crater wall suggests that they were derived from the upper part of the section. The dark-matrix boulders are coherent and appear to be the latest ejecta to fall on the crater rim. One of these, Outhouse rock, was the source of several igneous and metaclastic fragments. Most of the dark-matrix breccia s may be derived from a deeper horizon near the present crater floor.

Several types of evidence other than the fresh-rayed appearance argue for the youthfulness of North Ray crater. Spallation exposure ages of 27 to 51 m.y. have been reported for five North Ray rocks. Within that time interval, a very thin regolith (approximately a centimeter thick) formed locally; it thickens to 15 cm or more where it forms fillets around the friable light-matrix boulders.

South Ray and Baby Ray craters are fresh blocky craters in the southwestern part of the Apollo 16 landing site. Rays from South Ray can be traced as far as 10 km from the crater to the vicinity of North Ray crater. Although South Ray crater itself was not actually visited by the astronauts, Cayley plains materials ejected from it probably are present at most stations. Station 8 was purposely located on a bright ray from the crater to insure collection of South Ray materials;

dark-matrix breccias and light-gray igneous rocks were the two main rock types sampled. They appear to represent two lithologic units in South Ray crater, dark-matrix breccias being the upper unit.

The South Ray event, if correctly dated by the 1- to 4-m.y. exposure ages in the boulders, apparently deposited ejecta recognizable only in the coarse debris at station 8, about five crater diameters away. Associated soils are reported to give much older ages. No ejecta from the younger Baby Ray crater were recognized in the sample suite, although such materials may be present in small amounts.

Three sampling localities were established on Stone mountain at the south limit of the traverse area with the objective of collecting materials representative of the Descartes mountains. The two highest stations (4 and 5) appeared on premission photographs to be outside ray patterns related to South Ray crater, but contamination by South Ray ejecta appears likely at Station 4. The location of station 4a on the edge of ejecta from Cinco a crater suggests that samples collected might contain local material from a depth of 15 m on Stone mountain. Sampling at station 5, on the wall of a small crater shadowed from South Ray and void of visible blocky ray material, would be expected to include rocks of the Descartes mountains. Station 6, on a bench at the base of Stone mountain very near a ray, may be a mixture of fragments from the Cayley plains and materials of the Descartes mountains.

Chapter E.-Apollo 16 rocks are classified by a descriptive scheme into three groups: crystalline rocks, subdivided as igneous (C,) or metamorphic (C2); glass (G); and breccias (B,-B,), subdivided on the basis of clast and matrix colors and proportions. These rock-type symbols are used throughout this volume.

The crystalline igneous rocks consist of 1 certain and 1 possible anorthosite, 11 fine-grained ophitic to intersertal rocks of troctolitic to anorthositic composition, and 1 troctolite enclosed in fine-grained meltrock of the same composition. Derivation of the fine-grained igneous rocks by impact melting of feldspathic plutonic source rocks is indicated by the common occurrence of unmelted relics derived from coarse-grained plutonic rocks and a bulk compositional range like that of the plutonic rocks with essentially the same compositions.

Metamorphic crystalline rocks studied consist of 1 medium-grained granoblastic rock considered to be a product of metamorphism in a plutonic environment prior to excavation and 10 poikiloblastic rocks. Gradation from poikiloblastic to unequivocally igneous textures in these rocks is taken as evidence of metamorphic origin with minor melting.

Five breccia types have been derived by comminusion of a first-cycle breccia that consisted of anorthositic clasts in a fine-grained matrix ranging from melt texture to metamorphic texture. The first-cycle breccia is considered to be multiring-basin ejecta because it contains clasts of plutonic rock whose origin appears to be deep in the lunar crust. These breccias have been modified to varying degrees by subsequent smaller impacts.

Rocks representative of first-cycle breccias are sufficiently abundant in the Apollo 16 collection that least-metamorphosed samples may be identified. From some such samples displaying minimum modification, it should be possible to date the crystallization of the original crustal rocks, the preexcavation metamorphism of these rocks, and the time of excavation. A review of age data shows that most samples selected for isotopic measurement are so severely modified by subsequent impact that the ages are ambiguous. The samples petrologically most favorable for dating significant and identifiable events in the histories of the rocks are tabulated with the hope that they will help in obtaining unambiguous ages, because such data from Apollo 16 rocks are now so scarce that basin chronologies are only speculation.

The distribution of the various sample types shows no significant differences between Cayley and Descartes materials. Statistical and compositional data on soils support the view that the Cayley Formation and materials of the Descartes mountains are facies of the same ejecta deposit. The Cayley Formation may contain a somewhat higher proportion of matrix consisting of melt and powdered rock.

Chapter F.-The appearance of the regolith is generally that of a rocky gray soil. Rays from young craters in hard substrata are distinguishable mainly as local concentrations of blocky fragments. The brightness of a ray appears to result from a combination of the density and the angularity of fragments, both of which are higher for South Ray than for North Ray crater.

The regolith thickness on the plains has a median value of between 6 and 10 m based on photogrammetric measurements of concentric craters. The thickness of regolith on Stone mountain ranges from a minimum of 5 to 10 m to more than 20 m and may vary greatly owing to the accumulation of mass-wasted debris on a softer, weaker bedrock that may underlie much of the Descartes mountains.

Regolith compositions for most of the site are chemically similar except for North Ray soils, which are significantly enriched in alumina and depleted in iron,

titania, and nickel by comparison with the remaining stations. Soils from station 4 tend to be intermediate in titania and nickel content with respect to soils from the plains and North Ray crater. As a group, the soil samples are a homogenized mixture of the bulk rock analyses from the entire site.

Chapter G.-South Ray crater ejecta totaling 5 to 10 million m^3 are scattered over the Apollo 16 landing site in an irregular pattern that reflects a nonuniform mantle of debris. The ejecta thin rapidly from about 10-15 m at the crater rim to an estimated 1 cm or less of equivalent uniform thickness at the southern sample localities (stations 4, 5, 6, 8, and 9) and to less than 1 mm at the northern localities (stations 11 and 13). The power function best describing this thinning has a slope of approximately -3.0. The fragment population on the lunar surface (for sizes larger than 2 cm) can account for most of the total volume of ejecta, although an equal amount of finer grained material can be accommodated by the model.

Ray material from South Ray Crater can be determined best by the combined evidence of computer-enhanced orbital photographs and the density of fresh rock fragments observed on the lunar surface. Station 8 has the highest potential for materials from South Ray; next most likely are stations 9, 6, 4, and 5. The probability of identifying South Ray ejecta from field data for areas farther away than these stations (3.5-4 km from the crater) is remote. Possible exceptions are station 2 samples taken within a bright ray patch in the central part of the landing site.

Chapter H.-An investigation of the photometric properties of the Apollo 16 landing site indicates that albedo values of several areas, including the rim of South Ray crater, are 50 to 55 percent, the highest measured at any Apollo site. Measurements for the sampled areas range from 15 percent at the central area, 20 percent in the Stone mountain and station 8 areas, to 24 percent at North Ray crater.

The polarimetric properties of the north and east wall of North Ray crater reveal that very little, if any, crystalline material is present in that area and that, most of the rocks are more highly shocked than the Fra Mauro breccias at Cone crater.

Chapter I.-Four highland terrain types have been morphologically defined in the Descartes mountains in and adjacent to the Apollo 16 landing site. Lineated patterns of crater chains, ridges and scarps, and crosslineations represent three of these. These features exhibit both erosional and depositional characteristics whose orientations show that they were formed by the Imbrium impact event. The main highlands mass probably is a tongue of Imbrium basin ejecta. The fourth highland terrain type is represented by isolated mountains inferred to be older Nectarian massifs projecting through the mantle of Imbrium ejecta.

The mountain terrain can be traced beneath the Cayley plains. The plains materials are thin enough along some margins to reveal a subdued reflection of the buried mountain terrain but thick enough in central parts to conceal the mountainous unit. The gradational character of the morphologic contact between plains and mountains does not indicate intergradation between the units but rather the overlapping of Cayley fill on the edge of slightly older mountain terrain.

The smooth to gently undulating surface of the Cayley plains indicates high mobility of the plains-forming materials at the time of their deposition. Of the hypotheses currently offered, the concept that the plains represent fluidized ejecta from one or more multiring basins is most consistent with the morphologic evidence.

Chapter J.-The ejecta deposits from craters that penetrated materials beneath the Apollo 16 landing site, together with the morphologic characteristics of the craters themselves, provide the best clues for a stratigraphic interpretation of the region. The Cayley plains, whatever their source, consist of three textural rock units: light-matrix breccias, dark-matrix breccias, and nearly holocrystalline rocks. These materials are locally mixed but form a gradational assemblage compatible with a crudely layered sequence of rocks whose chemical composition is grossly homogeneous.

At the north end of the traverse area, samples from the ejecta of North Ray crater reveal a population dominated by friable light-matrix breccias. These rocks, easily eroded, account for the convex upper slopes of the crater wall and the rounded and deeply filleted boulders on the rim and ejecta blanket. The lowermost materials of the crater's floor mound are most likely represented by coherent glass-rich dark-matrix rocks found as sparse unfilleted blocks on the rim. The third main lithologic type is coherent light-gray igneous-textured rock that occurs interstitially in light-matrix breccias and as inclusions within dark-matrix breccias. This type, the holocrystalline rocks, reaches sizes of 50 cm at station 8 and occurs as smaller angular rocks in the central part of the landing site.

The relative abundances of the holocrystalline rock and the dark-matrix breccias at stations 8 and 9 and the photographic evidence for layering within South Ray and Baby Ray craters suggest that the crystalline rocks occur as large lenslike masses underlying and grading upward into melt-rich to melt-poor breccias

within the upper 150 m over much of the site. A discontinuous resistant layer at about this depth, becoming shallower in the South Ray area, may be reflected as benches in some crater walls (such as South Ray) and by floor mounds in other kilometer-size craters within the Cayley plains. In the south-central and eastern parts of the landing site plains and everywhere in the nearby mountains, evidence for this layer is lacking.

The materials of the Descartes mountains in and adjacent to the traverse area show little evidence of layering. The dominant rock type below the regolith at the highest point sampled on Stone mountain is most likely light-matrix breccia. The upper 100 m or so of the North Ray crater wall appears to have the same lithology, possibly representing similar materials of Smoky mountain. The lack of coherent blocks in the ejecta of a fresh Copernican crater (Dollond E), about 1 km in depth, 35 km south of the landing site, and the high reflectance of the Descartes mountains indicate that they are made up mainly of friable light-matrix breccias.

Chapter K.-Several hypotheses have been proposed to explain the origin of the terra plains and the hilly and furrowed terra, both of which are nonvolcanic according to evidence from the Apollo 16 mission. Orbital and surface results of the mission, together with postmission photogeologic investigations, suggest that ejecta from the Imbrium basin constitutes a major part of both plains and mountains at this site.

The younger Orientale basin provides a model for investigating basin deposits. Both erosional and depositional landforms occur in the ejecta blanket around the basin, and conspicuous lineations, together with lobate escarpments, strongly indicate lateral flow of materials. Pitting and grooving by secondary impact occurred contemporaneously with deposition of primary hummocky ejecta. Smooth plains deposits appear to be a late-stage fluid facies that ponded in topographic lows. Extrapolation from this young well-preserved basin to the older and larger Imbrium basin implies similar origins for similar morphologic features. Hummocky ejecta, plains, and secondary craters are recognizable around Imbrium. The close spatial association of Cayley-type plains with the Fra Mauro formation is strong evidence for a genetic relation to Imbrium. Furthermore, ridged Fra Mauro-type materials shown on Apollo orbital photographs appear to extend as far as the Kant plateau, forming a depositional unit that partly filled the crater Descartes.

The hypothesis considered most defensible is that primary ejecta from the Imbrium basin, which itself must have included a mixture of preexisting crustal materials, and probably debris incorporated en route, formed rugged deposits as far away as the Kant plateau. The resulting Descartes mountains were sculptured penecontemporaneously by secondary projectiles, also from Imbrium. Fluid, perhaps partly molten, ejecta entrained in these debris flows pooled in topographic lows. The morphology of plains within the belt circumferential to Imbrium is produced by a planar facies of ejecta from Imbrium. Because the ages of the Cayley-type planar surfaces, as determined by crater-erosion models and crater-frequency distributions, are equivalent to those of Orientale ejecta, "crater-clocks" appear to have been reset in some way by the Orientale event.

The Cayley Formation may have been somewhat analogous to a gigantic ignimbrite-incorporating lenses or pods of molten material in a matrix of cooler debris that flowed into topographic lows and produced subplanar deposits. The molten blobs must have retained heat long enough and been of sufficient magnitude to mobilize and thermally metamorphose the debris around them. Since igneous textures developed, cooling must have been relatively slow locally, possibly allowing this partly molten material to acquire the anomalous remanent magnetism recorded at the surface.

The Cayley Formation and the materials of the Descartes mountains, both largely derived from the Imbrium basin, may be veneered by debris from the Orientale basin or smoothed by the seismic effects of that basin impact. Nectaris ejecta (Janssen Formation) is undoubtedly present at depth. Conclusive identification of these various basin deposits in the samples returned from the Apollo 16 site awaits further investigation.

B. APOLLO 16 REGIONAL GEOLOGIC SETTING

By CARROLL ANN HODGES

CONTENTS

ILLUSTRATIONS

GEOGRAPHY

Apollo 16 landed at approximately 15”30' E., 9” S. on the relatively level Cayley plains, adjacent to the rugged Descartes mountains (Milton, 1972; Hodges, 1972a). Approximately 70 km east is the west-facing escarpment of the Kant plateau, part of the uplifted third ring of the Nectaris basin and topographically the highest area on the lunar near side. With respect to the centers of the three best-developed multiringed basins, the site is about 600 km west of Nectaris, 1,600 km southeast of Imbrium, and 3,500 km east-northeast of Orientale. The nearest mare materials are in Tranquillitatis, about 300 km north (fig.1).

GEOLOGIC DESCRIPTION OF CAYLEY PLAINS AND DESCARTES MOUNTAINS

The principal geologic objective of the mission was investigation of two major physiographic units, the Cayley plains and the Descartes mountains (fig. 2). Materials of both local units had been interpreted as volcanic before the mission (Milton, 1968; Wilhelms and McCauley, 1971; Milton, 1972; Hodges, 1972a; Elston and others, 1972a,b,c; Trask and McCauley, 1972; Head and Goetz, 1972), mainly on the basis of their topographic expression. Much of the surrounding central highlands was assumed to be largely primitive crustal material, bombarded repeatedly by impact.

The Cayley plains are of Imbrian age according to stratigraphic relations, crater size'-frequency distributions, and crater degradation models (Wilhelms and McCauley, 1971; Trask, and McCauley, 1972; Soderblom and Boyce, 1972). The type area of the Cayley Formation is east of the crater Cayley, north of the landing site (Morris and Wilhelms, 1967); the name was extended to the apparently similar plains material at the Apollo 16 site (Milton, 1972; Hodges, 1972a). These materials were presumed to be representative of the widespread photogeologic unit, Imbrian light plains, which covers about 5 percent of the lunar highlands surface (Wilhelms and McCauley, 1971; Howard and others, 1974). Characteristics include relatively level surfaces, intermediate albedo, and nearly identical crater size-frequency distributions.

The plains were first interpreted as smooth facies of Imbrium basin ejecta (Eggleton and Marshall, 1962), but as the characteristics and apparent age of the materials were better defined, a volcanic origin became the favored hypothesis (Milton, 1964; Milton, 1968; Wilhelms and McCauley, 1971; Milton, 1972; Hodges, 1972a; Elston and others, 1972a,b,c; Trask and McCauley, 1972). Frequency distributions of superposed craters are lower on the plains than on the Fra Mauro Formation (Imbrium ejecta), and plains materials are superposed on Imbrium sculpture, indicating that the plains postdate the Imbrium basin. This age relation is further supported by the crater-erosion model (Boyce and others, 1974). In morphology and mode of occurrence, the plains resemble mare materials; surfaces are relatively level, and the plains are confined to craters and broad depressions, suggesting local derivation and fluid emplacement. In the landing site area and elsewhere, craters 0.5 to 1.0 km in diameter commonly have conspicuous central mounds on their floors. Throughout the central highlands

helms and McCauley, 1971), Cayley-type plains are especially prominent in large old craters-Ptolemaeus, Albategnius, and Hipparchus. Where adjacent to the maria, as at the type area of the Cayley Formation, the plains are embayed or overlapped by mare lavas. Orbital geochemical data obtained during the Apollo missions indicate that the higher albedo of the plains materials is produced by an aluminum-to-silicon ratio higher than in rocks of the maria (Adler and others, 1973).

FIGURE 1.-Lunar near side. *A*, Location of major features mentioned in the text; Apollo landing sites indicated by numbers. B, Major rings of near-side multiring basins in relation to Apollo 16 landing site. From Wilhelms and McCauley (1971).

In several places, large subdued craters appear to he mantled by Cayley-type materials, suggesting that a relatively thin deposit was emplaced on an older surface. To account for the apparent differential compaction in the upper layer, ash falls or flows, or possibly mass-wasted debris, were proposed as the depositional materials (Howard and Masursky, 1968; Cummings, 1972). In the large crater Alphonsus, dark conelike structures interpreted as volcanic vents occur along graben in the plains material, an association that supported the volcanic interpretation of the plains (McCauley, 1969).

The Descartes mountains topography is virtually unique on the Moon. No other deposits of identical morphology have been recognized, although similar hilly and furrowed materials of Imbrian age have been mapped in several places (Wilhelms and McCauley, 1971). Sixty kilometers south of the landing site, the materials overlap and nearly fill the degraded 50-km crater Descartes; they are clearly depositional and perhaps 1 km or more thick (Milton, 1972). No genetic relation to a local impact crater is apparent, and the morphology of the hills and furrows suggested an origin analogous to terrestrial volcanic extrusions or fissure cones to Trask and McCauley (1972). A partly gradational relation with the Cayley Formation was proposed prior to the mission (Milton, 1972; Hodges, 1972a; Elston and others, 1972a,b,c). Although superposed crater populations indicate an Imbrian age for most of the Descartes mountains (Trask and McCauley, 19721, a patch of unusually high albedo near the north rim of the crater Descartes was interpreted as a Copernican pyroclastic deposit (Head and Goetz, 1972).

As a result of the wide acceptance of these volcanic interpretations, developed independently by several authors, premission models of lunar history generally incorporated: (1) a Moonwide, postbasin, premare episode of fluid or pyroclastic volcanism producing Cayley-type plains and (2) a later and more localized phase of relatively viscous extrusive activity, best exemplified by the Descartes mountains. The Apollo 16 mission was designed to test these hypotheses.

The impact origin of the rocks returned from the landing site forced reinterpretations of the geologic units (pl. 1), Textures of the highly feldspathic samples are nearly all indicative of shock metamorphism of various degrees. The rocks are mainly breccias, but even the relatively few crystalline rocks contain "ghost clasts" indicating thermal metamorphism and recrystallization.

New interpretations of the landing-site geology must

now explain not only the brecciated nature of the rock samples but also all of the characteristics previously ascribed to volcanism. Extrapolation of the data from the Apollo 16 site to similar photogeologic units elsewhere imposes new constraints on the framework of lunar geologic history.

RELATION IN TIME AND SPACE TO BASINS AND CRATERS

Impact sources and emplacement mechanisms for the geologic units at the landing site and for similar materials elsewhere are not readily apparent. Although local derivation of the rocks has been suggested (Oberbeck and others, 1974a, b; Head, 1974), large multiringed basins now appear to have had pervasive influence throughout the Moon's geologic history (Howard and others, 1974) and probably contributed material to the landing site. Youngest and best preserved of these basins is Orientale, whose outer and most conspicuous ring is the Cordillera, 930 km in diameter. Next youngest-and largest on the near side-is the Imbrium basin, whose outer ring, the Apennine, is 1,340 km across; this basin and its ejecta (Fra Mauro Formation) form the stratigraphic and structural base of the Imbrian System (Wilhelms, 1970). The sequence of basin formation becomes progressively ambiguous with increasing age, but Nectaris, nearest the Apollo 16 site, is one of the best preserved of the pre-Imbrian basins on the near side. Its most prominent ring, the Altai, is 840 km in diameter. Its ejecta blanket, the Janssen Formation (Stuart-Alexander, 1971), denotes the base of the Nectarian System, immediately preceding the Imbrian System in the time-stratigraphic nomenclature established on the east limb and farside areas of the Moon (Stuart-Alexander and Wilhelms, 1975). Because of age and proximity, each of these enormous impact events almost certainly influenced the latest stratigraphic and structural development of the entire central highlands including the landing site area.

Inasmuch as multiringed basins formed throughout the Moon's early history, unraveling the stratigraphic column at any given place requires an estimate of the thickness of ejecta contributed by these basins as well as by locally derived material.

Nectaris basin.-The Apollo 16 area, only 600 km from the center of Nectaris, is well within range of the continuous ejecta from the Nectaris basin, but the Imbrian age of the Cayley and Descartes units sampled precludes their derivation from that basin. Further, no deposits as fresh in appearance as the Descartes mountains occur elsewhere around the Nectaris basin. The Nectaris ejecta that should be present at the site must be buried by these younger materials.

Imbrium basin.-The Apollo 16 site is about 1,600 km southeast of the center of the Imbrium basin and

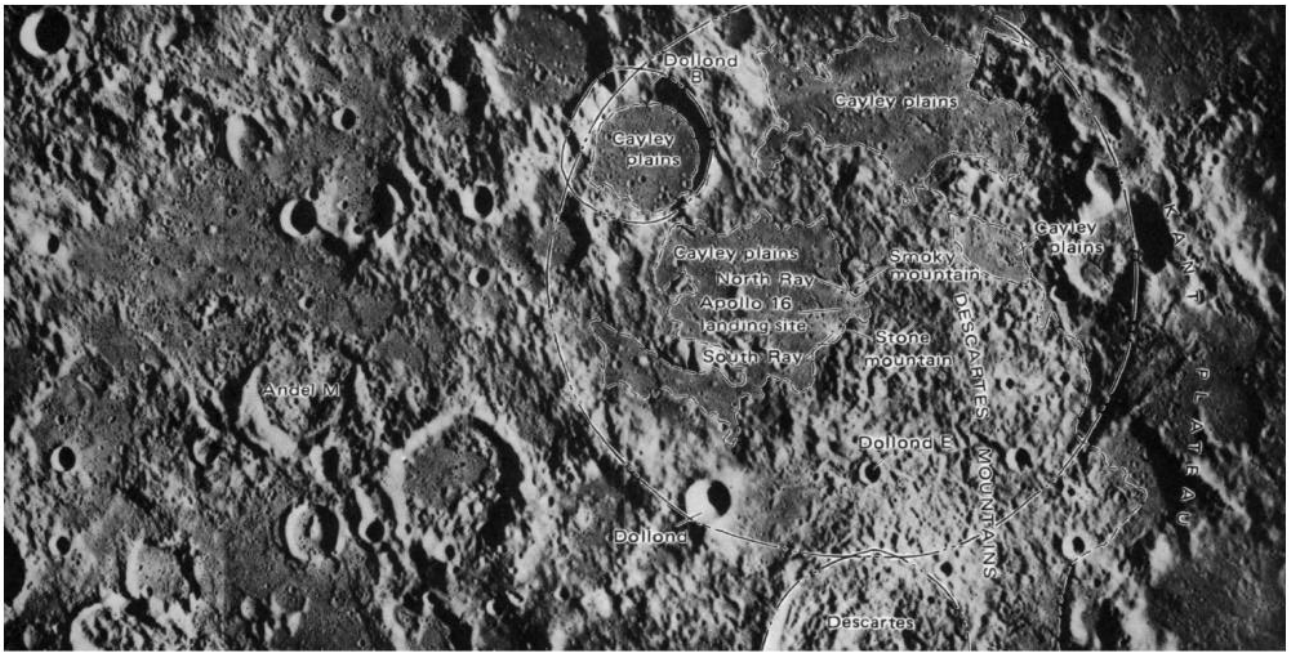

FIGURE 2.-Apollo 16 landing site and vicinity. Andel M, 130 km west of the site, may be filled with as much as 1 km of mixed Imbrium ejecta and debris from its destroyed north rim. Prominent ridges and furrows trending predominantly southeast reflect Imbrium sculpture (secondary cratering) and possible flow lineations in primary ejecta. (Apollo 16 mapping-camera frames 439, 440, 441, 442.)

within a well-defined belt of plains peripheral to that basin in both the central highlands (Eggleton and Schaber, 1972) and on the north (Lucchitta, 1978). Although the site is beyond the range of Imbrium ejecta previously mapped (Wilhelms and McCauley, 19711, this spatial association of plains and basin suggests a genetic relation (Eggleton and Marshall, 1962; Eggleton and Schaber, 1972). Size-frequency distribution of superposed craters, crater degradation models, and stratigraphic relations indicate that the central plains are younger than the Fra Mauro Formation (Wilhelms and McCauley, 1971; Greeley and Gault, 1970; Soderblom and Boyce, 1972), whereas two patches of northern plains are equivalent in age to Fra Mauro Formation (Boyce and others, 1974).

The Descartes mountains may be composed of Imbrium ejecta banked against the Kant plateau, analogous to the deceleration ridges (Trask and McCauley, 1972) of the Hevelius Formation trapped by preexisting crater walls around Orientale (Hodges, 1972b; Hodges and others, 1973). Smaller scale analogs have been described within the ejecta blanket of a crater only 3.5 km in diameter (Head, 1972). Discontinuous Fra Mauro materials occur west of the site where the crater Andel M (fig. 2) appears to have been partly filled by Imbrium ejecta that destroyed its north rim (Moore and others, 1974).

Orientale basin.-The Apollo 16 site is about 3,500 km from the center of Orientale-well beyond any previously recognized extent of that basin's ejecta. The Cayley-type plains, however, appear to be contemporaneous with the Hevelius Formation (McCauley, 1967), which is the continuous ejecta from Orientale and which includes a conspicuous planar facies of broad extent, mainly at the distal margin of the textured ejecta (Soderblom and Boyce, 1972; Hodges and others, 1973). In order to account for the age of the plains surfaces, as deduced from cratering models, Orientale was proposed as the source of the uppermost deposits of both mountains and plains at the Apollo 16 site (Chao and others, 1973; Hodges and others, 1973). Theoretical analyses of ejecta volume argue that ejecta from Orientale may be dispersed over the entire Moon (Moore and others, 1974); broad distribution of crater ejecta is demonstrated photogeologically by young craters such as Tycho, whose rays extend more than 3,000 km (Baldwin, 1963).

Local craters. -Because of stratigraphic constraints, local craters are an unsatisfactory source for the materials at the Apollo 16 site. The Cayley plains are younger than any large adjacent craters, all of which have clearly been sculptured by Imbrium ejecta. A pre-Imbrian crater 150 km in diameter centered on the landing site has been conjectured (Milton, 1972; Head, 19741, but materials formed by such a crater would be several kilometers deep at the landing site and are not likely to have been included in the sample collection. Head (1974) proposed that the plains were essentially floor materials of a 60-km crater whose rim crest includes Stone and Smoky mountains. This seems impossible, however, for such a crater would have to be younger than the Descartes mountains of Imbrian age, yet older than the pre-Imbrian crater Dollond B (fig. 2), an obvious incongruity; even allowing the Descartes mountains and the plains to be pre-Imbrian would require the plains to be sculptured, and they are not. Furthermore, this mechanism, requiring local origin within craters, cannot be extrapolated, inasmuch as craters containing Cayley-type plains are generally considerably older than the enclosed plains, and some plains (for example, at the Cayley Formation's type locality) are not within craters.

A possible derivation of plains materials by local secondary cratering was advocated by Oberbeck and others (1975), who demonstrated that the mass of ejecta from a secondary crater far exceeds the mass of the primary projectile at increasing distances from the continuous ejecta blanket. The pervasiveness of Imbrium sculpture caused by secondary projectiles around the Apollo 16 site indicates that such cratering, together with mass wasting and extensive lateral transport, could have concentrated material in topographic lows, although the crater size-frequency distributions of the surficial plains suggest a younger age for the deposits than is accountable by this postulate. The potential sources for rocks returned from the Apollo 16 mission are reexamined in Hodges and Muehlberger (this volume) after presentation of field data and pertinent orbital information.

To summarize the position of the Cayley plains and Descartes mountains in space and time: (1) The units are Imbrian in age, and the uppermost plains deposits are essentially contemporaneous with the formation of the Orientale basin; cratering ages of the Descartes materials are not so well defined because of their rugged topography, but they are at least as old as Imbrian. (2) Because of proximity to the Nectaris basin, stratigraphy at the Apollo 16 site must surely include Nectaris ejecta at depth, but the basin is too old to have produced the materials now at the surface. (3) The site is within the "sphere of influence" of the Imbrium basin, as indicated by the sculpturing produced by gouging of secondary projectiles, and Imbrium deposits may well be present. (4) The hypothesis that Orientale ejecta reached the site is based largely on the apparent contemporaneity of that basin with the surficial plains deposits. Deposition of Orientale ejecta on the order of several tens of meters (a speculation not represented on the accompanying geologic map, pl. 1) seems required to "reset" the Imbriuni "crater clocks."

C. APOLLO 16 TRAVERSE PLANNING AND FIELD PROCEDURES

By WILLIAM R. MUEHLBERGER

CONTENTS

ILLUSTRATIONS

GEOLOGIC OBJECTIVES

The geologic objectives of the Apollo 16 mission were to understand better the nature and development of the highland area north of the crater Descartes, including an area of Cayley plains and the adjacent Descartes mountains, and to study processes that have modified highland surfaces. The objectives were to be met through the study of the geologic features both on the surface and from orbit and through analyses of the samples returned.

The plans for the mission finally evolved from backroom discussions and formal review between interested personnel: scientists, engineers, and, foremost, the astronauts themselves. The premission plan as finalized shortly before launch underwent modification during the mission as the science support team evaluated revised times available for traverses, problems that arose during the mission, and changing geologic concepts of the area being investigated.

Highlands materials had been collected at the Apollo 14 and 15 landing sites (fig. 1): from the continuous ejecta blanket of the Imbrium basin at Apollo 14; from the base of the Apennine front, the outer ring of mountains bounding the Imbrium basin, at Apollo 15. Each of these sites yielded highlands materials of different types that could be related to Imbrium basin formation.

At the Apollo 16 site, materials of both a widespread highlands plains unit and the rugged Descartes mountains were of interest; neither geologic unit had yet been sampled in the Apollo reconnaissance of the Moon.

Ray materials from two small but conspicuous Copernican craters, North Ray and South Ray, both on the Cayley plains, mantle a considerable part of the traverse area, on both plains and adjacent mountains

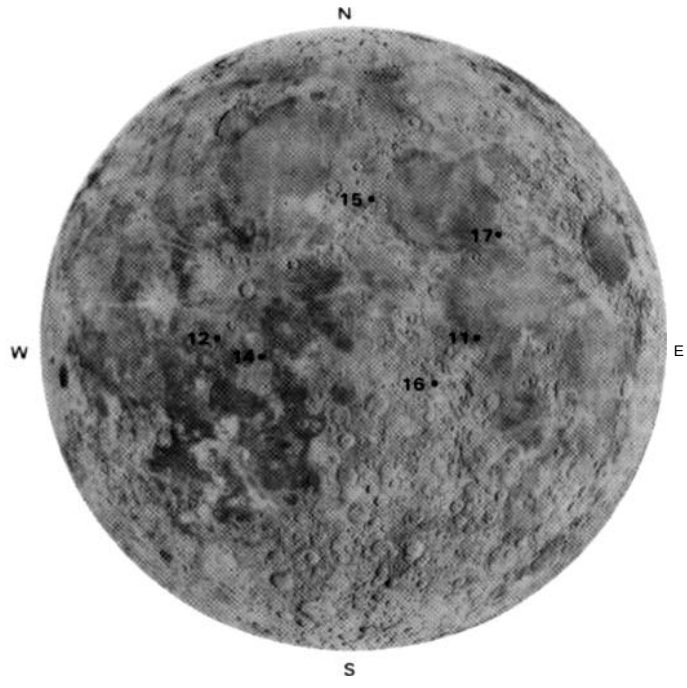

Figure l.--Near side of the Moon showing the Apollo landing sites

(Hodges, 1972a; Elston and others, 1972a, b). Impact craters of Imbrian to late Copernican age are prominent throughout the region (fig. 2). Rimless to low-rimmed, irregular depressions were mapped as craters of either secondary impact from Theophilus, 300 km to the east, or volcanic origin.

FIGURE 2.-Apollo 16 landing site, traverses, and regional lunar features. From AFGIT (1973) and Hodges and others (1973). Reprinted with permission of the American Association for the Advancement of Science and Pergamon Press.

Lithologic layering in the Cayley plains was suggested by albedo bands and ledges in the walls of several craters and by mounds in the floors of craters about 1 km in diameter. Lithologic layering in the materials of the Descartes mountains was suggested by topographic benches and bands of slightly varied albedo on the flanks of Stone mountain. Materials at depth beneath the Cayley plains were interpreted as including both the Fra Mauro Formation derived from the Imbrium basin and ejecta from the nearer but older Nectaris basin (Hodges, 1972a). Elston and others (1972b) projected the flank of a highly cratered pre-Imbrian hill beneath the traverse region. The depth to these units was unknown, but all were believed to be well below the depth of local cratering and therefore unlikely to be sampled in the traverse area.

PREPARATION FOR FIELD GEOLOGY AT DESCARTES

The name of the game in traverse planning is maximum science return. Most surface experiments and the central station of the Apollo Lunar Surface Experiments Package (ALSEP) that telemetered data to Earth required deployment by the astronauts, or required astronaut voice data transmission as in the procedure for the Lunar Portable Magnetometer. Each of these types of operations required rapid deployment (using minimum time), and a definite period of time was allocated to each experiment.

The geologic experiment was more difficult to structure, and the observations, sampling, and photography necessary to satisfy the collective geologic community required time and equipment beyond that available. For example, a fourth traverse or Extravehicular Activity (EVA) was requested by the Field Geology Experiment Team (with the concurrence of the astronauts) in order to study South Ray crater and its ejecta blanket. This request was denied because it would have gone beyond the time limits deemed safe for the LM systems. As time was extremely limited, an intricate system of priorities was established for both station locations and tasks performed at each station. The development of priorities involved many individuals and advocate groups for the various aspects of the traverse activities. The final system of priorities and contingency plans appeared in the "Lunar Surface Procedures" and "Science Contingency Plan" documents for the mission.

The field training of the astronauts developed their abilities to identify and describe the significant geologic features in view, to sample and document photographically the geologic units at a sampling site, to document the significant relations of areas remote from the traverse line by use of telephoto cameras and Description, and to integrate previous observations into a general geologic picture of the landing site.

Both sampling procedures and photographic techniques evolved with experience during training and throughout the actual missions. Sampling procedures focused on obtaining a truly representative collection of materials at the site while staying within severe weight restrictions. In addition to standard sampling procedures (illustrated in fig. 3), several special techniques were used to: (1) support studies of the surface character of the regolith, the optical properties of the

FIGURE 3.-Sampling equipment and techniques used on Apollo 16. ***A,*** Sample 61295 broken from large rock under gnomon. Regolith samples were taken from fillet surrounding rock. Photograph taken to include LRV to assist in locating sample areas. Station 1, Plum crater. AS16-109-17804. B, Gnomon in standard position with color chart leg toward sun and near sample to be collected. Gray scale and color chart on leg and wand gives true color; bands are 2 cm wide, for photographic scale; wand is mounted in gimbels to give local vertical. Station 5, cross-sun view. AS16-110- 18024. C, Same as B but with sample 65035 removed. Station 5, cross-sun view. AS16-110- 18025. ***D,*** Sampling area of B and C after collection of rake sample. Gnomon leg at right edge. Station 5, cross-sun view. AS16-110-18026. ***E,*** Sample 60018 being chipped from large rock by Astronaut Charles Duke. Rake being used for scale. Wires in rake are spaced 1 cm apart. Cuff checklist of notes strapped to astronaut's wrist, above hammer. Camera lens sun-shade and sample bags hanging from a clip below the camera are visible. Station 10. AS16-11-18689. ***F,*** Astronaut John Young breaking chips from spa11 zone, Outhouse rock, North Ray crater. Sample bags being carried by hand because clip under camera fell off. Each bag is numbered and called out by astronaut when sample is placed in it. Camera and mounting bracket on astronaut's chest, and cuff checklist clearly visible. AS16-116-18647. G, Tongs being used as scale for sample site. Astronaut John Young pulling rake. Rim of North Ray crater; LRV in background; white breccia boulder sampling area on skyline. AS16-106-17340. ***H,*** Tongs holding rock 60115, just removed from small depression (arrow) in which rock had lain on lunar surface. Station 10. AS16-114 18446. I, Closeup stereo view of boulder 1 at station 8 showing textural details of breccia not visible in small samples returned. AS16-108-17693/17694. J, Scoop being used as locator. Dark stripe on handle used as guide by the astronaut to give proper distance for closeup photography. Sample 60275 marked by arrow. Sampling station at LM. AS16-117-18833. ***K,*** Area of J after removal of sample 60275 with scoop. AS16-117-18835. L, Scoop, gnomon, and sample collection bag (SCB). The unlatched and open top shows two single core tubes (drive tubes) stowed within the bag. This bag can be carried by hand or attached to the astronaut's life support system. Individual samples in their numbered bags are stored in the SCB. Station 4, down-sun, before sampling. AS16-107-17464. ***M,*** Double core attached to extension handle. Lower tube about half driven. Upper tube (number 29) visible. Station 8, AS16-108-17682. N, Double core hammered to total depth. Station 8, location changed from that shown in ***M.*** AS16-108- 17686. 0, Hinged rack (in open position) on rear of LRV, showing (right-to-left) rake, both tongs, and penetrometer drum in stowed position for travel. Lunar portable magnetometer deployed at end of 15-m cable. Other equipment under seats. AS16-114- 18433.

lunar surface, the unabraded surfaces of lunar rocks, boulder erosion and filleting, the adsorption of mobile elements in shaded areas, cosmic ray tracks in large and small boulders, and chemical homogeneity throughout single units and (2) support future studies on uncontaminated lunar soil. Horz and others described these procedures and special samples returned, including an X-ray description of the cores collected.

Photographic requirements included two panoramas at each station, one taken immediately upon arrival at the station, the other just prior to leaving the station, so that the undisturbed surface could be studied, sample locations more easily identified. and a stereobase established for detailed study. Telephoto surveys were made from two stations to obtain a stereobase of Stone and Smoky mountains for analysis of lineaments like those first recognized on Mount Hadley during Apollo

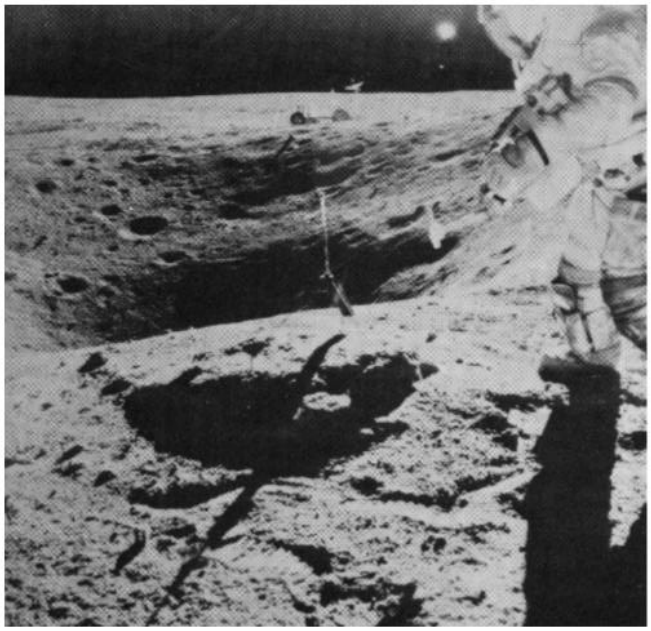

A

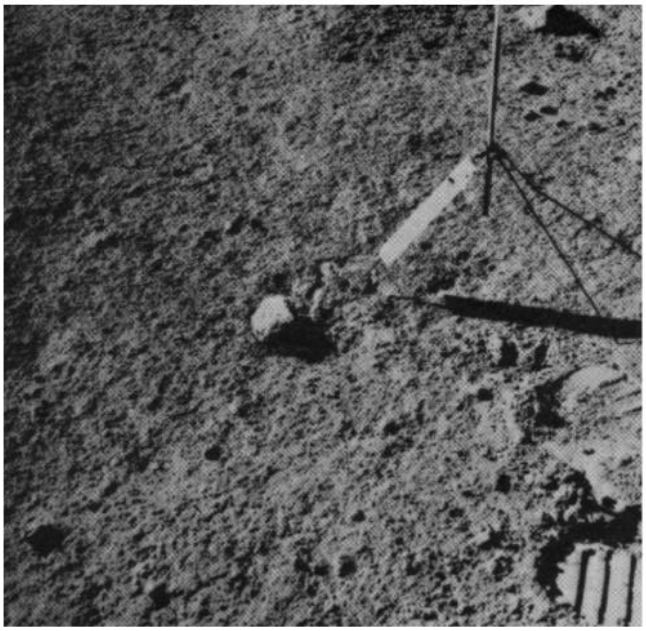

B

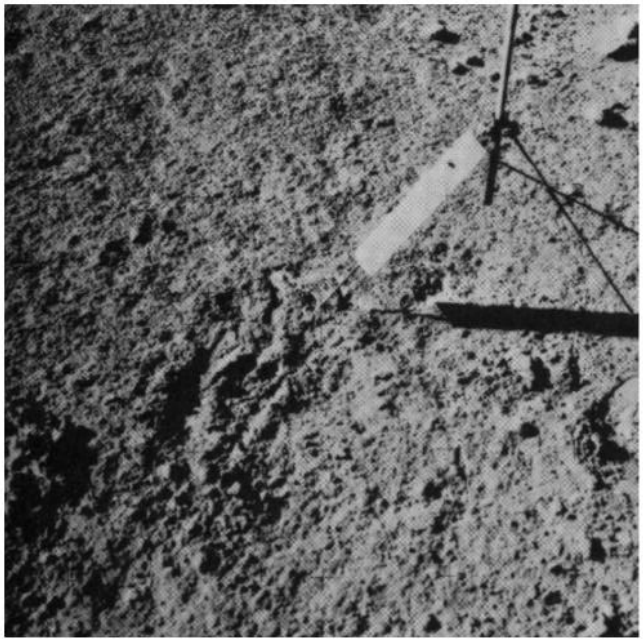

C

D

15. In addition, two polarimetric surveys were made at station 11: one to establish calibration control in the near-field of a sampled area and one of the inaccessible interior of North Ray crater taken from the rim.

Finally, the photographs required included a standard set for sample documentation, closeup stereopairs for analysis of rock textures, and "flight-line" stereo, that is, a series of photographs perpendicular to a boulder that would provide a stereo base for study.

TRAVERSE DESIGN

The three traverses (one per EVA) were designed to optimize investigations of the Cayley plains and the Descartes mountains (fig. 4). For that purpose, a preliminary photomosaic and topographic base map, plate 2, was prepared from existing Apollo 14 Hasselblad photographic coverage 9 months before the mission. This allowed detailed traverse planning to start

E

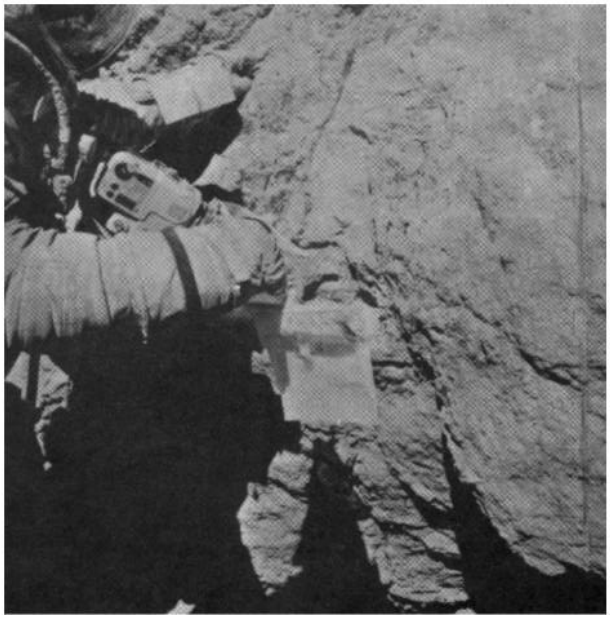

F

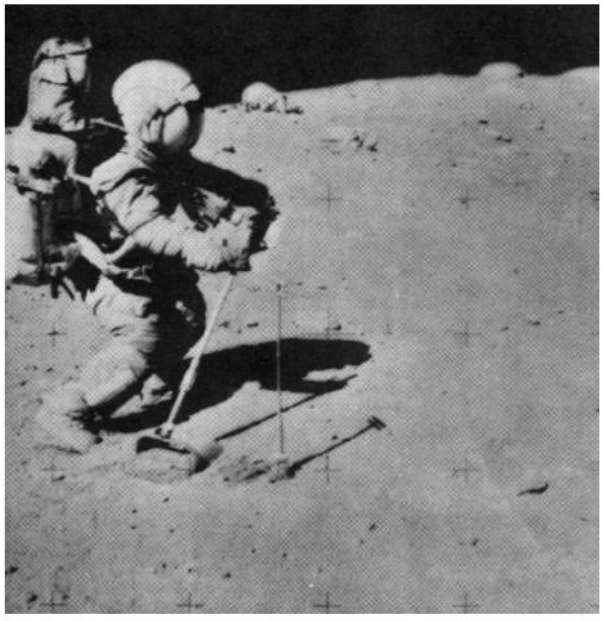

G

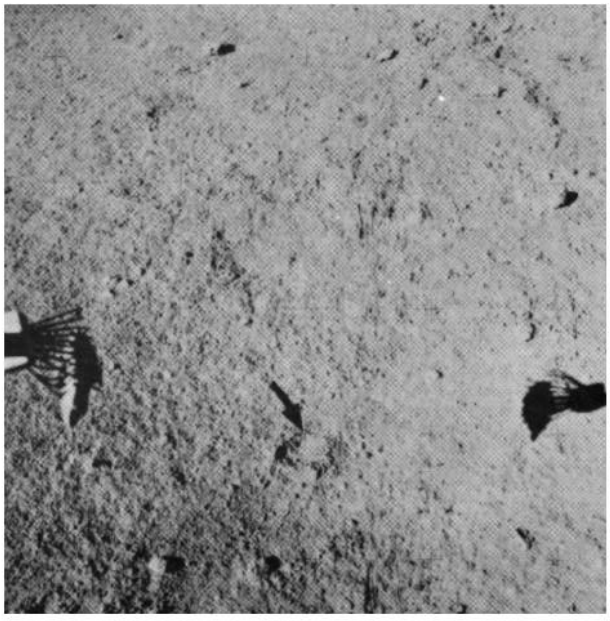

H

spite the low resolution of the photography and long before more accurate maps became available. The Cayley Formation was to be sampled during each traverse in order to determine lateral variations of the stratigraphic section between North Ray and South Ray craters, the petrology of the formation throughout the area, and the characteristics of the upland plains regolith. The prime sampling areas were located at Flag and Spook craters and in the vicinity of the LM and ALSEP, where crater dimensions suggested that the unit might be sampled to depths of approximately 60 m. Avoiding ray material so as to obtain locally derived samples of Cayley Formation was a major consideration in the LM-Spook-Flag sampling areas. Prime sampling sites for deeper parts of the Cayley were in the ejecta of North Ray and South Ray craters.

The short distance between Flag and Spook craters, about 1 km, made it possible early in the lunar surface activities (EVA-11 to test the lateral continuity of bedrock layers. Good stratigraphic correlations in these craters could provide a solid base for extending the stratigraphy into the LM-ALSEP area and a geologic basis for the interpretation of the Active Seismic Experiment profile. It was hoped that the stratigraphy could then be carried northward through Palmetto to North Ray crater and southward to South Ray crater. Both Flag and Spook craters are degraded and have a veneer of South Ray ejecta across or near them. Station

I-L

I-R

J

K

1 was located on Plum crater, a small fresh crater on the rim of Flag crater, thought large enough to have penetrated the entire Flag crater ejecta blanket, and station 2 was on Buster crater, thought to have penetrated the upper layer of the underlying Cayley Formation even though it lies on the outer part of the ejecta blanket of Spook crater. A third station, for sampling, coring, and experiments in soil mechanics in the ALSEP area, was moved late in the planning stages to the end of EVA-2 so that maximum sampling time could be spent at Flag and Spook craters.

Deeper parts of the Cayley Formation were assumed to have been excavated by the larger North Ray and South Ray impacts and exposed near the rim of North Ray crater (stations 11,12, and 13, fig. 4) and in the ray deposits of South Ray crater (station 8).

On the second traverse, stations 4, 5, and 6 on the flank of Stone mountain were the principal sampling

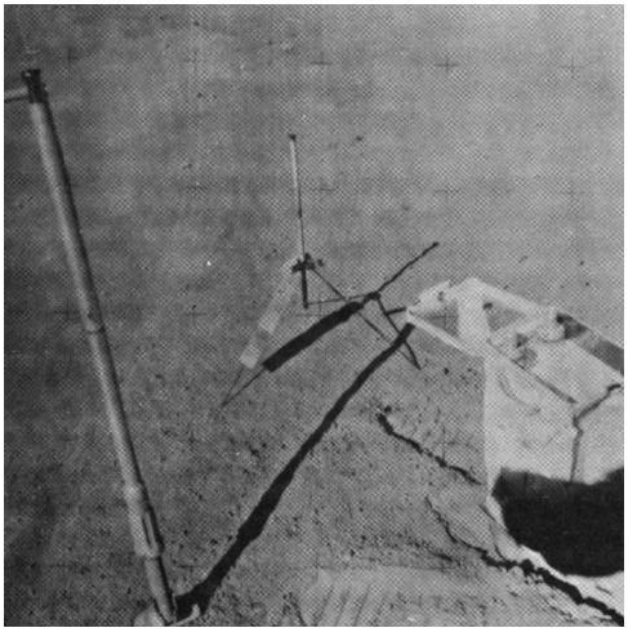

L

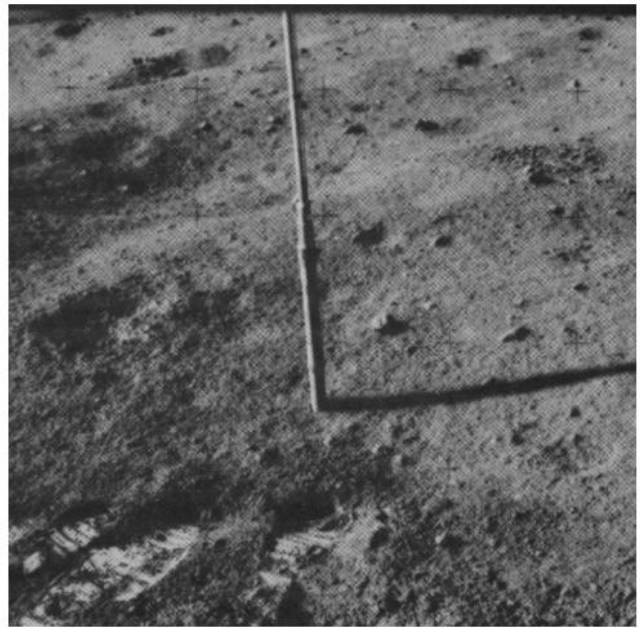

M

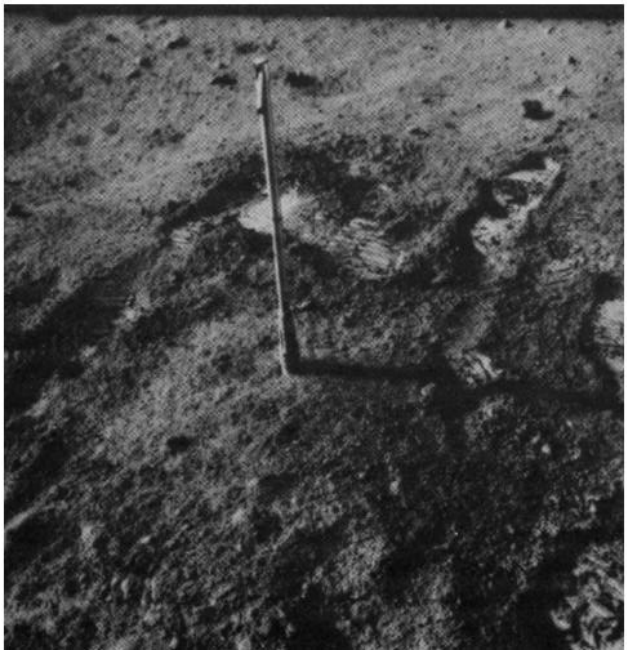

N

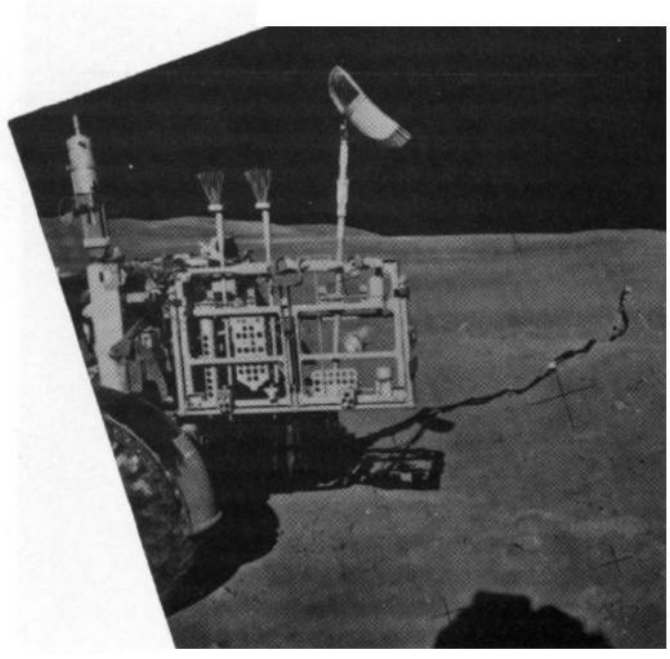

O

sites for Descartes mountains materials (fig. 4). These stations were on benches delineated on the premission topographic map (U.S. Army Topographic Command, 1972). The station farthest upslope (station 4) was located between Cinco *d* and e, a pair of craters that must penetrate the regolith, excavating blocks of Stone mountain material. It was hoped that ray material from South Ray crater, anticipated at these stations, could be recognized and avoided. In addition to employing a wide variety of sampling techniques, penetrometer tests of soil were to be performed; the elevation of the station would permit good telephoto viewing of the rim and interior of South Ray and Baby Ray craters on the plains. Locations of the lower stations on Stone mountain (5 and 6) were spaced at equal intervals down the slope but subject to change if the astronauts observed outcrops, blocky-rimmed craters, or other features of particular interest on their outbound traverse. Station 14, on the lower slopes of Smoky mountain, was planned for the third traverse in order to compare the two mountain units.

The rim of North Ray crater, nearly 1 km in diameter and more than 200 m deep, was the prime site for obtaining the deepest samples of Cayley plains. The younger South Ray crater was believed inaccessible because of the blockiness of the ejecta blanket and the large deep craters (Trap-Wreck-Stubby) that obstructed the direct route from the LM. Although many large blocks were observed in the ejecta of North Ray crater, there appeared to be relatively smooth approaches along which the astronauts could drive to the crater rim or at least to within walking distance of it. Seven stratigraphic layers within the crater were interpreted on the basis of albedo differences (Elston and others, 1972a, b, c) visible on premission photographs having a resolution no better than 5 m. Lateral variations in these bands across the crater, a large dark central mound on the crater floor, and a 25-m-long dark boulder on the crater rim were identified as features of interest. Stations 11 and 12, approximately 200 m apart on the crater rim, were located as end points of a sampling strip that would provide materials representative of all layers penetrated, except possibly the top one. Station 12 was at the huge dark block named "House rock" by the astronauts, assumed, in premission planning, to be visible from a distance and therefore useful as a navigation aid. To guarantee samples from the uppermost layers of the Cayley

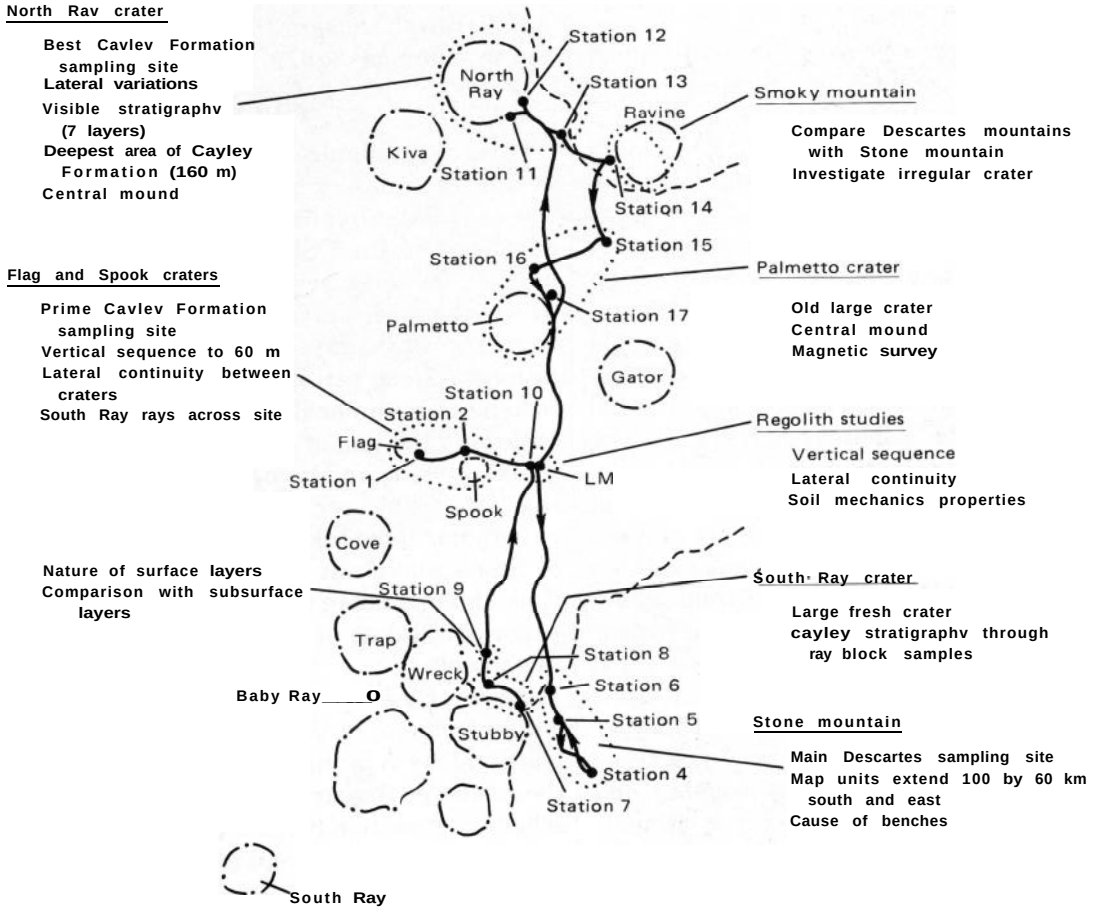

FIGURE 4.-Planned traverses and geologic objectives.

plains, station 13 was established far out on the ejecta blanket. A wide variety of photographic techniques was planned to document the compositional, textural, and stratigraphic relations of the returned samples: panoramas from several locations for stereoviewing, 500-mm telephotography of far crater wall, near- and far-field polarimetric surveys, close-up stereo for textural details of individual boulders, "flight-line" stereo of large boulders, as well as conventional photographic documentation during sampling.

Palmetto crater, about the same diameter as North Ray crater, is older and very subdued; a few large fresh craters occur near its rim. Stations 16 and 17 (fig. 4) were selected as the best places for sampling Palmetto ejecta. In addition, the outbound traverse was specifically planned along the Palmetto rim so that the astronauts could observe features within the crater and on its ejecta blanket not visible on the premission photographs and thereby recommend changes in the plan for the end of the traverse. Station 15 was planned at a small fresh crater for sampling the local top layer of the Cayley Formation to establish lateral continuity. Stations 15, 16, and 17 were also planned as magnetometer stations designed to determine whether magnetic anomalies occur around a large crater (Palmetto).

Rays from South Ray crater were visible across much of the landing site area on premission photographs, but the nature of the ejecta in rays was unknown. Either a blanket of debris of various sizes or a string of blocks and associated fines that produced secondary craters, or perhaps a combination of both, was thought to account for the apparent characteristics. Ascertaining the composition of rays was essential in order to assign samples collected to their proper source craters.

Ideally the procedure for sampling these rays would have included intensive study of several widely separated patches, as each patch represents only a small volume of the crater ejecta. The more patches studied, the better the stratigraphic sampling of the crater, despite the fact that most ray material in the vicinity of the LM was likely derived from only the upper quarter or less of the crater. South Ray material was expected in cores from the LM/ALSEP and station 8 areas and in some of the surflcial samples returned. Station 8, near the rim of Stubby crater in the brightest ray patch accessible, was planned specifically to obtain materials from South Ray crater. Sampling by all techniques available was designed to obtain a variety of rock types representative of stratigraphic units. Trenching and coring was expected to indicate the thickness of near-surface units; special samples from the top and bottom of large boulders and from the soil beneath such boulders might provide an exact date of the South Ray impact. Photographs of secondary craters and the boulders that formed them would indicate azimuths toward the source.

The objectives of station 9 required a mature regolith surface, free of recent contamination by ejecta from fresh young craters. The station location had to be selected by the crew as they traveled, although the general area was delimited prior to the mission. The primary purpose of this station was to study the surface of the regolith visible in photographs and telescopes and analyzed by nonpenetrating geochemical and geophysical devices. The station had to be in a patch of Cayley Formation of "typical" or "average" albedo such that the data could be extrapolated regionally. A series of successively deeper samples were to be collected to determine the nature of the regolith. Samplers were designed to collect uppermost layers of surface grains, and a surface skim sample was to be collected, as well as a deeper scoop sample directly under the skim. A special vacuum-sealed short core was designed to protect the most pristine sample yet returned from the Moon, and several padded bags were included to preserve fragment surfaces (see Horz and others, 1972, for details).

A very readable booklet on details of premission planning for various surface and orbital experiments and hardware aboard the Apollo 16 mission was written by Simmons (1972).

THE MISSION

Several mechanical and operational problems arose during the mission that prevented exact execution of the premission plans. Because a mechanical problem developed in the CSM engine, the lunar landing was delayed for three revolutions, or nearly 5 hours. This delay changed the mission plans. To keep the astronauts' work day within acceptable medical limitations, a sleep period was assigned first upon landing instead of an immediate EVA. This change precluded observing the flanks of Stone mountain for lineaments like those seen on Mount Hadley at the Apollo 15 landing site. The second of two planned telephoto panoramas to be taken during EVA- 1 for stereo study of Stone mountain was cancelled because of lack of time and was taken instead at the start of EVA-3. This panorama, taken at high sun angle, shows no shadow, lineaments.

During EVA-2 (fig. 5), problems with the LRV navigation system, a lack of landmarks, and difficult trafficability combined to stop the astronauts short of the prime goal near Cinco e. In order to preserve the schedule at station 8 and 9 and to keep enough time at station 10 to do the preplanned tasks and, if required, to remove the broken cable on the Heat Flow Experiment, station 7 was cancelled. This station, planned for 15-minutes duration, was intended for sampling of a

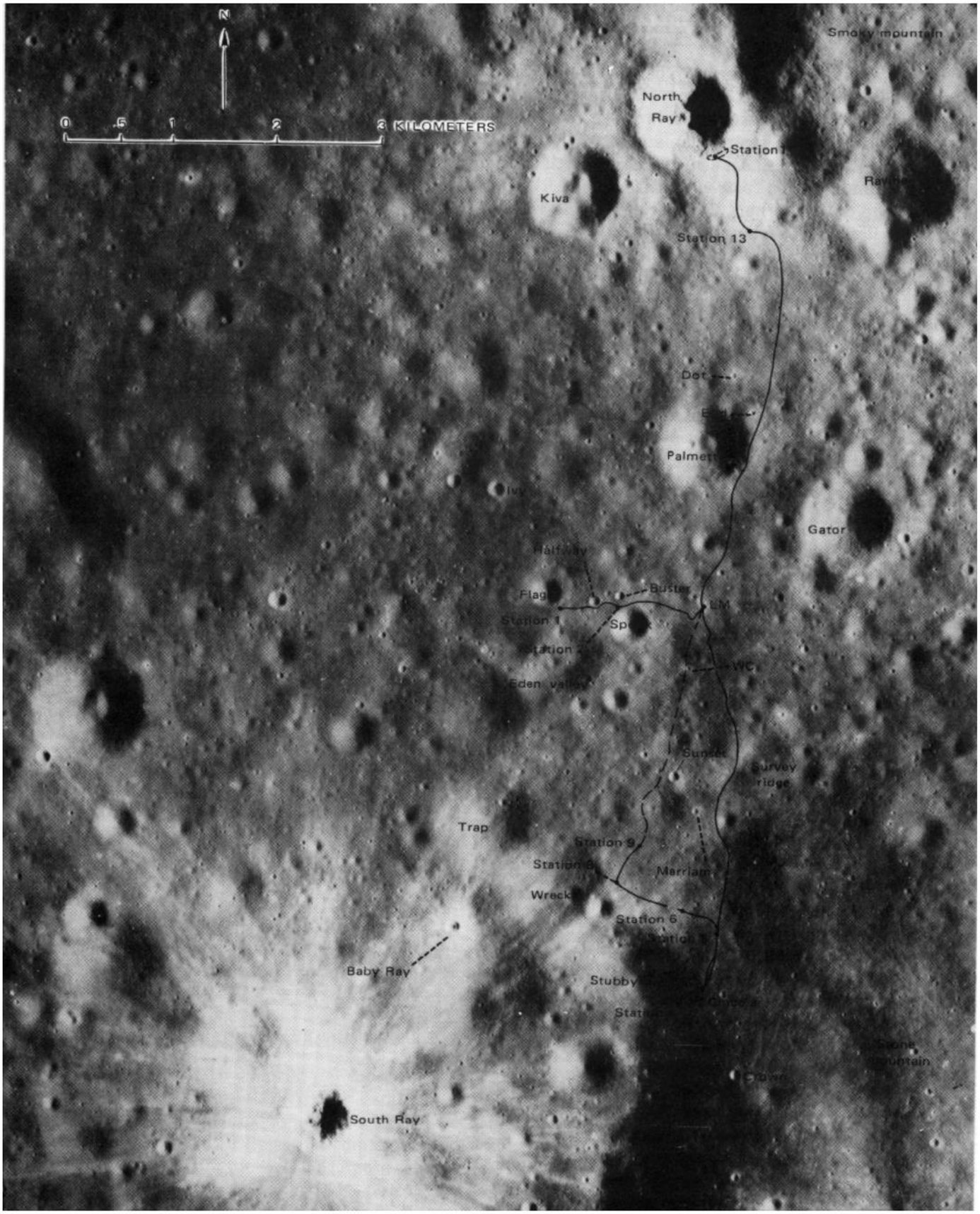

FIGURE 5.-Actual traverses. Apollo 16 panoramic-camera frame 4618.

fresh crater near the mapped Descartes-Cayley contact and a telephoto survey of Smoky mountain and the interior of Stubby crater.

EVA-3 was shortened from 7 to 5 hours when it was decided to lift off from the lunar surface at the preplanned time rather than extend the lunar surface stay and risk problems with nearly depleted LM systems. All activities other than those scheduled for North Ray crater were cancelled. The astronauts drove the LRV to the rim of the crater without difficulty, allowing time for nearly all of the preplanned tasks for stations 11 and 12 to be accomplished. The near-field polarimetric survey was cancelled and a second abbreviated telephoto panorama into North Ray crater was taken from near House rock. The operational aspects of the mission are described in the Apollo 16 preliminary science report (Baldwin, 1972). Despite exigencies that developed through the mission, all of the primary geologic tasks were carried out: sampling of the Cayley plains, of ejecta from North Ray and South Ray craters, and of materials from Stone mountain, representative of the Descartes mountains; photographic coverage of all sampling areas, the entire traverse route, and telephoto views of all important points remote from the traverse route.

HINDSIGHT

Photogeologic interpretations for this mission were hampered by the low resolution of the best available premission photographs. As it turned out, nearly all the large blocks (5 m or larger) had been located (Boudette and others, 1972), but because the announced resolution of the photographs was 5 m or poorer, it was not certain whether features at or near the limit of resolution were real or simply artifacts of photoprocessing. The number of boulders identified and the blockiness predicted from radar studies of the site convinced us that travel through the rays from both South Ray and North Ray craters would be difficult if not impossible. The virtual absence of rocks on North Ray, except for those identified before the mission, was startling. Had the spacing of blocks on South Ray rays been known, the mission might have been designed differently: an alternative considered was a dash to Stone mountain along with deployment of the ALSEP on EVA-l, followed by EVA's to South Ray and Baby Ray craters, and then to North Ray crater. Better geologic data from the youngest crater rims could have helped immeasurably to determine the nature of the Cayley Formation, its composition, and stratigraphic makeup. Data from a fresher or larger crater on Stone mountain, remote from South Ray crater ejecta, could have better defined the character of the materials composing the Descartes mountains.

Certainly if we had better understood, before the mission, the enormity of the events forming the Imbrium and Orientale basins and the potential extent of their ejecta, we would have considered geologic alternatives to the volcanic interpretation of the units at the Apollo 16 site. The geologic field training might thus have been different, many of the special sampling experiments might never have been scheduled for this mission, and as a result, the time available for geologic traverses would have been allocated differently.

Dl. FIELD GEOLOGY OF APOLLO 16 CENTRAL REGION

By GERALD G. SCHABER

CONTENTS

ILLUSTRATIONS

TABLES

THE LM/ALSEP STATION

The central region of the Apollo 16 landing site includes three major areas-LM/ALSEP, station 1, and station 2-all underlain by materials of the Cayley plains. The LM/ALSEP station comprises five general areas-Lunar Module or LM, Apollo Lunar Surface Experiments Package or ALSEP, station 10, station 10, and the Lunar Roving Vehicle or LRV final parking site-ranging from approximately 70 m east to 140 m southwest of the LM (pls. 3 and 8; fig. 1). All five sites lie within but at the east edge of distinct ray material ejected from South Ray crater 5.7 km to the southwest (fig. 2).

The Cayley plains in the LM/ALSEP region are broadly undulating and slope to the southwest; the maximum relief within a radius of 400 m from the LM

site is 25 m (fig. 3). The amount of surface covered by 2- to 20-cm fragments ranges from 1.3 to 6 percent and averages about 2 percent (fig1 4). Blocks as large as 0.5 m are relatively common (fig. 5). The largest boulder (33 m north of ALSEP) is several meters across. The rocks are uniformly distributed, not deeply buried, and are poorly filleted, some are perched, unburied, and lack fillets entirely. The rocks with little or no fillet are

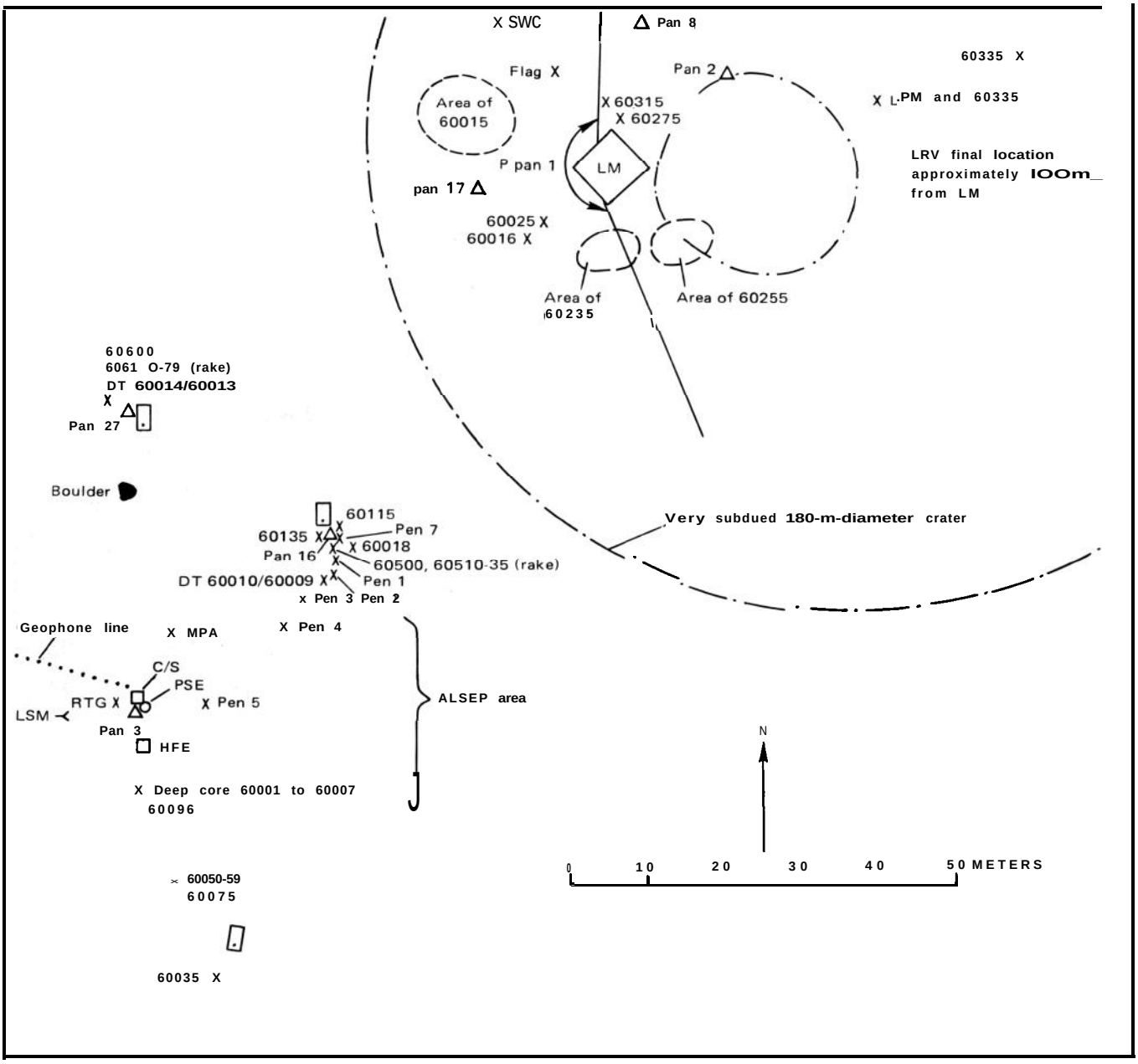

EXPLANATION

◌	Crater rim	PSE	Passive seismic experiment
X 60335	Sample locality and number	LSM	Lunar surface magnetometer
DT	Drive tube	HFE	Heat-flow experiment
P pan	Partial panorama	RTG	Radioisotopic thermoelectric generator
△ Pan 2	Panorama location and number	MPA	Mortar package assembly
▯	LRV. dot on front	LPM	Lunar portable magnetometer
X Pen 5	Penetrometer reading, location and number	swc	Solar wind composition
c/s	Central station		

FIGURE l.-Planimetric map of the **LM/ALSEP** area.

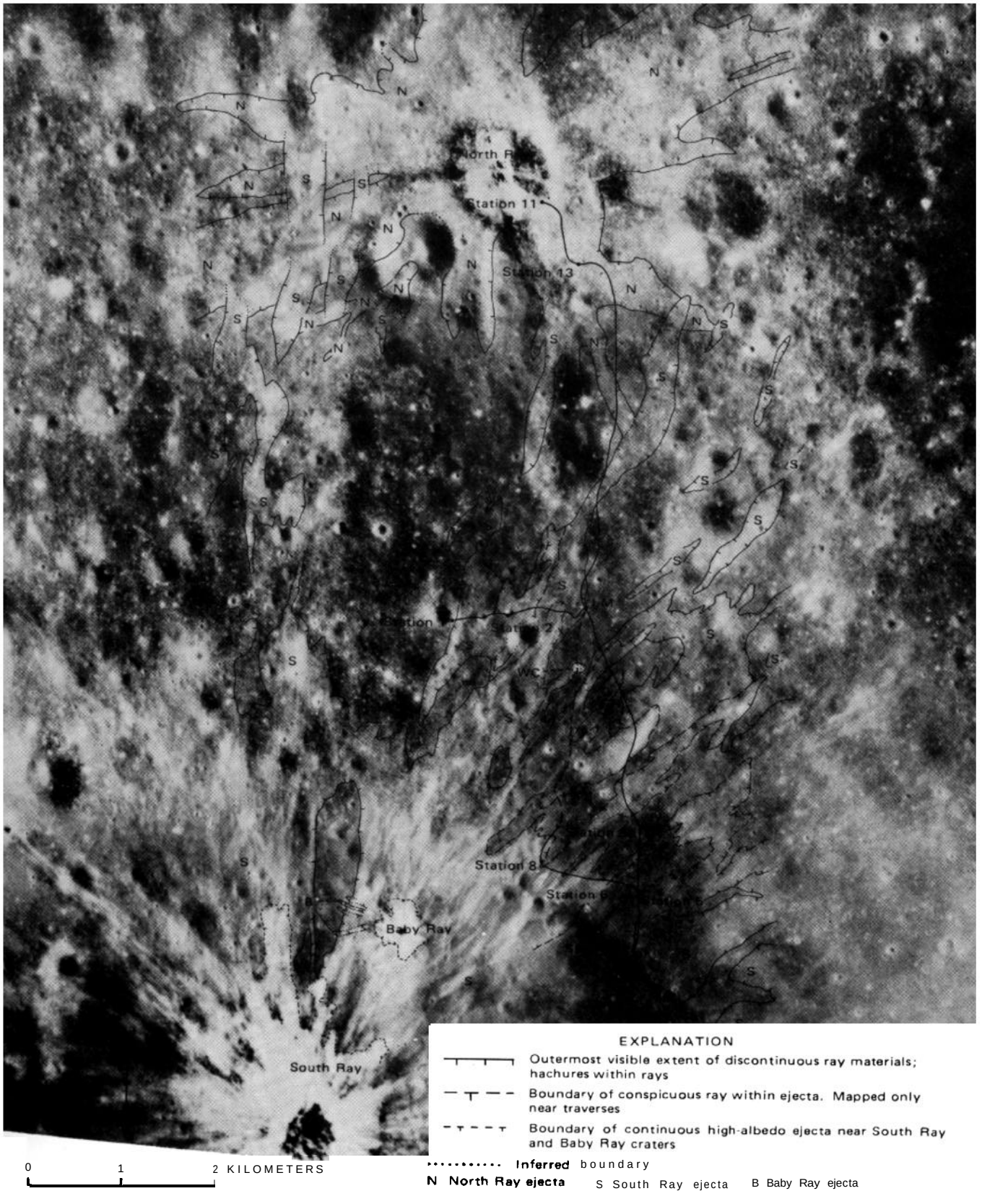

Figure 2.-Distribution of ejecta near the Apollo 16 landing site. Derived from second-generation film positives of Apollo 14 orbital photographs AS14-69-9520 and 9522 (500 mm), using stereoanalytic plotter (from Muehlberger and others, 1972).

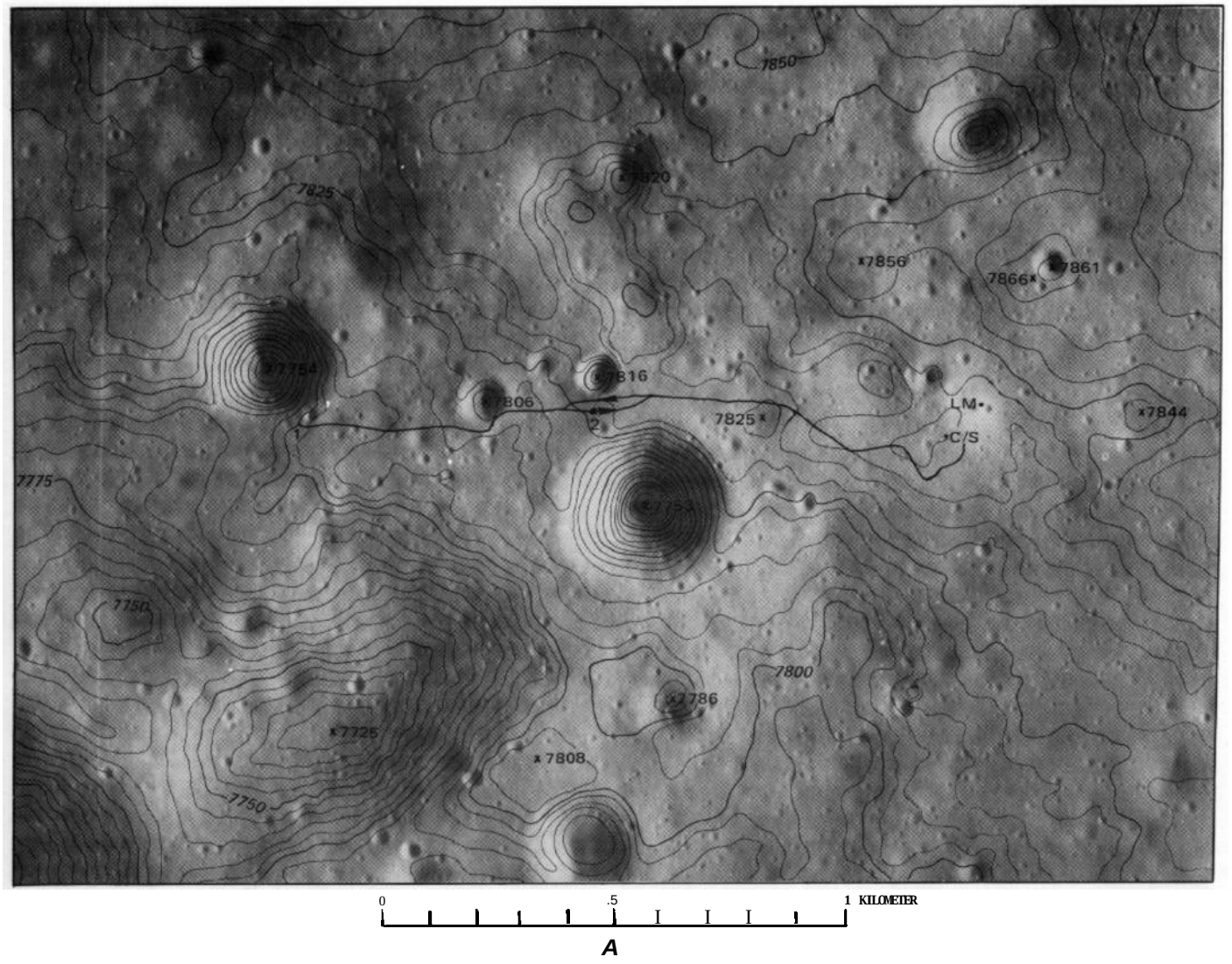

FIGURE 3.-Map and stereopairs of the central part of the landing site. ***A,*** Contour map of Apollo 16 central landing site region superimposed on Apollo 16 panoramic photograph, frame 4618. LM sites and EVA-l traverse indicated. Contour interval, 5 m: arbitrary datum. Geographic names on figure 6. Topography compiled on AP/C plotter by G. M. Nakata from panoramic-camera photographs AS16-4618 and 4623. *B*, Stereopair showing the hummocky nature of the Apollo 16 landing site and central traverse region. Area of coverage identical to 3A. C, Stereopair showing the Lunar Module (arrow) on the lunar surface in the Descartes highlands. Note the relatively fresh 30-m-diameter crater 10 m east of the LM. Same photographs as in 3A and *B* greatly enlarged.

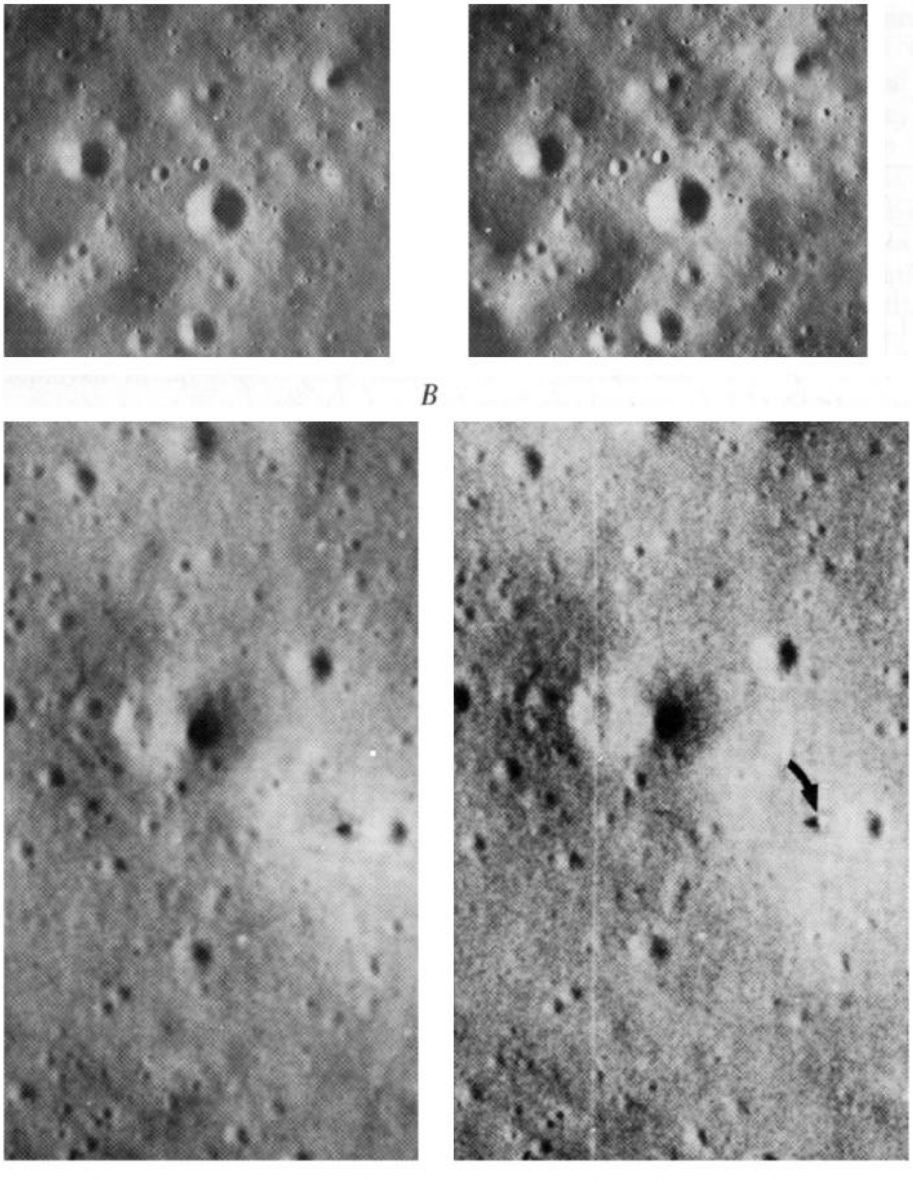

B

C

FIGURE 3.-Continued.

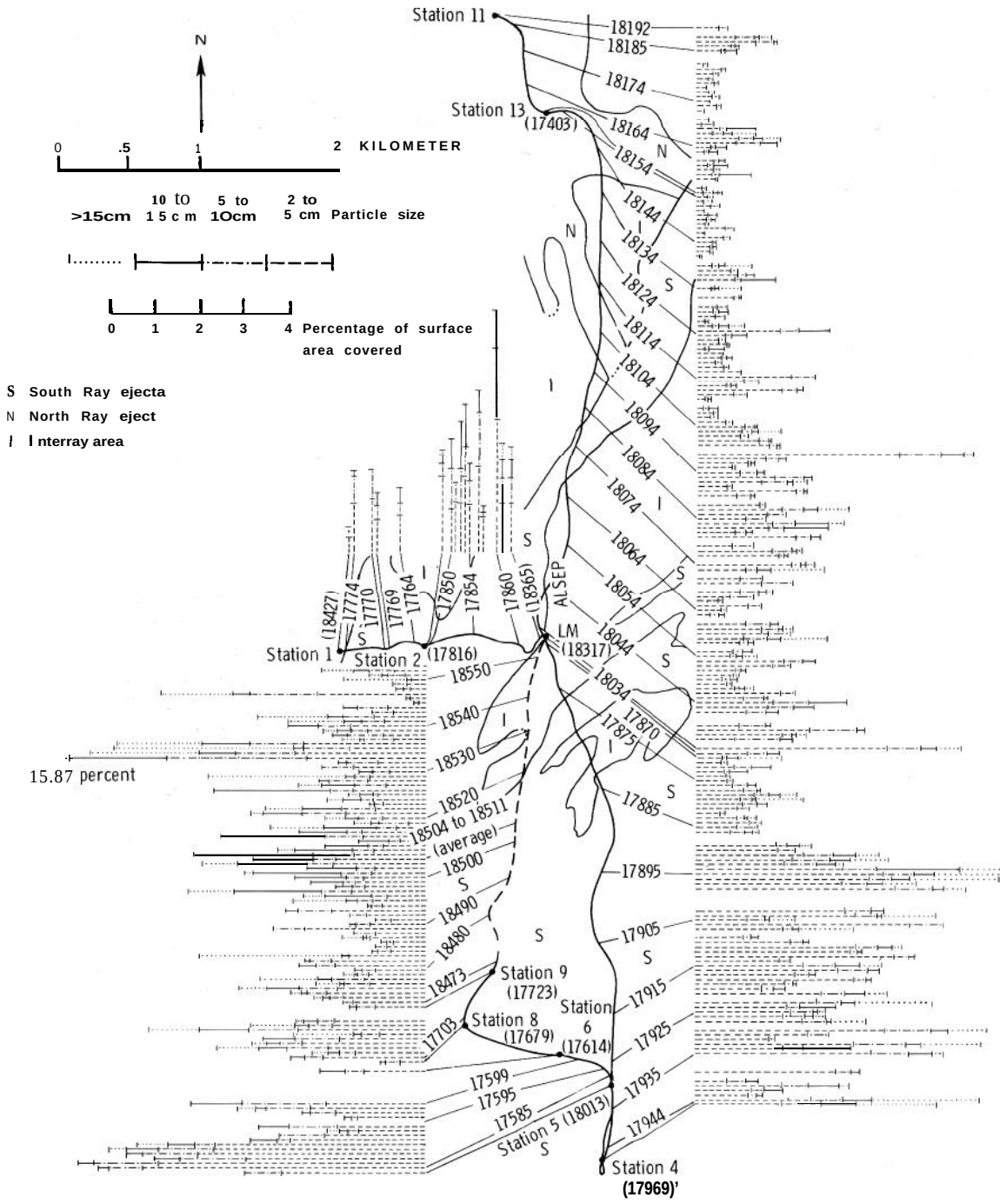

FIGURE 4.-Size distribution of fragments larger than 2 cm as determined from lunar surface photographs. Each line represents a size-distribution determination from a single photograph. Length is proportional to surface area covered by fragments as shown by bar scale. Five-digit numbers identify photographs; leaders tie them to their approximate positions along the traverse path (from Muehlberger and others, 1972).

thought to represent ejecta from South Ray crater. The largest boulder near ALSEP has a well-developed fillet and may have been ejected from the older North Ray crater.

The LM landed on the western wall of a very subdued crater, approximately 180 m in diameter, 10 m west of a moderaely subdued crater about 30 m in diameter. There are eight very subdued craters 125 m to 360 m in diameter within a radius of 400 m from the LM (fig. 6). Ejecta from these craters with excavation depths of 25 m to 70 m may be included in the material sampled at this station.

The ALSEP was deployed in an intercrater area about 3.5 m higher than the elevation of the LM. Stations 10 and 10' were on.the western rim crest of the crater in which the LM landed (fig. 6). Smaller, younger craters are common in the LM/ALSEP area, ranging from numerous 0.5 m to 2 m secondaries (probably produced by ejecta from South Ray crater) to less common primary craters as large as 40 m in diameter. Samples collected in the LM/ALSEP area include all eight categories of rocks described in the petrology section of this report (Wilshire and others, this volume; Wilshire and others, 1973): crystalline rocks (igneous, metaclastic), glass, and five types of breccias (table 1). The only other station where all rock types were collected was station 11. LM/ALSEP and 11 were the most thoroughly sampled of mission 16 stations.

The source areas and depths of the LM/ALSEP samples are not known with certainty, but some assumptions can be made. As the LM site is on the eastern edge of a distinct ray from South Ray crater (fig. 2), a large proportion of the samples collected may be from that source. The 30-m crater just east of the LM site (figs. 1, 3A), however, may have ejected material from as deep as 6 m in the floor debris of the LM crater. A possible secondary source of sampled material is the reworked ejecta from the eight very subdued craters mapped within a 400-m radius of the LM (fig. 6).

Many of the rocks collected in the LM/ALSEP area are at least partly glass coated and range from highly angular to subround (figs. 7-10). In general, the fine-

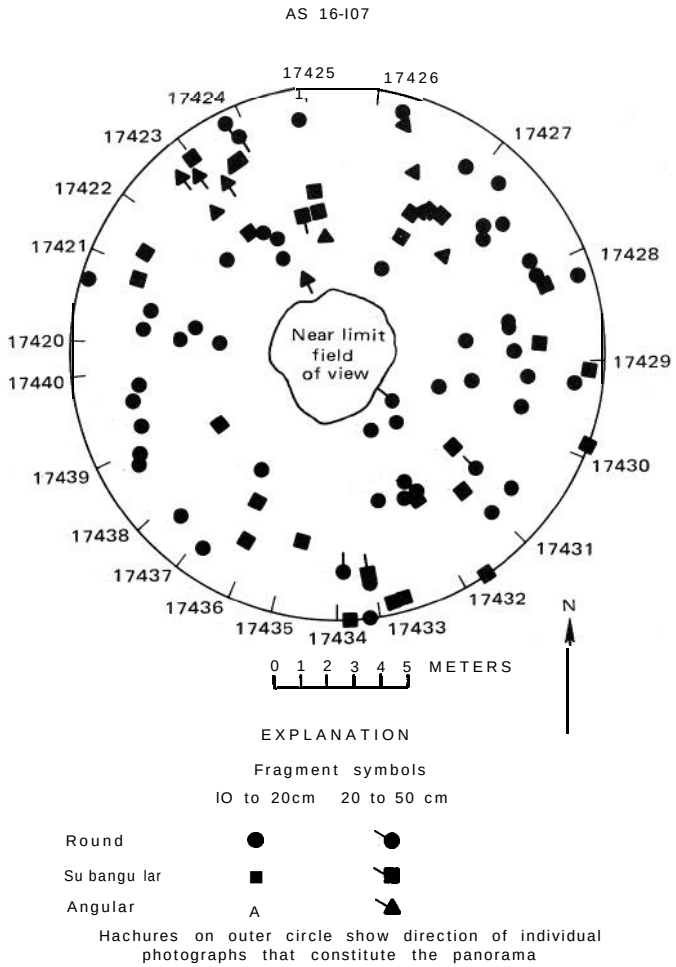

FIGURE 5.-Rock distribution within 10 m of the panorama site north of the LM (see pl. 3, pan 8).

TABLE *L-Number and percentages of rocks (>2 g) documented at the LM/ALSEP station*

category	Number of rocks collected	Percentage
Igneous:		
C_1	3	5.4
Metaclastic:		
C_2	11	19.6
Breccia:		
B_1 (light matrix, light clast)	14	25.0
B_2 (light matrix, dark clast)	4	7.1
B_3 (light and dark clast)	6	10.7
B_4 (dark matrix, light clast	8	14.3
B_5 (dark matrix, dark clast)	1	1.8
Glass:		
G		16.1
Total		100.0

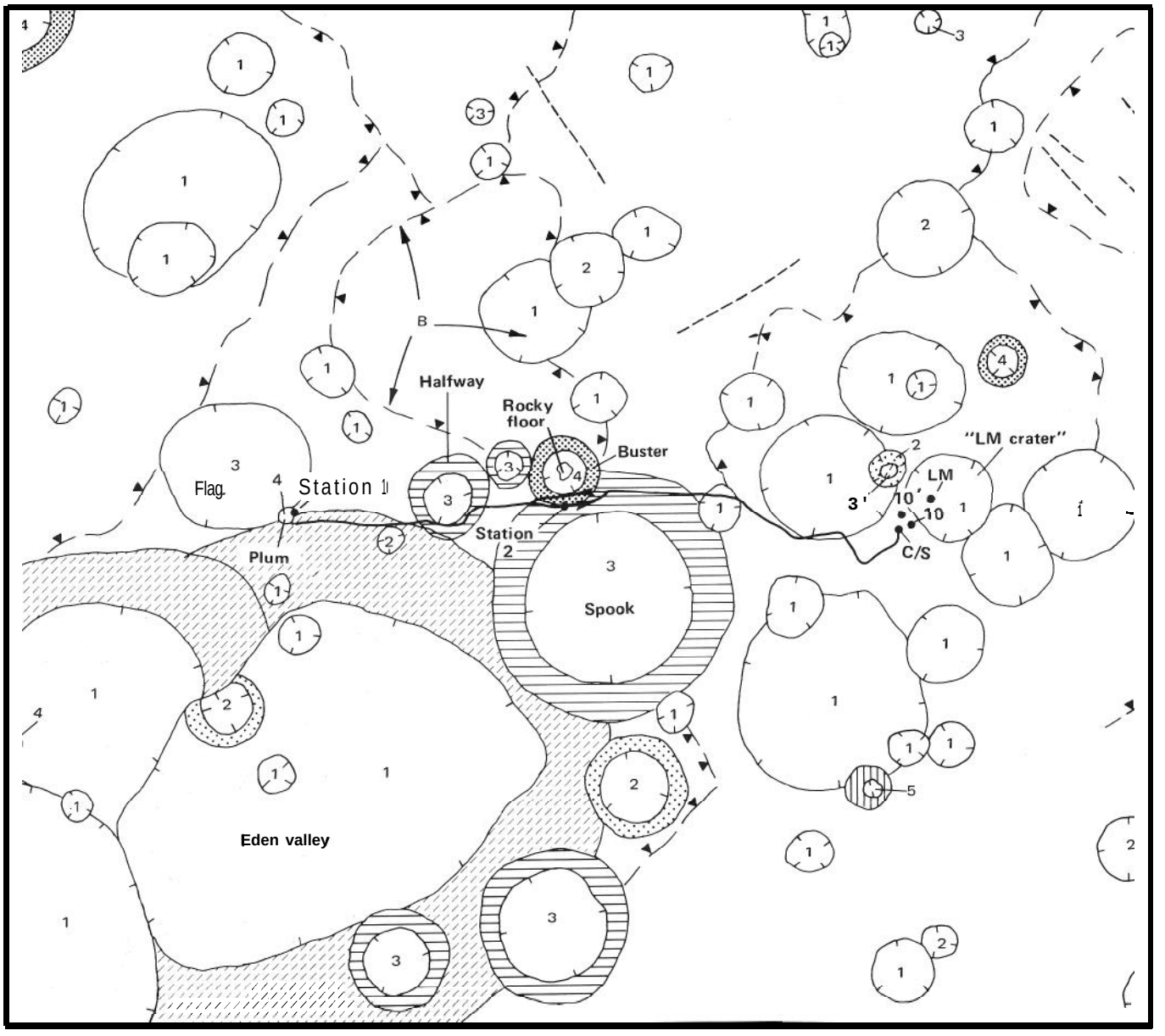

0 .5 1 KILOMETER

EXPLANATION

Lineament

Base of subdued scarp; barbs point downslope

Crater rim crest

5 Freshest crater rim

1 Most subdued crater rim

B Ridge near Buster crater

FIGURE 6.-Sketch map of landing site and central region showing distribution of fresh to greatly subdued craters of significant size and their relation to EVA- 1 traverse stations.

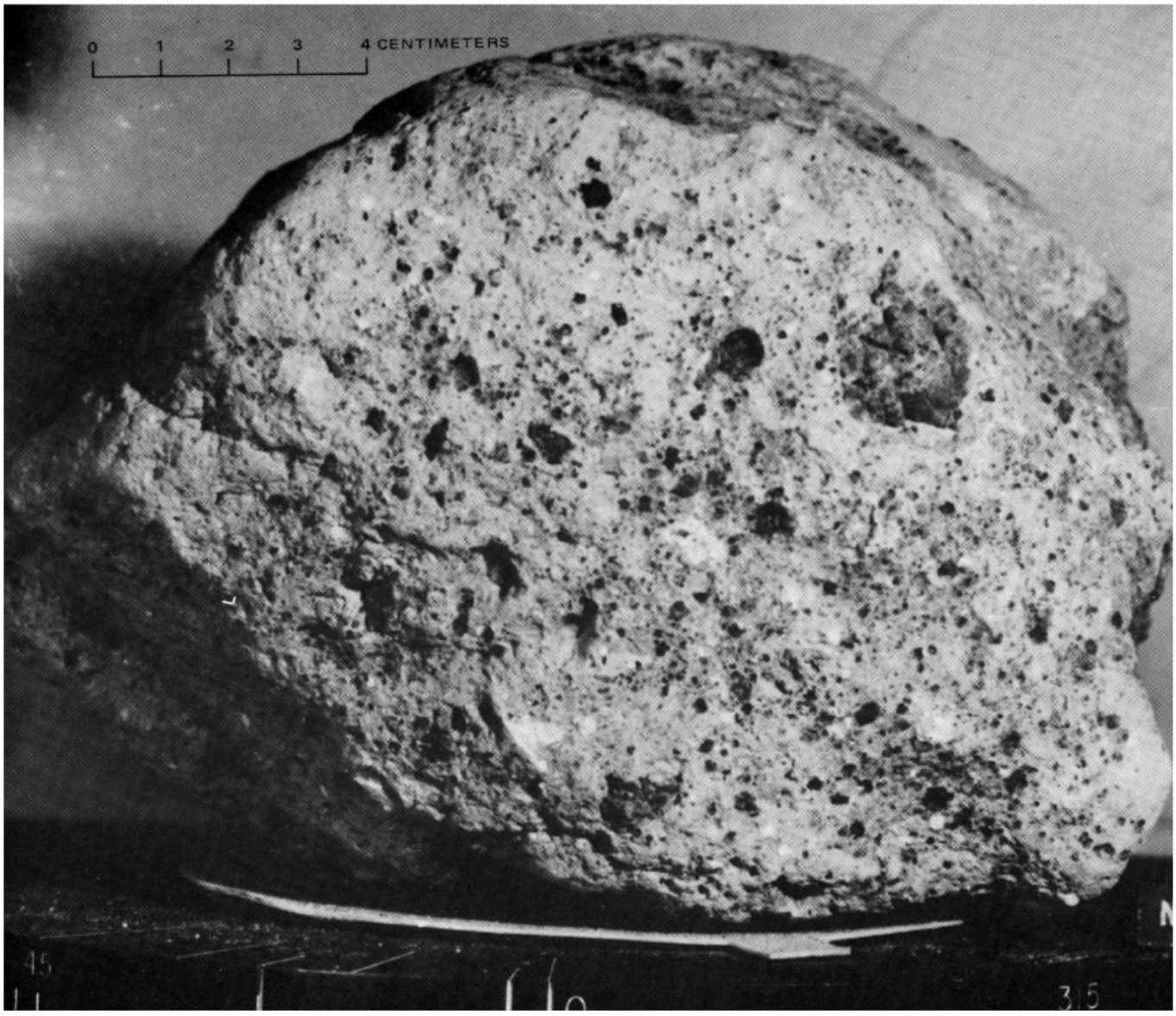

FIGURE 7.-Sample 60016. NASA photograph S-72-43829.

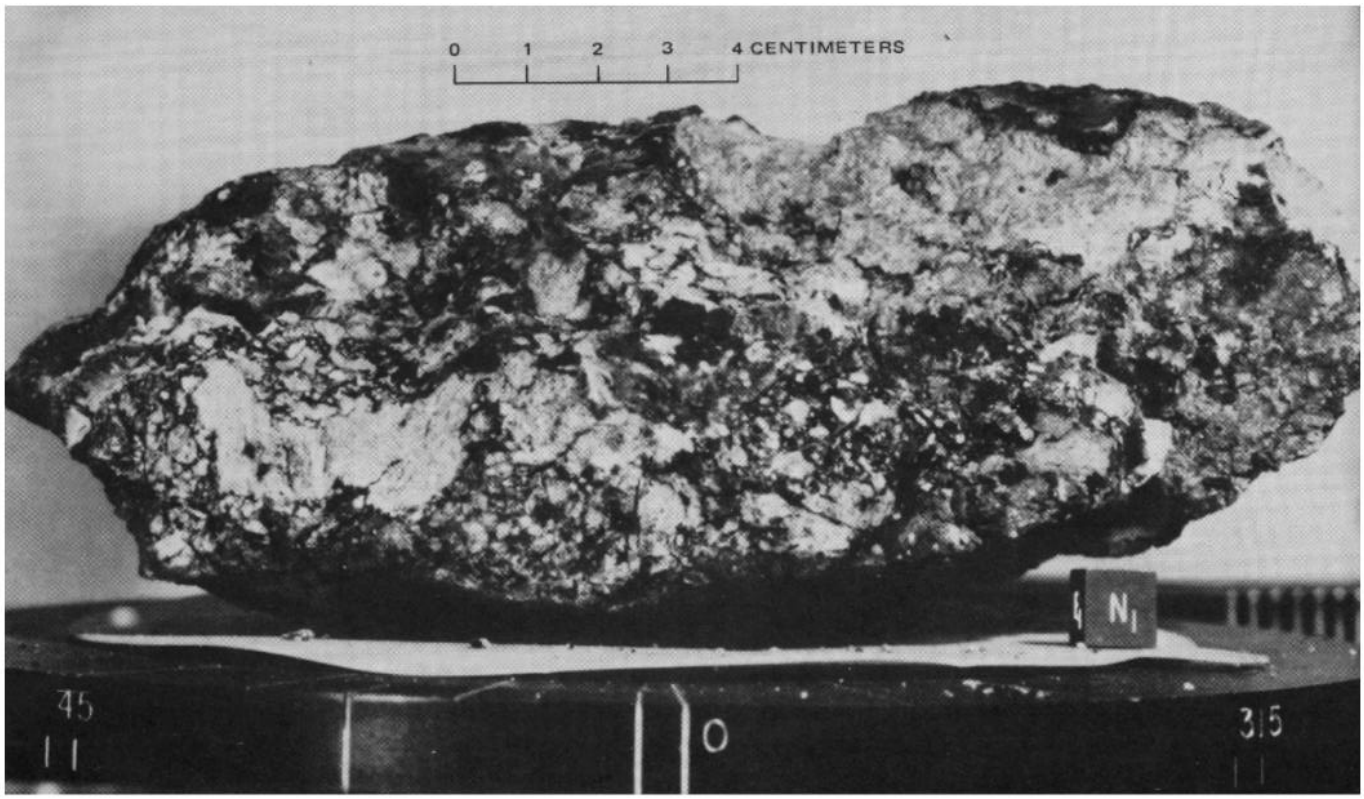

A

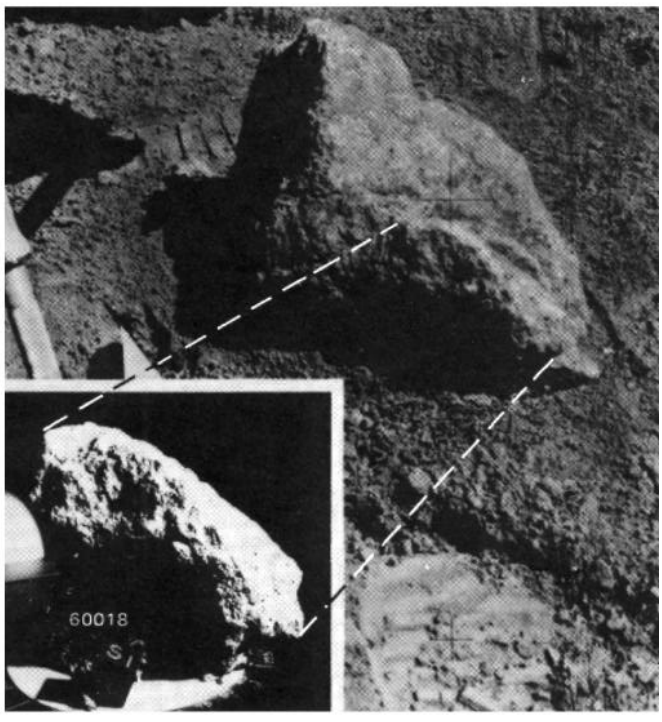

B

Figure 8.-Sample 60018. *A*, NASA photograph S-72-41499B. *B*, Approximate lunar orientation reconstructed in Lunar Receiving Laboratory compared with enlarged part of EVA photograph AS16-116-18689, taken cross-sun, looking north (inset photograph, S-72-41840). Reconstruction by R. L. Sutton.

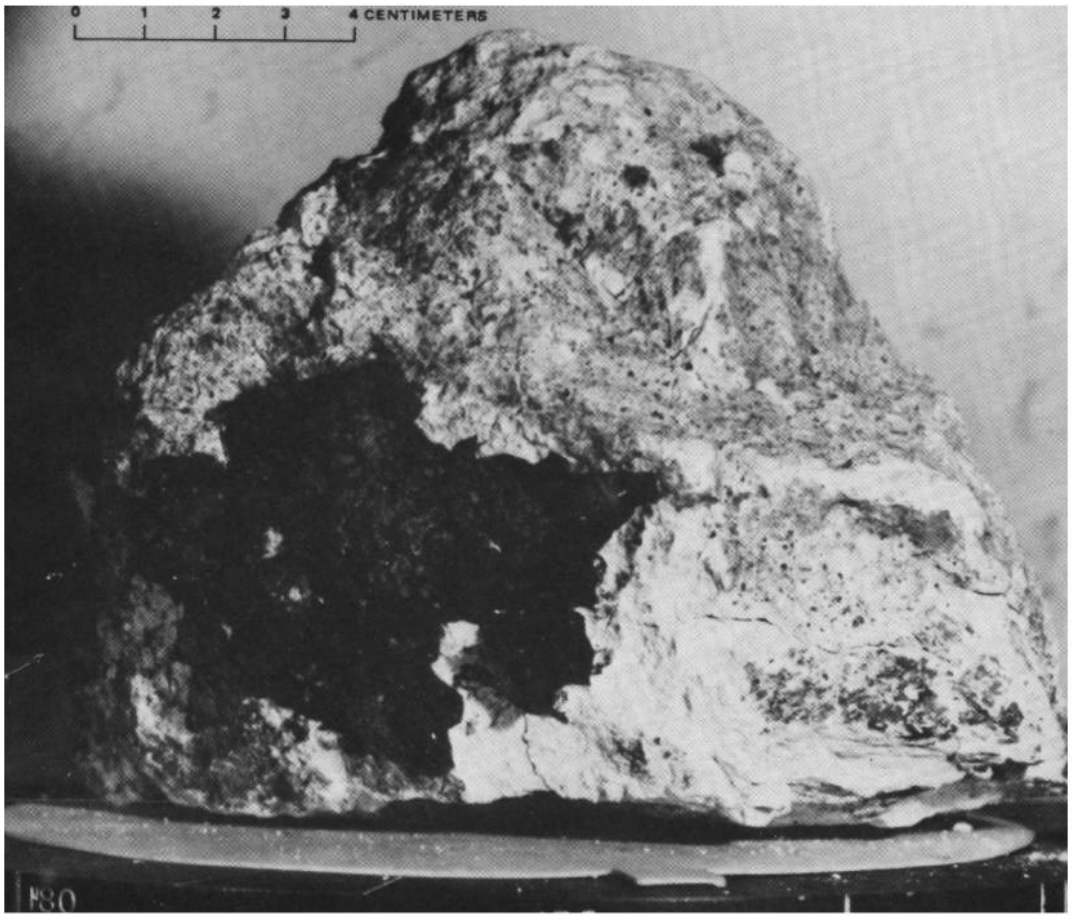

A

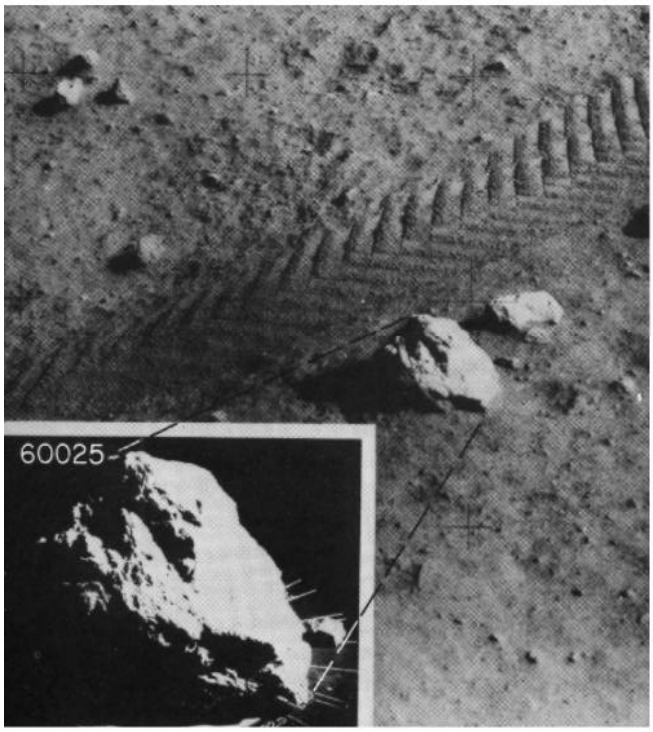

B

Figure 9.-Sample 60025. *A*, NASA photograph S-72-42593b. *B*, Approximate lunar orientation reconstructed in LRL, compared with enlarged part of EVA photograph AS16-110-17666, taken cross-sun, looking north (inset photograph, S-72-44019). Reconstruction by R. L. Sutton.

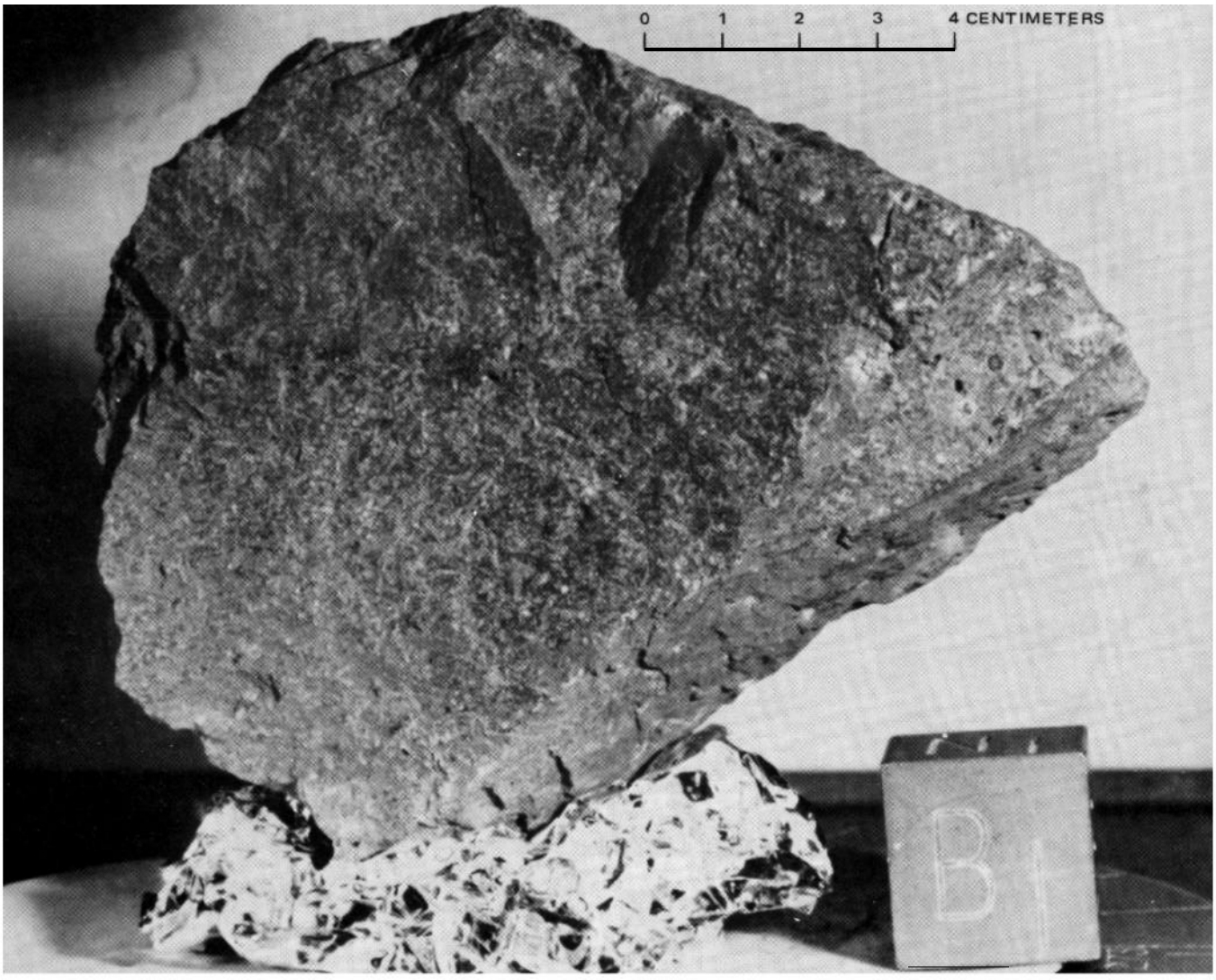

A

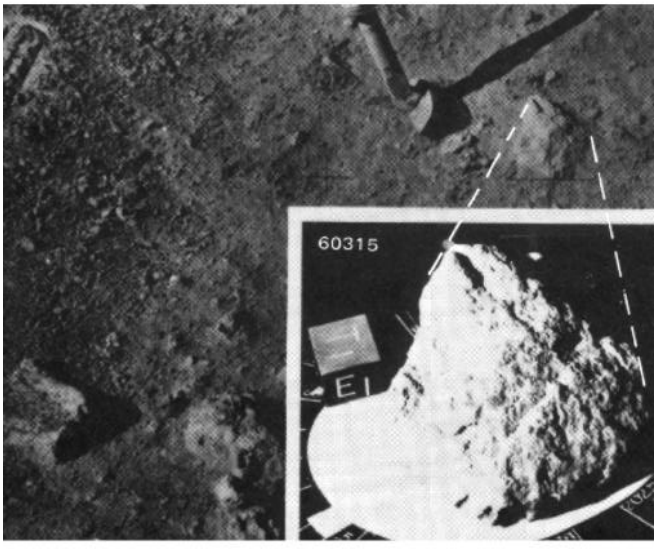

B

FIGURE 10.-Sample 60315. *A*, NASA photograph S-72-41572. *B*, Approximate lunar orientation reconstructed in the LRL compared with an enlarged part of EVA photograph AS16-117-18836, taken oblique to sun, looking southwest (inset photograph, S-72-41842). Reconstruction by R. L. Sutton

grained chalky and crystalline rocks, approximately 5 percent of the rocks observed by the crew, are smaller (6- to 12-cm range) than most breccia fragments.

Documentation photographs of the samples collected at the LM/ALSEP station show that most of the rocks were either perched or only slightly buried, indicating that many samples from this station may be South Ray material.

The soil in the LM/ALSEP area is in general medium gray, but patches of high-albedo soil are present near the ALSEP. White soils are more abundant to the west (toward stations 1 and 2), where they underlie a thin, darker surface layer. The soil in the LM/ALSEP area generally is firm except in the intercrater area of the ALSEP, where it was found to be exceptionally loose and powdery. Soil of the intercrater regions associated with very subdued 200- to 300-m diameter craters typically is less compact than the walls and rim crests of such craters (Schaber and Swann, 1971).

Special samples collected at LM/ALSEP include a deep drill core at the ALSEP, double-core tubes at 10 and lO', rake samples at 10, and the Lunar Portable Magnetometer (LPM) sample at the LRV final park position (fig. 1). The deep-core, rake, and double core-tube samples may contain North Ray crater ejecta but should contain material representative of the Cayley plains beneath the LM/ALSEP station. The deep drill core (223 cm) may have penetrated the ejecta from the "LM" crater and the subdued crater, 270-m diameter, immediately west of the station (see fig. 6). Two Lunar Portable Magnetometer readings were taken in the LM/ALSEP vicinity, the first the ALSEP site, the second at the LRV final park position (approximately 80 m east of the LM). The ALSEP site remanent field strength was very high, 231 gammas, the LRV park reading considerably lower, 121 gammas. This difference represents a field magnitude gradient of 370 gamma/km, the maximum recorded during the mission. The minimum gradient measured was 1.2 gammas/km between station 5 and the LRV final park position (Dyal and others, 1972, p. 12-5).

Near the LRV final park location (fig. l), two LPM measurements were made to calculate the magnetic field of a surface rock sample (60335) in order to determine the total magnetization. The magnetic field was found to be below the resolution of the LPM (Dyal and others, 1972, p. 12-6).

The passive seismometer (PSE) deployed at the ALSEP station was the most sensitive of the four lunar seismograph stations in operation at that time. On the basis of the initial 45-day record of operation, seismic events occurred at a rate of 10,000 per year; the rate at the Apollo 14 site was 2,000 per year, and at the 12 and 15 sites, 700 per year (Latham and others, 1972, p. 9- 1). The higher sensitivity of the Apollo 16 seismometer has been attributed by Latham and others to the depth and elastic properties of the regolith, the inference being that the Apollo 16 regolith is deeper or weaker, or both.

The results of both the active and passive seismic experiments at Apollo 16 indicate that the regolith is not underlain by competent lava flows. Rather, the seismic velocities recorded suggest that a brecciated or .mpact-derived debris unit of undetermined depth underlies a 12.2-m-deep regolith. Petrographic analysis of the returned samples (almost entirely breccias) supports this hypothesis.

STATION 1

Station 1 was located near the rim of Plum crater approximately 1,400 m west of the LM and 45 m lower. Plum crater, 30 m across and 5 m deep, is on the rim of Flag crater, 290 m in diameter (pl. 5, pans 4 and 5; fig. 11) and 40 m deep. When formed, Flag crater probably penetrated 60 m into the underlying Cayley plains material, but it has been partly filled by talus. The crater is subdued, having only a slightly raised rim, and no rocky exposures are visible in its walls or floor. Small subdued craters as large as 10 m in diameter are common in the area.

The east part of station 1 appears to be crossed by a very faint ray from South Ray crater, but rock fragments >2 cm are less abundant (0.6 to 1.8 percent) than at station 2 or at the LM/ALSEP area (figs. 2, 4, 12).

Rocks larger than 10 cm cover only 0.2 percent of the surface at this station, whereas at station LM/ALSEP rocks of similar size cover 0.3 to 0.9 percent (fig. 4). The crew mentioned that South Ray crater ray material was visible about 50 m east of the station 1 area.

Samples (>2 g) collected at station 1, in table 2, are predominantly breccias of types B_2 B_3, and B_4. The complete absence of B1 breccias, at least in the samples collected, may be significant with respect to the low

TABLE 2.-*Number and percentages of rocks (>2 g) documented at station 1*

Category	Number of rocks collected	Percentage
Igneous:		
C_1	1	3.3
Uetaclastic:		
C_2	2	6.7
Breccia:		
B_1	0	0
B_2	3 (1 in rake)	10.0
B_3	10 (7 in rake)	33.3
B_4	4 (3 in rake)	13.3
Glass:		
G	10 (7 in rake)	33.3
Total	30	99.9

proportion of South Ray material in this station area relative to station LM/ALSEP, where 25 percent of the samples are breccias.

Four large samples, 61016 (B_4; 11,745 g), 61135 (B_3; 245 g), 61195 (G; 586 g), 61295 (B_3; 172 g), were collected from the rim crest of Plum crater (pl. 5, pan 5), and are probably ejecta from that crater (figs. 13-15). Large samples 61015 (B_2; 1,803 g) and 61175 (B_3; 543 g) were collected away from the Plum rim crest and in an arc concentric to and about 30 m from the rim crest of Flag crater (pl. 5, pans 5 and 6; figs. 16, 17). These samples may represent original ejecta from Flag crater, or possibly Flag rim materials reejected by Plum crater, which undoubtedly penetrated the upturned bedrock beneath Flag crater. A distinct, but smooth and somewhat subdued bench occurs in Plum approximately 3 m below the surface. No outcrop is visible, but the benched topography suggests a change in cohesion of the materials in the walls of the crater. This change may reflect the contact beween Flag ejecta and raised bedrock in the eroded rim of Flag crater and may be the source area of the large, filleted, partly buried boulder from which sample 61295 (B_3) was collected (fig. 15*B*; pl. 5, pan 5).

The largest of the Plum crater samples are B_3 and B_4 type breccias, whereas samples related to Flag crater are in the B_2 and B_3 categories. The B_2 breccias at this station may represent the deepest excavation level (60 m) of Flag crater, a stratigraphic horizon not tapped by the smaller Plum crater (5 m). Sampling of all rock types present at this station may not have been statistically sufficient because of time constraints.

At two places on the rim of Plum crater, the astronauts noted white regolith beneath a top layer of gray soil 1 to 2 cm thick. At one of these places, the light material lay beneath the gray on the fillet of a large boulder (fig. 18). This suggests that the fillet was formed by one of two mechanisms: (1) shedding of light material from the rock followed by postfillet deposition of a thin dark layer or (2) deposition of light material followed by darkening of the surface. White soil was observed at the trench site on the northeast rim west of Plum crater, where the top centimeter of gray soil was underlain by several tens of centimeters of white soil.

Other samples collected at station 1 included those from the trench (61240, 61245 to 61249, 61255 and 61220), a fillet soil (61280 at 61295-boulder), and two surface soil samples (61160 and 61180).

The crew observed that the large rocks were clearly more abundant on the rim crests of both Flag and Plum craters than in the intercrater areas, indicating that

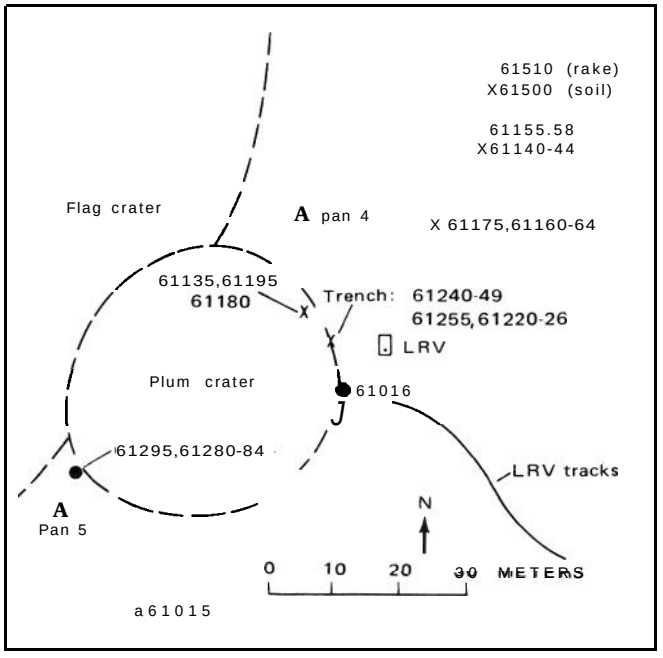

FIGURE 11.-Planimetric map of station 1.

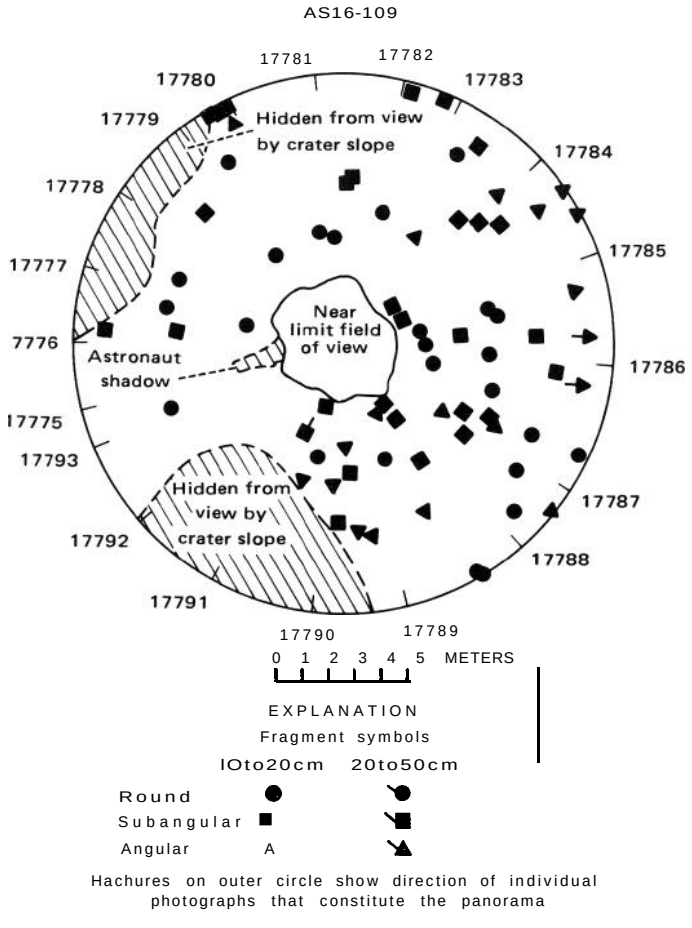

FIGURE 12.-Rock distribution within 10 m of site of panorama 4 station 1.

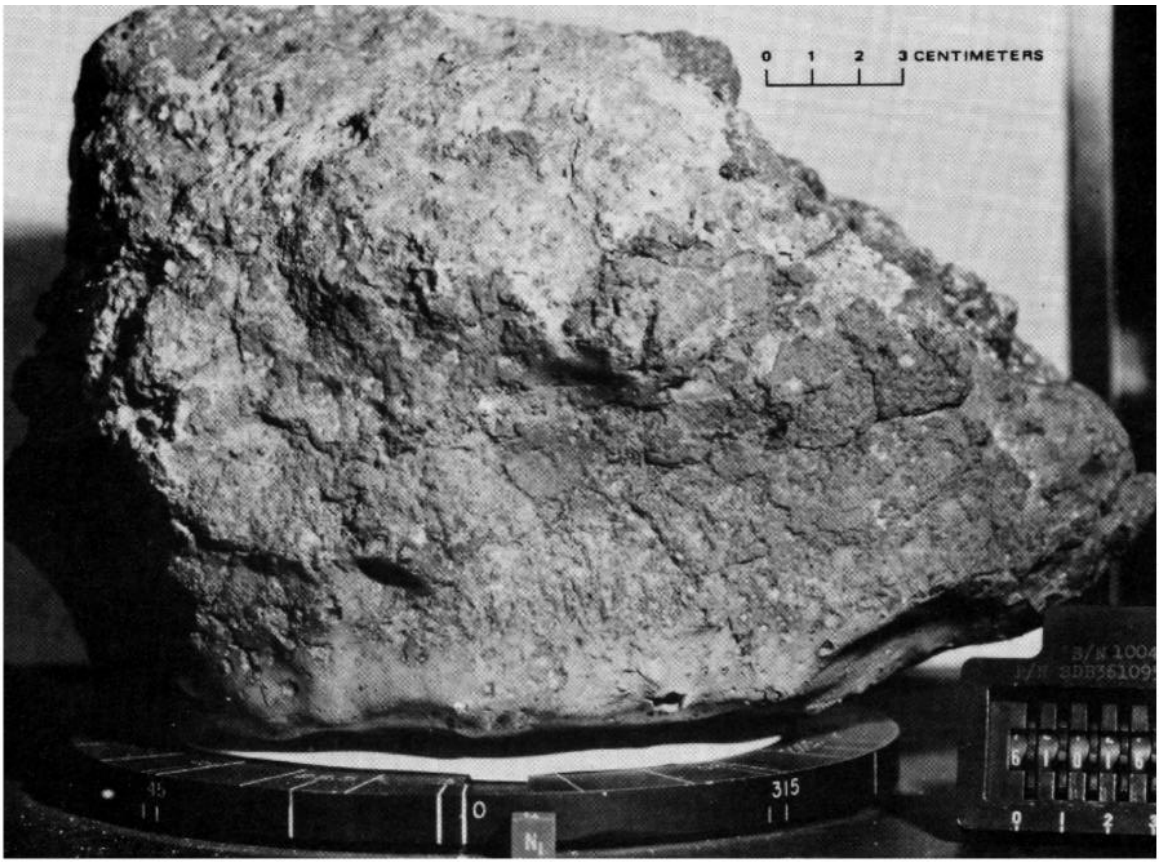

FIGURE 13.-Sample 61016. NASA photograph S-72-41545. (See Sutton, fig. 24*B*, this volume, for lunar orientation).

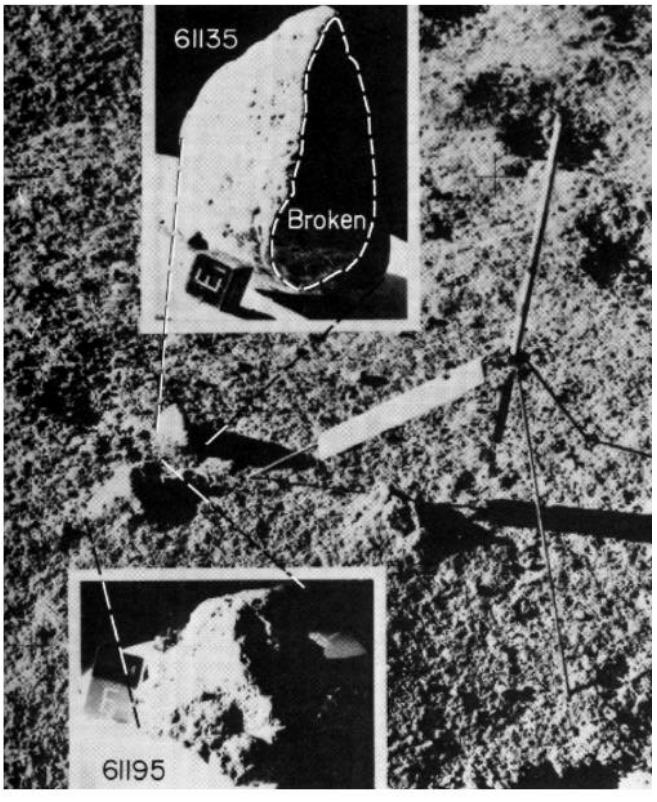

Figure 14.-Samples 61135 and 61195 showing approximate lunar orientations reconstructed in the LRL compared with an enlarged part of EVA photograph AS16-114-18405, taken cross-sun, looking south (inset photographs, S-72-41609 and 43315, respectively). Reconstruction by R. L. Sutton.

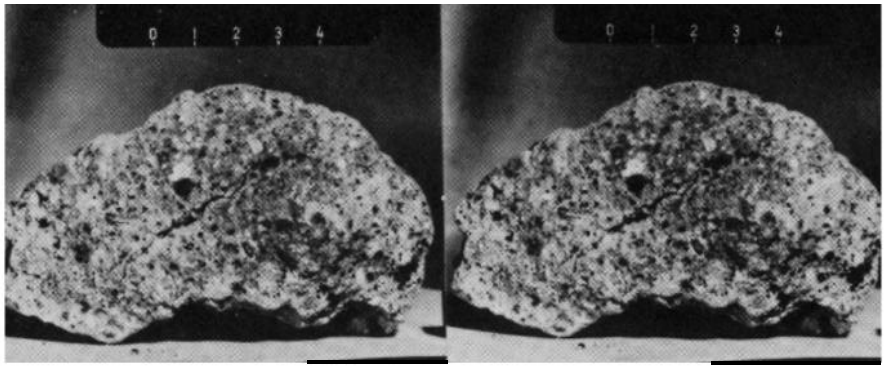

A

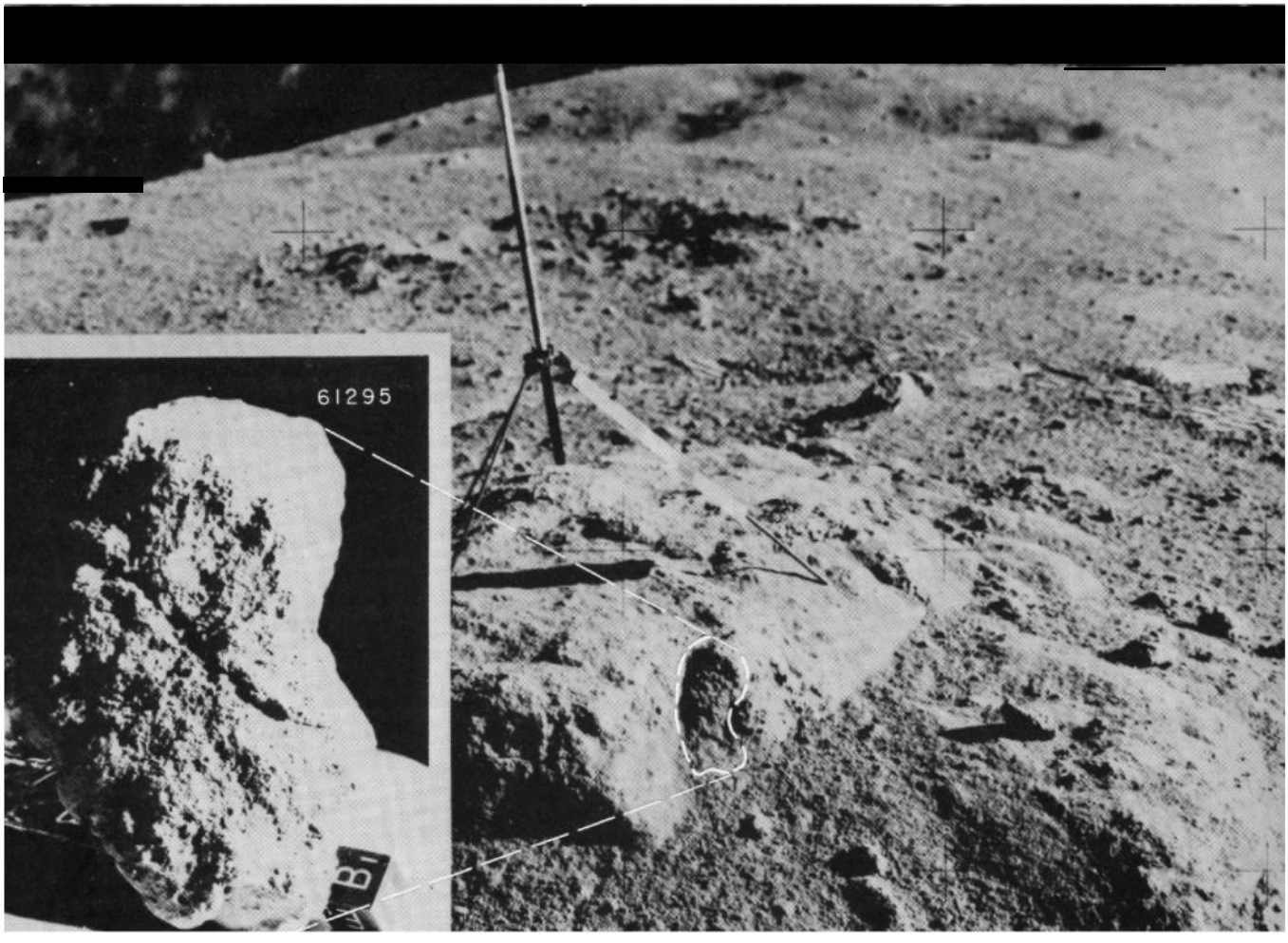

B

FIGURE 15.-Sample 61295. *A*, Stereopair composed of NASA photographs S-72-40946B and 40946. *B*, Approximate lunar orientation reconstructed in the LRL compared with an enlarged part of EVA photograph AS16-114-18412, taken cross-sun, looking north (inset photograph, S-72-40967). Reconstruction by R. L. Sutton.

these craters are the most recent source of the deposits. Two very large craters 180 m south of station 1 (450-m diameter and 630-m diameter, "Eden valley") may have contributed ejecta to the area from depths of 90 to 130 m before the impact at Flag crater (fig. 6). The significance of these materials in the collected samples has not been ascertained.

The surface rocks at station 1 are considerably less abundant, more eroded, less angular, and distinctly more buried than at station LM/ALSEP , demonstrating (pls. 3, 4, and 5) the scarcity of fresh South Ray ejecta at station 1.

STATION 2

Station 2, located approximately 850 m west of the LM, is just north of Spook crater (370 m diameter) and on the blocky south rim of Buster crater (90 m diameter) (pl. 5, pan 6; fig. 19). The area is crossed by a faint ray of high-albedo material thought to be derived from South Ray crater, 5.7 km to the southwest (fig. 2). Subdued, grooved lineaments radial to South Ray crater cross the area.

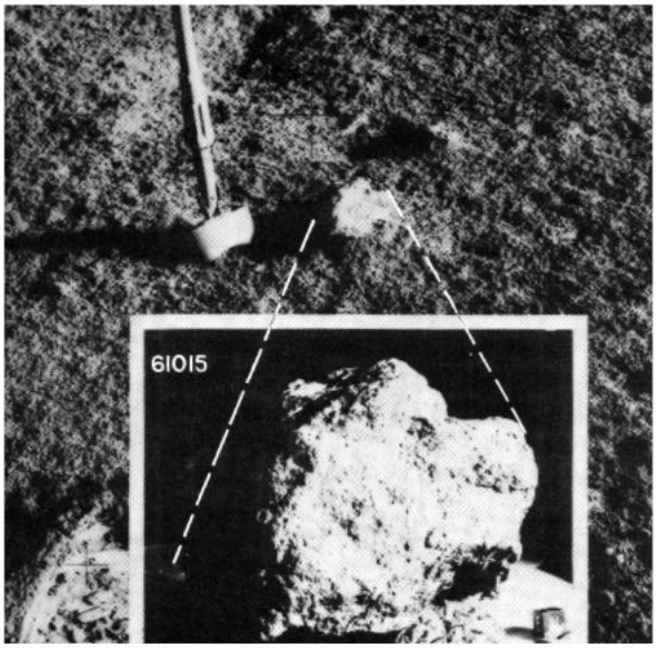

FIGURE 16.-Sample 61015 showing approximate lunar orientation reconstructed in the LRL compared with an enlarged part of EVA photograph AS16-109-17808, taken cross sun. looking north (inset photograph, S-72-4105). Reconstruction by R. L. Sutton.

Fragments as large as 0.5 m, but mostly 5 to 10 cm, are scattered over the station area; they cover 1.6 to 2.6 percent of the surface, averaging 2.0 percent (figs. 4, 20). Rocks larger than 5 cm cover 0.4 to 1.5 percent of the surface, averaging less than 0.8 percent. Most fragments are angular to subangular and are perched or only slightly buried. Fillets are rare.

Station 2 lies within the continuous ejecta blanket of both Spook and Buster craters. Samples collected should include some material from both craters, although Buster is more clearly associated with surface rock fragments. Spook crater is symmetrical with a subdued but slightly raised rim; no rock exposures are discernible on the walls. Buster crater is about 100 m north of Spook crater and is superimposed on its outer rim. The rim of Buster is fairly sharp, the inner walls fairly steep. Ninety percent of the floor and a large part of the walls and rim of Buster crater are covered by blocky debris that trends northeast across the crater floor (pl. 5, pan 6). The rocks in the crater floor, as large as 5 m, are angular. The crew discerned northeast-trending planar structures dipping northward within the blocks and a parallel organization of the blocks.

Buster crater penetrates about 18 m into the south end of a subtle ridge, 15-18 m high (maximum) and 700 m long, that trends northwest from the station area ("B" in fig. 6). The conspicuous blocks on the floor of Buster crater may have been derived from this ridge. Halfway crater, 155 m west of Buster and off the ridge, is slightly more subdued and has very few associated blocks. The nature and distribution of the blocks in the floor and walls of Buster (pl. 5, pan 7) suggest that it penetrated a more coherent substrate than most craters of similar size and age in this region. A bench recognized in the blocky part of the wall of Buster crater may represent the change in coherence between the regolith and the inferred bedrock.

Spook crater penetrated 75 m into the Cayley plains; its location on the northeast edge of the "Eden valley" crater complex (penetration to 120 m) suggests that some of the material ejected may be from the earlier "Eden valley" impact (fig. 6).

A total of eight rocks larger than 2 g were collected from the station 2 vicinity; they represent both crystalline and breccia types, as shown in table 3.

The percentage of the B_1 breccias collected from stations LM/ALSEP (25 percent), station 1 (0 percent), and station 2 (37 percent) appears to show a relation to the presence of continuous-ejecta deposits from South

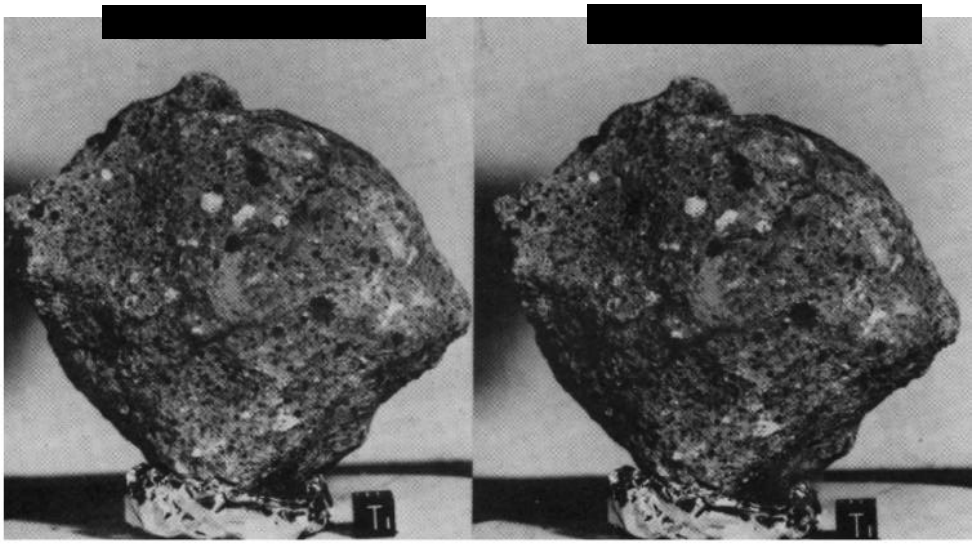

A

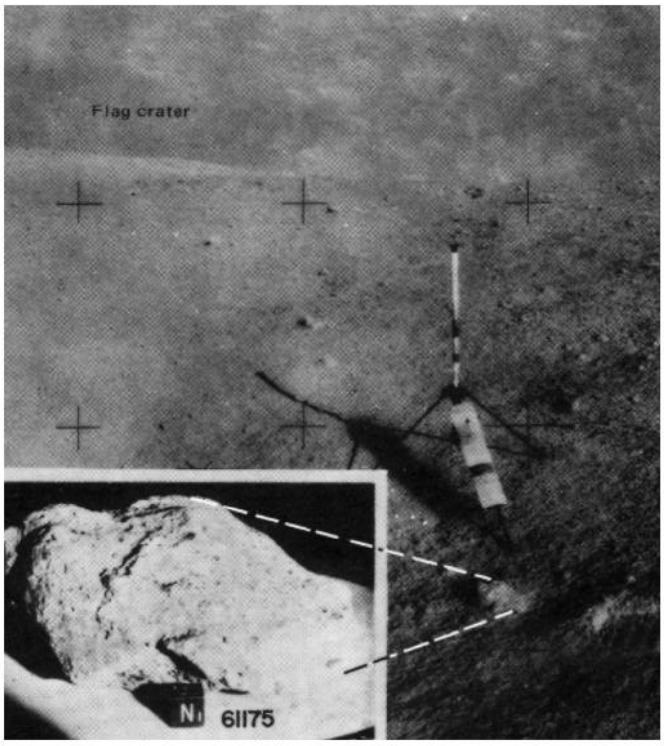

B

FIGURE 17.-Sample 61175. *A.* Stereopair, NASA photographs S-72-411 97 and 41197B. *B,* Approximate lunar orientation reconstructed in the LRL compared with EVA photograph AS16-109-17798, taken down sun, looking west (inset photograph, S-72-40966). Reconstruction by R. L. Sutton.

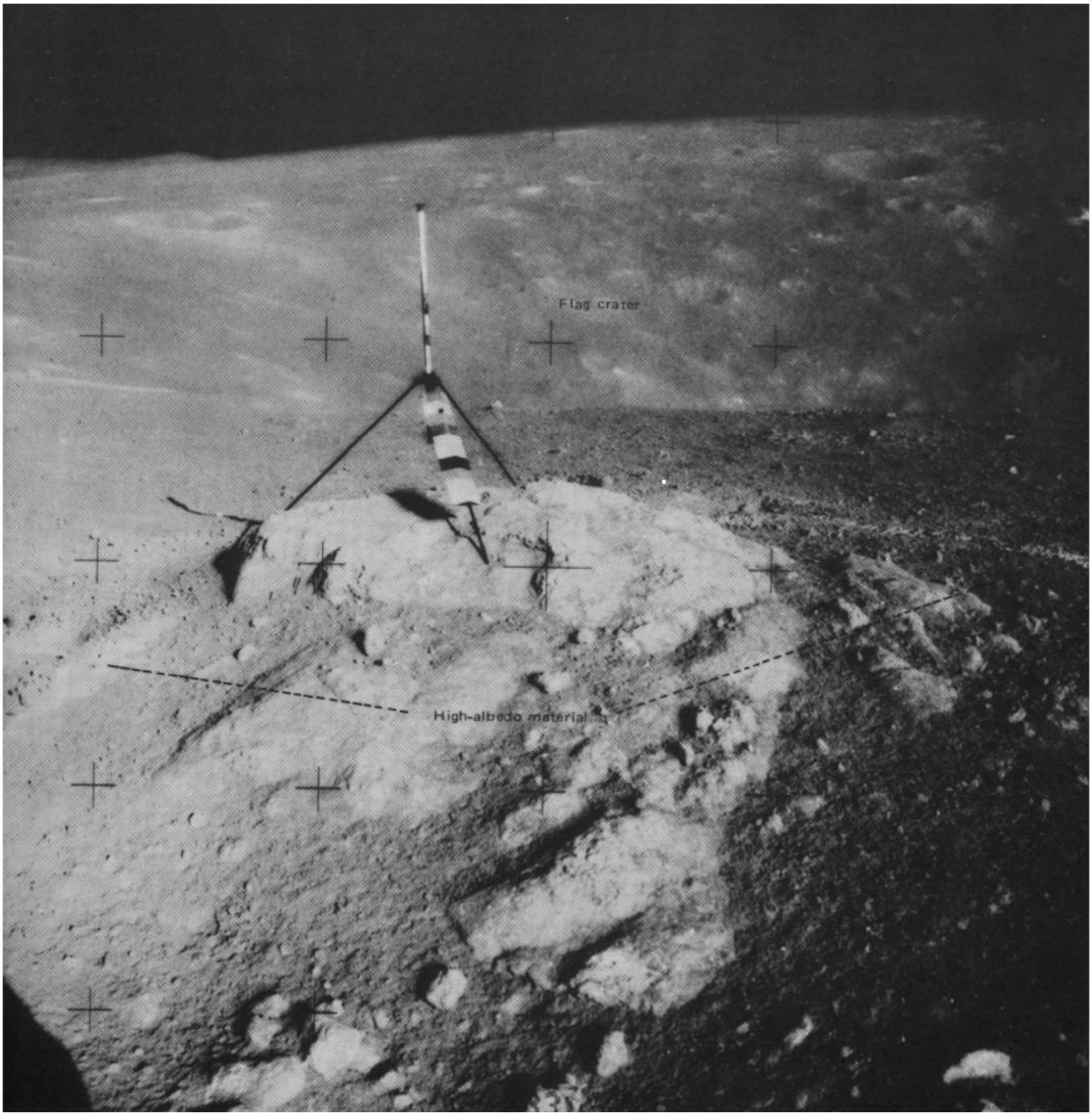

FIGURE 18-Large filleted boulder showing high-albedo material kicked by astronauts (AS16-109 17802).

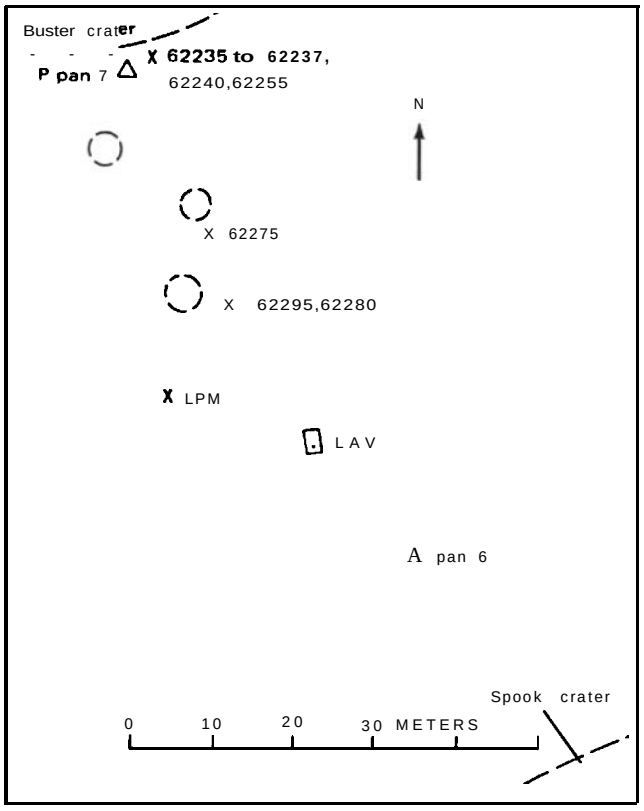

FIGURE 19.-Planimetric map of station 2. For explanation of Symbols see Figure 1.

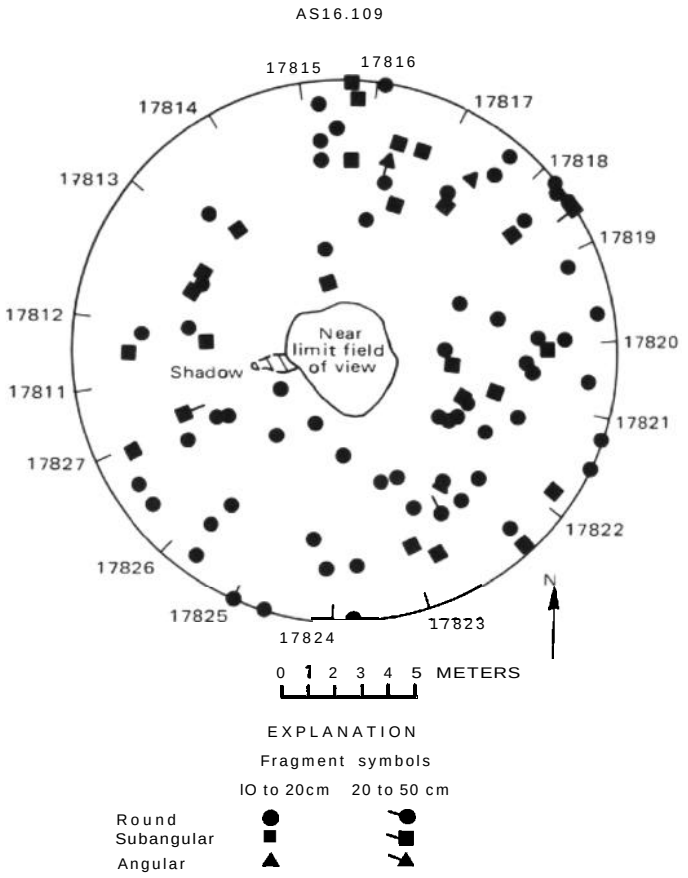

FIGURE 20.-Rock distribution within 10 m of site of station 2 panorama.

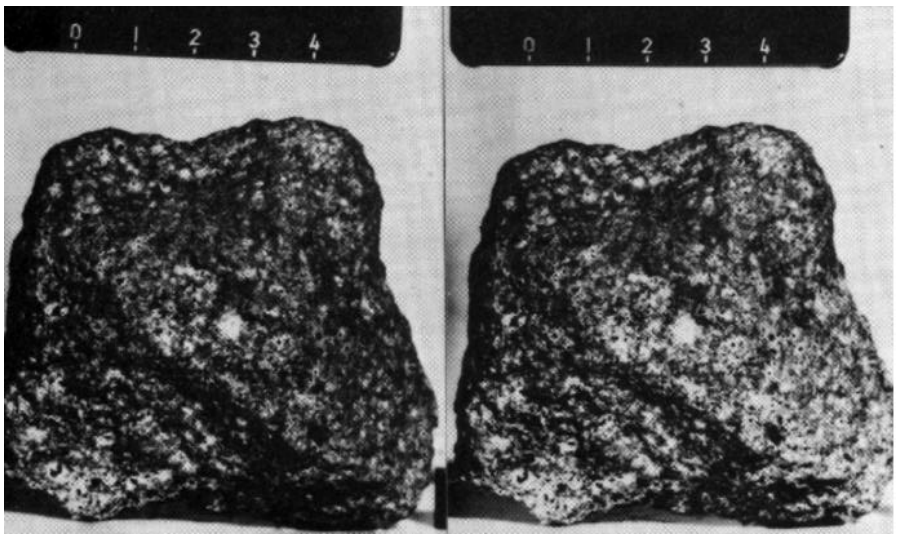

A

FIGURE 21.-Sample 62235. *A*, Stereopair (NASA photographs S-72-41280 and 41280B). *B*, Samples 62235, 62236, and 62237 showing approximate lunar orientation reconstructed in the LRL compared with an enlarged part of EVA photograph AS16-109-17838, taken cross-sun, looking south (inset photographs. S-72-41424, 41837, and 41838, respectively. Reconstruction by R. L. Sutton.

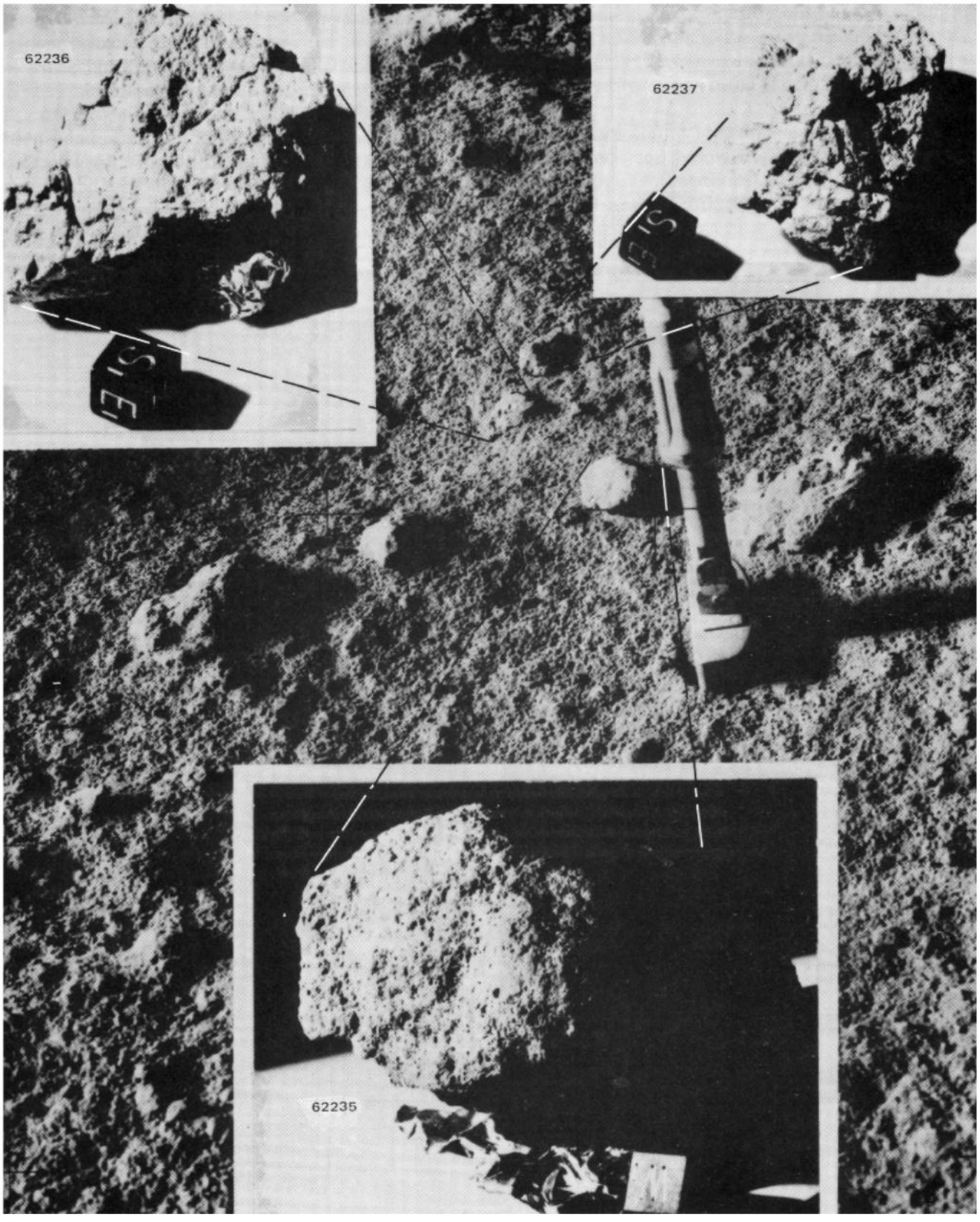

B

FIGURE 21.-Continued.

TABLE 3.-*Number and percentages of rocks (>2g) documented at station 2*

Category	Number of rocks collected	Percentage
Igneous:		
C_1	1	12.5
Metaclastic:		
C_2	1	12.5
Breccia:		
B_1	3	37.5
B_2	2	25.0
B_3	1	12.5
B_4	0	0
Total	8	100.0

Ray crater. South Ray ejecta crosses stations LM/ALSEP and 2 but is extremely sparse at station 1. This relation does not appear to hold, however, when the sample types collected at stations 6 and 8 are examined. Although these stations are much closer to South Ray crater, no B_1 breccias were collected from either site. If indeed the B_1 rocks at the stations LM/ALSEP, 1, and 2 sites are related to South Ray ejecta, they would have to represent a very shallow horizon within that crater, deposited primarily downrange. The association is tenuous at best. Breccia type B_4 was not sam-

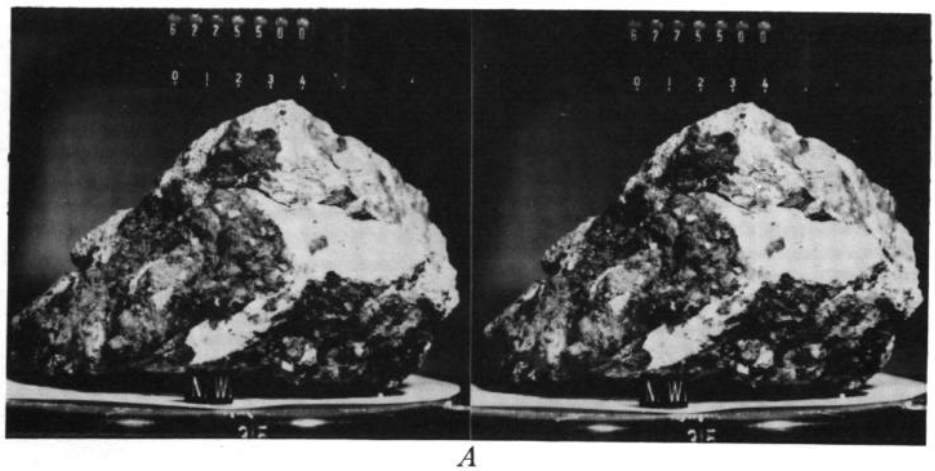

A

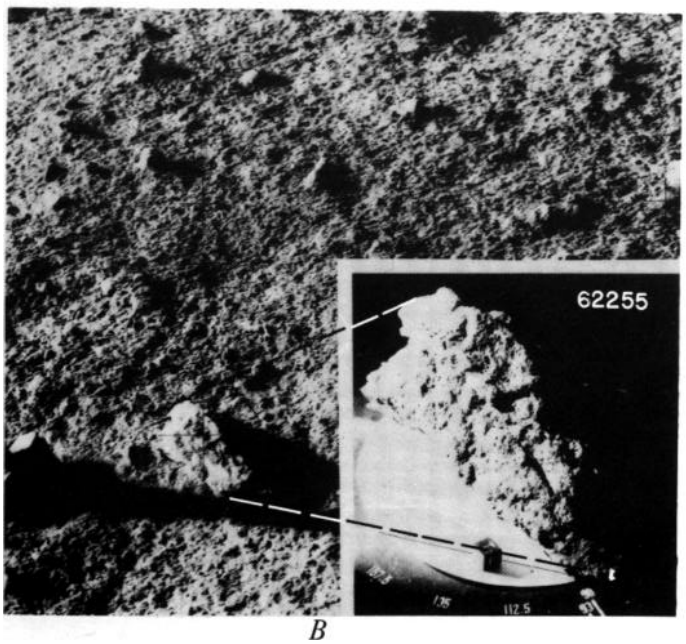

B

FIGURE 22.-Sample 62255. ***A,*** Stereopair (NASA photographs S-72-41823B and 41823). ***B,*** Approximate lunar orientation reconstructed in the LRL compared with an enlarged part of the EVA photograph AS16-**109-**17844, taken cross-sun, looking south (inset photograph, S-72-41834). Reconstruction by R. L. Sutton.

pled at station 2 but made up 14 percent of the rocks collected at LM/ALSEP and 13 percent of those re turned from station 1.

The planimetric map of station 2 (fig. 19) clearly shows that most sampling was done closer to Buster crater rim than to Spook crater. The samples collected nearest Spook were 6229 (C_1) and 62280 (soil) at a distance of about 70 m. Photographs and orientation diagrams for the station 2 large rocks are shown as figures 21 to 24.

Astronaut Duke commented regarding Buster crater, "The blocks are angular, but they are definitely coming out of Buster." The most recent source of collected samples therefore may have been Buster crater, which probably reexcavated much Spook crater material.

The surface soil at station 2 is medium gray with a higher albedo soil below the upper centimeter or so, similar to light soil at the ALSEP and at station 1. The compaction and granularity of the soils are typical of

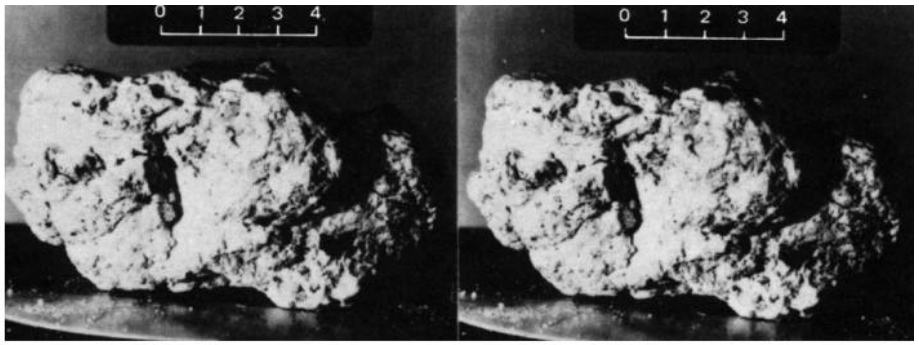

B

FIGURE 23.-Sample 62275. ***A,*** Stereopair (NASA photographs S-72-40922B and 40922) ***.B,*** Approximate lunar orientation reconstructed in the LRL compared with an enlarged part of EVA photograp h ASl6-109- 17846, taken cross-sun, looking south. The sample is fragile and minor breakage has occurred; shadow details were impossibl e duplicate accurately in the laboratory (inset photograph, S-72-41426). Reconstruction by R. L. Sutton.

the area. Small craters as much as 2 m in diameter are distributed fairly uniformly; they are generally subdued but a few small fresh craters, possibly South Ray secondaries, have sharp rims on which cloddy ejecta is discernible.

SUMMARY

The samples collected from stations LM/ALSEP, 1, and 2 most probably represent materials of the Cayley plains to depths of 70 m or more and materials from the upper layers within South Ray crater. The proportions of rock types collected from each station were constrained by time available and may not be clearly indicative of the rocks present at depth.

The variety of rock types collected at stations LM/ALSEP, 1, and 2 indicates that the Cayley plains breccias are heterogeneous and suggests that they are composed of pockets of both light and dark breccias deposited by a turbulent process characteristic of large-basin ejecta emplacement.

The great amount of South Ray ejecta. within the central plains of the landing site, suggested by the distribution of high-albedo materials radial to that crater (fig. 2), appears to be a heterogeneous collection of light and dark breccias including all types collected throughout the region traversed during the mission.

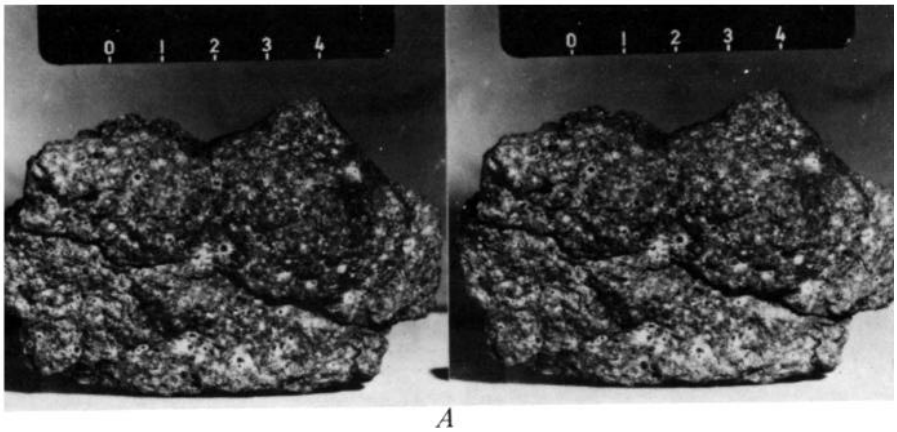

A

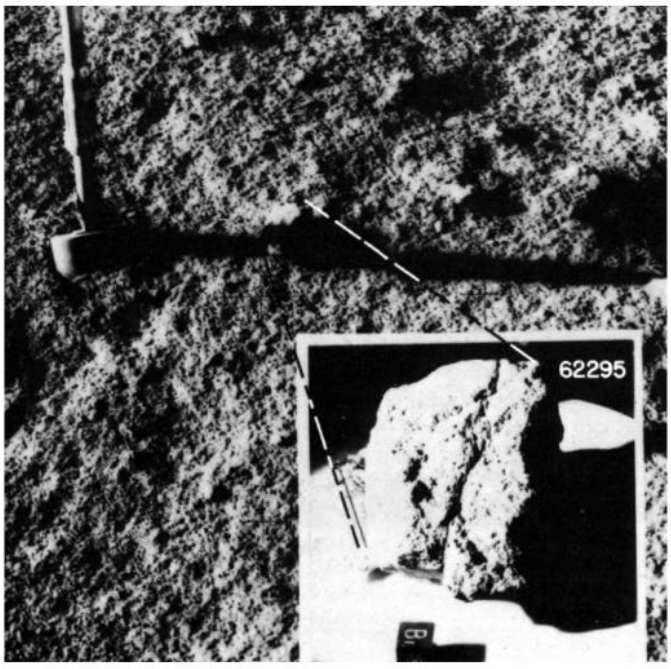

B

FIGURE 24.-Sample 62295. A, Stereopair (NASA photographs S-72-44492 and 44492B). B, Approximate lunar orientation reconstructed in the LRL compared with an enlarged part of EVA photograph AS16-109-17848, taken cross-sun, looking south (inset photograph, S-72-42563). Reconstruction by R. L. Sutton.

D2. GEOLOGY OF NORTH RAY CRATER

By GEORGE E. ULRICH

CONTENTS

ILLUSTRATIONS

TABLES

INTRODUCTION

North Ray crater was the primary sampling target of the last of three traverses made during the Apollo 16 mission. Its apparent youth minimizes the chance of contamination by ejecta from younger craters; its deep exposures, 230 m into the subsurface, reveal stratigraphic differences to approximately that depth. Orbital and surface photographs illustrating the vertical sequence of units exposed in the wall of North Ray crater, together with the rocks and soils collected on its rim and ejecta blanket and the crew's first-hand observations, provide the controlling data for interpreting a stratigraphic model in this area of the landing site. This model is extended to the larger region explored by Apollo 16 in Ulrich and Reed (this volume).

PHYSIOGRAPHIC SETTING

North Ray crater lies at the foot of Smoky mountain and is one of the highest sampling sites in the landing area. Its setting is well illustrated from a surface perspective on plate 11 (pan 34). Station 4, on Stone mountain, is at approximately the same elevation; the rim of South Ray crater, 10 km to the south, is about 170 m lower (fig. 1). About 1 km across, North Ray crater straddles a ridge approximately 50 m high and a little narrower than the crater rim. The crest of this ridge, informally named North Ray ridge, is nearly parallel to the base of Smoky mountain. Its similarity in morphology to Smoky mountain and to the Descartes highlands in general was not recognized until after the mission when orbital photography with low-sun-angle illumination became available (fig. 2). The top of the ridge is 400 m below the top of Smoky mountain, which suggests that the ridge may be a downfaulted segment of the mountain and therefore that North Ray crater may expose material from part of the Descartes mountains in its walls.

That part of the crater interior visible from the rim is shown by the postmission topographic map (fig. 3). The crest is rounded but falls off rapidly to the steep crater wall, whose upper slopes are generally convex, ranging from 27" at the top to 34" in the lower half. Precipitous drops in the foreground slopes below the rim crest made photographing the lowest parts of the crater wall impossible. Only the upper 60 percent of the crater wall is observable from the vantage point at station 11 (figs. 3, 4). The rounded form of the crater rim, the smooth walls with few blocky areas, and the predominance of breccias in the observable rocks on the surface are evidence that the target materials impacted by North Ray crater were breccias of relatively low strength.

BLOCK DISTRIBUTION AND ROCK TYPES

The concentration of blocks on the rim of North Ray crater was considerably lower than anticipated. The low frequency of fragments was observed on the approach to the crater rim. Fragments range from 25 m to less than 1 m in maximum diameter. Most of the large boulders observable on postmission orbital photographs, mapped here on figure 5, had been identified on premission photographs. Within 10 m of the site of panorama 18 (pl. 8), fragments 10 cm and larger cover 4.3 percent of the surface (figs. 4, 6A); at station 13, 0.75 km away, they cover only 0.5 percent with about one-fourth as many fragments (fig. 6B and panorama 23, pl. 7). Nearly 70 percent of the fragments counted at these stations are rounded (fig. 6; table 1). At station 11, more than 20 percent are larger than 20 cm in diameter, at station 13, only 10 percent.

All the blocks with discernible textures are clastic in appearance. Their matrices range from dark to light gray, as seen in the black-and-white photographs. The

TABLE 1.—*Distribution of blocks at North Ray crater by size and shape*

[Number of blocks counted and percentage of total within 10 m of center of station panoramas. Data from figure 6]

Shape	10–20 cm	20–50 cm	>50 cm	Total	Shape percent
Station 11—rim crest					
Rounded	145	35	0	180	69.0
Subangular	44	11	0	55	21.0
Angular	13	3	10	26	10.0
Total	202	49	10	261	
Size percent	77.4	18.8	3.8		100.0
Station 13—outer ejecta blanket					
Rounded	41	6	0	47	68.1
Subangular	13	1	0	14	20.3
Angular	8	0	0	8	11.6
Total	62	7	0	69	
Size percent	89.9	10.1	0		100.0

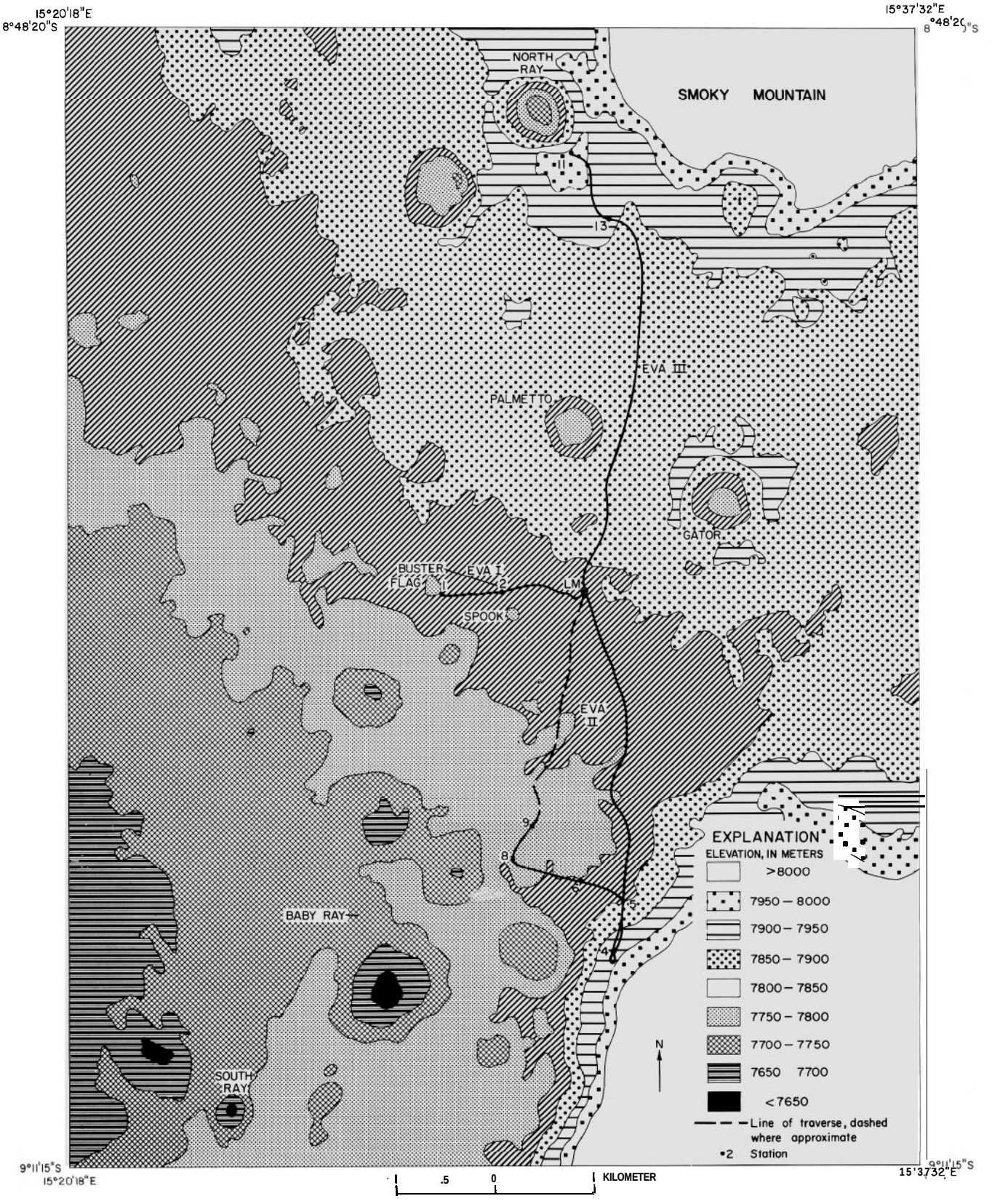

FIGURE 1.-Hypsographic map of the Apollo 16 site showing topographic zones in 50-m increments. Modified from MuehIberger and others (1972) and AFGIT (1973). Copyright 1973 by the American Association for the Advancement of Science.

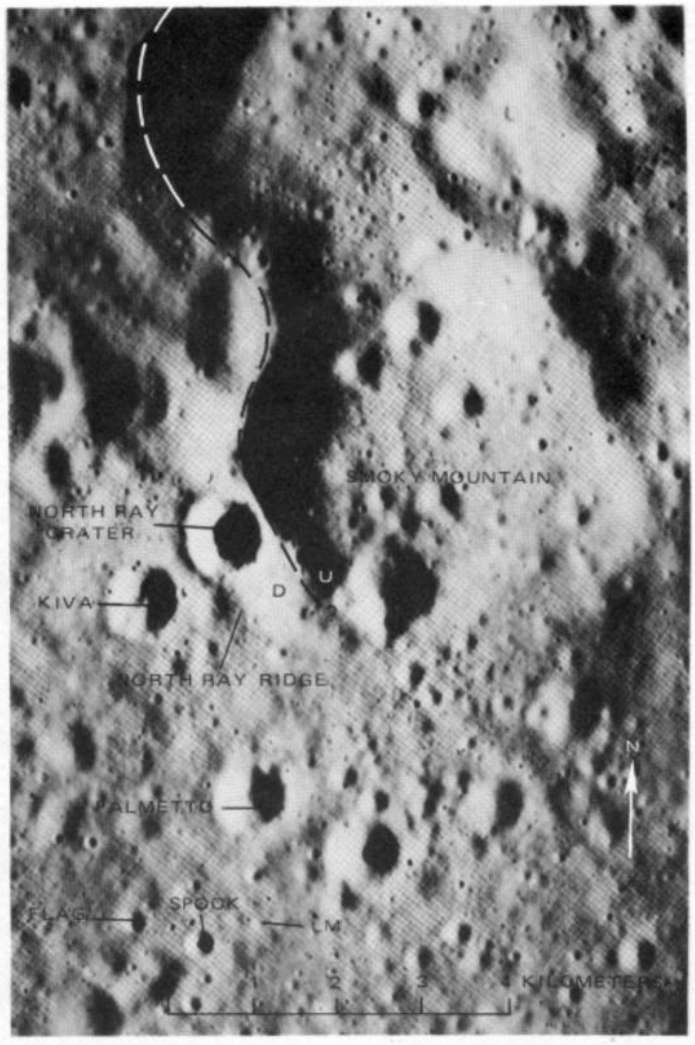

FIGURE 8.--Northern part of Apollo 16 landing site, showing principal named features. Dashed line, possible fault; U. upthrown side; D, downthrown side. Apollo 16 panoramic camera frame 4558, sun elevation 16". From Ulrich (1973) Reprinted with permission of Pergamon

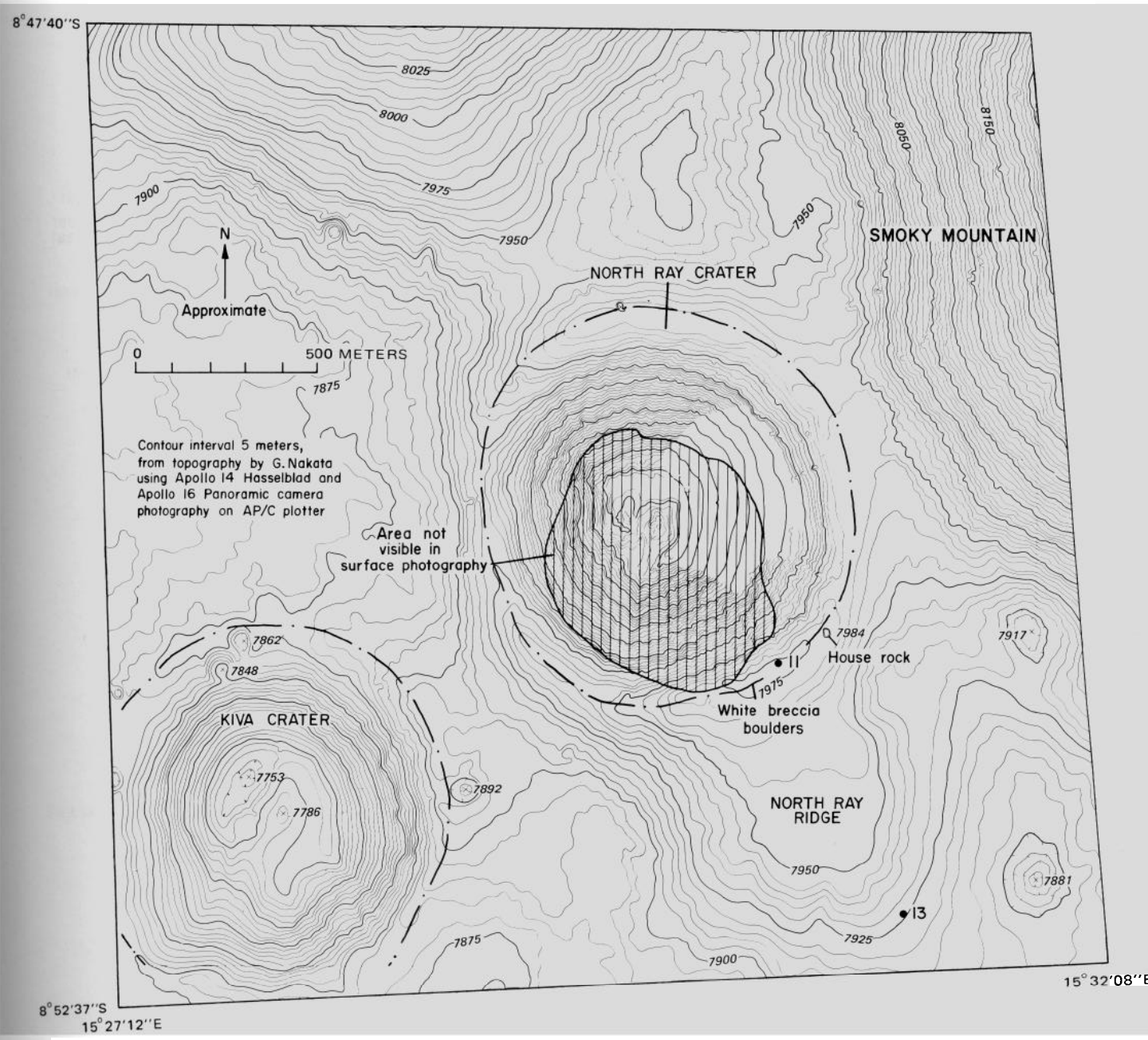

FIGURE 3.-Topographic map of North Ray crater showing station localities and area visible from rim. Contour interval 5 m. Topography by G. M. Nakata from Apollo 16 panoramic camera frames 4618 and 4623. From Ulrich (1973). Reprinted with permission of Pergamon Press.

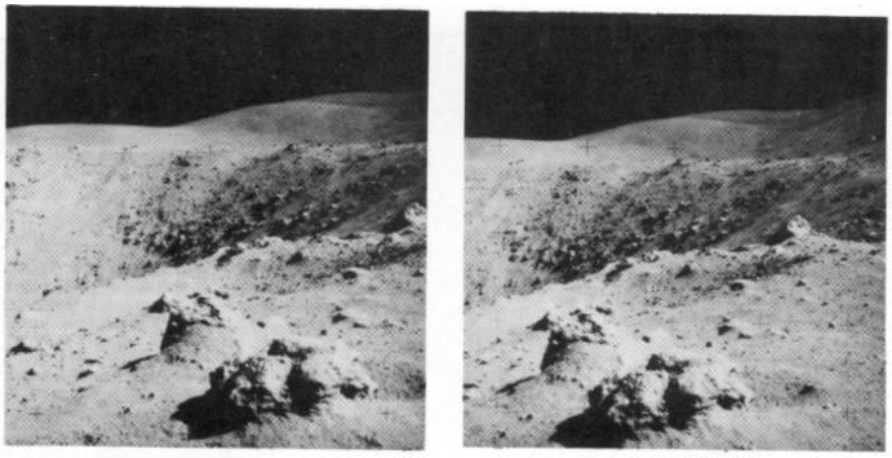

Figure 4.-Stereopair showing northeast wall of North Ray crater from east panorama station. Foreground shows typical slopes inside rim crest. AS16-106-17301, 17302.

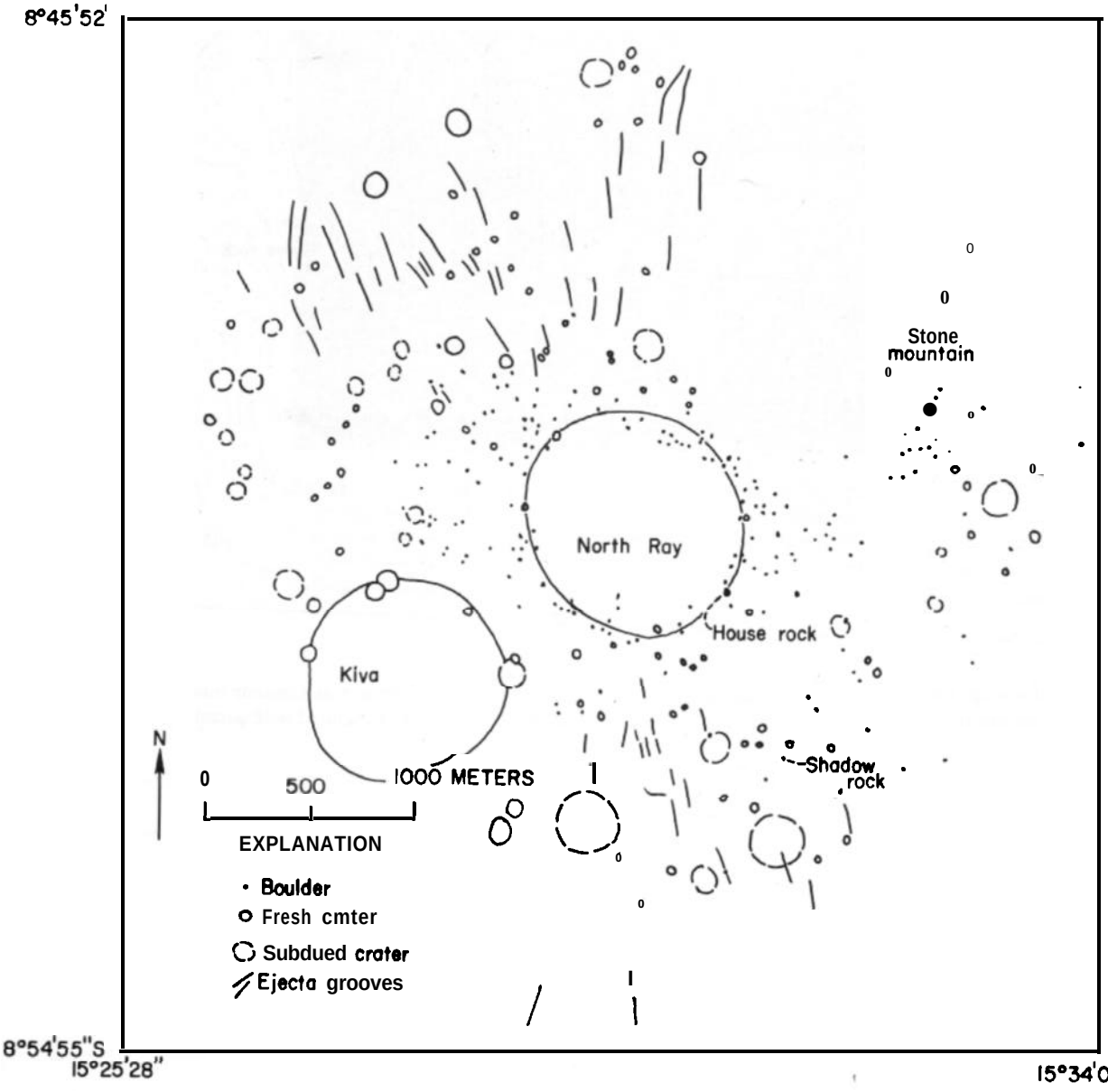

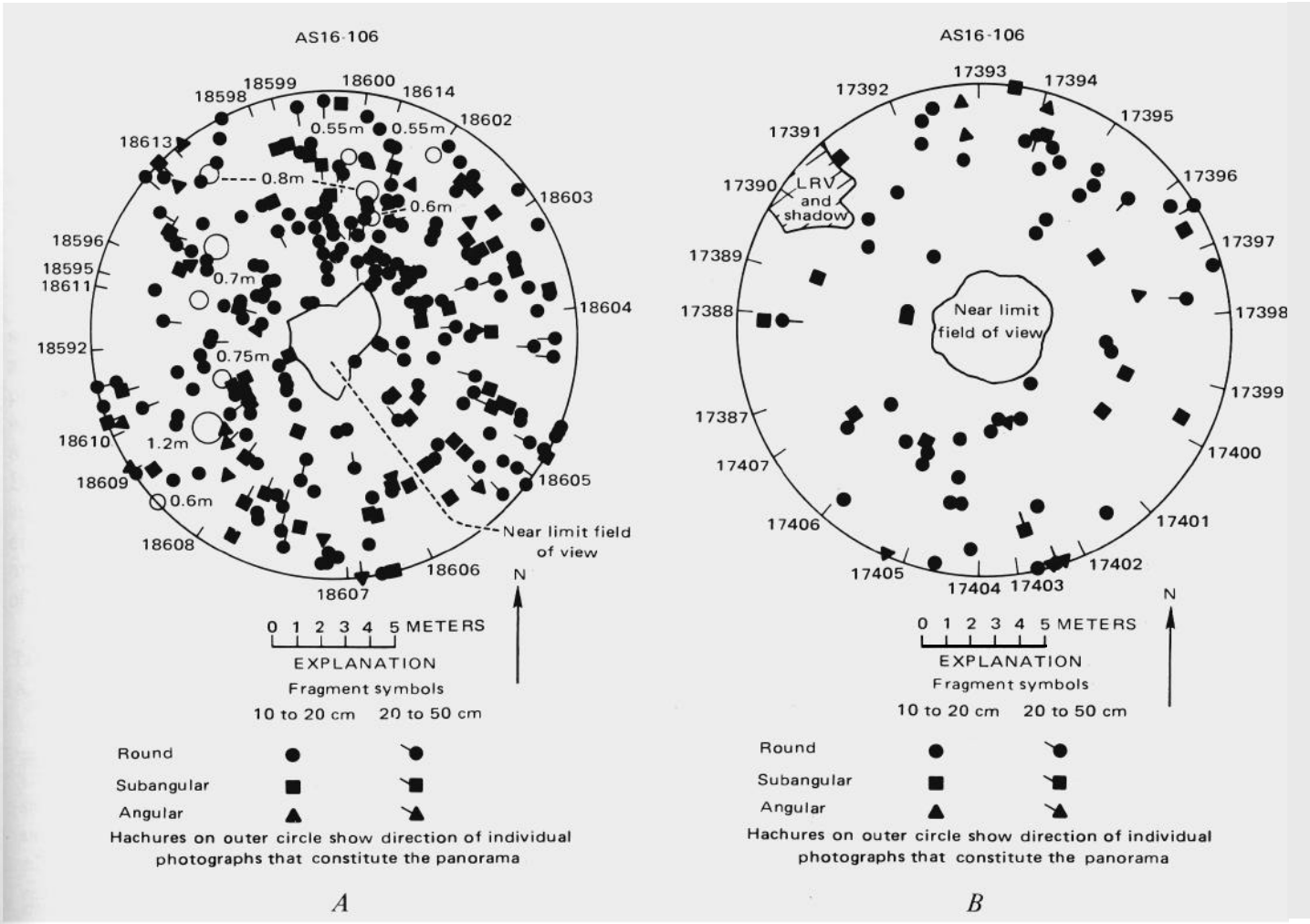

FIGURE 6.-Block distribution within 10 m of sites of station 11 and station 13 panoramas. ***A,*** Station 11. B, Station 13. From Muehlberger and others, 1972.

(FIGURE 5.—Map of boulders, craters, and ejecta grooves in North Ray crater area. Data from Apollo 16 panoramic camera frames 4563 and 4623.

dark-matrix rocks consistently exhibit angular edges and pronounced jointing, and few have soil fillets developed at their bases (figs. 7-9).

Light-matrix boulders are distinctly more rounded more crudely jointed, and more deeply filleted by soil inferred to be their own residual debris (figs. 10 and 11). The rock sample characteristics, discussed below and by Wilshire and others (this volume), reflect similar differences in coherence or friability. Megascopically and microscopically, textures indicate that variations in rock colors and coherence are produced by differences in amounts of impact melt incorporated in the rocks and in rates of cooling.

Of more than 800 rocks in the near field of four photographic panoramas taken on the rim and ejecta blanket of North Ray crater, 70 to 90 percent are relatively light colored (fig. 12). These include the light- and medium-gray-matrix breccias (B1, B2, and B, of Wilshire and others, this volume) and probably some igneous and metaclastic rocks (C, and C2,) that are indistinguishable from the light-matrix breccias in surface photographs. Rocks consisting largely of glass (class G of Wilshire and others, this volume) may be counted as dark rocks (dark-matrix breccias, B, and B,) except where large amounts of light-colored soil adhered to their surfaces. The percentage of dark rocks increases from about 10 in the western part of the southeast rim (panorama 19 and sketch, pl. 8) to nearly 30 at a location midway between the White breccia boulders and House rock. About 20 percent of the fragments at Shadow rock are dark.

SAMPLE LOCALITIES

In order to reconstruct the stratigraphic sequence in North Ray crater, the distribution and concentration of the several rock types with respect to their location on the crater wall and floor were studied. The sampled area is subdivided into four localities, the White cia boulders, the Interboulder area, the House rock a.rea and the Shadow rock area (fig. 13), whose names Were derived from descriptive terms used by the crew. All but Shadow rock are on the crater rim crest. Shadow rock is approximately 0.75 km southeast of the

TABLE 2.—*Rock samples greater than 2 g from the House rock area*

Sample No.	Weight group (g) 2–25	25–100	100+	Classification (Wilshire and others, this volume, table 1)	Geologic significance
67915	----	----	×	B_4	Representative of House and Outhouse rocks.
67935	----	----	×	[1](C_2)	Metaclastic matrix from Outhouse rock.
67936	----	×	----	C_1	Same as 67935, in impact-spall zone.
67937	----	×	----	B_4	Dark-matrix breccia from impact spall zone.
67945	×	----	----	B_4	Rock from "east-west split."
67946	×	----	----	(B_4)	Do.
67947	×	----	----	(B_4)	Do.
67955	----	----	×	B_1	Light-matrix clast from Outhouse rock.
67956	×	----	----	C_1	Igneous fragment from Outhouse rock.
67975	----	----	×	B_2	Fragment in soil near Outhouse rock.

( ) Provisional classification by Wilshire and others, this volume, table 1.

TABLE 3.—*Rock samples greater than 2 g from the White breccia boulders area*

Sample No.	Weight group (g) 2–25	25–100	100+	Classification (Wilshire and others, this volume, table 1)	Geologic significance
67016	----	----	×	[1]$B_3(B_2)$	Large loose rock on crater rim crest.
67025	×	----	----	$B_3(B_2)$	Coherent fragment, possibly from 67016.
67035	----	----	×	B_2	"Three-rock" breccia 20 m inside rim crest.
67215	----	----	×	Unclass	Unopened rock in padded bag.
67415	----	----	×	B_1	Friable rock at base of light-matrix breccia boulder.
67435	----	----	×	[2](B_4)	Glass-coated; may be dark- and light-matrix breccia.
67455	----	----	×	B_2	Fragments off top of 6 m light-matrix breccia boulder.
67475	----	----	×	B_4	Clast from the same boulder as 67455.
67485	×	----	----	(C_2)	Fragment in soil near 67455 light-matrix boulder.
67486	×	----	----	(B_1)	Do.
67487	×	----	----	(C_2)	Do.
67488	×	----	----	(C_2)	Do.
67489	×	----	----	(C_2)	Do.
67515	----	×	----	B_2	Breccia in rake sample near 67455 light-matrix boulder.
67516	×	----	----	$B_3(B_1)$	Do.
67517	×	----	----	$B_3(B_1)$	Do.
67518	×	----	----	$B_3(B_1)$	Do.
67519	×	----	----	$B_3(B_1)$	Do.
67525	×	----	----	$B_3(B_1)$	Do.
67526	×	----	----	$B_3(B_1)$	Do.
67527	×	----	----	$B_3(B_1)$	Do.
67539	×	----	----	$B_3(B_1)$	Do.
67549	----	×	----	B_2	Do.
67555	×	----	----	B_2	Do.
67556	----	×	----	B_2	Do.
67557	×	----	----	Unclass	Do.
67558	×	----	----	Unclass	Do.
67559	----	×	----	(C_2)	Olivine basalt* in rake sample near 67455 boulder.[3]
67565	×	----	----	C_2	Basalt* in rake sample near 67455 boulder.
67566	×	----	----	C_2	Do.
67567	×	----	----	G	Breccia in rake sample near 67455 boulder.
67568	×	----	----	G	Do.
67569	×	----	----	G	Do.
67575	×	----	----	G	Do.
67576	×	----	----	G	Do.
67605	----	×	----	B_2	Fragment from soil sample in rake area.
67615	×	----	----	C_2	Basalt* in rake sample 10 m inside rim crest.
67616	×	----	----	C_2	Do.
67617	×	----	----	C_2	Basaltic breccia* in rake sample 10 m inside rim crest.
67618	×	----	----	C_2	Do.
67619	×	----	----	C_2	Do.
67625	×	----	----	C_2	Metaclastic rock in rake sample 10 m inside rim crest.
67626	×	----	----	G	Breccia in rake sample 10 m inside rim crest.
67627	----	×	----	G	Do.
67628	----	×	----	G	Do.
67629	----	×	----	G	Basalt* clast from light-matrix breccia.
67635	×	----	----	B_1	Breccia in rake sample 10 m inside rim crest.
67636	×	----	----	B_1	Do.
67637	×	----	----	B_1	Do.
67638	×	----	----	B_2	Do.
67639	×	----	----	B_2	Do.
67646	×	----	----	B_2	Do.
67647	----	×	----	Unclass	Do.
67648	×	----	----	B_2	Do.
67655	×	----	----	B_2	Do.
67665	×	----	----	(B_2)	Do.
67666	×	----	----	B_2	Do.
67667	×	----	----	C_2	Ultramafic?* in rake sample 10 m inside rim crest
67668	×	----	----	C_2	Basaltic breccia* in rake sample 10 m inside rim crest
67669	×	----	----	(B_2)	Breccia in rake sample 10 m inside rim crest
67676	×	----	----	C_2	Basalt* in rake sample 10 m inside rim crest

[1]$B_3(B_2)$ Alternative classification by Wilshire and others (this volume).
[2]) Provisional classification by Wilshire and others (this volume).
[3] Interpretation from Smith and Steele (1972).

crest, but still on continuous North Ray ejecta. For each of the four areas, the rock samples weighing more than 2 g are tabulated and their geologic significance indicated in tables 2 to 5. Their occurrence by rock type is graphically compared in figure 14. The larger soil samples and their location and geologic significance are given in table 6.

HOUSE ROCK AREA

The largest boulder visited and one established as a sampling target before the mission is House rock. It is an angular, predominantly dark-matrix boulder, approximately 25 m long and 12 m high, at the northeastern limit of the crater-rim-crest traverse area (figs. 8, 13; pl. 8, pan 28). It was so named when Astronaut Duke, on first observing it at station 11, compared its size to that of a house. Less than 1 m away on the south end of House rock is a 3-m boulder of similar texture, anonymously named Outhouse rock, the source of most of the rock samples collected at this locality.

TABLE 4.—*Rock samples greater than 2 g from the Interboulder area*

Sample No.	2–25g	25–100	100+	Classification (Wilshire and others, this volume)	Geologic significance
67015	----	----	×	[1]$B_3(B_2)$	Large loose rock inside rim crest.
67055	----	----	×	$B_2(B_3)$	Collected for abundant black clasts (more than 67035).
67075	----	----	×	B_1	Found as two broken pieces of white shocked rock.
67095	----	----	×	G	Collected for appearance as "really black glass."
67115	----	----	×	[2](B_3)	Same location as 67095; more rounded.
67235	----	----	×	Unclass	Unopened rock in padded bag.
67705	×	----	----	(G)	Fragment in rake soil on rim crest.
67706	×	----	----	Unclass	Do.
67715	×	----	----	B_4	Basalt* probably clast from light-matrix breccia.[3]
67716	×	----	----	B_4	Breccia, probable clast from light-matrix breccia.
67717	×	----	----	B_4	Do.
67718	----	×	----	(B_3)	Do.
67719	×	----	----	B_4	Do.
67725	×	----	----	B_4	Breccia in rake sample on rim crest.
67726	×	----	----	B_4	Do.
67728	×	----	----	G	Fragment in rake sample on rim crest.
67729	----	×	----	G	Do.
67735	×	----	----	$B_3(B_2)$	Do.
67736	×	----	----	C_2	Olivine basalt with ultramafic inclusion; zapped on all sides.*
67737	×	----	----	B_4	Basalt* probable clast from light-matrix breccia.
67738	×	----	----	B_4	Do.
67739	×	----	----	B_4	Fragment in rake sample on rim crest.
67745	×	----	----	B_4	Basalt* in rake sample on rim crest.
67746	×	----	----	C_2	Norite?* in rake sample on rim crest.
67747	×	----	----	C_2	Troctolite?* in rake sample on rim crest.
67748	×	----	----	C_2	Fragment in rake sample on rim crest.
67749	×	----	----	B_2	Breccia in rake sample on rim crest.
67755	×	----	----	B_2	Do.
67756	×	----	----	B_2	Do.
67757	×	----	----	B_2	Do.
67758	×	----	----	B_2	Do.
37759	×	----	----	B_2	Do.
67766	×	----	----	B_2	Do.
67769	×	----	----	B_2	Do.
67775	×	----	----	B_2	Do.
67776	×	----	----	B_2	Do.

[1]$B_3(B_2)$ Alternative classification by Wilshire and others (this volume).
[2]( ) Provisional classification by Wilshire and others (this volume).
*Interpretation from Smith and Steele (1972)

TABLE 5.—*Rock samples greater than 2 g from the Shadow rock area, station 13, on outer North Ray ejecta*

Sample No.	2–25g	25–100	100+	Classification (Wilshire and others, this volume)	Geologic significance
60017	----	----	×	[1]$B_4(B_3)$	Large rock broken off from 2 m area on southwest side of Shadow rock.
63335	----	×	----	[2](B_3)	Chip rock broken off from 2 m area on southwest side of Shadow rock.
63355	----	×	----	B_4	Do.
63505	×	----	----	(B_4)	Fragment in rake soil 5–10 m west of Shadow rock
63506	×	----	----	C_1	Do.
63507	×	----	----	B_3	Do.
63508	×	----	----	B_3	Do.
63509	×	----	----	B_2	Do.
63525	×	----	----	(B_4)	Do.
63526	×	----	----	(B_4)	Do.
63527	×	----	----	(B_4)	Do.
63528	×	----	----	(B_4)	Do.
63529	×	----	----	(B_4)	Do.
63535	×	----	----	(B_4)	Do.
63537	×	----	----	(C_2)	Do.
63538	----	×	----	(C_2)	Do.
63545	×	----	----	(C_2)	Do.
63546	×	----	----	(B_4)	Do.
63547	×	----	----	(C_2)	Do.
63549	----	×	----	(C_2)	Do.
63555	×	----	----	(B_4)	Do.
63556	×	----	----	(C_2)	Do.
63557	×	----	----	(B_4)	Do.
63558	×	----	----	(C_2)	Do.
63559	×	----	----	(G)	Do.
63566	×	----	----	(G)	Do.
63567	×	----	----	(G)	Do.
63568	×	----	----	(G)	Do.
63575	×	----	----	(G)	Do.
63577	×	----	----	$(B_4(C_2))$	Do.
63578	×	----	----	(B_3)	Do.
63579	×	----	----	(B_3)	Do.
63585	----	×	----	(C_2)	Do.
63587	×	----	----	(B_3)	Do.
63588	×	----	----	(B_3)	Do.
63589	×	----	----	$(B_3(B_2))$	Do.
63595	×	----	----	(B_3)	Do.
63596	×	----	----	(B_3)	Do.
63597	×	----	----	(B_3)	Do.
63598	×	----	----	(B_3)	Do.

[1]$B_4(B_3)$ Alternative classification by Wilshire and others (this volume)
[2]( ) Provisional classification by Wilshire and others (this volume).

TABLE 6.—*North Ray crater soil samples greater than 26 g*

Sample No.*	White breccia boulder area	Interboulder area	House rock area	Shadow rock area	Geologic significance
63320–4	----	----	----	×	"Shadowed" soil on surface under northwest overhang of Shadow rock.
63340–4	----	----	----	×	Soil beneath 63320 under northwest overhang of Shadow rock.
63500–4	----	----	----	×	Rake soil 5–10 m west of Shadow rock.
67010	----	×	----	----	Residue in sample collection bag No. 7
67020	×	----	----	----	Residue in Buddy Secondary Life Support System bag with rock 67016.
67030–4	×	----	----	----	Residue in sample bag with rock 67035.
67410	×	----	----	----	Residue in sample bag with rock 67415.
67450	×	----	----	----	Residue in sample bag with rock 67455.
67460–4	×	----	----	----	Fillet at boulder from which 67455 and 67475 were collected.
67480-4	×	----	----	----	Reference soil for comparison with 67460; same location as sample 67510.
67510–4	×	----	----	----	Soil in rake sample near large, light-matrix breccia boulder.
67600–4	×	----	----	----	Rake soil collected about 25 m east of 67510; inside rim crest.
67610	×	----	----	----	Soil in rake sample from same location as 67600.
67700–4	----	×	----	----	Rake soil from half way between White breccia boulders and House rock.
67710–4	----	×	----	----	Soil in rake sample from same location as 67700.
67910	----	----	×	----	Residue in sample collection bag No. 4.
67940–4	----	----	×	----	Soil from "east-west split" between House and Outhouse rocks.

*-4 indicates sample was sieved in LRL into newly numbered fractions, 1 through 4, for less than 1 mm, 1–2 mm, 2–4 mm, and 4–10 mm, respectively.

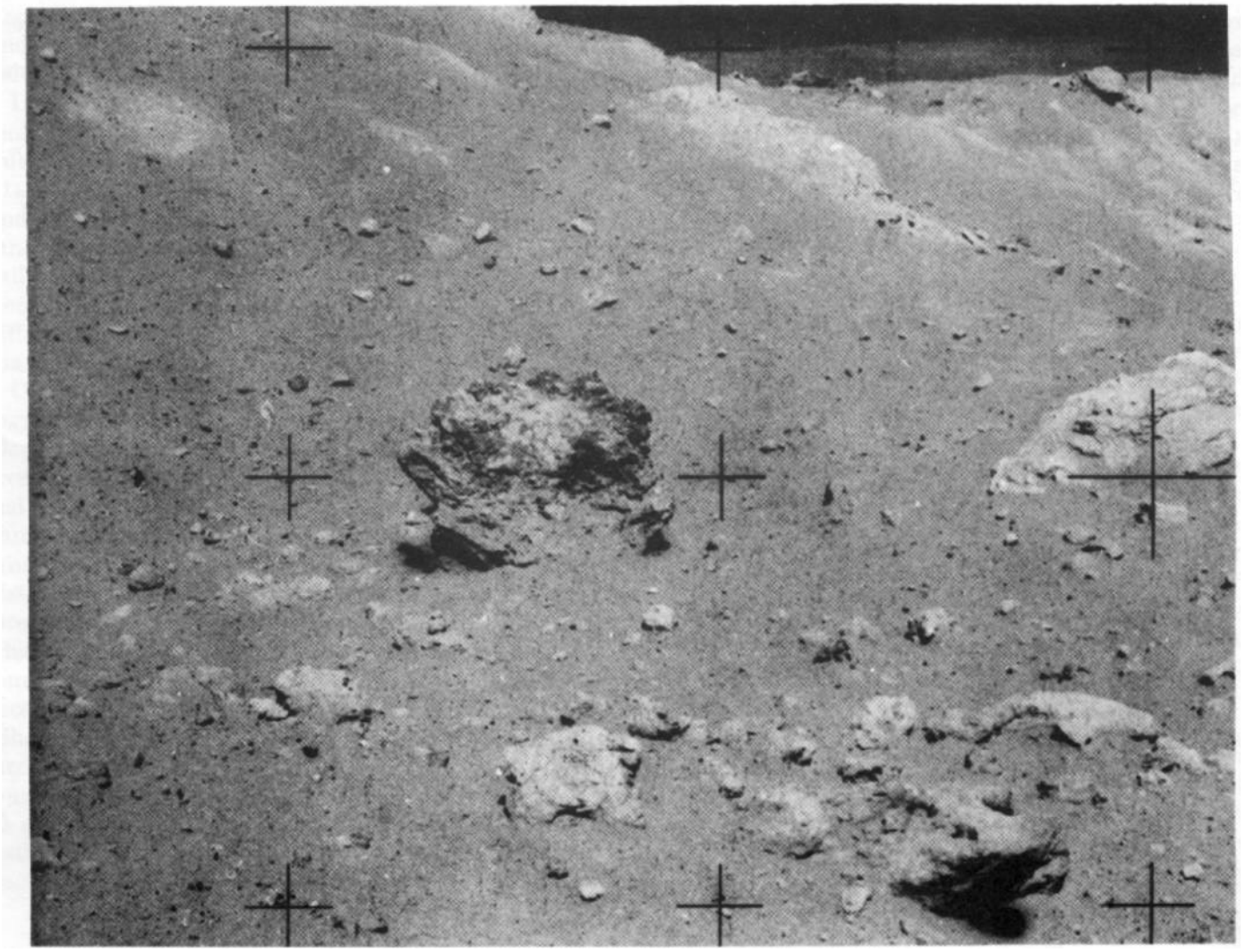

FIGURE 7.-Dark-matrix breccia boulder in White breccia boulder area. For location see panorama 19, pl. 8.

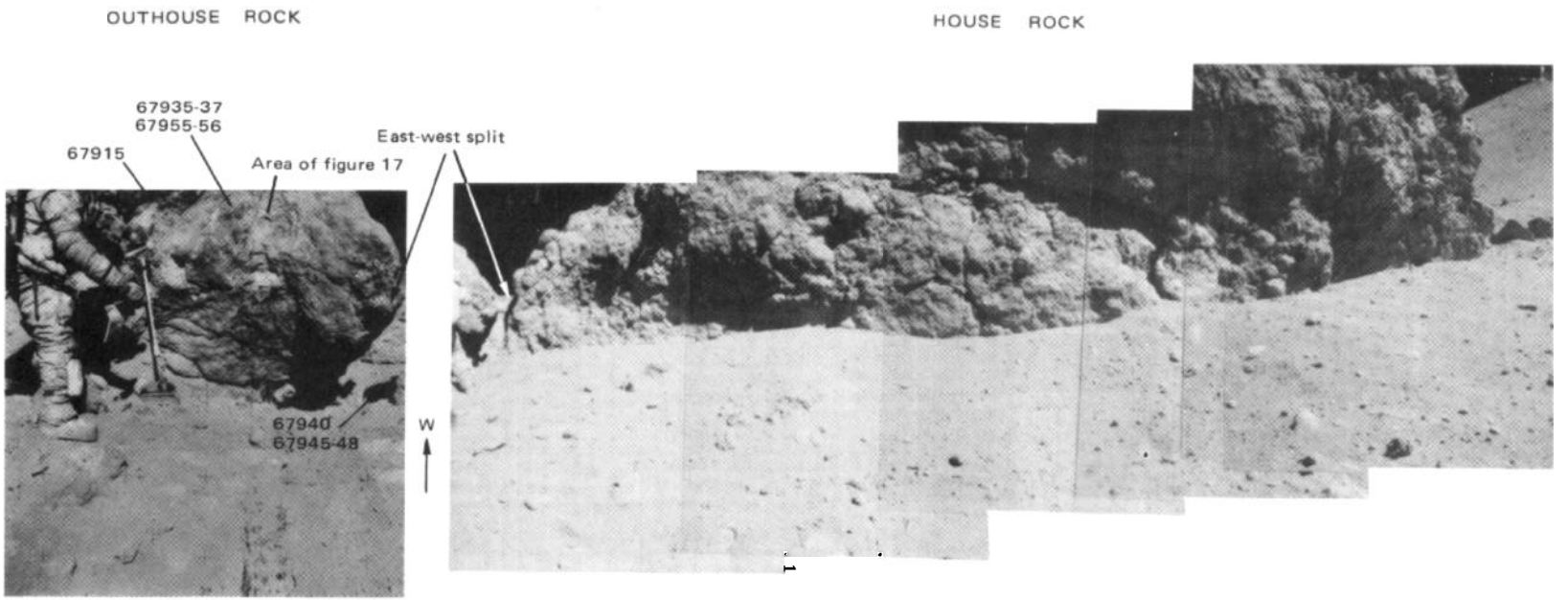

FIGURE 8.—House rock and Outhouse rock panorama at station 11, showing east face of dark-matrix breccia boulders. Note lack of fillet at base and angular, jointed faces. AS16–116–18653 (left) and 106–17349 to 19354.

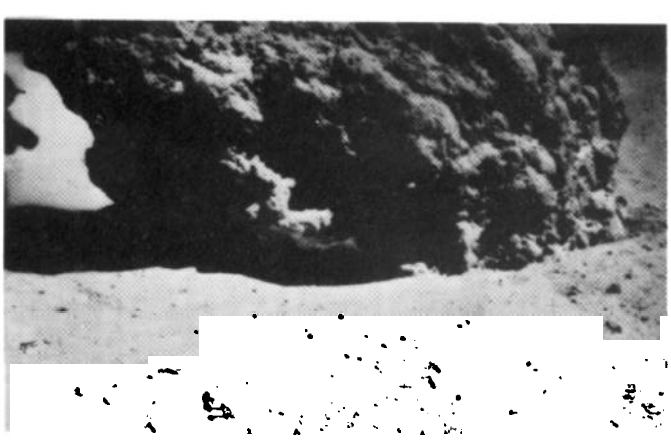

A

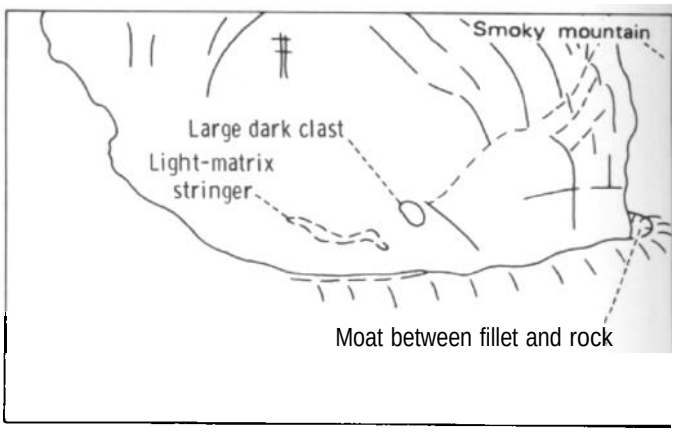

B

FIGURE %--Shadow rock panorama at station 13. ***A,*** South face of 5-m-wide boulder of dark-matrix breccia. AS16- 106-17413 to 17415. B. Sketch map of fractures and clasts.

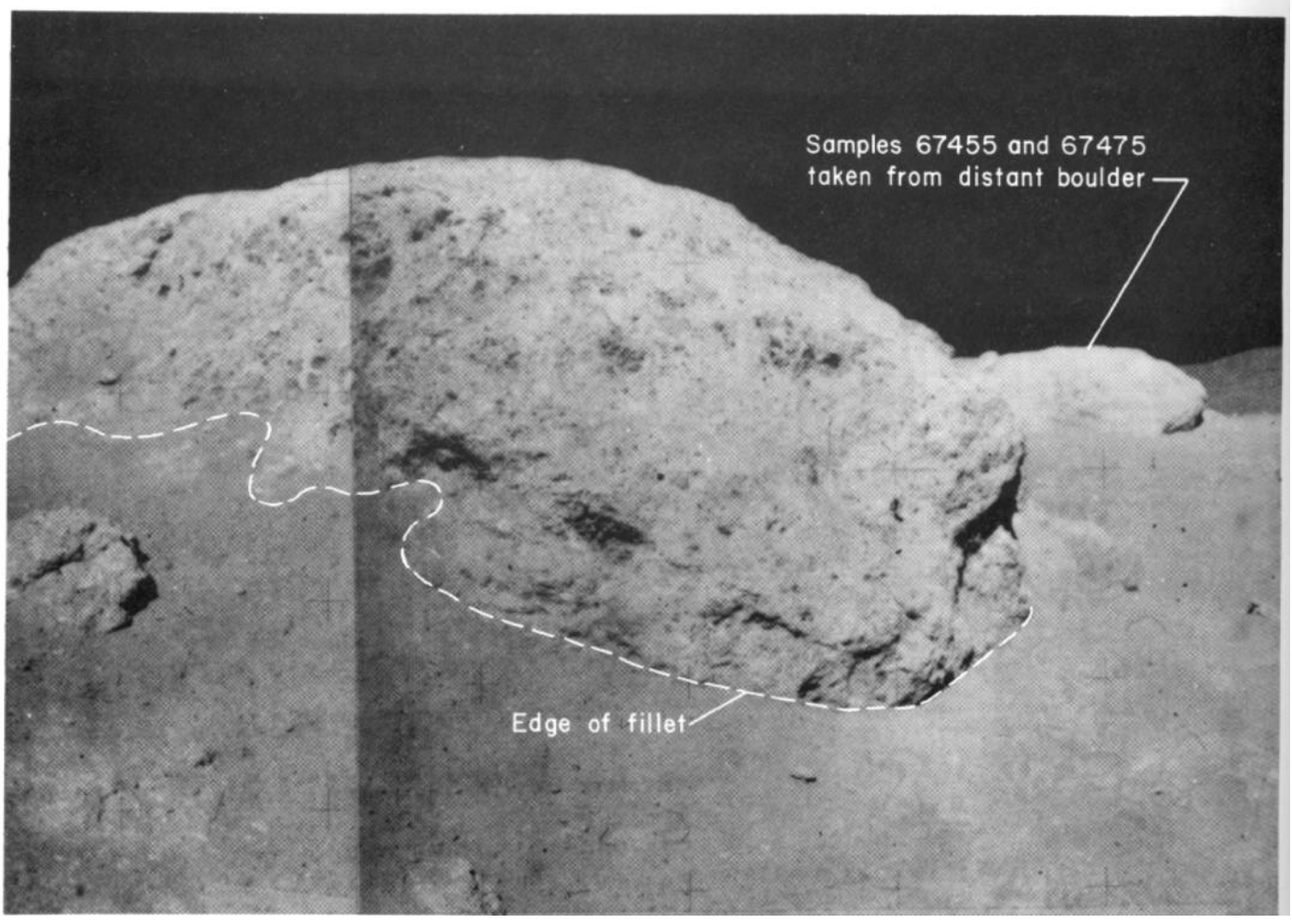

FIGURE 10.--white breccia boulders showing rounded outlines and deeply filleted margins. AS16-106- 17325 and 17326.

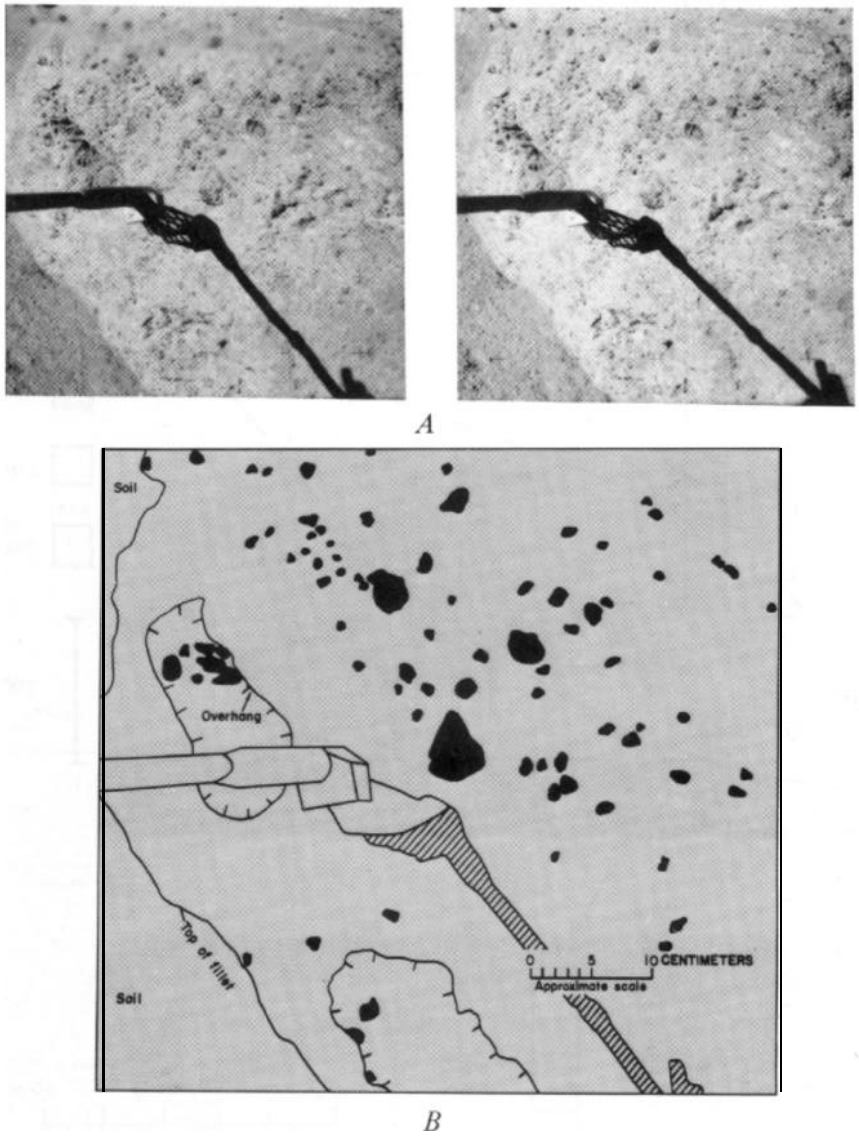

FIGURE 11.-Surface texture and distribution of dark clasts, White breccia boulder. *A,* Stereopair showing surface texture. AS16 106-17327 to 17328. B, Sketch map showing distinction of dark clasts and top of fillet.

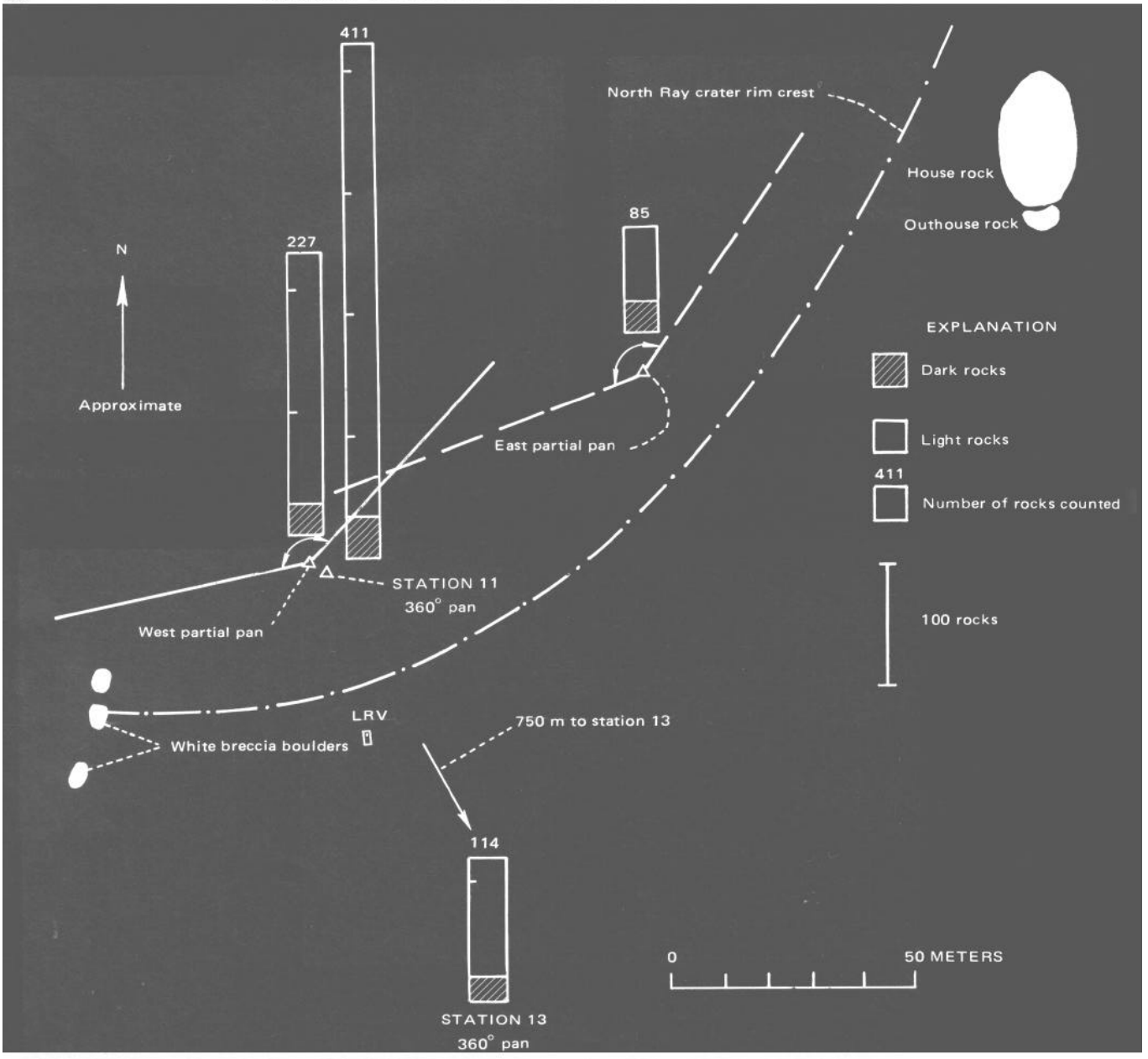

FIGURE 12.-Proportions of light and dark fragments counted in surface panoramas. Data from plate 7, pan 23, plate 8, pans 18 and 19, and plate 9, pan 20. Boulder map from Sutton (this volume).

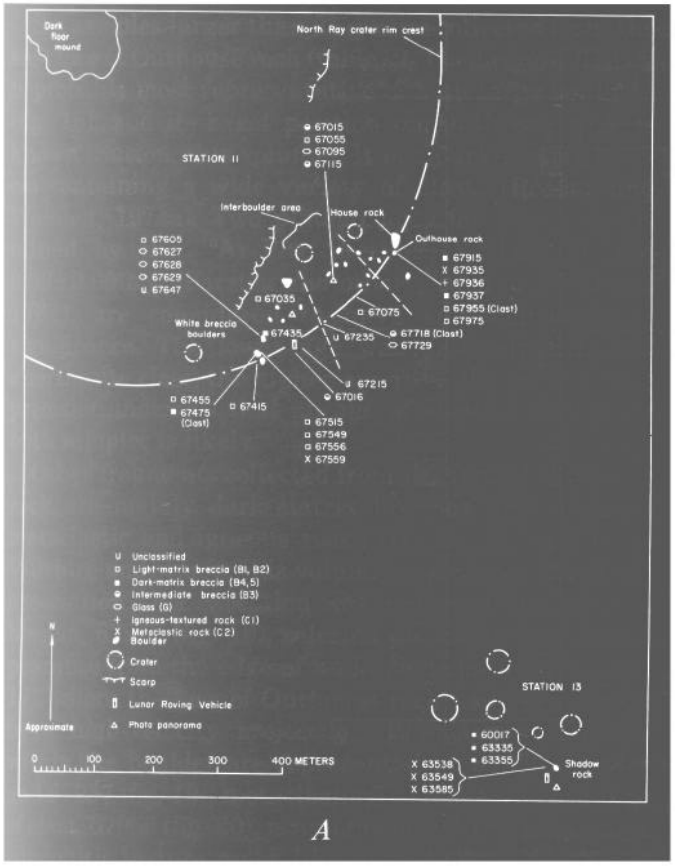

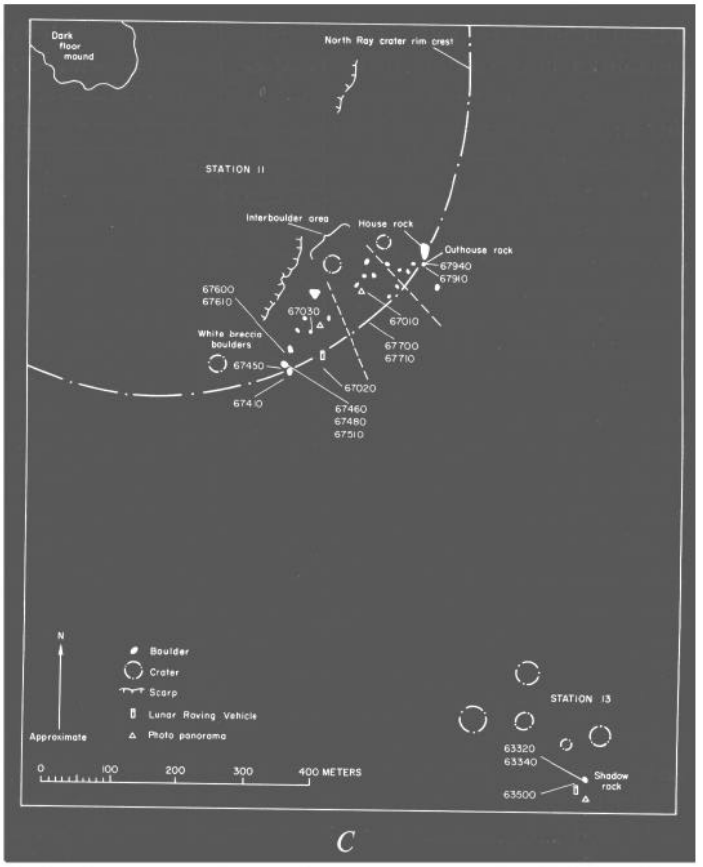

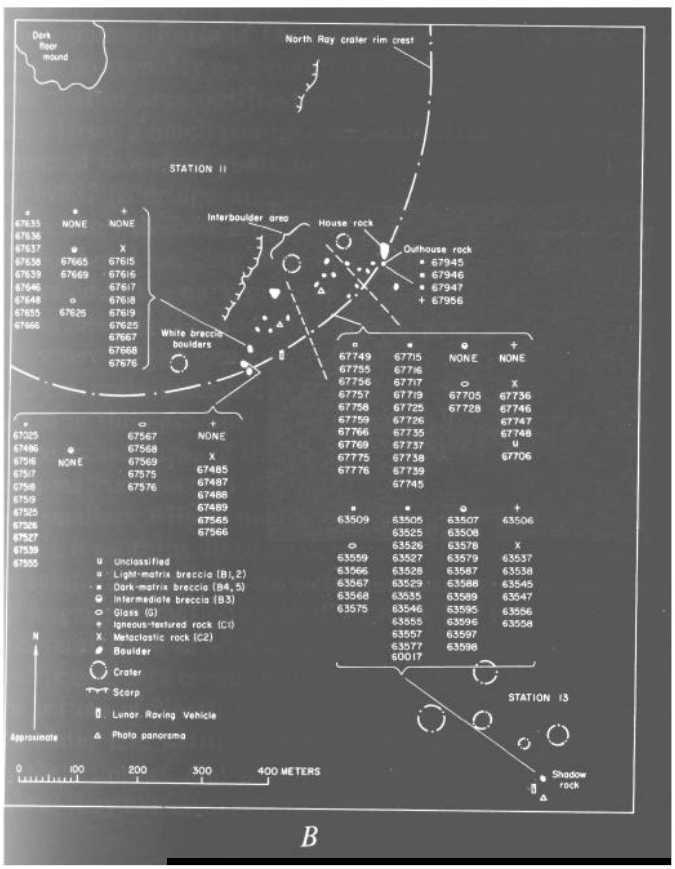

FIGURE 13.-Location of rocks and soils collected at stations 11 and 13. ***A,*** Rocks weighing more than 25 g. ***B,*** Rocks weighing 2 to 25 g. ***C***, Soil samples weigh more than 26 g.

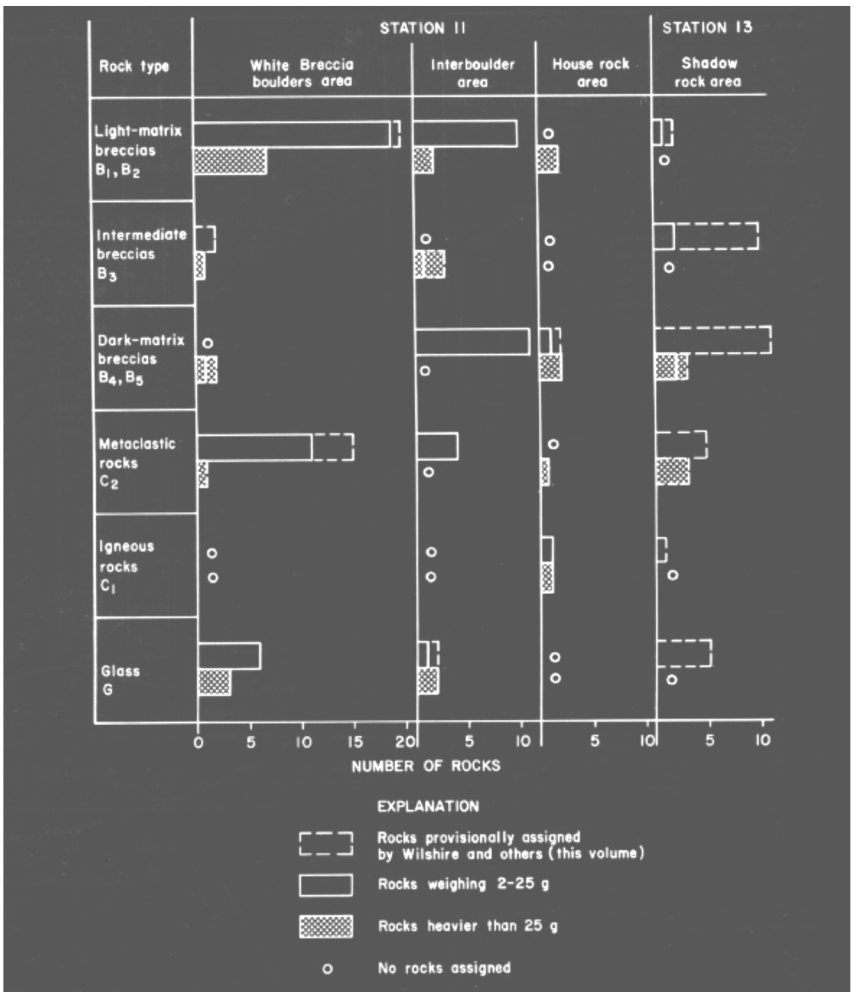

FIGURE 14.—Abundance of rock types collected from four localities at North Ray crater.

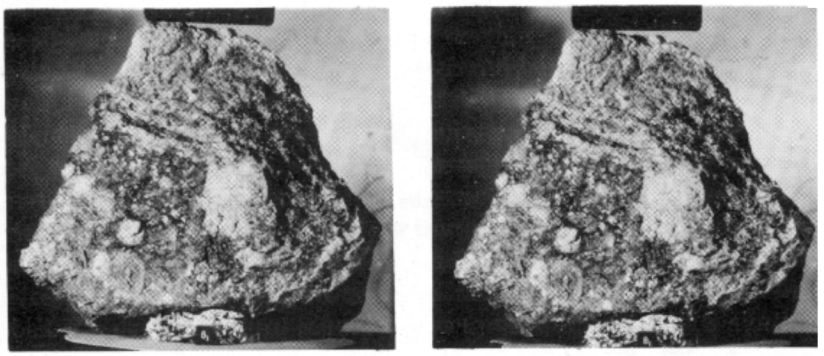

FIGURE 15.—Sample 67915, a dark-matrix breccia, the largest fragment collected from Outhouse rock. Scale in centimeters. NASA S–72–43917 and 43917B.

Six samples larger than 25 g were collected from the east face of Outhouse rock (table 2). The largest, 67915, is probably most representative of both large boulders (fig. 15), and its exact position on Outhouse rock is known (Sutton, this volume). It is a dark-matrix breccia containing a wide variety of clasts (Roeder and Weiblen, 1974a). Two plateau ages for 67915 determined by the ^{40}Ar-^{39}Ar method, 3.91 ± 0.05 and 3.99 ± 0.05 b.y. (Kirsten and others, 1973, p. 1760 and 1762), are considered to have selenochronologic significance. The lower age was determined on an anorthosite clast, the higher age from the matrix. The precision indicates that an age of about 3.95 b.y. for both samples is likely.

Other fragments collected from the face of Outhouse rock are mainly dark-matrix breccias and coherent metaclastic and igneous rocks (B4, B_5, C_2, and C_1 of Wilshire and others, this volume), a common lithologic association. One exception was a clast of light-matrix breccia, 67955 (fig. 16), selected for its unshocked appearance from the edge of an impact-spalled area (fig. 17), where the face of Outhouse rock had been struck by a high-velocity projectile. Other types of clasts within the boulder are represented by 67935 (fig. 18) and 67937 (fig. 19), metaclastic (C_2) rocks. A third type of clast, 67956 (fig. 20), is an igneous (C_1) rock having a subophitic texture much like that of 68415 (see Reed, fig. 9B, this volume) and 65055 (see Sanchez, fig. 20, this volume). Parts of Outhouse rock are highly fractured, presumably as a result of the North Ray impact. The spalled area outlined on figure 17 apparently resulted from a much younger impact within the past few hundred thousand years based on ^{26}Al measurements on 67937 (Eldridge and others, 1973, p. 2119). Other rocks likely to show effects of this event are 67935 and 67936. Local melting during the North Ray event is indicated by the dark glass splashes on the face of Outhouse rock (fig. 17) and the glass coating on fragments elsewhere on the rim crest.

Loose undocumented fragments and soil were collected in the east-west split between House and Outhouse rocks. Three of the four small rocks collected are dark-matrix breccias (67945-47, fig. 21). The fourth and smallest, 67948, may be a relict inclusion of mare basalt; it contains 40 to 50 percent mafic minerals with an ophitic texture (fig. 22). These rocks are most likely all fragments spalled from the large boulders.

Several lines of evidence suggest that these dark-matrix boulders came from a lower horizon near or at the bottom of North Ray crater. They are perched on the crater rim within the shallow depressions formed by their impact and are not overlain by subsequent debris; they are clearly late arrivals in the sequence of crater ejecta. This perched position is typical of the deepest material in terrestrial impact and explosion craters. In size and color, the rocks resemble the coarse rubble on the crater floor and, by comparison with the central mounds in nearby craters, may represent a more resistant stratum near the floor of the craters (Hodges, 1972a; Ulrich and Reed, this volume). Dark rocks are sparse on the crater rim crest (10-30 percent, fig. 12). The more abundant light-matrix breccias here and radially away from the rim probably represent shallower materials overlying the dark-matrix rocks in the crater wall. The large 10-m blocks in the northeast wall of the crater appear in telephotographs to be light-matrix breccias (fig. 23, and pl. 9, pan 36) with some degree of lateral continuity, suggesting at least a crude stratigraphic relation to the materials above and below. The slightly convex shape of the crater wall as seen from the southeast rim (fig. 4) indicates that relatively softer, less coherent materials in the upper wall overlie more resistant material at depth.

WHITE BRECCIA BOULDERS

A group of rounded light-colored boulders was another major sampling target at the rim of North Ray, about 50 m west of the LRV parking spot. The sampling done in the vicinity of the LRV was within this area, and the largest number of samples from station 11 was collected at this westernmost location, as shown in figure 13. The classification and geologic significance of all the rocks weighing more than 2 g (figs. 13A, B) are given in table 3.

The most distinctive characteristics of the rocks here are the well-rounded profiles, deeply filleted margins, and light-gray to white color (fig. 10). The lengths of the largest boulders are about four times their height. The returned samples typically are light-matrix breccias, which are generally very friable and contain coherent clasts of dark-matrix breccia (fig. 11). The rock probably most representative of these boulders is sample 67455 (fig. 24), collected from several loose fragments on top of a boulder approximately 6 m long and 1.5 m high (figs. 10 and 25A). A light-colored clast from this sample has a plateau age of 3.91 ± 0.12 b.y. determined by the ^{40}Ar-^{39}Ar method (Kirsten and others, 1973, p. 1762), essentially the same as the age of 67915 from Outhouse rock. This rock, like many of the rocks of this group, crumbles so badly that it is impossible to reconstruct its lunar orientation. The friable texture is expressed microscopically by extensive irregular fracturing through the matrix and around the more coherent clasts (fig. 25B), referred to as glass selvages by Wilshire and others (this volume, fig. 4A).

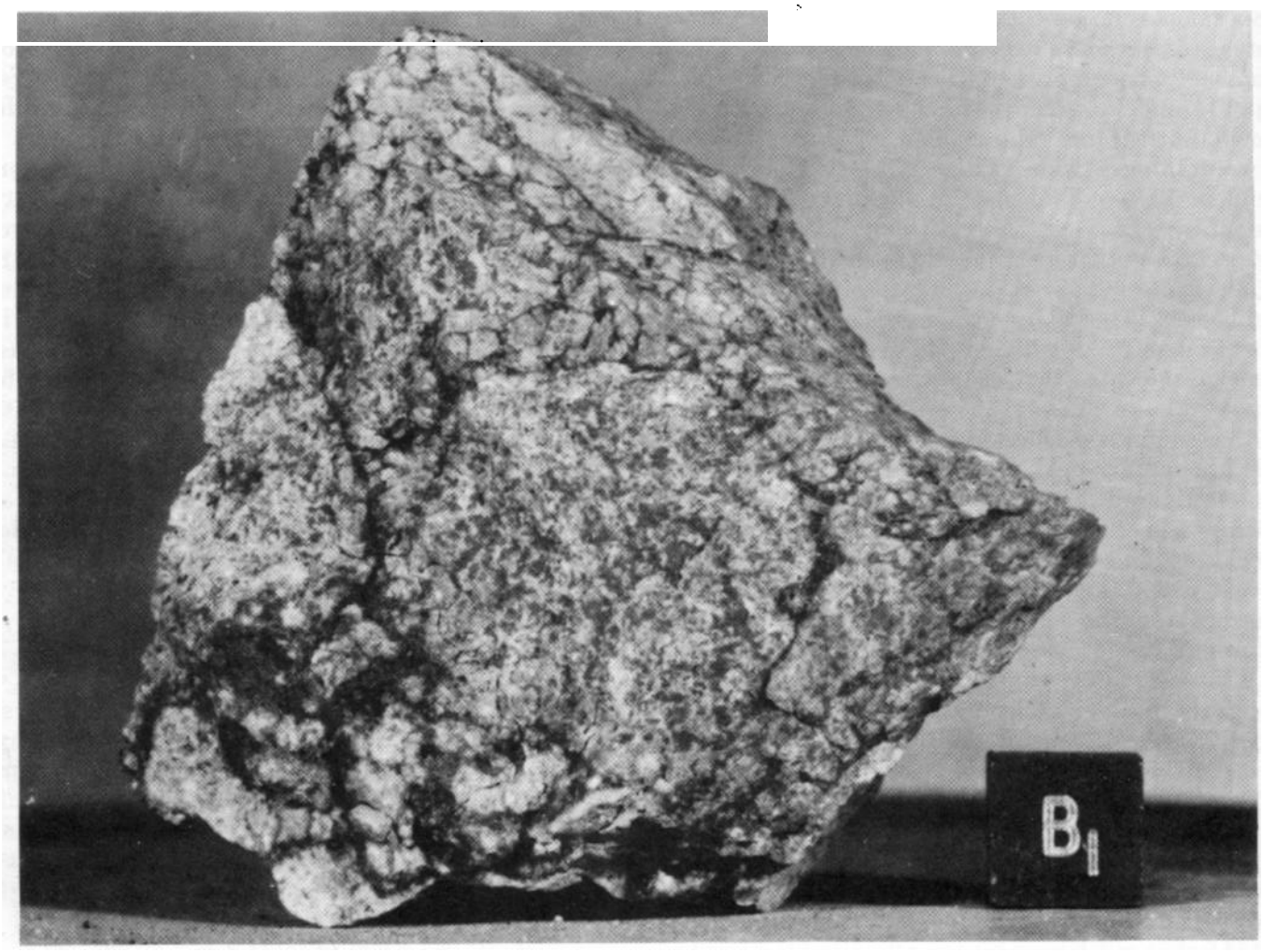

Figure 16.-Sample 67955, a clast of light-matrix breccia from Outhouse rock. Cube is 1 cm. NASA S-72-45681.

FIGURE 17.-Impact-spalled area on east face of Outhouse rock. AS16-106-17345.

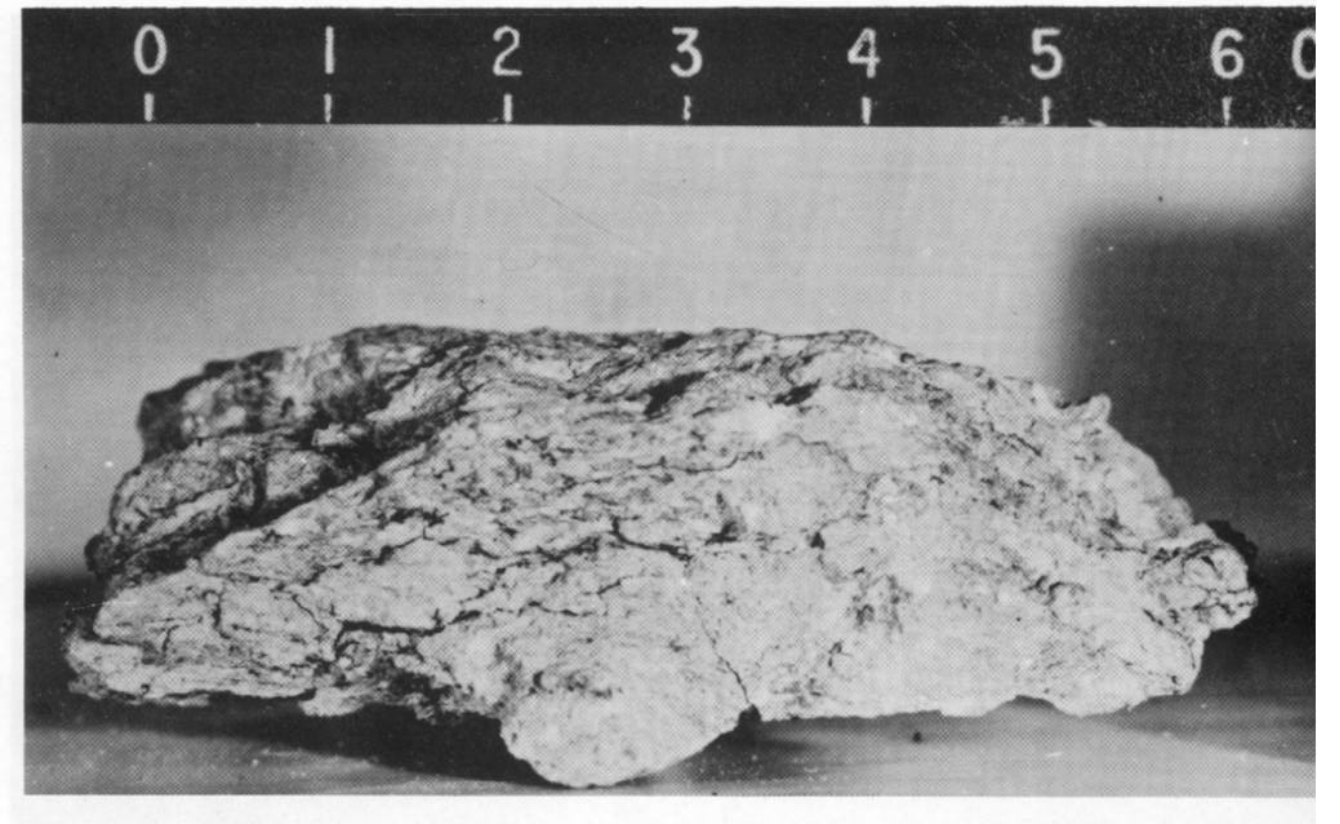

FIGURE 18.-Sample 67935, a metaclastic rock broken off the east face of Outhouse rock. NASA S-72-37784.

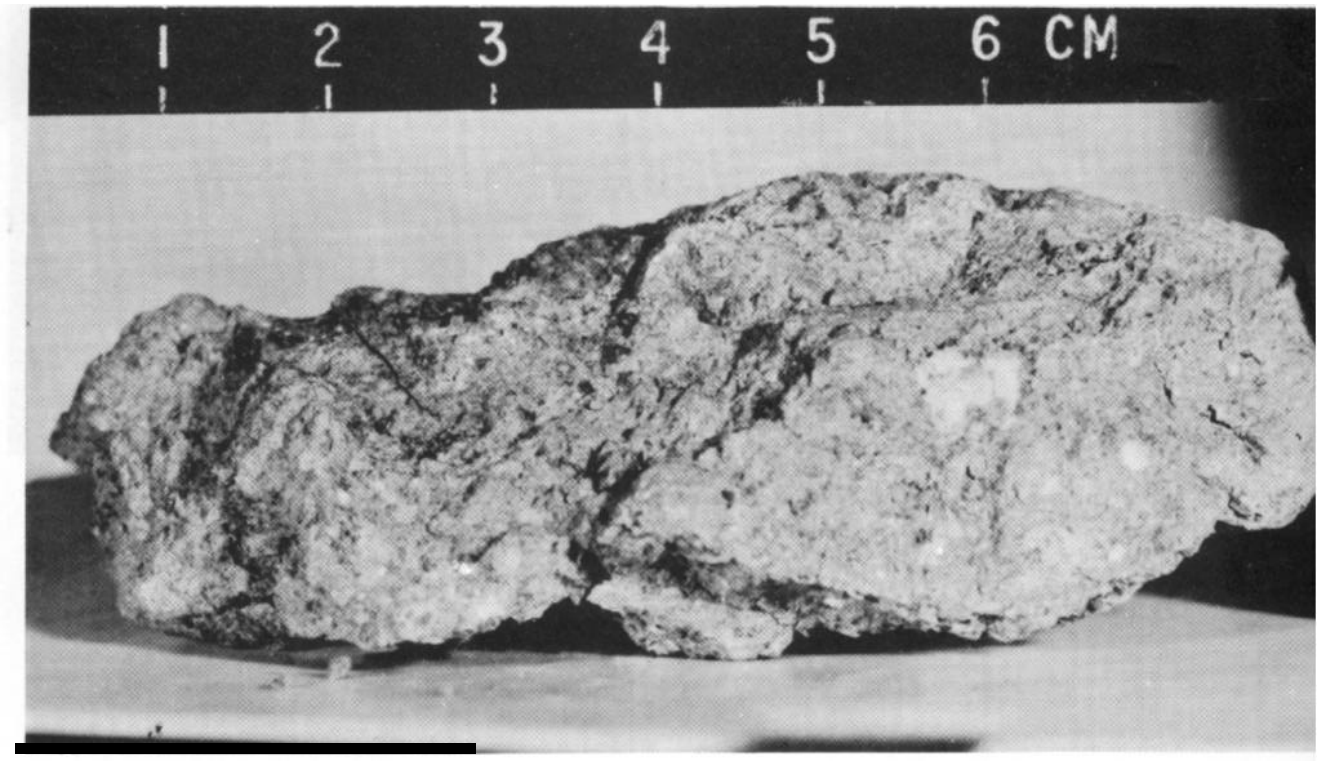

Figure 19.-Sample 67937, a metaclastic rock from Outhouse rock. NASA

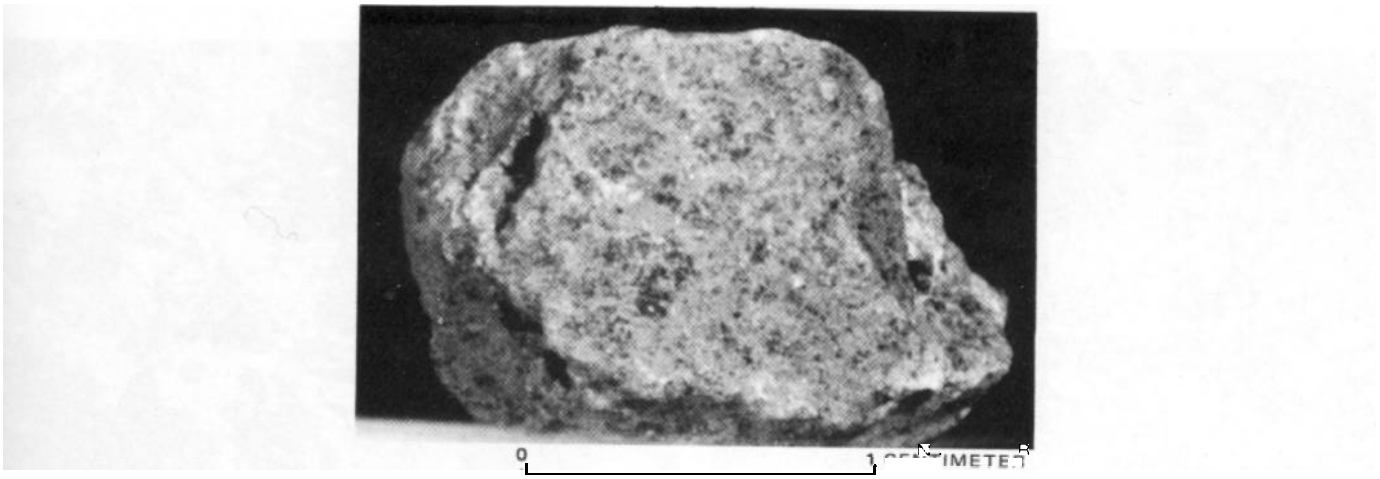

FIGURE 20.-Sample 67956, a rock with igneous texture from Outhouse rock. NASA S-72-37547.

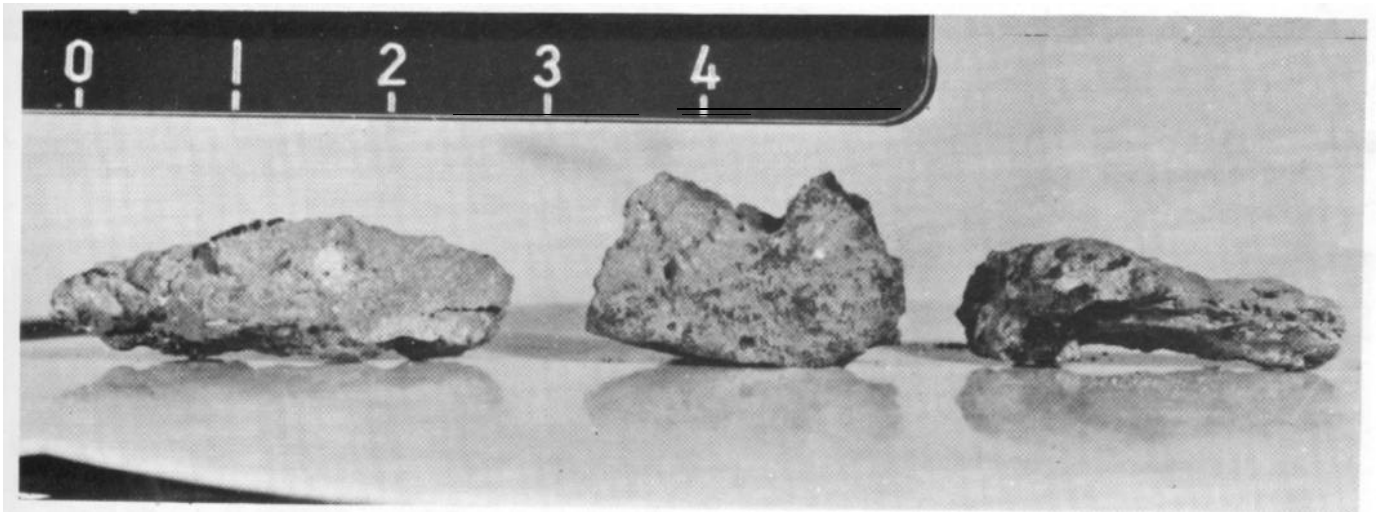

FIGURE 21.-Three dark-matrix breccias collected from the east-west split between House and Outhouse rocks; left to right, 67945, 67946, 67947. Scale in centimeters. NASA

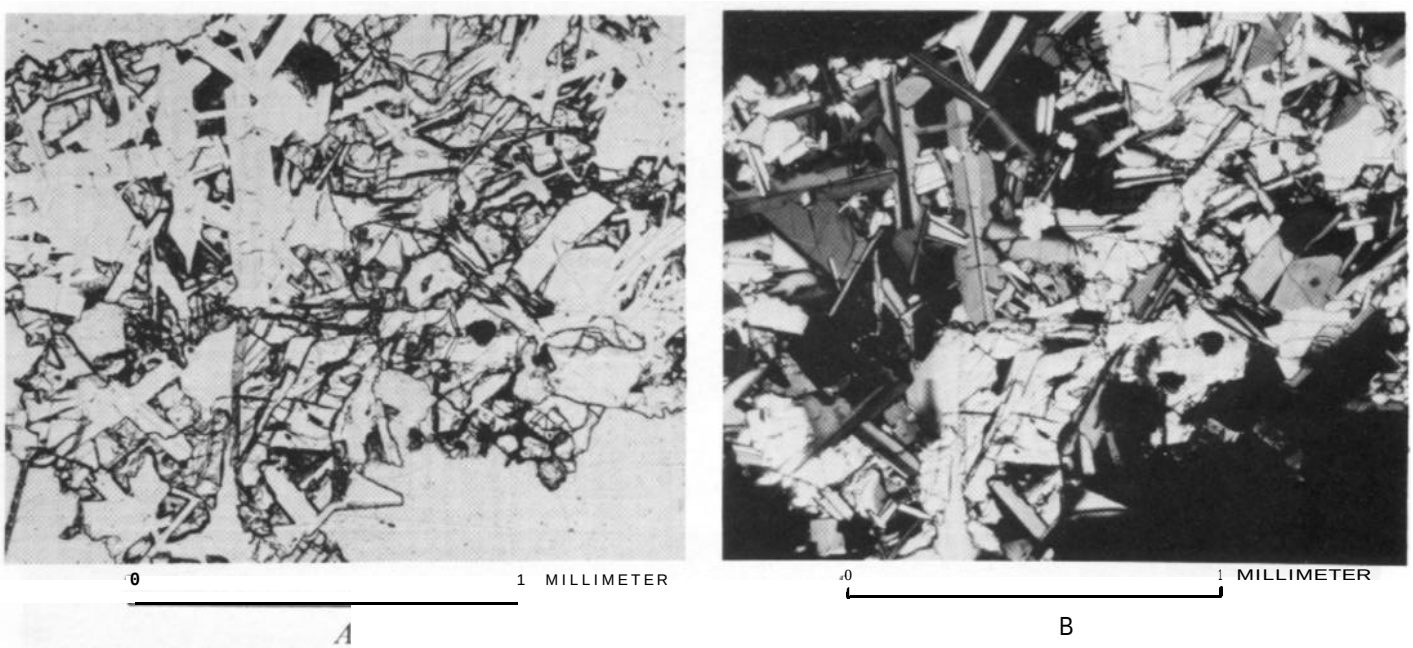

FIGURE 22.-Ophitic fragment 67948 (1.59 g) collected from the east-west split between House and Outhouse rocks. A, Photomicrograph of 67948, 15 showing pyroxene (high relief) and plagioclase laths. Plane-polarized light. B. Same samples as A, cross-polarized light.

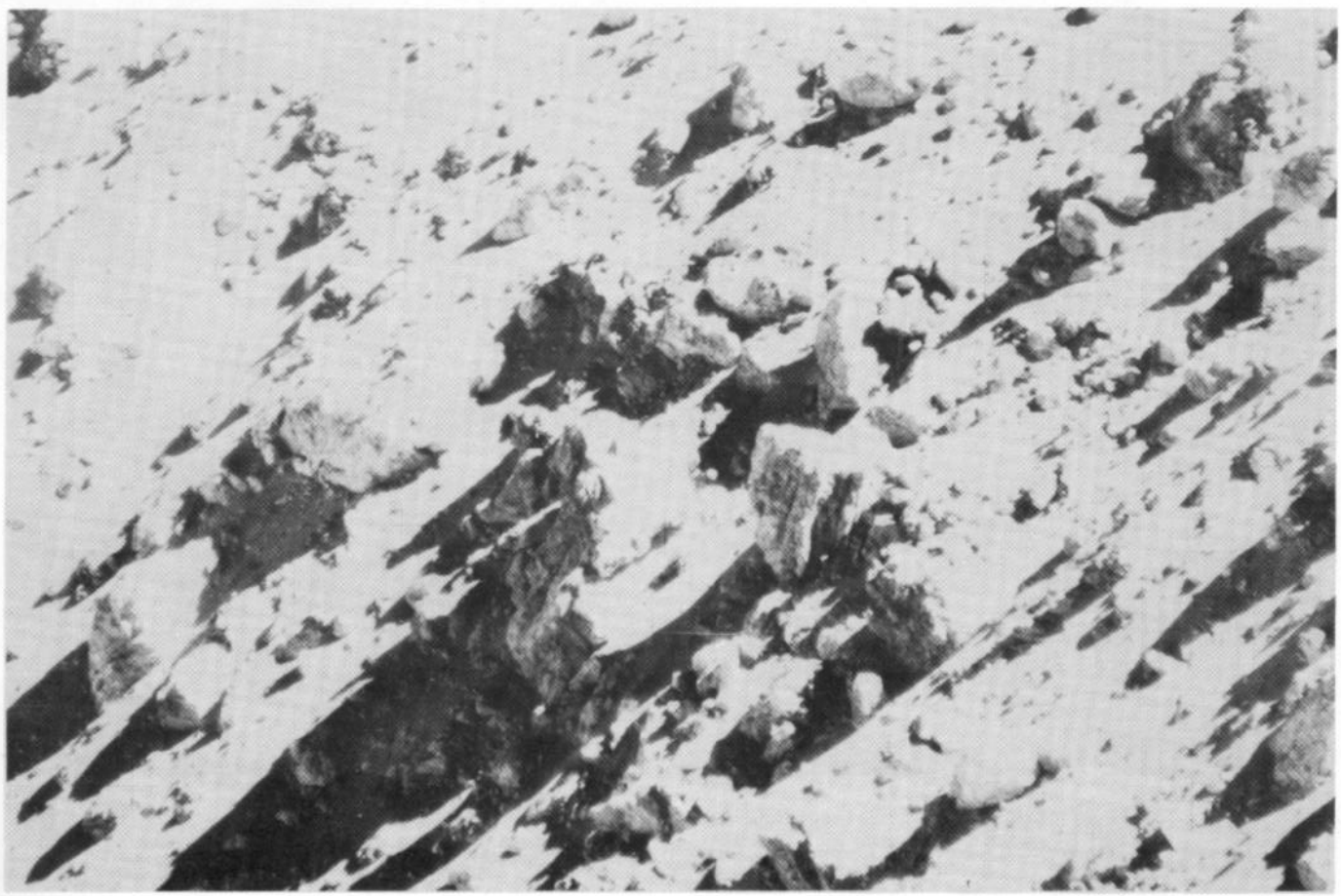

FIGURE 23.-Telephotograph of large light-matrix breccia blocks on northeast wall of North Ray crater. Intentionally underexposed to enhance textures in shadows. From AFGIT (1973). Reprinted with permission of the American Association for the Advancement of Science.

Figure 24.-Broken fragments and fines of sample 67455, a light-matrix breccla collected from the top of a White breccia boulder illustrated in figures 10 and 254. Note few small dark clasts. NASA S-72-38194. Cube is 1 cm.

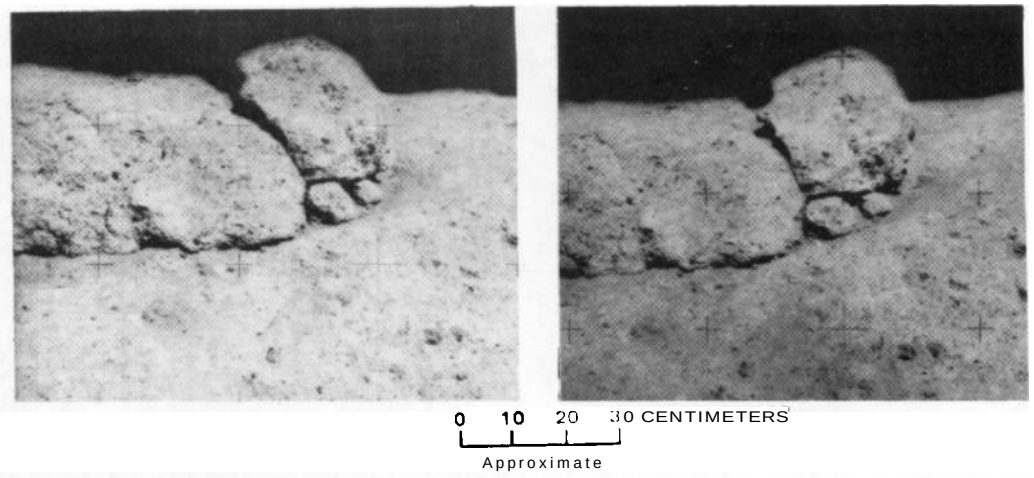

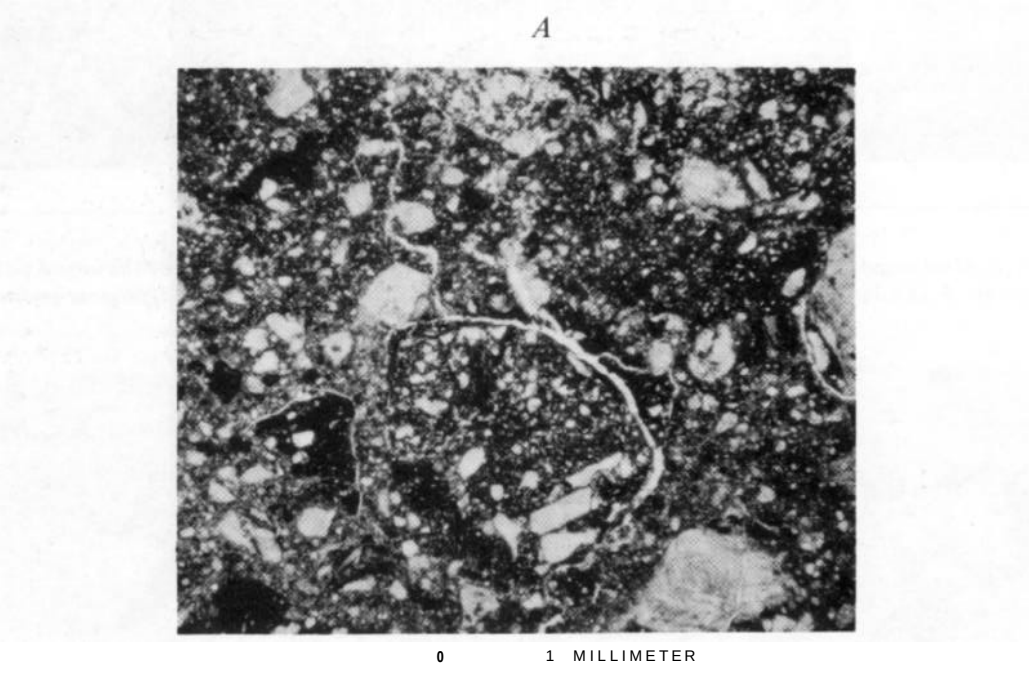

FIGURE 25.--Sample 67455. ***A,*** Stereopair of the top of a White breccia boulder and the fragments of sample 67455 before sampling. AS16-106-17331 17332. ***B.*** Photomicrograph of 67455, 57 illustrating irregular fractures that penetrate the matrix of shocked feldspar grains but avoid dark-matrix Plane-polarized light.

The rapid mechanical breakdown of these rocks relative to the dark-matrix boulders may be explained by a combination of thermal cycling, which doubtless causes unequal expansion of the dark clasts and light matrix, and micrometeorite bombardment of the surface whereby the rock disintegrates along the irregular fractures and the more coherent fragments collected in the rake samples are preferentially preserved. These processes do not appear to be as effective in the dark-matrix boulders.

A dark-matrix breccia clast (67475) collected from the same boulder as 67455 illustrates very well the criteria by which some clasts can be identified, even when separated from their host. Three views of 67475 (fig. 26) show the weathered surface, a fresh dark-matrix surface, and a surface coated with the feldspathic host material. Fragment 67718 from a rake sample in the Interboulder area is another specimen whose surfaces reveal its relation to the host (see Smith and Steele, 1972, p. 81).

Other samples in the White breccia boulder area that exceed 100 g in weight and probably represent the majority of rocks there are shown in figure 27. The only crystalline rocks recognized by Wilshire and others (this volume) are 16 rake samples classified as metaclastic (C_2); all but one of these weigh less than 25 g. Their occurrence as smaller rocks suggests only that they are residual coherent clasts "weathered" out of the local boulders. Two examples of such clasts within light-matrix breccias are 67415 and 67455 (fig. 28).

One rock, 67215 (also weighing more than 100 g), was collected because of its unabraded rock surface. It is described by Horz and others (1972, p. 7-25) as a moderately tough breccia. This rock has not been studied (as of this writing).

INTERBOULDER AREA

Approximately midway between the White breccia boulders and House rock is a sampling area chosen because it was relatively free of large rocks (fig. 13). From this location, a third photographic survey (east panorama, pl. 9, pan 20; and fig. 4) was taken of the far crater wall. (Table 4 and figs. 13A, B, and *29A-E* show the types of breccias collected in this area.) Light-matrix breccias, typified by 67055 and 67075 (fig. *29B, C*), are abundant but not as predominant as in the White breccia boulder area. The appearance of sample 67075 in this section is typical of a crushed anorthosite (B_1) breccia (fig. 30). Samples 67015 and 67115 (fig. 30A, *E*), assigned to the intermediate B_3 class by Wilshire and others (this volume) are considered here to be light-matrix breccias because of their matrix color and friable textures. The one dark-matrix fragment collected (67718, 49 g) is covered with white material (Smith and Steele, 1972, p. 82-l) indicative of its former location within a light-matrix host. Rock 67095 (fig. 29D), glass-coated and cemented, is a good example of the glass of class G of Wilshire and others (this volume). Astronaut Young associated it with a l-m secondary crater on the North Ray rim; it may be an exotic arrival postdating the North Ray event or, alternatively, a fragment of late-stage melt from North Ray.

Fragments weighing less than 25 g and collected in the Interboulder area (see figs. 13B, 14) reflect a concentration of intermediate-gray-matrix breccias (B_3) collected mainly in the rake sample (67715-67776). This breccia class appears to be transitional between the light- and dark-matrix breccias and is most commonly listed with light-matrix breccias as an alternative designation by Wilshire and others (this volume). Its origin may be considered similar to that of the light-mat&ix breccias, with some enrichment in the dark glass components. Consequently, a selective concentration of more resistant clasts of B_3 material occurs as residuum from an inferred light-matrix (B, and B_2) host rock. Rock 67235, like 67215 from the White breccia boulder area, has not been studied as of this writing but is described by Horz and others (1972, p. 7-25) as a hard recrystallized breccia in appearance.

SHADOW ROCK'AREA

Station 13 was planned for the outer edge of the continuous ejecta blanket of North Ray crater. The objective was to collect a radial sample in the region where the shallowest stratigraphic material would be present. As the outer edge of the ejecta blanket was not identifiable, the astronauts selected a location in the vicinity of several large boulders described while enroute to the crater rim crest.

The primary source of rock samples greater than 25 g was the single large boulder named Shadow rock, about 5 m long and about 4 m high. It has a distinct moat around its base (fig. 9), presumably part of a shallow secondary crater created by impact of the boulder when ejected from North Ray crater. No.fillet of material was shed from its surface. Its shape and apparent resistance to erosion suggest that it is similar to the dark-matrix breccias in the House rock area. And its color and texture are typical of dark-matrix rocks (illustrated close-up in figure 31).

Of the rock samplescollected at station 13, (table 5) only one, 60017, weighs more than 100 g (fig. 32). It is very dark, fine grained, and vesicular and apparently has a high percentage of glass in its matrix. Prominent elongate vugs or vesicle pipes were noted by Astronaut

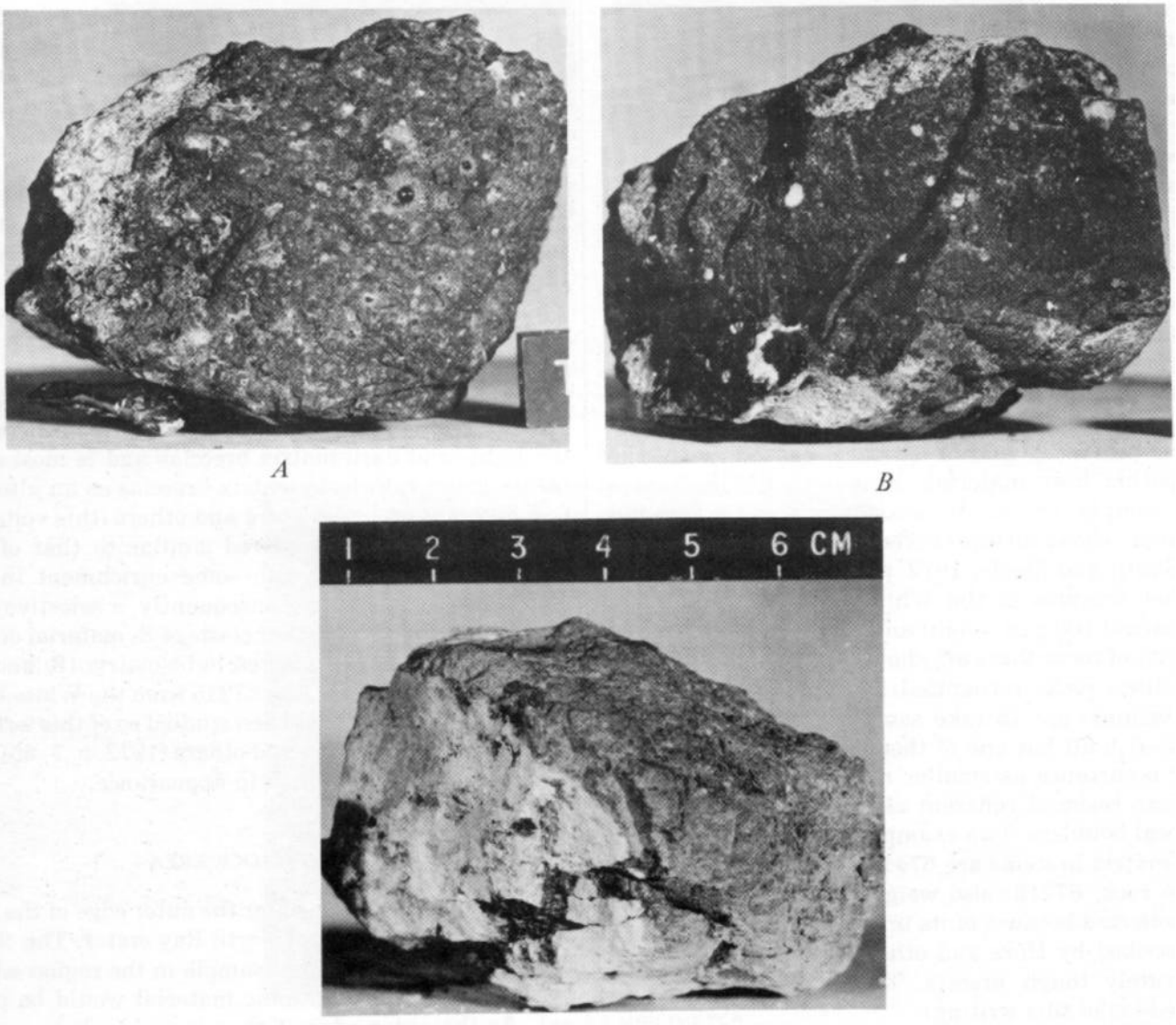

Figure 26.-Sample 67475, a dark-matrix clast from the White breccia boulder of 67455. ***A,*** Weathered surface with glass-lined zap pits (NASA S-72-43359). ***B,*** Fresh broken surface showing white feldspathic clasts (NASA S-72-43363). C, Broken surface showing coating of light feldspathic matrix of host material (NASA S-72-37958).

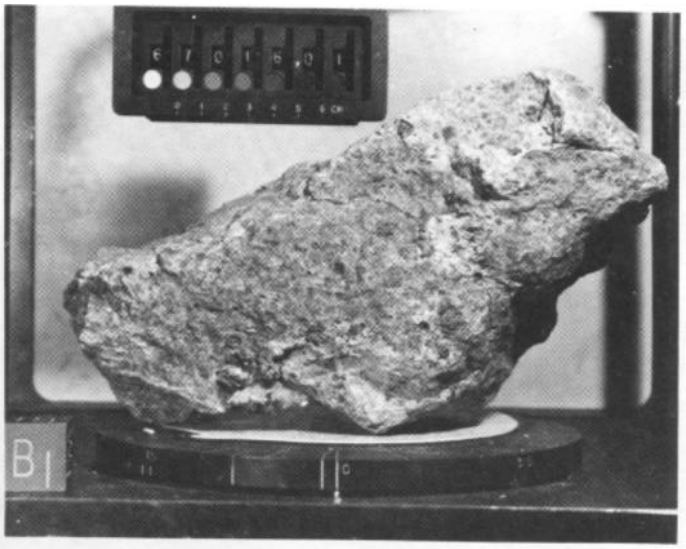

A

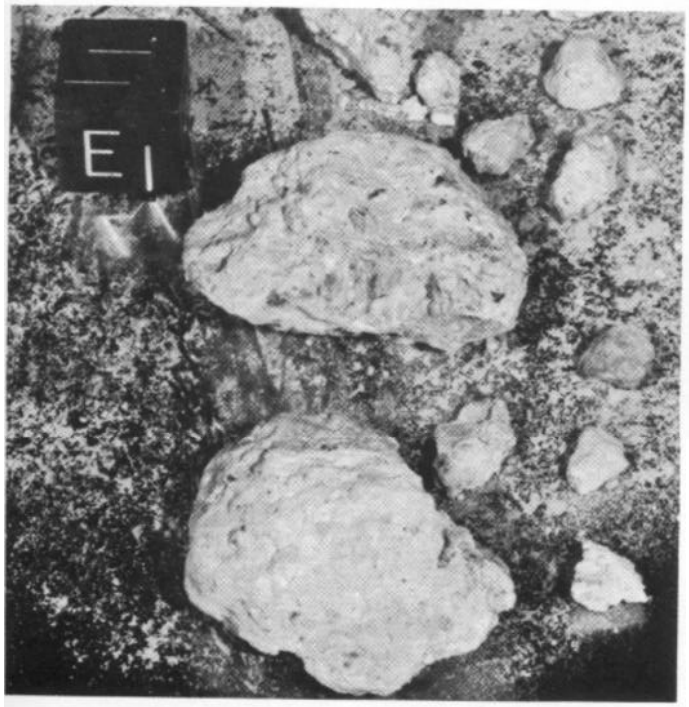

B

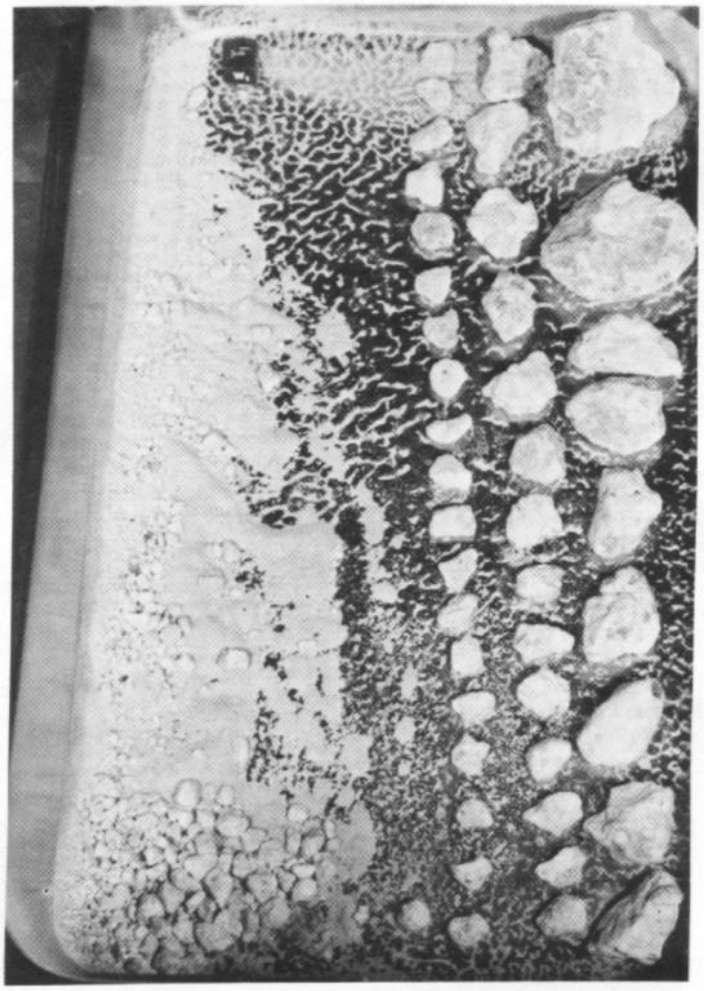

C

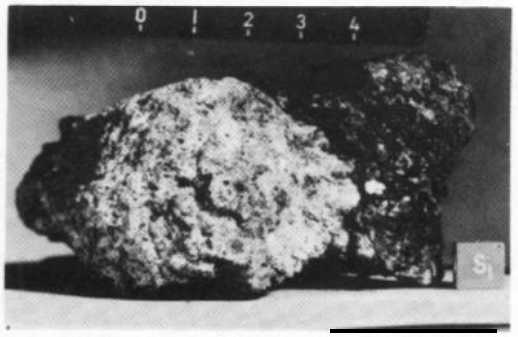

D

FIGURE 27.-Sevcrd rocks heavier than 100 g collected in the White breccia boulder area. A, Part of 67016, intermediate-gray matrix (B_3 of Wilshire and others, this volume\. S-72-39230. B. 67035, light-matrix (B_2) broken in transit, S-72-37542. C:, 67415, light-matrix (B_1) broken in transit, .S-72-39038. D, 67435. half light, half dark. (B_4 of Wilshire and thin volume). S-72-43897 stereopair.

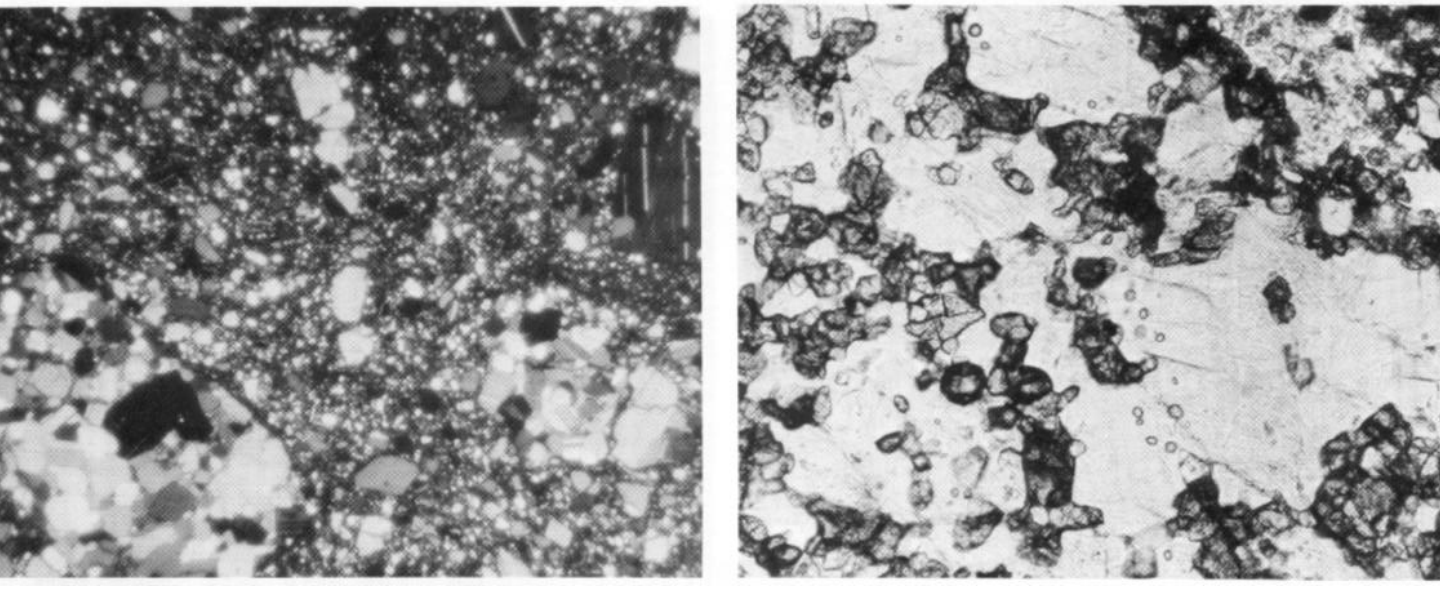

FIGURE 28.-Photomicrographs of metamorphic clasts within light-matrix breccias. A, Granoblastic plagioclase clasts in matrix consisting predominantly of crushed feldspar: 67415 14; cross-polarized light. B, Poikiloblastic plagioclase enclosing mafic minerals: 67465 57; light.

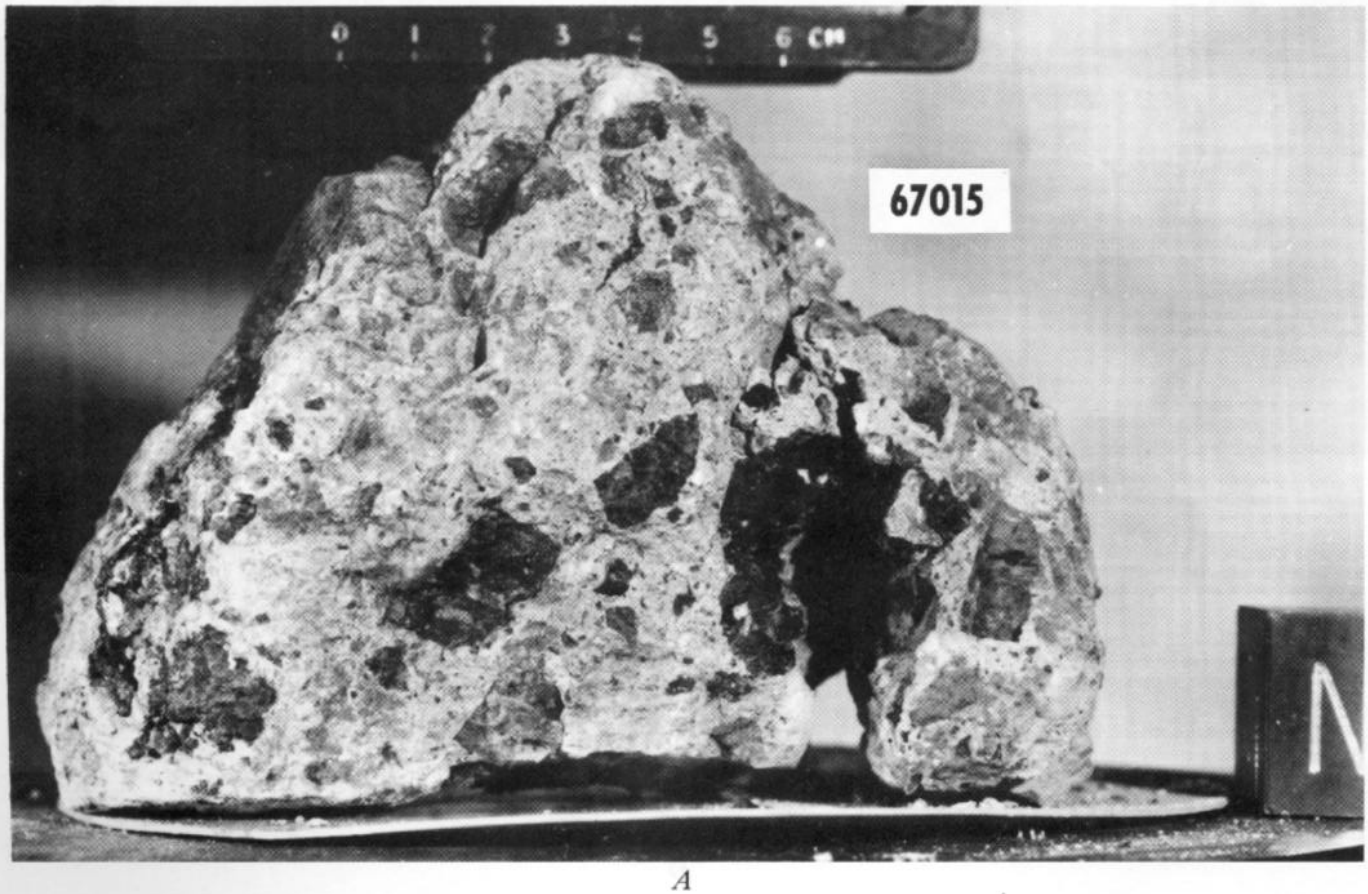

29.-Caption on facing page.

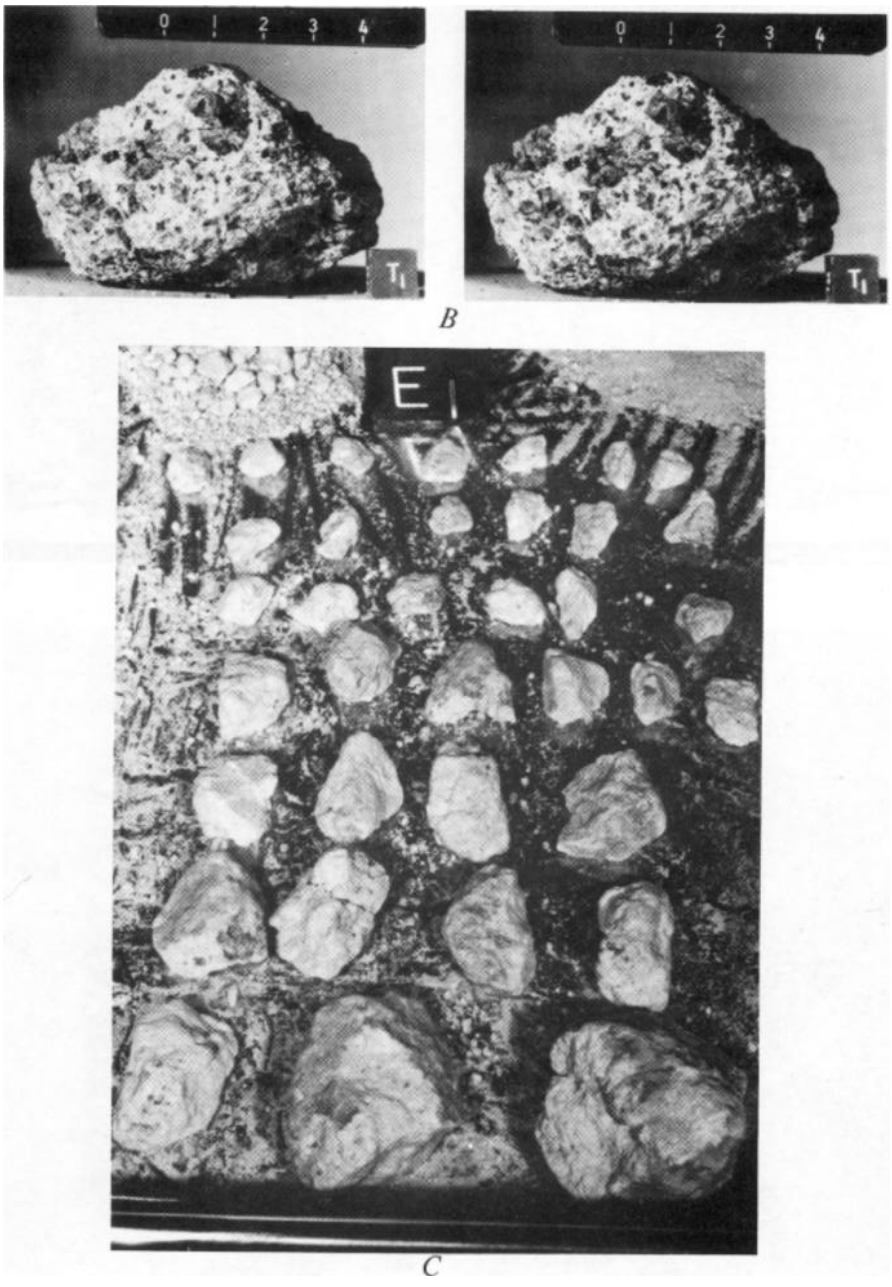

FIGURE 29.-Rocks heavier than 100 g collected from the Interboulder area. *A, 67015,* light-matrix (B_3 of Wilshire and others), S-72-37216. B, 67055, light-matrix (B_2), S 72-43880 stercopair. C, 67075,light-matrix (B_1), S-72-37539. D, 67095, glass coated (G), S-72-43076 stereopair. E, 67115, light-matrix (B_3 of Wilshire and others), ,S72-37718.

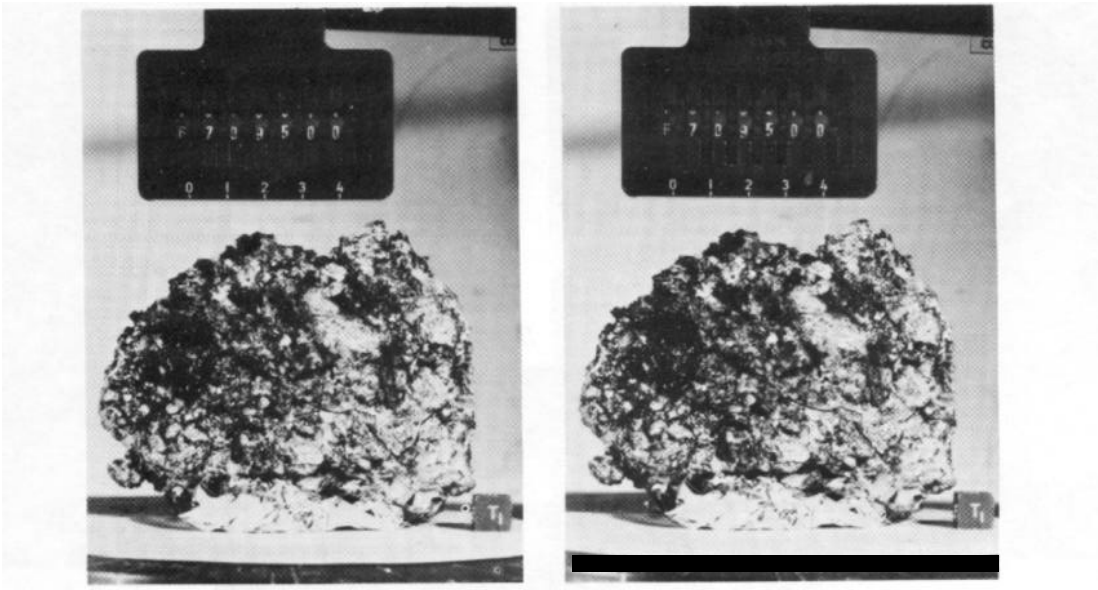

D

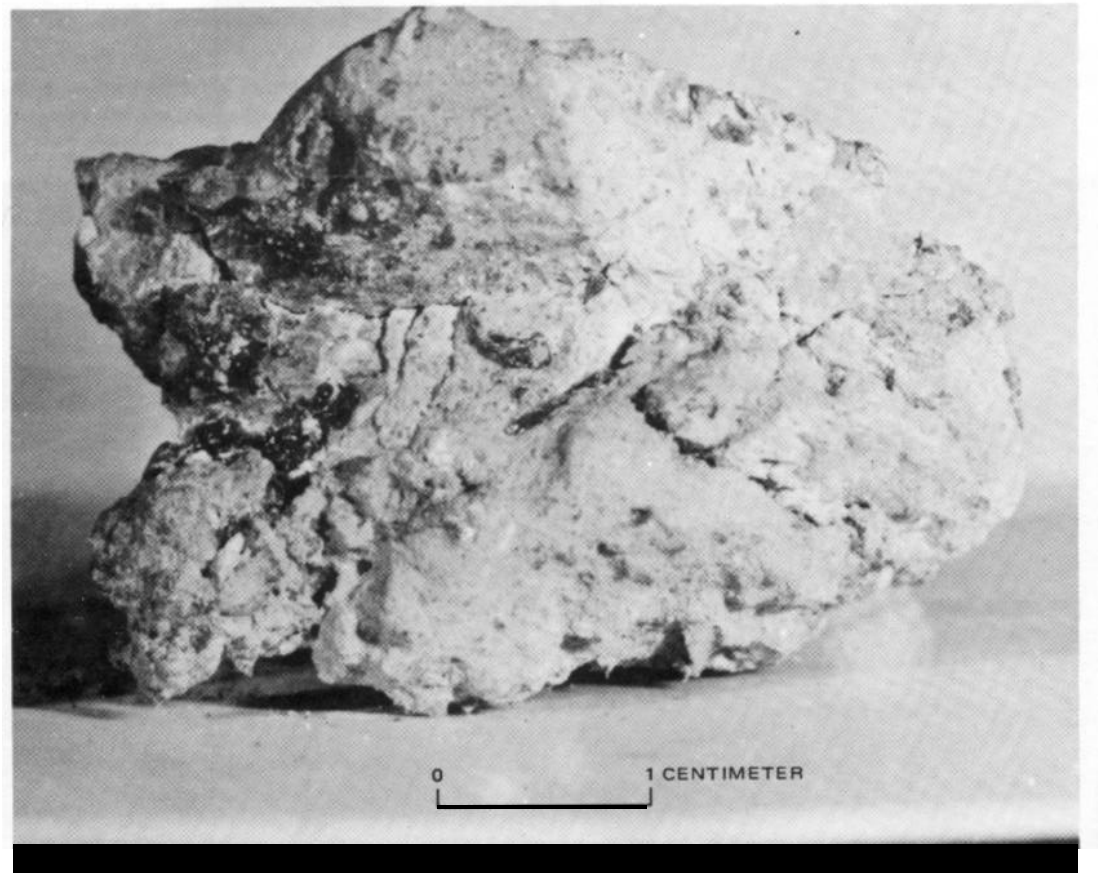

E

FIGURE 29.-Caption on preceding page.

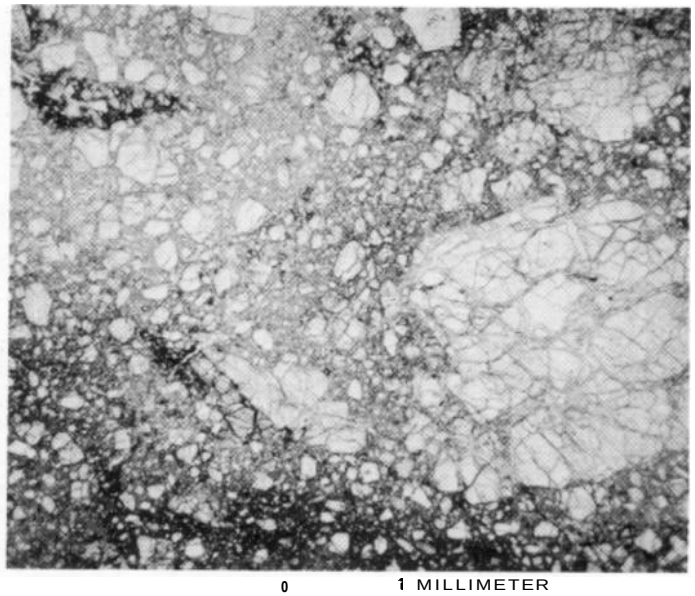

A

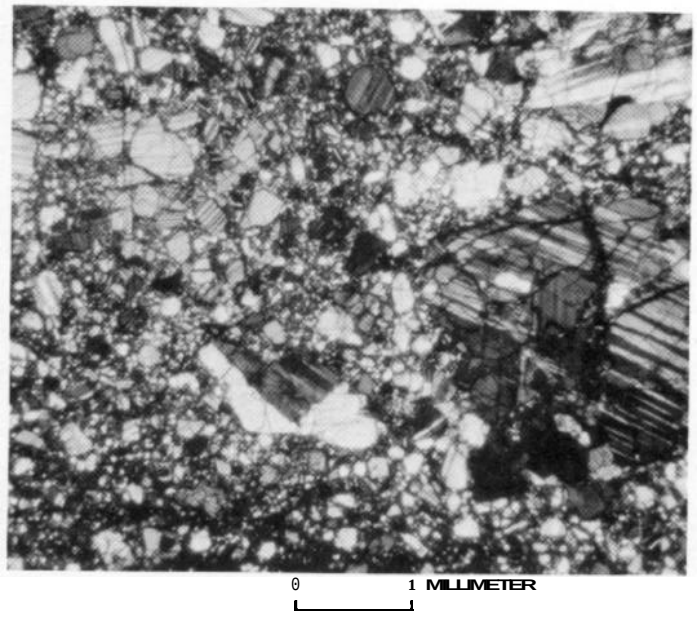

B

FIGURE 30.-Photomicrographs of a typical light-matrix hreccia from the Interboulder area. *A*, Plane-polarized light. B, Cross-polarized light. Glass occurs as veinlets within larger plagioclase clasts and in fine-grained matrix.

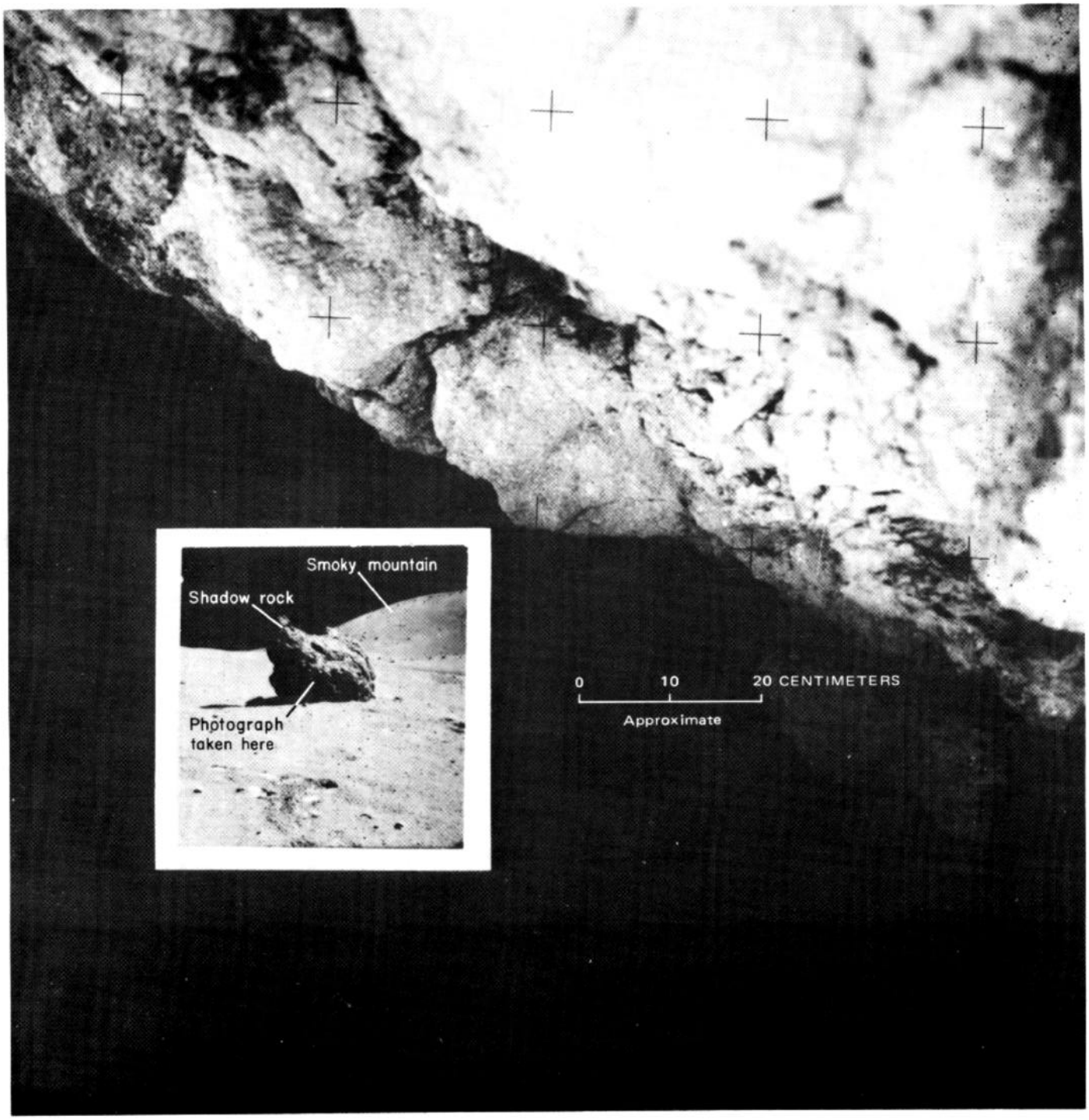

FIGURE :31.-Surface texture of Shadow rock. Closeup of overhanging southwest corner (arrow). AS16-106-17410; inset photograph AS16- 106- 17393: view is northeast.

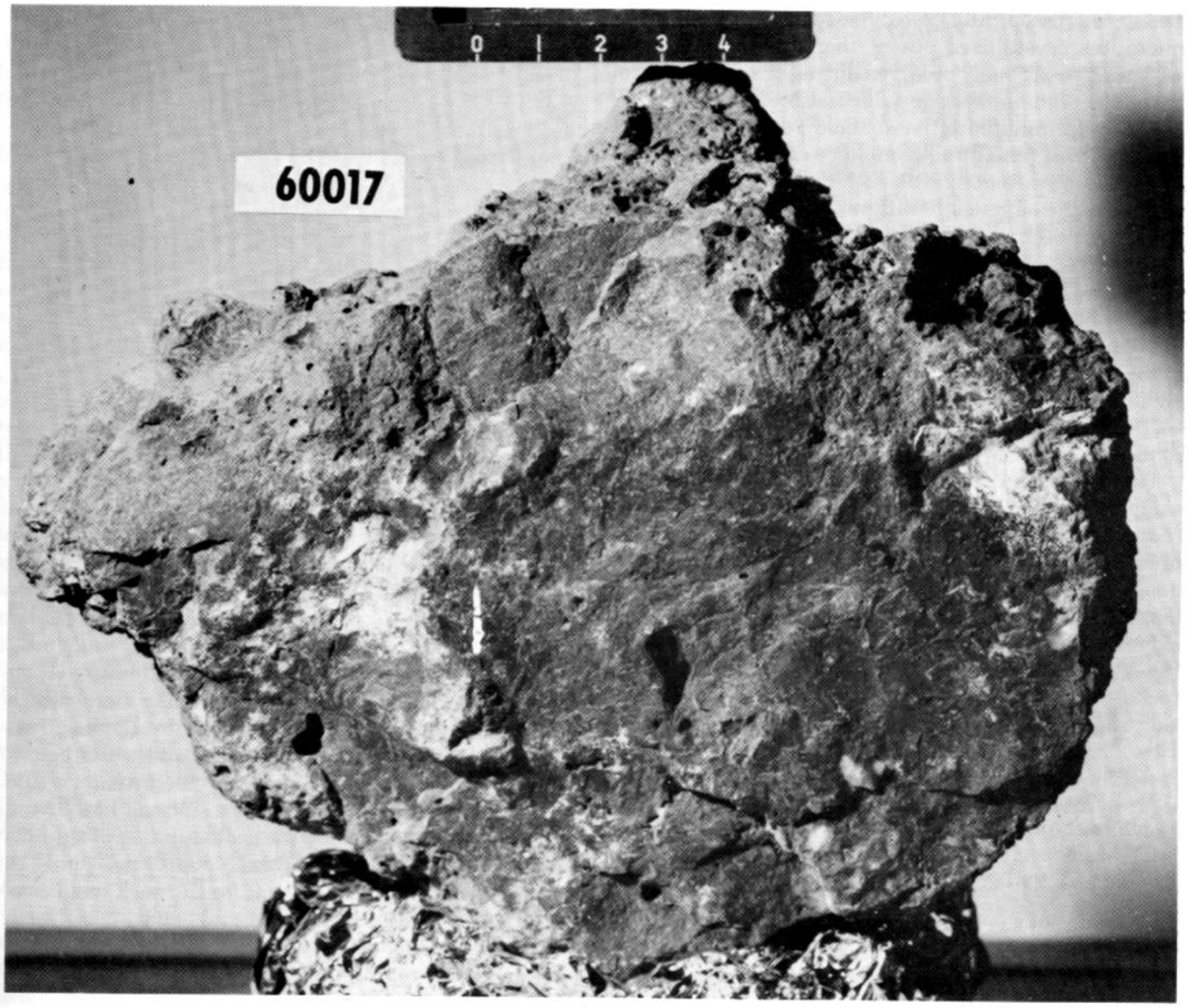

FIGURE 32.-Dark-matrix breccia, 60017, (B_1) from near Shadow rock. Scale in centimeters. NASA S-72-36943.

Duke. Microscopically, it can be seen that plagioclase microlites crystallized out of the glassy matrix and vesiculation probably occurred during the quenching of the glass; some late-stage vesiculation is indicated by abruptly terminated laths at some vesicle boundaries (fig. 33). The remaining samples weighing more than 25 g are dark-matrix (B_4, B_5) and metaclastic (C_2) rocks. Of the samples less than 25 g, a large number (nine) are tentatively classified as intermediate-gray-matrix breccias (B_3) (Wilshire and others, this volume); 11 are dark-matrix breccias (fig. 14). Metaclastic and glassy rocks collected in the rake sample, 5 to 10 m west of Shadow rock, probably represent rocks high in the North Ray walls. Removal from these assignments of samples of uncertain classification (fig. 14) leaves few samples that can be interpreted with confidence.

The most significant rocks, then, are the largest samples derived from a known local source, Shadow rock. Like House rock and Outhouse rock, Shadow rock must have been derived from North Ray crater and deposited late in the ejecta sequence; otherwise later deposits would have banked against its northwestern side. Whereas most of the local blocks are light colored (fig. 12), Shadow rock belongs to a small group of dark rocks that are larger and more angular than most of the fragments (about 20 percent of all the blocks in view). It is probably part of a,discontinuous ray of dark resistant breccias from a deep unit that is overlain by light-matrix rocks in North Ray crater.

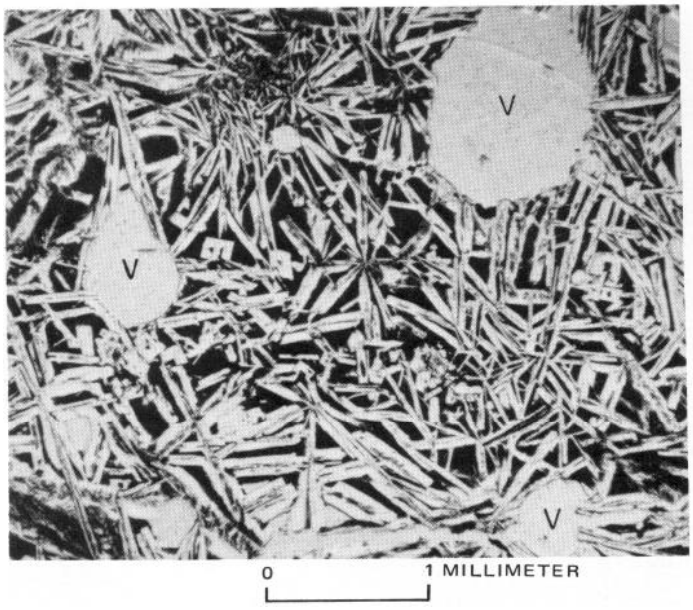

FIGURE 33.-Photomicrograph of 60017, 112, showing vesicles (V) that both conform to and crosscut plagioclase quench crystals in glassy dark-matrix breccia. Plane-polarized light.

NORTH RAY SOILS

The soils on the rim of North Ray crater are distinct from those at other sampling stations within the traverse area in that they are generally very thin and light in color. They are similar to one another in modal and chemical composition (Heiken and others, 1973, p. 261-263). Light-matrix breccias are especially abundant in .these soils (approximately 40 percent, G. J. Taylor and others, 1973, fig. 8).

The soils at each of the sampling localities (table 6) were described by the astronauts. At the White breccia boulders, where large fillets occur around the very friable rocks, Duke commented, "The regolith here * * * on this crater rim is really soft. We're sinking in on the slopes about six inches or so" (see fig. 10). Elsewhere it was a centimeter or less as indicated by the bootprints in the station 11 panorama (pl. 8, pan 18). At the Interboulder area, illustrated in the foreground of figure 4, descriptions were, "Right under the upper dull-gray soil there's a layer of whitish material, much like it was at South Ray" and "It's hard under there * * * there must be a big rock under here. I can't get the rake in * * * It's all white under here. Down about a centimeter or less, it's all white" (Duke). This color difference, gray on the surface and white below, was also described near Shadow rock (station 13) and everywhere else at the site except stations LM, 8, and 9. It is probably caused by the accumulation of agglutinates at the surface (Adams and McCord, 1973, p. 171), a process that may also account for the dark tongues of surface debris seen draping the upper wall of North Ray in figure 3. The lighter areas between these tongues may represent more active soil movement downslope, where darker soils have slid away. Low scarps commonly border the more stable gray slopes, and a few boulder tracks are present where larger fragments have rolled or slid downward.

The agglutinate contents of the darker soils, much lower than elsewhere in the traverse area, indicate a lack of maturity and thus the low relative age of North Ray soils (McKay and Heiken, 1973, p. 42). Exposure ages have been reported as 30 to 60 m.y. (Schaeffer and Husain, 1973, p. 1858; Kirsten and others, 1973, p. 1775; Turner and others, 1973, p. 1903; Marti and others, 1973, p. 2039).

At House rock, Duke, while attempting to sample the east-west split (fig. 8), reported, "This soil here is very hard and the rake really won't go into it. It's bending tines * * *. The purpose of sampling in the west-trending opening was to obtain materials (soil 67940) shielded from the solar wind and to identify, by

comparison with a nearby reference soil sample (67960), the components concentrated or redistributed by the solar wind. No chemical or modal differences are found in these soils (Heiken and others, 1973, p. 262); only minor contributions of soil-size particles spalled from the adjacent boulders are recognized. Adams and McCord (1973, fig. 4 and p. 170), however, found a lower reflectance for 67941[1] when compared with 67461 from the White breccia boulder area, even though the agglutinate contents are the same (20 percent). They attribute the lower reflectance of the House rock soils to enrichment in dark-matrix breccia fragments.

At Shadow rock the astronauts collected a soil sample from beneath the overhang on the west end of the rock in the deepest recess (fig. 31). It was hoped that the sample had been permanently in shadow since the rock was emplaced, and the investigators intended to determine whether volatile elements had been concentrated in such a cold trap. The shadow at the time of sampling is shown in figure 34; the sun elevation angle was 46" above horizontal, its azimuth was 12" north of east. At sunrise and sunset, the maximum progression of the sun's azimuth is 1" to 2" north of an east-west line. This and the estimated movement of sunlight into the shadowed area (shown on fig. 34) during a single lunation make it unlikely that any exposed soil remains permanently shadowed, despite Astronaut Duke's observation that the shadowed area was downslope (beneath the rock). A second soil sample (63340) was collected from beneath the first and therefore was a buried soil rather than an exposed shadowed soil.

The North Ray soils have not been found to differ significantly in lithophile trace-element abundances; strontium contents are slightly higher in these soils than elsewhere, probably reflecting higher plagioclase contents in North Ray target materials (Philpott and others, 1973, p. 1433). North Ray rim soils (including 67941) exhibit no apparent differences in carbon content but as a group are significantly lower in carbon than all other Apollo 16 soils measured by Moore and others (1973, p. 1616). If carbon content is mainly a product of solar wind effects, the contribution on the rim of North Ray crater is relatively small and is the same for the east-west split as in unshielded areas.

The apparent meteoritic component in the North Ray soils is lower than elsewhere; this too is indicative of relative immaturity (see Freeman, this volume).

[1]The fifth digit "1" in sample numbers denotes the sieve fraction of soil that is less than 1 mm.

GEOPHYSICS

Geophysical data in the North Ray area consist of a single three-vector reading on the Lunar Portable Magnetometer at station 13. The resultant magnetic anomaly reported was about 300 gammas, down and to the southwest, the largest recorded at this site and larger than any recorded at Apollo 14 or 15 sites (Dyal and others, 1972, p. 12-7). This and the readings from station 2 and in the LM area are interpreted by Strangway and others (1973, p. 113-114) as indicative of a breccia blanket of the order of 1 km thick under the Cayley plains. This blanket, by their hypothesis, was emplaced within a field of a few thousand gammas cooled from a temperature higher than 700°C, forming a moderately welded rock mass with a high remanent magnetization.

The only lunar rocks known at this time (1974) to have stable magnetization sufficient to fit this model are a moderately welded, dark-matrix soil breccia (15498) from Dune crater at the Hadley-Apennine (Apollo 15) site and an Apollo 11 chip from soil 10085 (Strangway and others, 1973, p. 113). As unwelded materials and (surprisingly) highly welded and igneous rocks do not carry strong remanent magnetizations, it is possible that the large magnetic fields required are produced by local or regional impact events (such as 10-km or larger craters) wherein only the melted and rapidly cooled breccias retain the transient fields. The igneous-textured rocks cooled slowly enough that the short-lived impact-induced fields had disappeared by the time they passed through the Curie point. The melt-poor light-matrix breccias, never hot enough to pass through the Curie point, therefore were not magnetized.

SUMMARY

North Ray crater proved to be an excellent source for a large variety of samples and photographs representing the best available documentation for stratigraphic interpretations anywhere in the Apollo 16 traverse area. The rounded form of the crater rim and the convex shape of its generally smooth walls indicate a target material of relatively low strength.

Rocks on the rim and wall of North Ray crater are mainly of two types: light-matrix and dark-matrix feldspathic breccias with clasts and inclusions of glassy to crystalline texture. The large boulders (0.2 m and larger) are mainly light-matrix breccias (B_1, B_2 of Wilshire and others, this volume); many have well-rounded profiles and have accumulated deep fillets of soil by erosion of their friable surfaces. Similar rocks occur as possible outcrops in the upper half of the crater wall. Dark-matrix rocks (B_4, B_5) make up 10 to 30 percent of the boulders present and appear to be very

resistant. to erosion. Generally perched or sitting within shallow depressions, they are interpreted as the deepest material exposed in the crater wall and therefore the latest to be deposited on the crater rim.

The small fragments (2 to 25 g) collected in soils and rake samples reflect in part, the more resistant components contained interstitially and as clasts within the larger boulders. These include the coherent dark- and intermediate-gray (B_3) breccias, metaclastic (C_2) rocks, and holocrystalline fragments with igneous textures (C_1 of Wilshire and others). The metaclastic and holocrystalline rocks were documented from the matrix of only one boulder, the dark-matrix breccia called Outhouse rock. Light-matrix breccias and glass-coated fragments (G) are common locally in the smaller samples and as clasts from the dark-matrix breccias.

The sample suite is divided into four subgroups based on their locations. Three are on the rim crest of North Ray, the fourth is near the edge of the continuous ejecta blanket. Of 148 rock samples, only a fourth weigh more than 25 g, but these probably represent the abundance and distribution of rock types more accurately than do the smaller fragments. Light-matrix breccias characterize two of the three rim crest areas; dark-matrix breccias with associated metaclastic and igneous inclusions are typical of the large dark boul-

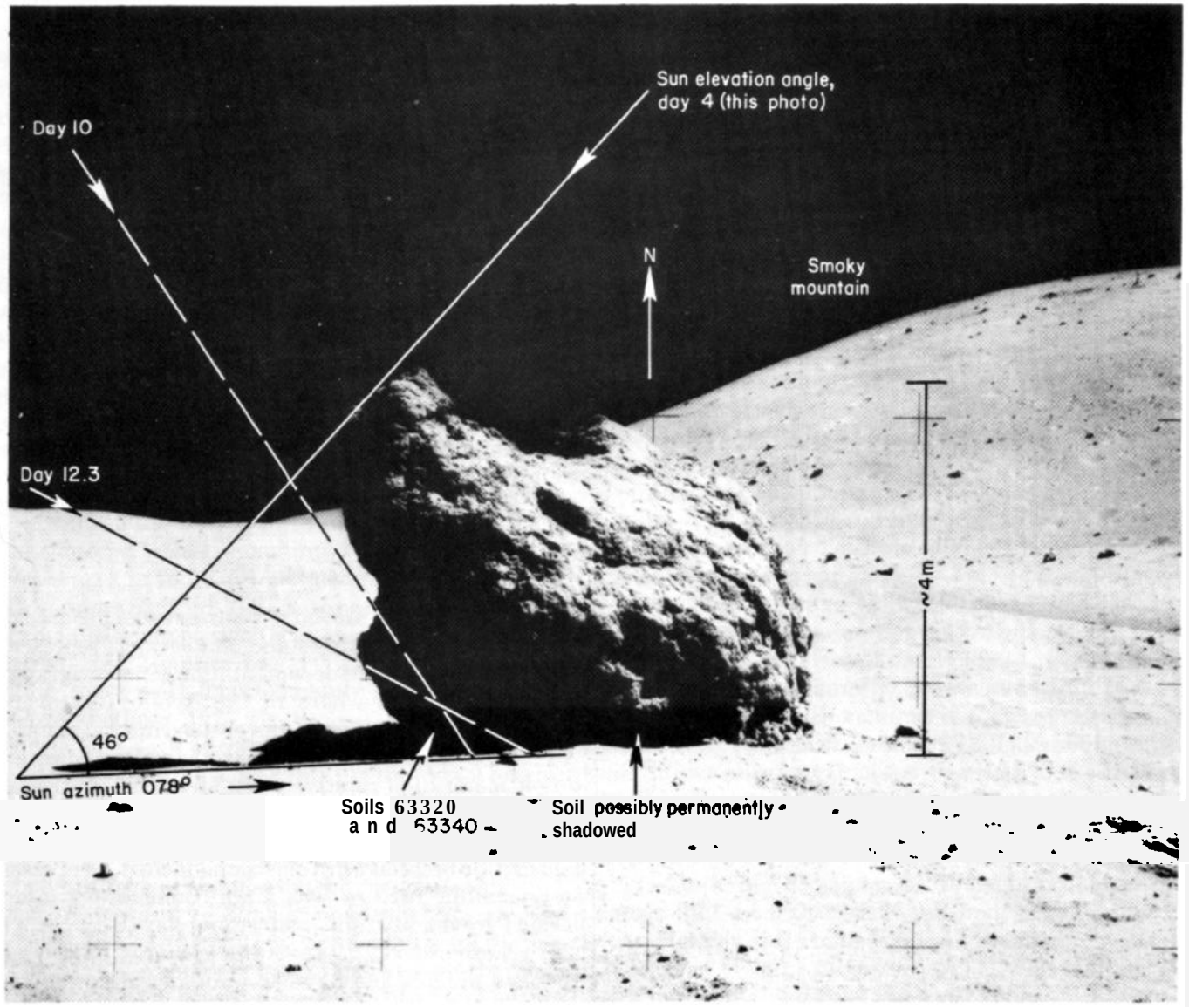

FIGURE 34.-Estimated exposur toesunlight beneath overhang of Shadow rock during one lunation. Predicted sun-elevation angles (dashed lines) for earth days 10 and 12.3 correspon to inclined surface on Shadow rock above soil sample 63320. Angle error due to changing sun azimuth is 2° to 3". AS16- 106- 17393.

ders at one rim crest site and at station 13, 0.75 km away. Shadow rock, at station 13, appears atypical of the normally light-colored block population on the outer rim. It is therefore interpreted as part of a discontinuous ray extending southeast from the crater rim. The light-matrix materials that constitute the main fragment population are derived from at least the upper half of North Ray (possibly deeper) and overlie a zone of dark material indicated by a small mound on the crater floor. The stratigraphic implications for other parts of the landing site are discussed by Ulrich and Reed (this volume).

The generally thin regolith (about 1 cm) thickens to 15 cm or more where it forms fillets around the friable light-matrix boulders. The soils on this fresh crater rim are generally very light gray but not as light as those immediately beneath the surface. Their mineral compositions, while distinct from other areas, are reported to be very similar within the North Ray ejecta blanket. Mass movement on the steep crater wall and rim has transported soil and a few blocks toward lower areas.

Magnetic readings from the Lunar Portable Magnetometer were high where measured at station 13. They are believed (Strangway and others, 1973) to reflect moderately welded breccias that were emplaced and cooled from temperatures higher than 700°C in a field of a few thousand gammas. In view of the apparent lack of remanent magnetization in more crystalline rocks, it is suggested here that the magnetic field was very short lived and was induced by a large local or regional impact event affecting only melt-rich breccias that cooled rapidly, thereby retaining the transient field.

D3. GEOLOGY OF AREAS NEAR SOUTH RAY AND BABY RAY CRATERS

By V. STEPHEN REED

CONTENTS

ILLUSTRATIONS

TABLES

INTRODUCTION

The surface of the southern part of the Apollo 16 ding site is dominated by fragmental debris derived m South Ray crater (fig. 1). Although the crater was of actually visited, several samples collected can be directly attributed to that impact event. Premission maps by Hodges (1972a) and Milton (1972) from Apollo 14 orbital photographs show a distinct ray pattern around the crater. Traverse station 8 was planned as a sampling site for ray material excavated from South Ray crater, station 9 as an interray sampling site. South Ray Crater, 680 m in diameter and 135 m deep, is near the western flank of the Descartes mountains on a plains surface underlain by the Cayley Formation. Mapped as a young Copernican crater by Hodges (1972a), it appears extremely fresh, with a sharp, raised rim and abundant blocky ejecta (fig. 2). A smaller, 130-m diameter crater, Baby Ray, lies about 1.8 km northeast of South Ray crater, also in smooth plains. Younger than South Ray crater (mapped as the youngest Copernican crater material by Hodges, 1972a), its rays overlie the South Ray debris.

The two major rock types collected in the station 8 and 9 areas are dark-matrix breccias and light-colored igneous rocks. This paper presents evidence that the samples collected are impact ejecta from South Ray crater and that they represent some of the materials visible in the walls of the crater.

DESCRIPTION OF SOUTH RAY AND BABY RAY CRATERS

SOUTH RAY CRATER

South Ray crater is a fresh-appearing blocky crater with a sharp, raised rim (figs. 2, 3). About 50 m below the rim crest, is a discontinuous terrace is visible on the low-sun photographs. The interior of the crater is exter-emely blocky; a large mound of blocky debris occupies the central part of the floor. A few dark patches are visible in the upper third of the crater wall.

On the high-sun Apollo 16 photographs, bright rays extend at least 15 km northeast, overlying North Ray crater ejecta, 10 km to the north (fig. 4) (ALGIT, 1972a and AFGIT, 1973). Blocks were deposited in abundance as far as Survey ridge, 4.5 km to the northeast, where the highest concentration of blocks found during the traverse occurred (Muehlberger and others, 1972).. It is likely that the 10-m relief on Survey ridge is constructional, made up of ejecta from South Ray, as ages with amplitudes of 10 to 30 m are common the plains. The ridge probably formed by the intersection of two large old subdued crater rims that. intercepted a mass of South Ray impact debris traveling on low: trajectory.

The ejecta are distributed asymmetrically around South Ray crater, being practically absent southwest of the crater. Boulders appear concentrated mainly in three directions (fig. 1) that correspond roughly to the three principal trends of high-albedo material. One of these blocky rays trends directly toward stations 8 and 9. Several linear grooves on the surface are radial to South Ray crater. At the ends or along the margins of many of the grooves are large boulders. The continuous ejecta thins rapidly outward from the crater, as several dark-haloed craters have excavated dark material from beneath the light South Ray ejecta.

BABY RAY CRATER

Baby Ray crater (figs. 3, 5) is a fresh blocky crater, 130 m in diameter, about 1.8 km northeast of South Ray crater on the rim of an old, subdued 1.1-km crater. Debris ejected from Baby Ray overlies South Ray ejecta. High albedo of the underlying South Ray material makes it difficult to trace the rays much farther than the limit of the continuous ejecta. Scattered blocks are visible in the orbital photographs and abundant in the telephotographs. In general, the blocks on Baby Ray are smaller and more numerous than on. South Ray.

The interior of Baby Ray crater is unusual-in the following respects. About one-third of the way down the western crater wall is a faint discontinuous concentric terrace (fig. 5). In the eastern wall are two distinct terraces, one in the upper wall, discontinuous across the crater, another that extends almost across the entire width of the crater. These may be slump features rather than terraces reflecting different lithologies. A small dark-haloed crater nested in the center of Baby Ray is similar to other nested craters of the same size range within the landing area. Some subsurface stratum, perhaps more consolidated than the overlying material, may have influenced this morphology (Quaide and Oberbeck, 1968).

GEOLOGY OF THE STATION AREAS

GENERAL DESCRIPTION

Of all Apollo 16 traverse stations, station 8, on the north edge of a high-albedo ray, had the highest probability of location in predominantly South Ray material. Station 8 was planned as a prime sampling station of ejecta from South Ray crater, 3.3 km (about 5 crater diameters) to the southwest. Station 9, between two visible rays near the rim of a 110-m subdued crater about 400 m northeast of station 8, was planned for collection of surface samples in Cayley plains in an area free of South Ray debris. Although stations 4, 5, and 6 were designed for collection of Descartes materials.

A

FIGURE 1.-South Ray crater and surrounding area. *A,* Geologic map. *B,* Apollo 16 panoramic camera frame 4623 on which the geologic map was compiled. *C,* Topographic map of the southern part of the Apollo 16 landing site. Prepared by G. M. Nakata from Apollo 16 panoramic camera frames 4618 and 4623.

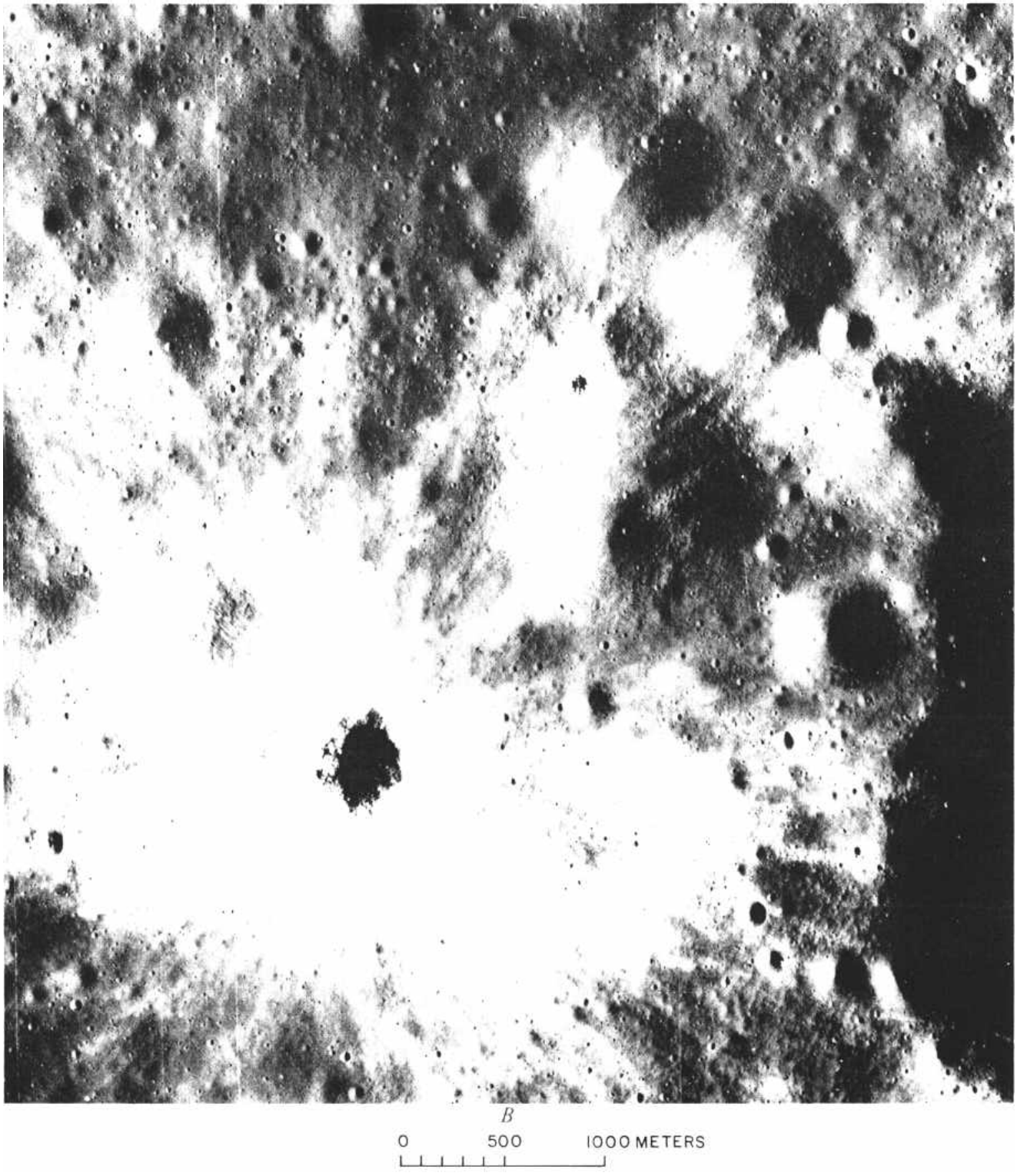

FIGURE l.-Continued.

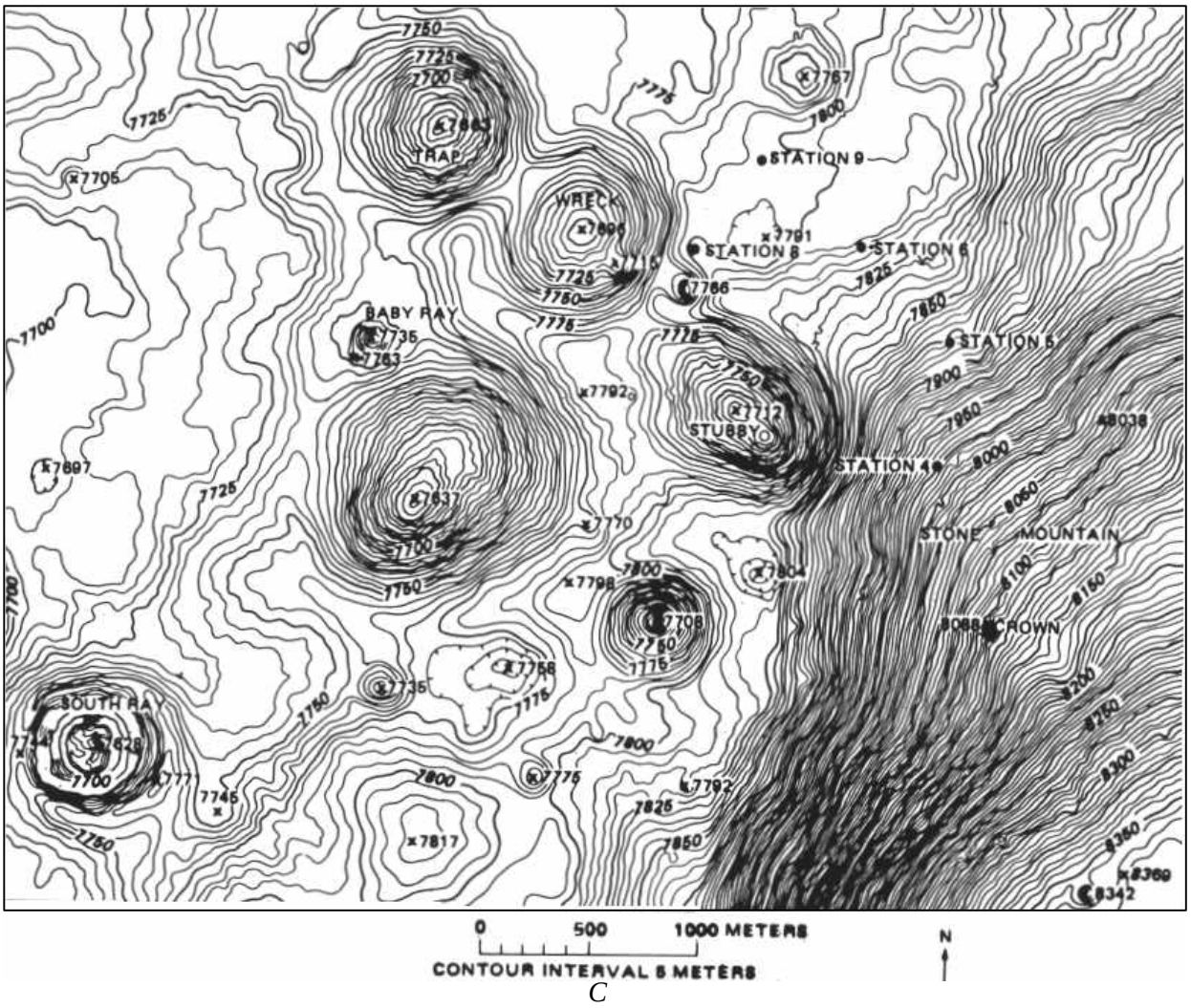

C

FIGURE 1.-Continued.

on Stone mountain, there is evidence (Sanchez, this volume; Muehlberger and others, 1972) of contamination by South Ray debris.

At station 8, fragments larger than 2 cm occupy about 3 percent of the surface, between stations 8 and 9, as much as .6 percent (Muehlberger and others, 1972). In the area of station 9, the fragment population drops to 2 percent, and in the LM/ALSEP area, fragments range from less than 1- percent to as much as 3 percent of the surface, the percentage of larger rock fragments (greater than 15 cm) decreasing northward.

The stratigraphy at stations 8 and 9 was complex prior to the deposition of South Ray ejecta. As station 8 is within the ejecta blankets or continuous rim deposits of four craters having a diameter of about 1 km, the regolith in the vicinity of these stations is probably made up of a series of several overlapping ejecta blankets. Superposed on this surface is debris excavated from South Ray crater. that apparently consists mainly of blocks with very minor distinguishable fines. Evidence against South Ray's being the source of fine material in the soils collected around these stations is the considerably older exposure age of the soils relative to the age of rocks more convincingly representative of South Ray crater (McKay and Heiken, 1973; Schaeffer and Husain, 1973; Adams and McCord, 1973; D. A. Morrison and others, 1973; Behrmann and others, 1973; Huneke and others 1973b; Kirsten and others, 1973; Drozd and others, 1974).

Counts of light and dark fragments in the down-sun photographs in the panoramas, where the reflectance most nearly approaches the albedo of the surface, indicate that at least. 75 percent are dark breccias. This estimate is probably somewhat low, as it is difficult to distinguish a dark-colored rock having a flat surface directed toward the sun from a light colored rock.

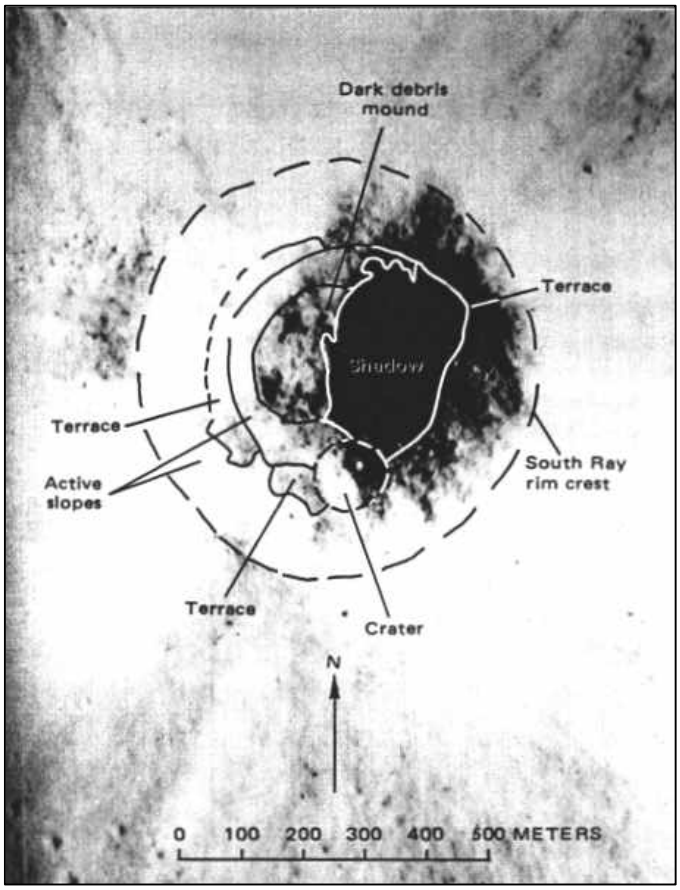

FIGURE 2.-Prominent features of South Ray crater. Photograph enlarged from Apollo 16 panoramic camera frame 4623 (fig. 1*B*).

SAMPLING

Three 0.5- to 1.5-m boulders were sampled at station one 0.5-m boulder at station 9 (figs. 6 and 7). Several soil samples and small fragments were collected from he surface. These samples are shown by rock type in table 1. The larger samples are pictured in figure 8 and photomicrographs of parts of the samples in figure 9.

STATION 8

DESCRIPTION

Station 8 is located on an undulating surface near two subdued 15- to 20-m craters. Regionally the surface slopes gently up to the northeast. Several scattered rock fragments, most of which are in the size range of 5-20 cm, are visible on the surface. The largest block in the area, one from which sample 68815 was collected, is about 1.5 m across.

A small (15-20 m) subdued crater provides direct evidence for the presence of South Ray ejecta in the station 8 area (fig. 10). Boulder 1, from which sample 68115 was collected (fig. 11), is perched on its rim. On the northeast wall, small fragments are abundant and small, fresh craters numerous. The opposite wall is nearly devoid of rocks and fresh craters. The downrange side of this old crater (the side facing South Ray crater) appears to have collected South Ray debris, whereas the uprange side was ballistically shadowed.

SAMPLING

Boulder 1. Boulder 1, approximately 1.5 m across, perched on the northeast rim of its own secondary crater, is rounded in appearance and friable (fig. 11). A large fragment chipped from the boulder (sample 68115) is a dark-matrix dark-clast breccia (B_5) that separated from the boulder along fracture planes intruded by glass. The boulder itself has a predominantly dark matrix with an abundance of light clasts (B_4?,fig. 12). Sample 68115 may represent only the matrix.

The presence of a few small vesicles (fig. 12) suggests that the boulder was at one time partly molten. One area where some of the light clasts have been smeared out appears to have been heated sufficiently to allow mobilization of the matrix. The many fractures in the rock probably account for its friable nature. Dark glass was injected along some of these fractures.

Boulder 2. Boulder 2, a light-gray rock about onehalf m across, was reported by Astronaut Duke to be representative of several he could see on the surrounding surface. Two samples were collected, 68415 from the side and 68416 from the top (fig. 13). The boulder appears homogeneous in photographs of its surface, but minor differences in phenocryst content are seen in the

TABLE 1.-*Samples collected at stations 8 and 9*

A. Boulder samples

	Rock type[1]	Location
68035	B_2	Small fragment near raked area.
68115	B_5	Boulder 1, station 8.
68415	C_1	Boulder 2, station 8.
68416	C_1	Boulder 2, station 8.
68815	B_5	Boulder 3, station 8.
69935	B_4	From top of boulder, station 9.
69955	C_1	From bottom of boulder, station 9.

B. Other samples

	Description	Location
68002168001	Double drive tube	10 m west of 15-m crater.
68120	Soil	Near boulder 1, station 8.
68500	do	From within rake area.
68505	C_2	Collected with the soil 68500.
68510	Rake fragments[2]	From 1 m^2 area near 15-m crater.
68820	Soil	At base of boulder 3, station 8.
68840	do	5 m from boulder 3, station 8.
69001	Single drive tube	10 m NW. of station 9.
69903, 69904	Surface samples	Near station 9 boulder.
69920	Soil	Beside station 9 boulder.
69940	do	Do.
69945	C_2	Collected with soil 69940.
69960	Soil	Beneath station 9 boulder.

[1]Rock types from Wilshire and others (1973, and this volume):
C_1-Crystalline igneous
C_2-Metaclastic
B_2-Light-matrix, dark-clast breccia
B_4-Dark-matrix, light-clast breccia
B_5-Dark-matrix, dark-clast breccia

[2] Twelve rake sampe fragments were collected from a 1-m-square area on the north rim of a 15-m subdued crater. Of the 12, 6 were igneous and metamorphic rocks, 6 partially melted breccias (LSPET, 1972). Of the rake fragments examined by Wilshire and others (this volume), 3 are B_2 breccias (68515, 68517, and 68519), 3 C_2 metaclastic rocks (68526, 68527, and 68535).

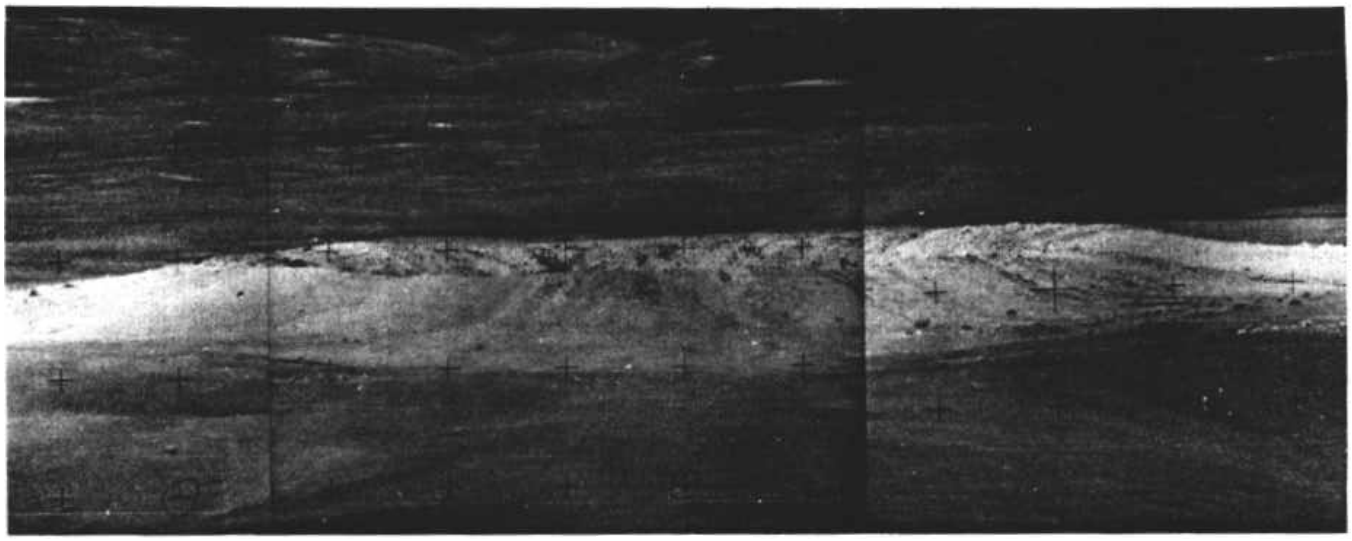

A

B

FIGURE 3.-Telephotographs of South Ray crater (top) and Baby Ray crater (bottom) taken from station 4 on Stone mountain (AS16-112-18246, 18247, and 18256, South Ray, and AS 16-112-18253 and 18254, Baby Ray). South Ray is about 680 m in diameter.

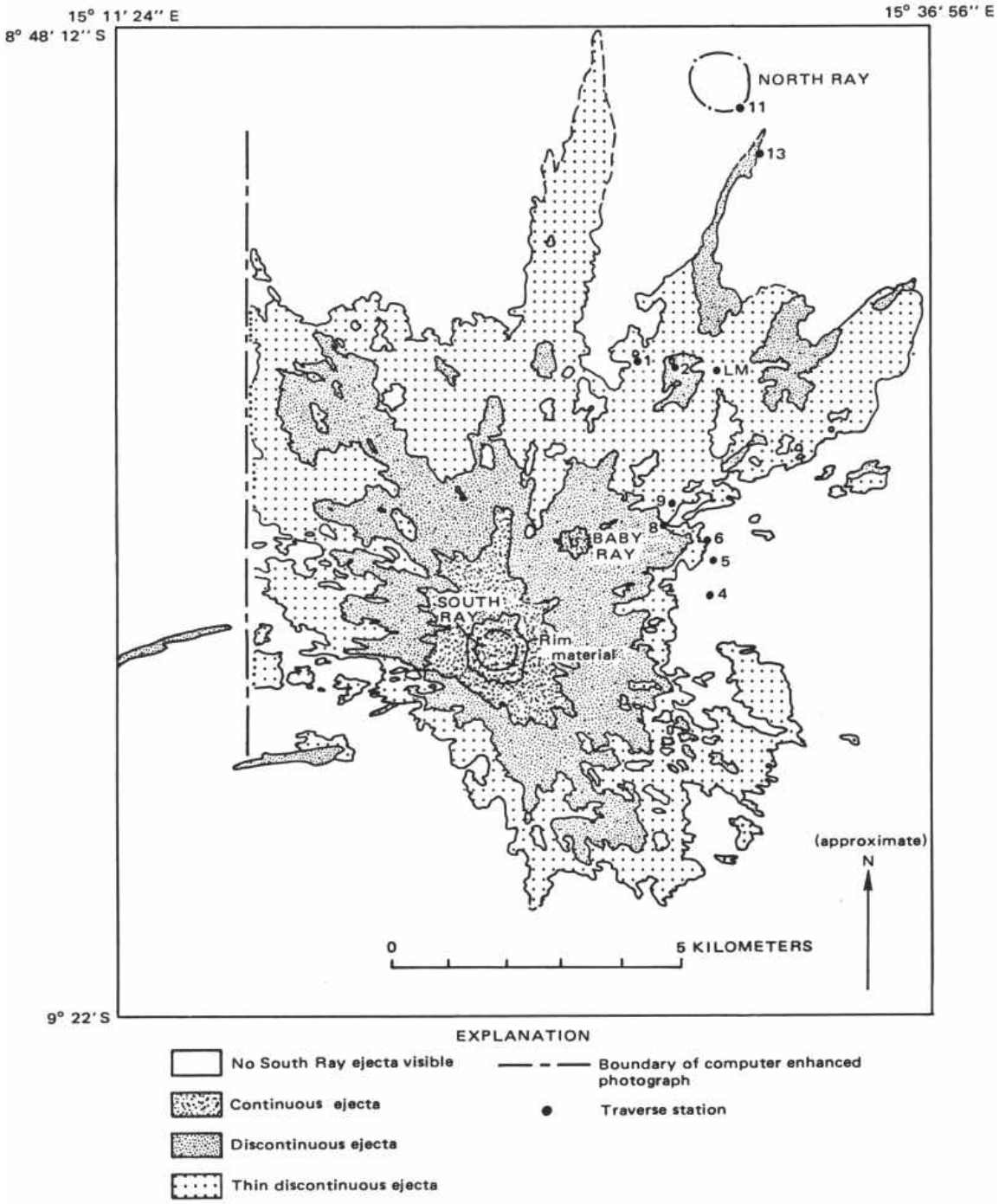

FIGURE 4.-Map of debris ejected from South Ray crater. Compiled on computer-enhanced Apollo 16 panoramic camera frame 5328.

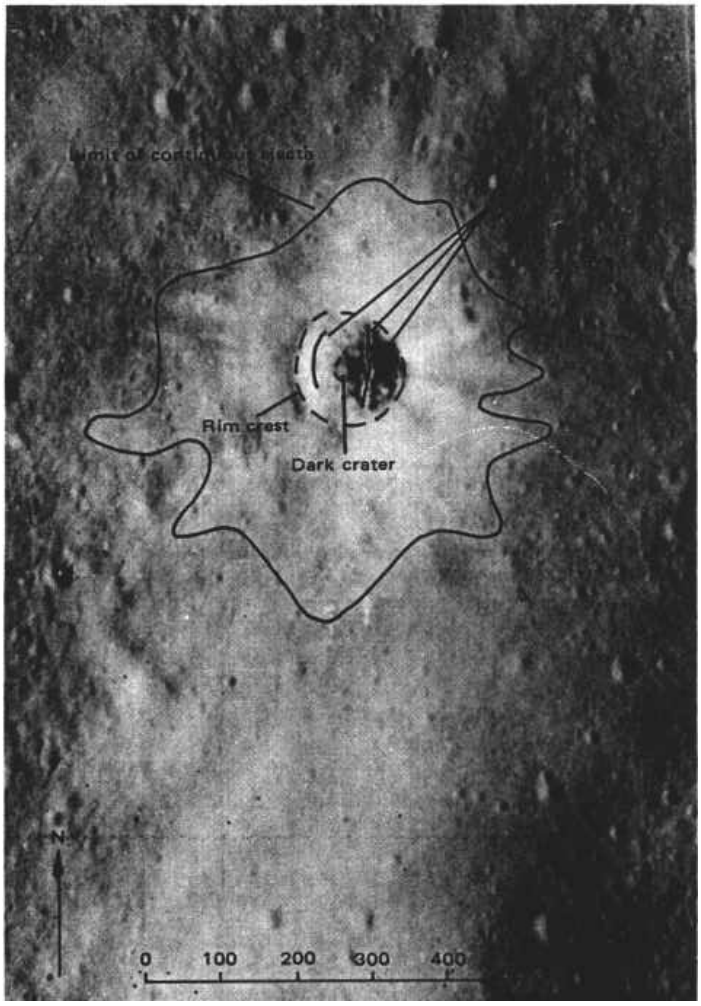

FIGURE 5.-Features of Baby Ray crater. Photograph enlarged from Apollo 16 panoramic camera frame 4623 (fig. 1*B*).

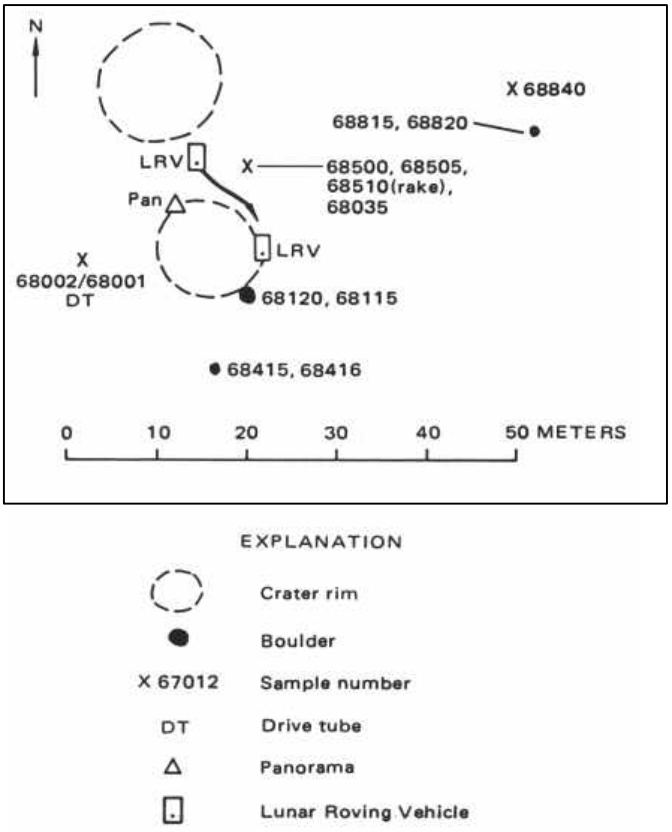

FIGURE 6.-Planimetric map of station 8 showing locations of samples.

samples. Both samples are fine-grained, highly feldspathic rock (Wilshire and others, 1973). Sample 68415, an igneous-textured rock, is composed of 79.3 percent plagioclase, 4.8 percent olivine, 4.4 percent augite, and 10.3 percent pigeonite (Helz and Appleman, 1973). Plagioclase An_{98-56} makes up 75 volume percent (Hodges and Kushiro, 1973). Both samples are texturally homogeneous but have a few shocked plagioclase inclusions in a fine-grained matrix (fig. 9*B*). It has been suggested that these rocks were produced not by partial melting of the deep lunar interior but rather by shock melting of an anorthositic rock (Wilshire and others, 1973; Helz and Appleman, 1973; Hodges and Kushiro, 1973; Walker, Longhi, Grove, and others, 1973; L. A. Taylor and others, 1973; and Warner and others, 1974) and rapid crystallization (Hodges and Kushiro, 1973; Nord and others, 1973) and that the inclusions represent unmelted anorthosite (Helz and Appleman, 1973, Wilshire and others, 1973).

Boulder 3. The third boulder sampled (fig. 14) at station 8, a 1.5-m dark boulder about 40 m northeast of boulders 1 and 2, is very coherent and angular and has only a few small fractures. Scattered large vesicles are visible. A "fillet" soil sample collected on the north side of the rock appears to be old regolith pushed up when the boulder landed rather than a fillet formed by rock degradation.

Sample 68815, termed a "fluidized lithic breccia," (Brown and others, 1973) contains a variety of basaltic and anorthositic clasts. Swirls of basaltic and feldspathic glasses or pockets of glass are common. Most of the material that has flowed is of plagioclase composition, whereas the basalt clasts have sharp unmelted boundaries (Brown and others 1973). Large, wormlike tubular vesicles are present (LSPET, 1972). Sample 68815, similar to 68115, is a dark-matrix dark-clast (B_5) breccia. The dark clasts in both differ only slightly from the matrix, and gas cavities are well developed in the matrices (Wilshire and others, 1973).

The bulk chemical compositions of rocks from station

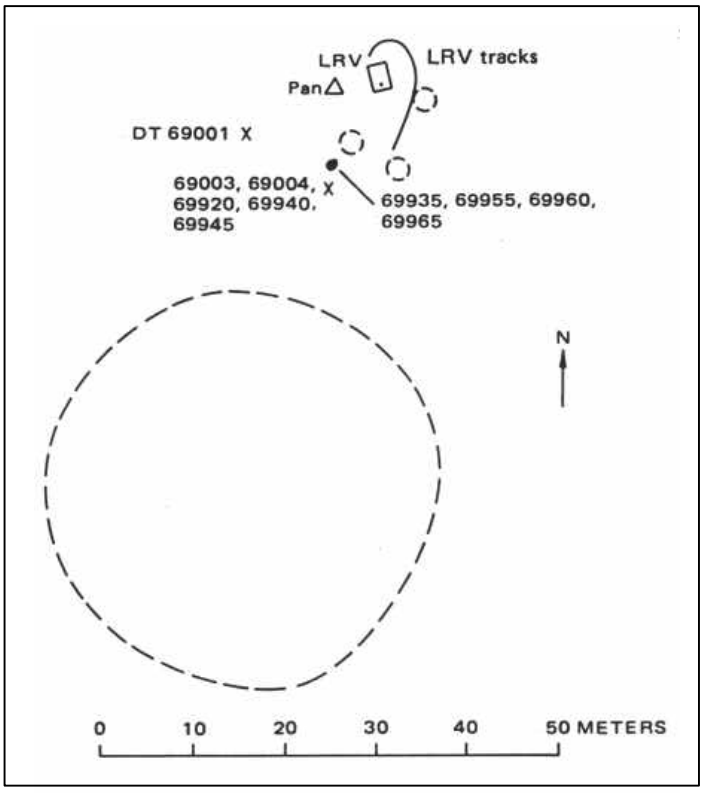

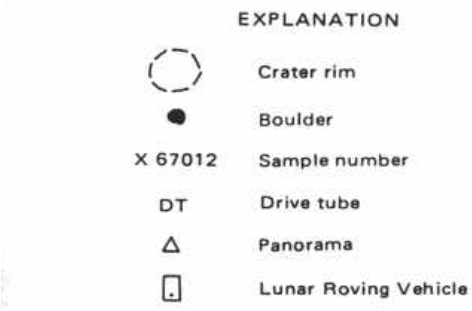

FIGURE 7.-Planimetric map of station 9 showing locations of samples. Symbols same as in figure 6.

8 boulders, shown in table 3, reveal a close similarity their chemistry that reflects a common source material despite the varied histories recorded in their textures.

TABLE 2.-*Chemical compositions of samples 68415, 68115, and 68815, station 8*

Rock type	C_1	B_5	B_5
Sample No.	68415,79	68115	68815,120
Source	Boulder 2 (Nava, 1974)	Boulder 1 (S. R. Taylor and others, 1974)	Boulder 3 (Scoon, 1974)
SiO_2	45.9	44.8	45.33
Al_2O_3	28.19	27.6	27.59
Fe0	4.01	5.10	5.17
Mg0	4.41	5.79	5.38
CaO	16.39	15.4	15.56
Na_2O	.47	.47	.48
K_2O	.060	.06	.17
H_2O	.....	.....	.05
TiO_2	.28	.34	.48
P^2O^5	.072	.....	.21
MnO	048	.....	.05
Cr_2O_3	.07	.....	.08
S			.06
Total	99.90	99.56	100.61

STATON 9

DESCRIPTION

Station 9, about 400 m northeast of station 8, is in an area of lower albedo. The surface is considerably smoother than at station 8, where there are many small, sharp-rimmed fresh craters. The small craters at station 9 are rimless and subdued. The fragment population varies in both size and abundance; fragments are fewer and mean size is smaller than at station 8.

SAMPLING

At station 9, the sampling was confined to the immediate vicinity of one boulder, about one-half m across, perched on the north rim of a small crater that may be a secondary crater formed by the boulder. Two rock chips were taken from the boulder, 69935 from the top and 69955 from the bottom. The photographs show that the rock consists predominantly of dark material but has a large component of light material (fig. 15), visible as discrete clasts as well as "streamed" through the boulder (fig. 16). Sample 69935 came from a predominantly dark part of the boulder. The boulder appears coherent, mostly angular, and is fractured throughout. Although most of the bottom was soilcaked, some of the rock is visible. One part of the bottom face is covered with dark glass. No glass was reported by the crew on the top, but apparently some glass has been injected into fractures.

Sample 69935 is a dark-matrix light-clast breccia (B_4). The sample from the bottom, 69955 (fig. 17), is an igneous (C_1) clast form within the dark matrix. Most of the other clasts in this boulder appear to be breccias.

Several soil samples designed to collect successively deeper regolith material were taken in the vicinity of the boulder: first, two surface samples (69003, 69004) collected the uppermost layer of regolith; then a skim sample (69920, penetration 5mm), a scoop sample (69940, penetration 3 cm), and a drive-tube sample (69001, penetration 27 cm) were taken. For comparison, a soil sample was collected from beneath the boulder.

AGE OF SOUTH RAY CRATER

The presence of distinct, light-colored rays in the vicinity of stations 8 and 9 in-orbital and surface photographs suggests a substantial thickness of South Ray-derived material in this region. The exposure ages of rocks and soils collected at stations 8 and 9, however, have generated some uncertainty, (McKay and Heiken, 1973) as to the amount of South Ray debris actually

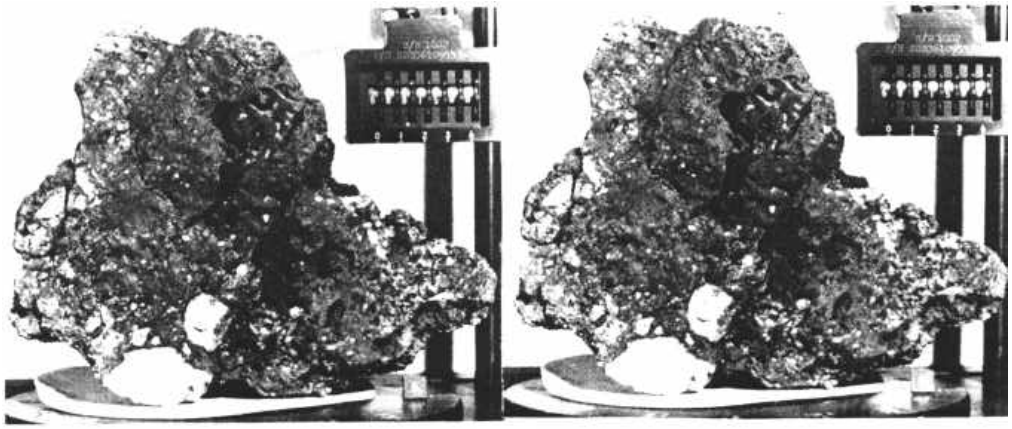

A

B

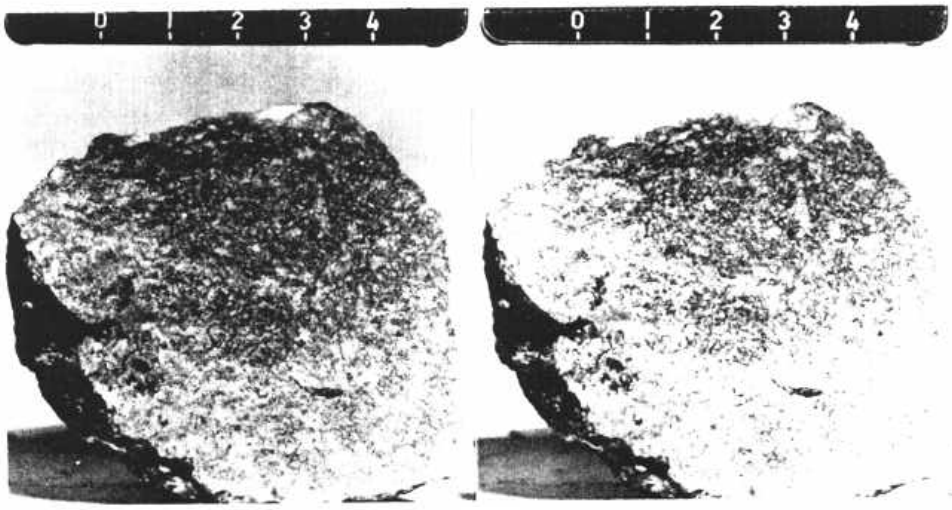

C

FIGURE 8.-Larger samples collected at stations 8 (*A-E*) and 9 (*F*). A, Sample 68115 (stereopair), from boulder 1. *B*, Closeup of 68115 showing boulder 3. *F*, Sample 69955 (stereopair). from

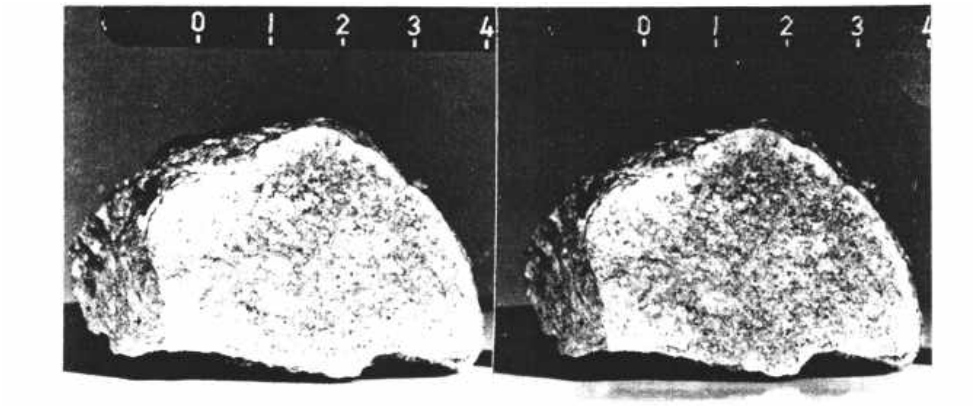

D

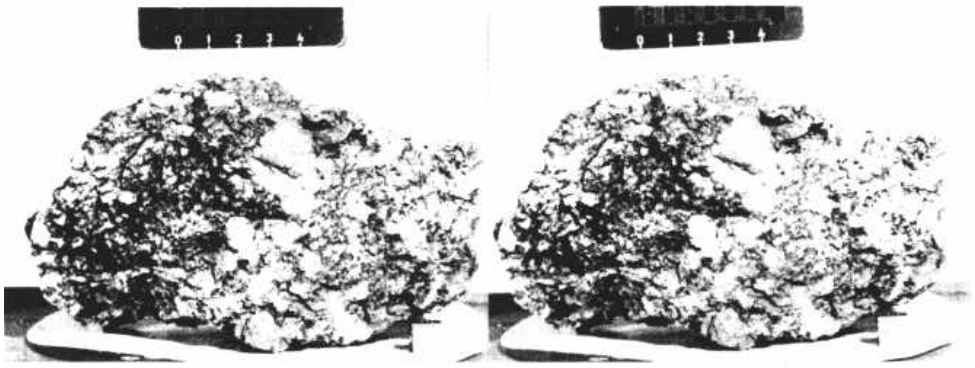

E

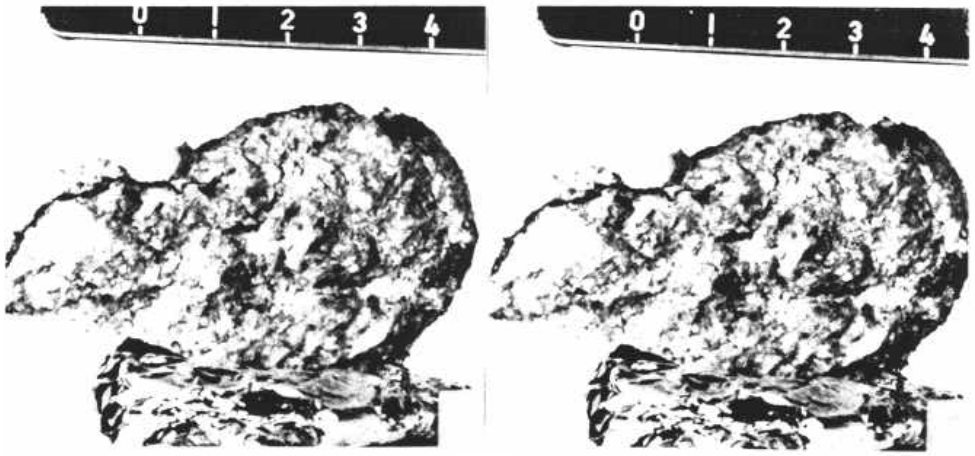

F

vugs. *C*. Sample 68415 (stereopair), from boulder 2. *D*, Sample 68416 (stereopair), from boulder 2. *E*, Sample 68815 (stereopair), from bottom side of the boulder. Scales in centimeters.

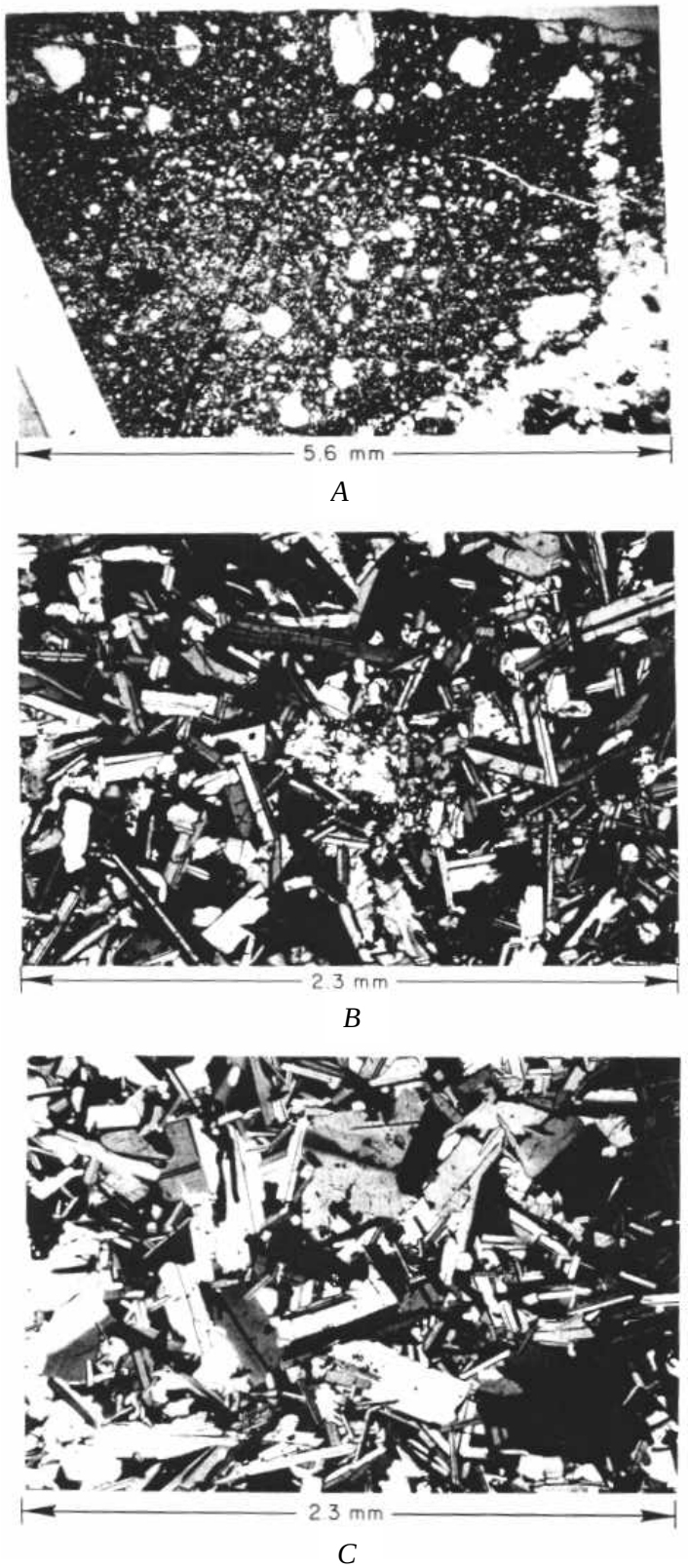

FIGURE 9. -Photomicrographs of rocks shown in figure 8. *A*, 68115, 95, plane-polarized light; glass and crushed plagioclase groundmass with relict plagioclast clasts. *B*, 68415, 142, cross-polarized light; subophitic plagioclase (twinned laths) and pyroxene with clast of shocked

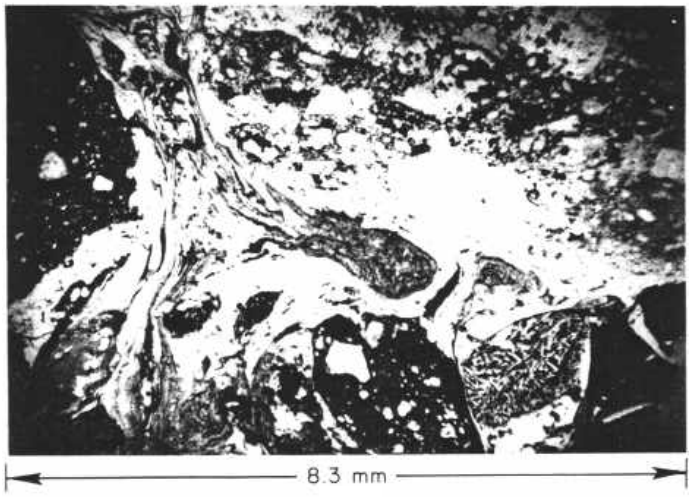

D

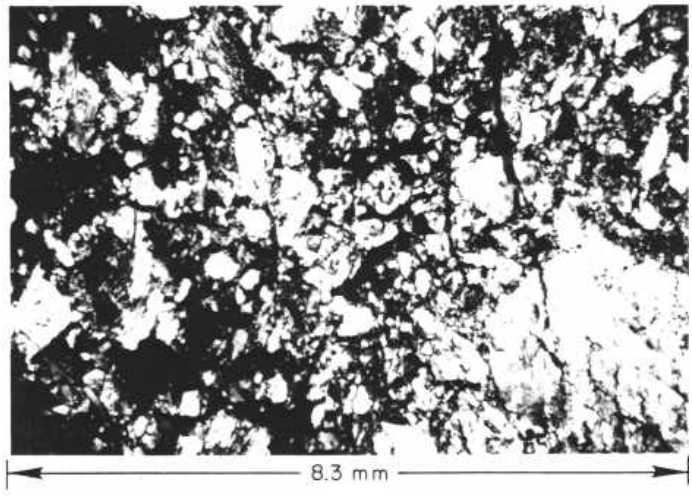

E

plagioclase in center. *C*. 68416, 78, cross-polarized light; seriate twinned plagioclase with pyroxene. *D*, 68815, 142, plane-polarized light; brown glass invading polymict breccia indicating several shock events. *E*. 69955, 30, cross-polarized light; shocked, partly melted coarse grained anorthosite.

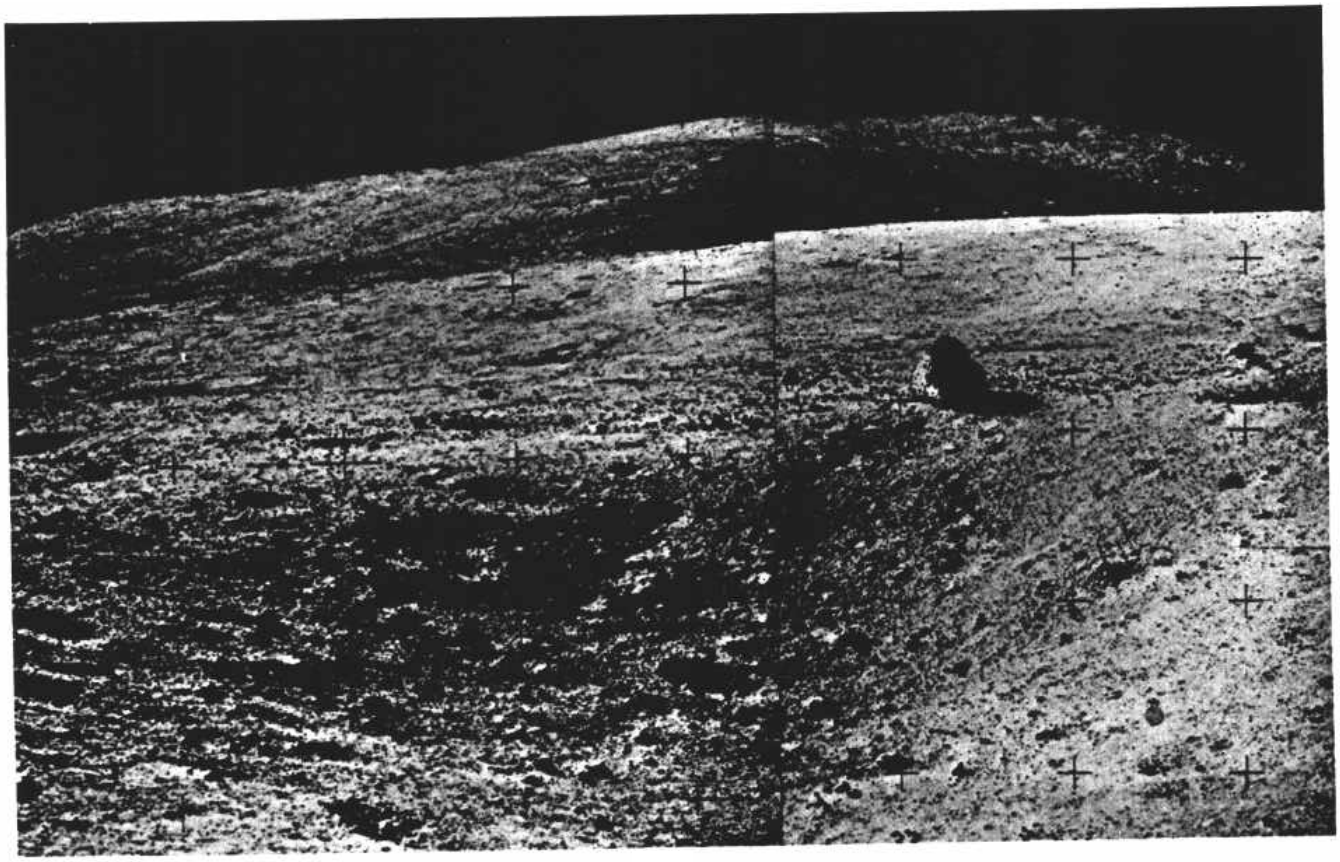

A

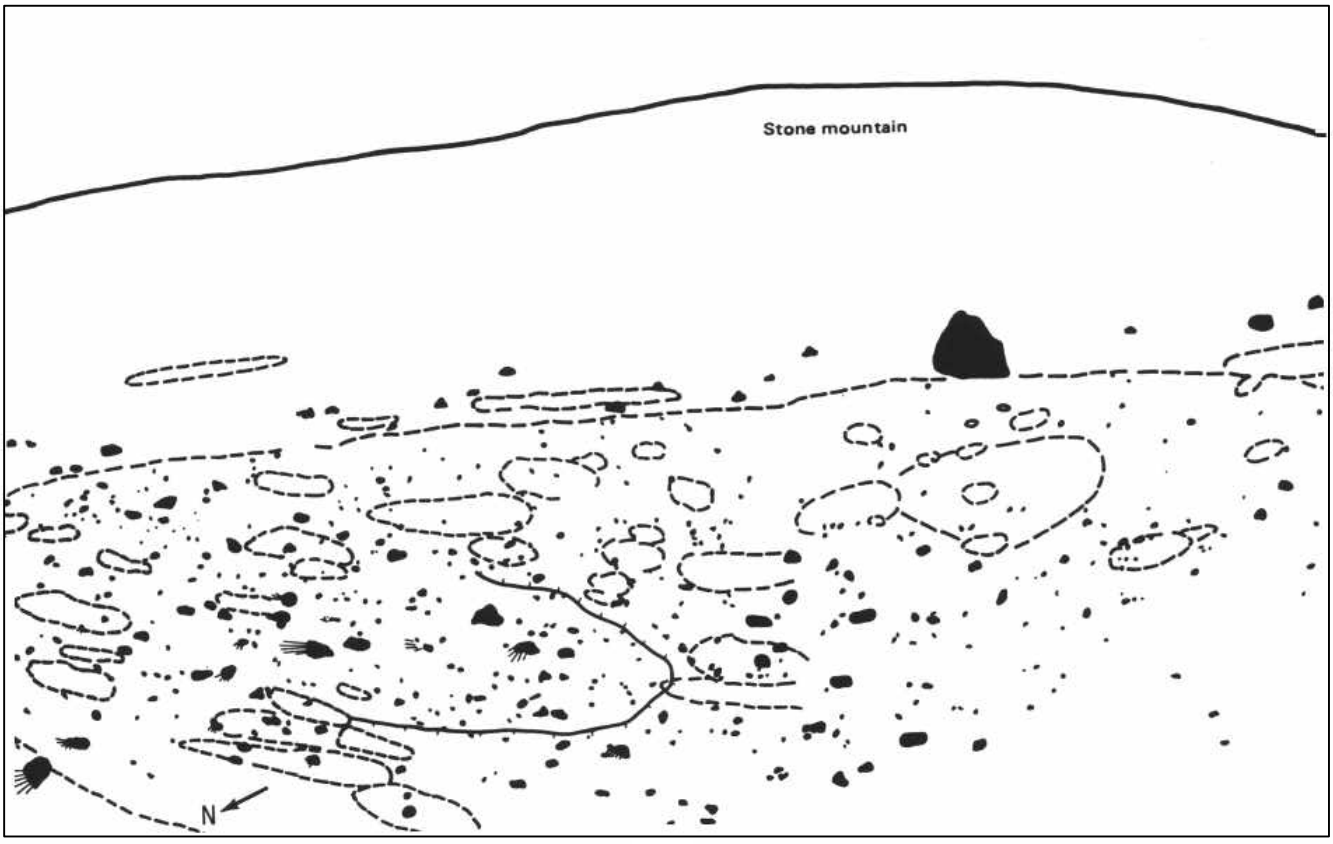

B

A

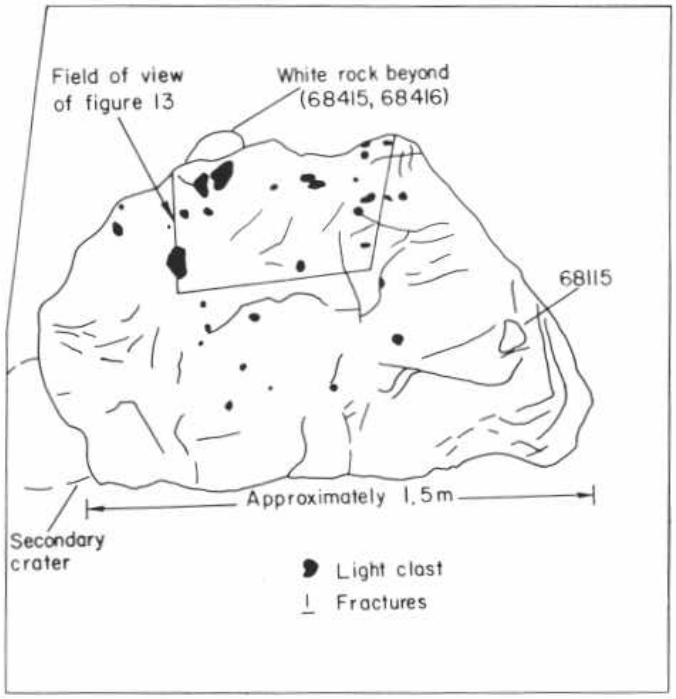

B

FIGURE 11.-Boulder 1, station 8. *A*, Photograph, view is southwest, AS16-108-17689. *B*, Sketch map.

< FIGURE 10.-Crater at station 8 that predates South Ray crater. *A*, Southeast view of 15-m crater. South Ray material is preferentially deposited on the downrange (left) side of the crater (AS16-108-17676). *B*, Sketch map of fragments (solid), fillets (whiskers), and craters (dashed) drawn from *A*.

A

FIGURE 12.-Boulder 1, station 8. *A*, Closeup view,

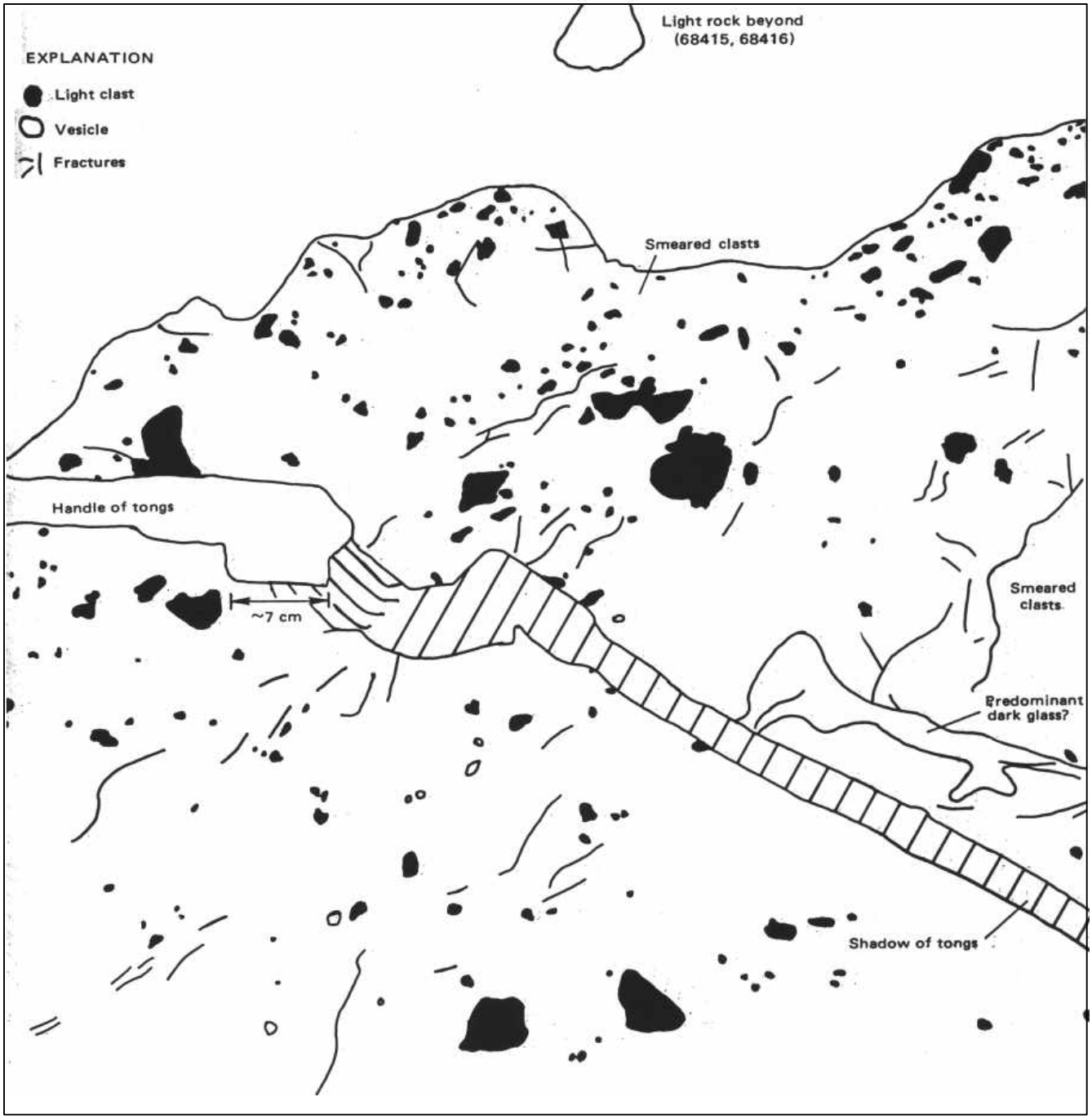

B

Apollo 16 photograph, AS16-108-17694 *B*, Sketch map.

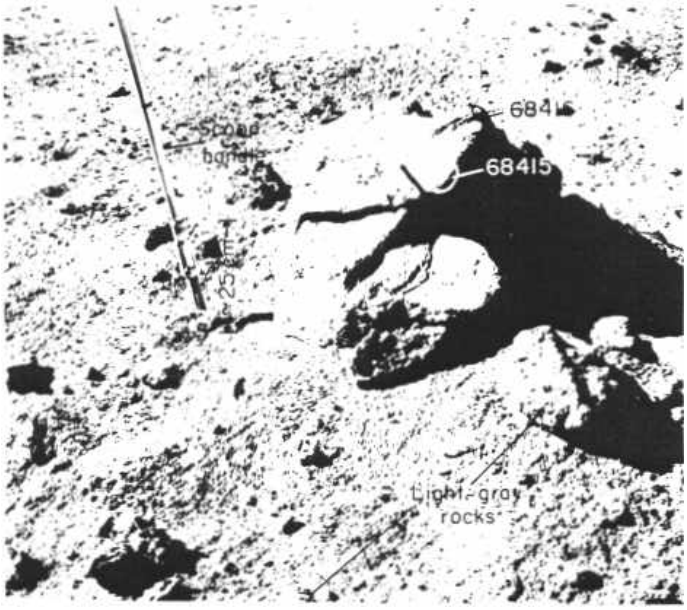

FIGURE 13-Boulder 2, station 8, showing location of samples collected; view is south (AS16-107-17549).

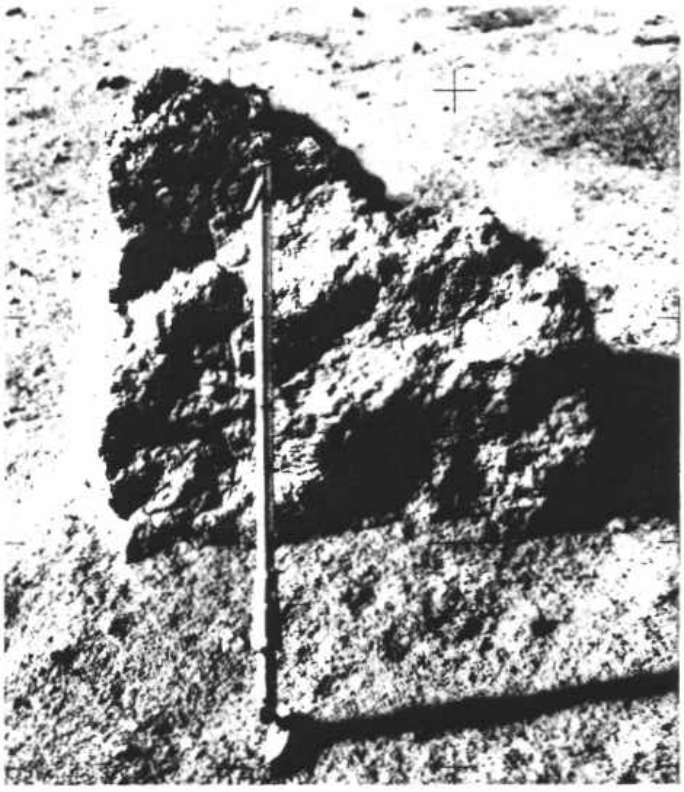

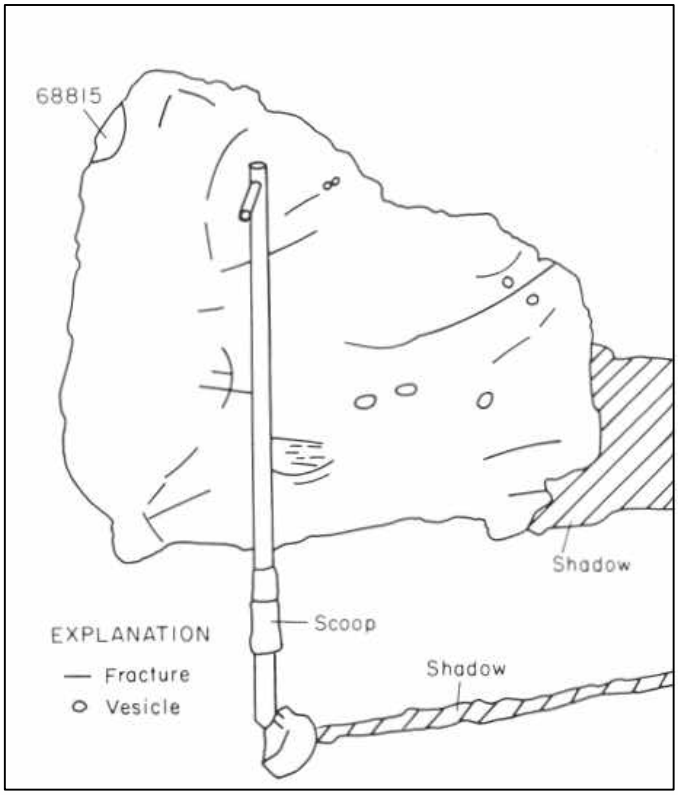

A *B*

FIGURE 14.-Boulder 3, station 8. *A*, Photograph before sampling, view is south (AS16-108-17700). *B*, Sketch map.

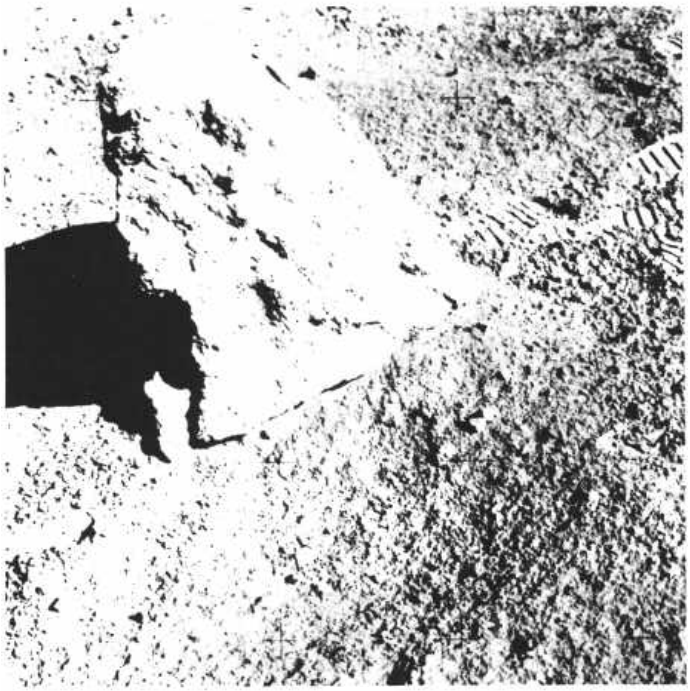

A

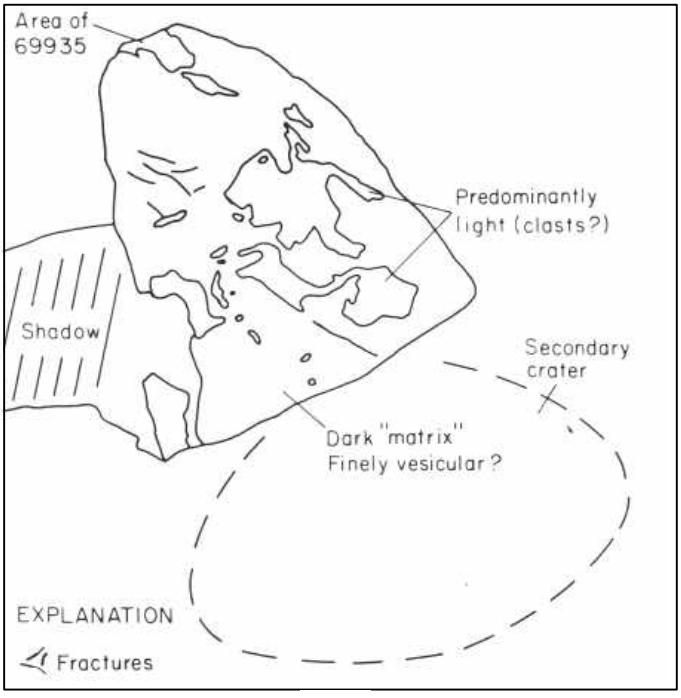

B

FIGURE 15-Station 9 boulder. *A*, Photograph, view is north, AS16-107- 17558. Boulder is about 50 cm wide. *B*, Sketch map.

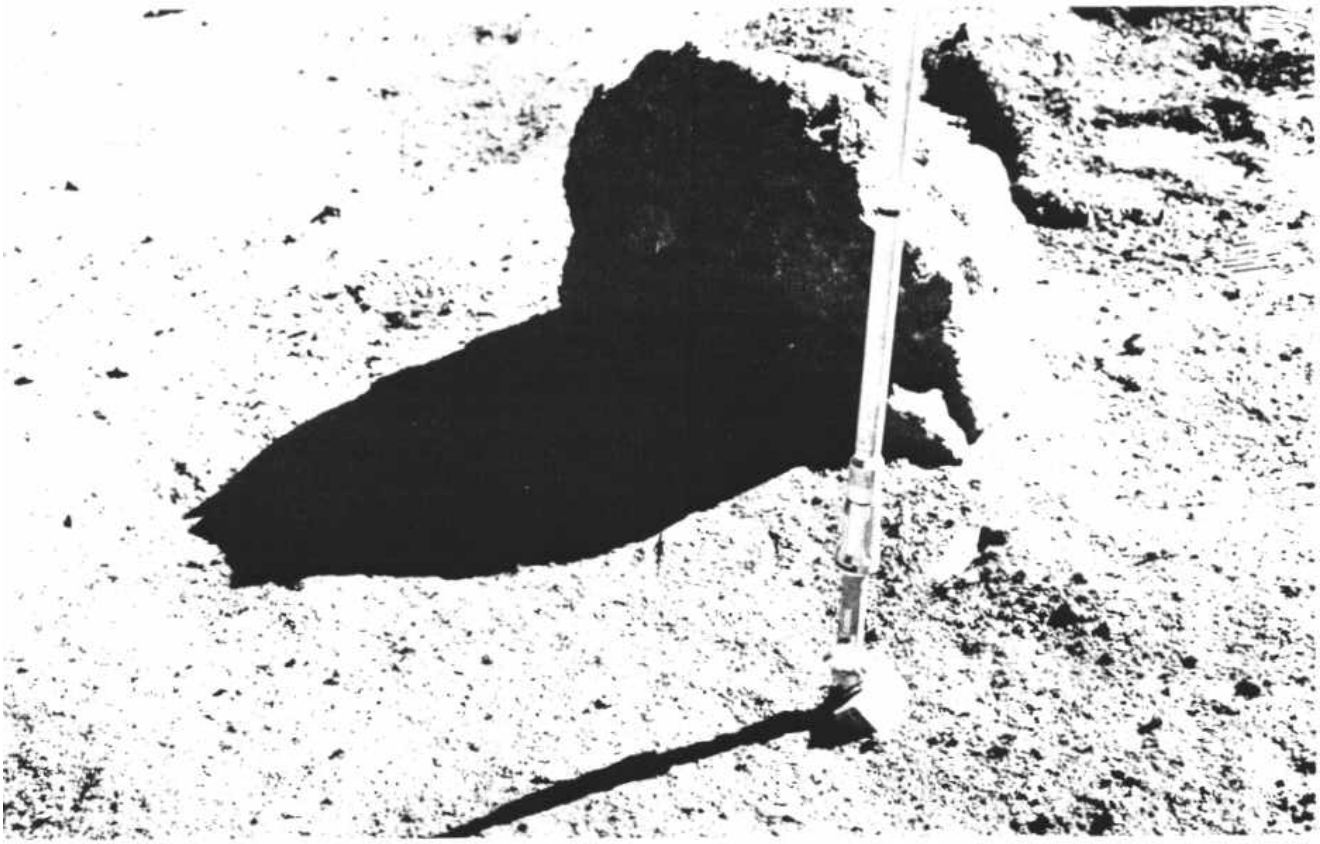

A

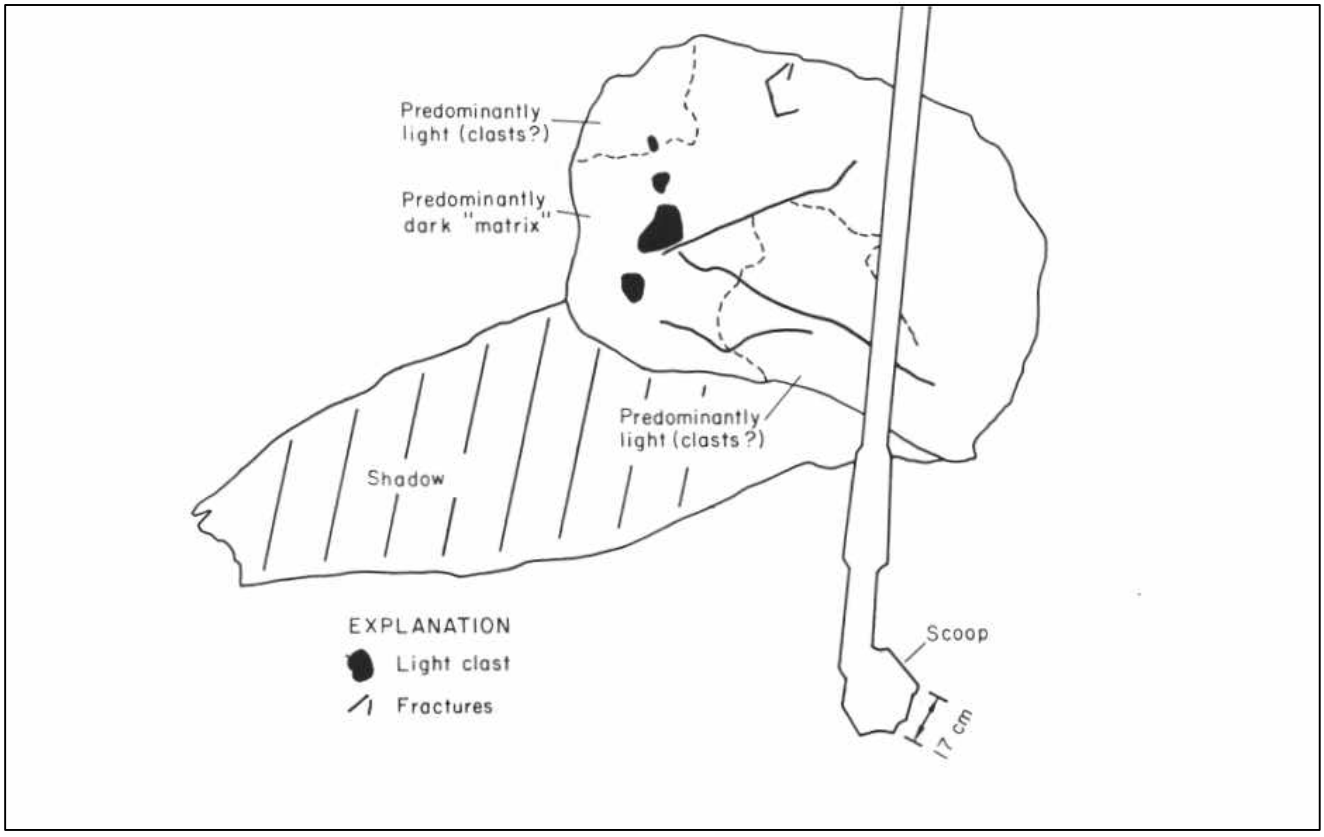
Predominantly light (clasts?)
Predominantly dark "matrix"
Predominantly light (clasts?)
Shadow
EXPLANATION
Light clast
Fractures
Scoop
17 cm

B

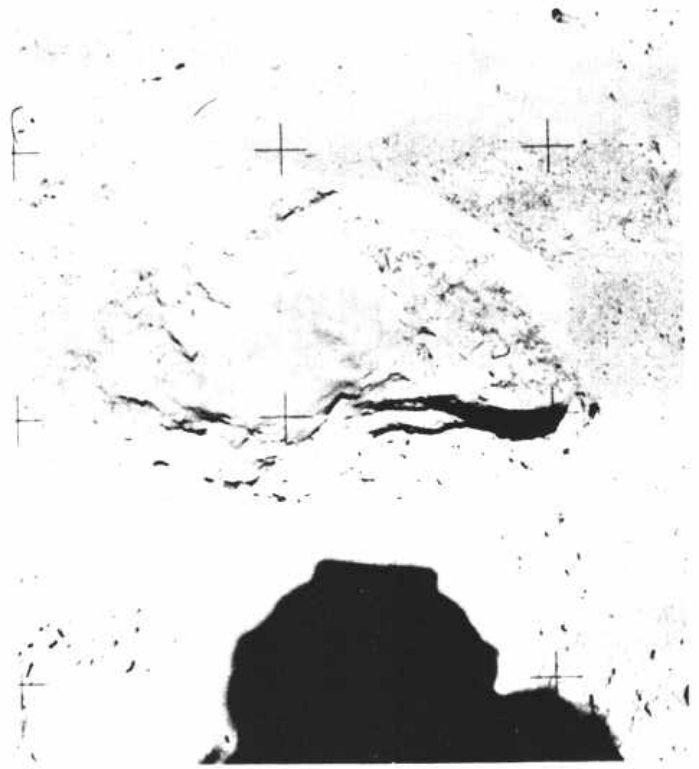

A

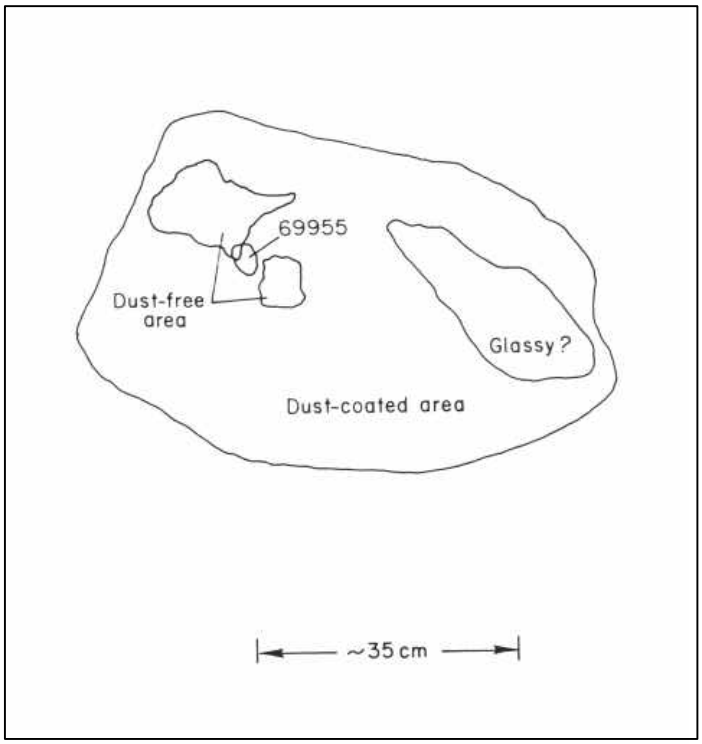

B

FIGURE 17.-Bottom of overturned boulder at station 9. *A*, Photograph before sampling, view is west, AS16-107-17576. *B*, Sketch map.

< FIGURE 16.-Station 9 boulder. *A*, Photograph, view is northeast (AS16-107-17558). *B*, Sketch map.

present. Exposure ages have been calculated for several station 8 and 9 rocks by several investigators (table 4).

The samples collected in the station areas appear to represent two lithologic units penetrated by the South Ray crater. Both light and dark fragments were collected, and light and dark blocks are visible on the rim of South Ray. The upper, dark unit (fig. 18) is about 50 m thick, the lower, light unit at least 70 m thick. (See Ulrich and Reed, this volume, for more detail.)

Most of the exposure ages for the station 8 and 9 boulders are about 2 to 3 m.y., which probably dates the South Ray impact. Older ages, however, indicate that exposure history may be complex or that the different dating techniques used have not yet been reconciled.

Neukum and others (1973) noted that the surface of 68415 is not saturated with microcraters, indicating it is freshly exposed rock. High exposure ages of 87-105 m.y. contradict this evidence but may represent an earlier exposure history for this boulder, preserved somehow in the material analyzed. Behrmann and others (1973) calculated an exposure age of 2 m.y. for 68815 and suggest that, prior to its ejection, it was buried at a depth greater than 7 m, which could place the boulder within the upper part of the dark unit prior to its excavation. Drozd and others (1973) calculated a 4.1-m.y.exposure age for 69955, 2 m.y. for 69935. They suggested that the boulder was in the upper few centimeters of the regolith in the South Ray target area, inverted from its present position for 2.1 m.y., then ejected from South Ray 2 m.y. ago. It seems unlikely, however, that a half-meter boulder near the surface of the South Ray impact point could have survived the event as well as the flight to station 9. More reasonably, the boulder was part of the upper dark layer and was ejected by the South Ray impact 2 m.y. ago. The boulders from which samples 68815, 68115, and 69955 were collected probably all represent the dark unit in South Ray crater, as all three are dark matrix (B_4 and B_5) breccias. The presence of light-gray rocks and fines on South Ray and Baby Ray craters and in the station areas suggests that igneous rocks 68415 and 68416 from boulder 2 are representative of the underlying light layer (impact melt). Crystallization ages reported for these rocks (table 4) are 3.68 to 4.09 b.y. and 3.87 to 4.00 b.y., respectively. These are inferred to represent the approximate age of emplacement of the fluidized material within the Cayley Formation as proposed by Hodges and Muehlberger (this volume). It seems fairly conclusive that the impact that formed South Ray crater occurred 2 to 3 m.y. ago and that the dark breccias and light igneous rocks sampled at stations 8 and 9 are representative of two discrete layers penetrated by South Ray.

The problem of assigning the samples collected at stations 8 and 9 to South Ray crater arises from the exposure ages of the fines (McKay and Heiken, 1973). Walton and others (1973) and Kirsten and others (1973) reported exposure ages of 180 m.y., 170 m.y., and 240 m.y. for 68841, 69941, and 69921, respectively. Schaeffer and Husain (1973) analyzed eight 2- to 4-mm fragments, obtaining exposure ages of 122 to 168 m.y. Adams and McCord (1973) stated that station 8 soils are mature, according to their high agglutinate content.

It appears that little fine debris was sampled that can be attributed directly to South Ray. Two explanations have been proposed: (1) the fines collected represent older regolith ejected by the South Ray impact (McKay and Heiken, 1973) or (2) there is little or no fine South Ray debris in these areas. If the soils do represent older ejected regolith, it would probably be indistinguishable from the preexisting regolith in the station areas. Size analysis of the soils (Butler and others, 1973), however, indicates that there may be recognizable mixing of South Ray and underlying fines and that the coarser fractions are likelier to represent the latest depositional material.

McKay and Heiken (1973) calculated that approximately 20 percent of the material ejected from South Ray was preexisting regolith, based on a regolith thickness of 10-15 m. As the regolith may not be more

TABLE 3.-*Reported exposure ages of rocks collected at stations 8 and 9*

Rock No.	Age (m.y.)	Method	Age source
68415	2-3	Microcraters	D. A. Morrison and others 1973.
	2.2+/-0.3	^{81}Kr-^{83}Kr and ^{81}Kr-^{78}Kr	Behrmann and others, 1973.
	95-105	Cosmic ray	Huneke and others, 1973a.
	87+/-5	^{40}Ar-^{39}Ar	Kirsten and others, 1973.
	92.5+/-13.3	^{81}Kr-Kr	Drozd and others, 1974.
68815	2.0+/-0.2	^{81}Kr-^{83}Kr and ^{81}Kr-^{78}Kr	Behrmann and others, 1973.
	1.7+/-0.4	^{22}Na-^{21}Na	Do.
	2.04+/-0.20	^{81}Kr-Kr	Drozd and others, 1974.
68115	2.08+/-0.32	^{81}Kr-Kr	Do.
68416	2-3	Microcraters	D. A. Morrison and others 1973.
	89+/-4	^{40}Ar-^{39}Ar	Kirsten and others, 1973.
69935	2-3	Microcraters	D. A. Morrison and others 1973.
	1.9+/-0.2	^{81}Kr-^{78}Kr	Behrmann and others, 1973.
	3.3+/-0.3	^{81}Kr-^{83}Kr	Do.
	2.2+/-0.3	^{22}Na-^{21}Na	Do.
	1.99+/-0.37	^{81}Kr-Kr	Drozd and others, 1974.
69955	4.25+/-0.41	^{81}Kr-Kr	Do.

TABLE 4.-*Reported crystallization ages for samples 68415 and 68416, station 8*

68415		
Age (b.y.)	Method	Source
3.84+/-0.01	Rb-Sr	Papanastassiou and Wasserburg, 1972a.
3.68+/-0.08	Total Ar	Kirsten and others, 1973.
3.85+/-0.06	^{40}Ar-^{39}Ar	Do.
3.96+/-0.08	^{207}Pb-^{206}Pb	Anderson and Hinthorne, 1973
4.09+/-0.04	^{40}Ar-^{39}Ar	Huneke and others, 1973a.
3.85+/-0.04	^{40}Ar-^{39}Ar	Do.
3.85+/-0.01	Rb-Sr	Tera and others, 1973.
68416		
3.87+/-0.08	Total Ar	Kirsten and others, 1973.
4.00+/-0.05	^{40}Ar-^{39}Ar	Do.

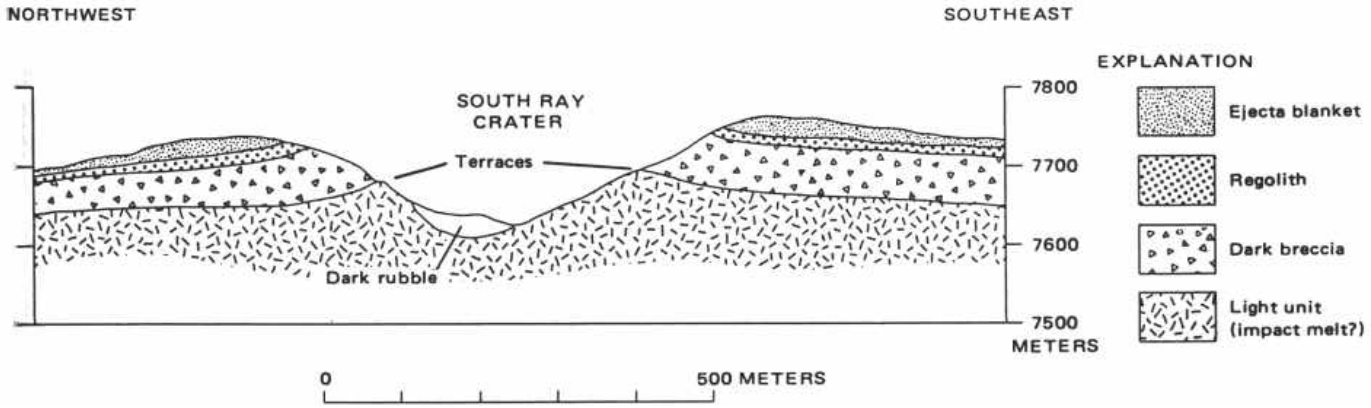

FIGURE 18.-Schematic cross-section through South Ray crater.

than 6-7 m thick (Freeman, this volume), older regolith in the ejecta may be considerably less than calculated. McKay and Heiken suggested that the amount of freshly produced fine material may be very small. It is possible, then, that little fine material in this area can be attributed directly to South Ray, either as older, preexisting regolith or as freshly produced fines.

If there is little or no soil produced by South Ray in the area, there must be another explanation for the high-albedo rayed surface at station 8. In several other station areas, the crew reported light-colored soil underlying a thin dark surface layer. At station 8, the soil appears to be a uniform gray. This uniformity may have been produced by churning of the upper few centimeters of the regolith as fragments from South Ray impacted. Such a process, in the absence of much fine debris, could generate a surface of higher albedo. The surface at station 8 (located on a prominent ray) has a rough appearance suggestive of such churning of the upper regolith, whereas the surface at station 9 has a lower albedo and is much smoother, compatible with a less prominently rayed terrain.

The apparent absence of primary South Ray fines is not surprising considering the intense mixing of the upper regolith as the rays were deposited. It is apparent that there was not a "blanket" of material deposited but rather that the high albedo was produced by a turbulent, churning disturbance of the older, darker regolith surface by South Ray ejecta, which deposited only sparse new material as blocks and fragments in the ray-covered area. This is consistent with the conclusion of Oberbeck and others (1974a, b, 1975) that beyond the continuous ejecta blanket, the proportion of primary material present is small, relative to the local material excavated by secondaries from the crater. These conclusions are also in agreement with a South Ray ejecta model proposed by Hodges and others (1973) (see also Ulrich and others, this volume) that presents an average thickness of ejecta based on fragment population, evenly distributed over 360° of arc. According to their preferred model, "an indeterminate, but small amount of South Ray ejecta should be expected in the interray areas, and the materials of the rays should be dominantly coarse debris."

D4. GEOLOGY OF STONE MOUNTAIN

By ANTHONY G. SANCHEZ

CONTENTS

ILLUSTRATIONS

TABLES

INTRODUCTION

Stone mountain is a westward projection of the Descartes mountains extending into the southeastern part of the Apollo 16 traverse area. It is approximately 550 m above the Cayley plains and has a domical morphology.

The largest craters on Stone mountain include Crown, 100 m in diameter, and two nearby unnamed craters, 80 m and 140 m in diameter; most range from 50 m down to the limit of resolution. The crater density on Stone mountain is qualitatively the same as that on the adjacent Cayley plains, but craters larger than 100 m are more abundant on the plains (fig. 1; see also Freeman, this volume). None of the resolvable primary craters on Stone mountain appear to be younger than

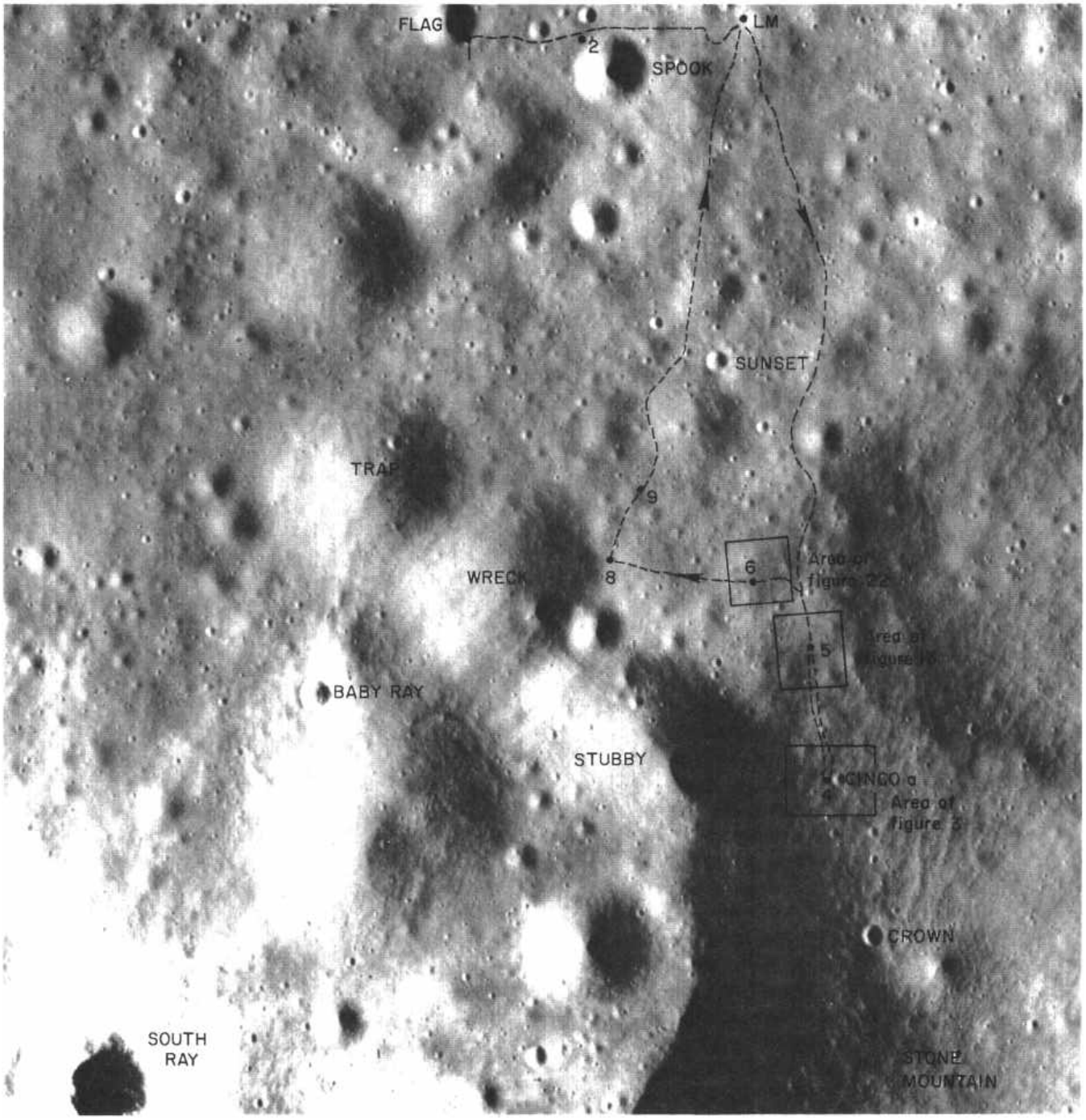

FIGURE 1.- Location of traverses 1 and 2, features discussed in text, and areas covered by figures 3, 13. and 22. Apollo 16 panoramic camera frame 4618.

the prominent South Ray and Baby Ray craters on the plains.

The average thickness of the regolith on Stone mountain based on radar data and concentric craters (Freeman, this volume) is estimated to be about 7 m. The surface is relatively smooth and undulating. The upper part of the regolith on Stone mountain probably includes ejecta from South Ray crater over much of the surface.

GEOLOGY OF THE STATION AREAS

The main objective of the sampling at stations 4, 5, and 6 was to collect materials characteristic of the Descartes mountains. This task was constrained by lack of outcrops, difficulty of recognizing craters that penetrated bedrock, contamination by South Ray ejecta, and the lack of obvious characteristics by which to distinguish Descartes material from Cayley. The contact between Cayley and Descartes material was not recognized on the ground; the crew noted the gradual increase in slope but observed no apparent difference in color or texture of regolith.

Station 4, the highest point reached, was about 150 m above the plain on Stone mountain (fig. 2) on a steep slope that was more blocky than expected owing to blocky ray material from South Ray crater. Station 5, lower on the slope and approximately 550 m north of station 4, was on a gently sloping bench near a 15-m crater in an area sparsely covered with blocks. Station 6 was on the edge of the Cayley plains at the base of Stone mountain. A subdued 10-m crater and several small craters are present in the station 6 area, and small blocks are fairly common.

The traverse route on Stone mountain is sprinkled with blocks in the 10- to 100-cm size range interspersed with smaller rocks down to the limit of resolution (2 cm). The crew observed that blocks less than 30 cm in size are the most abundant. Their observations were confirmed by block counts made from the station panorama (pl. 6, pans 9-12; table 1).

STATION 4

As a result of this study the location of station 4 has been redetermined at about 100 m east of the location reported earlier in Muehlberger and others (1972); the new location places the LRV on the outer part of the ejecta blanket of Cinco *a* crater. Two localities were occupied at station 4: station 4a (the LRV parking spot and principal sampling area, inside the northeast rim of a subdued doublet crater approximately 15 m across), approximately 40 m west of the rim of Cinco *a* crater, and 4b, about 50 m south of the LRV (figs. 3 and 4). The regional slope averages 10-15° down toward the northwest.

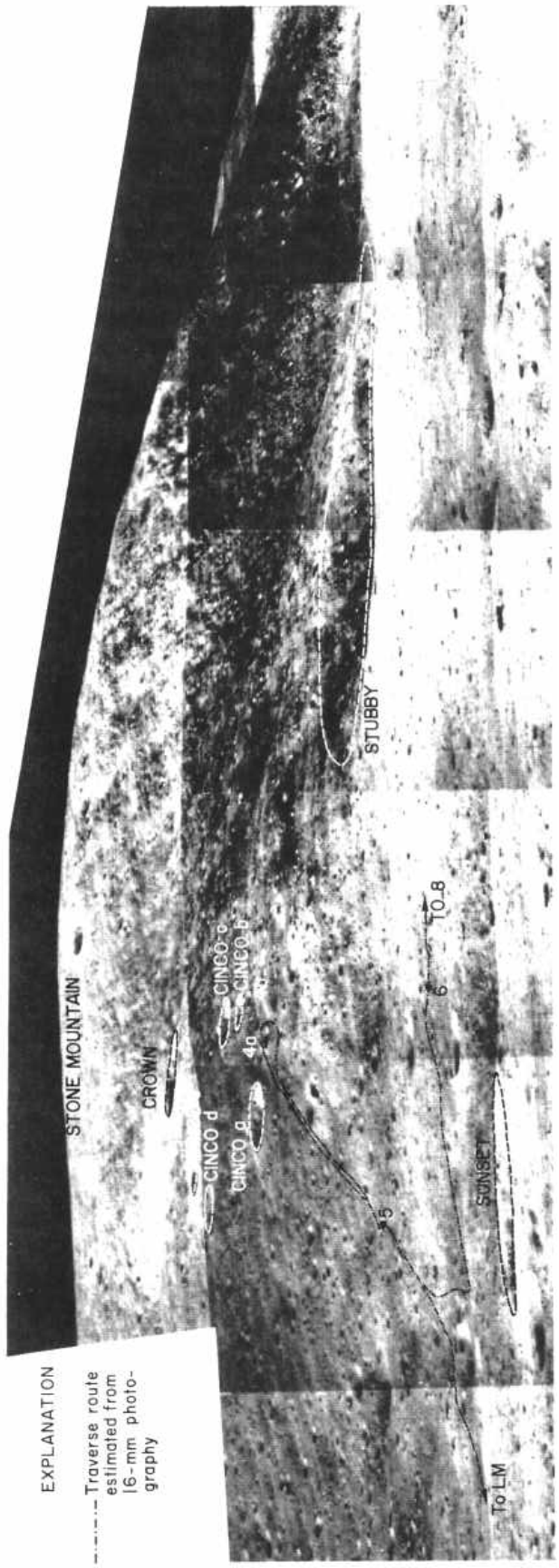

FIGURE 2.- Stone mountain showing locations of station 4, 5, and 6 and traverse line. Mosaic of 500-mm photographs from station 2. AS16- 112-18200, 02, 17, 19, 27-32.

the prominent South Ray and Baby Ray craters on the plains.

The average thickness of the regolith on Stone mountain based on radar data and concentric craters (Freeman, this volume) is estimated to be about 7 m. The surface is relatively smooth and undulating. The upper part of the regolith on Stone mountain probably includes ejecta from South Ray crater over much of the surface.

GEOLOGY OF THE STATION AREAS

The main objective of the sampling at stations 4, 5, and 6 was to collect materials characteristic of the Descartes mountains. This task was constrained by lack of outcrops, difficulty of recognizing craters that penetrated bedrock, contamination by South Ray ejecta, and the lack of obvious characteristics by which to distinguish Descartes material from Cayley. The contact between Cayley and Descartes material was not recognized on the ground; the crew noted the gradual increase in slope but observed no apparent difference in color or texture of regolith.

Station 4, the highest point reached, was about 150 m above the plain on Stone mountain (fig. 2) on a steep slope that was more blocky than expected owing to blocky ray material from South Ray crater. Station 5, lower on the slope and approximately 550 m north of station 4, was on a gently sloping bench near a 15-m crater in an area sparsely covered with blocks. Station 6 was on the edge of the Cayley plains at the base of Stone mountain. A subdued 10-m crater and several small craters are present in the station 6 area, and small blocks are fairly common.

The traverse route on Stone mountain is sprinkled with blocks in the 10- to 100-cm size range interspersed with smaller rocks down to the limit of resolution (2 cm). The crew observed that blocks less than 30 cm in size are the most abundant. Their observations were confirmed by block counts made from the station panorama (pl. 6, pans 9-12; table 1).

STATION 4

As a result of this study the location of station 4 has been redetermined at about 100 m east of the location reported earlier in Muehlberger and others (1972); the new location places the LRV on the outer part of the ejecta blanket of Cinco *a* crater. Two localities were occupied at station 4: station 4a (the LRV parking spot and principal sampling area, inside the northeast rim of a subdued doublet crater approximately 15 m across), approximately 40 m west of the rim of Cinco *a* crater, and 4b, about 50 m south of the LRV (figs. 3 and 4). The regional slope averages 10-15° down toward the northwest.

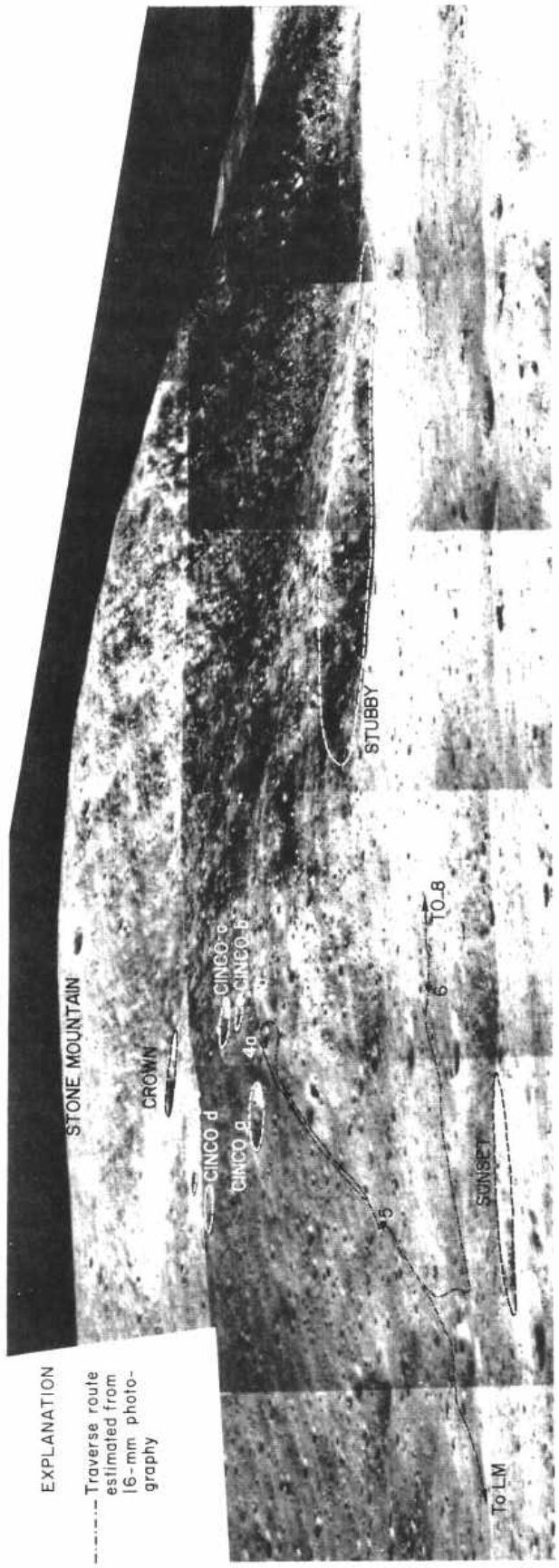

FIGURE 2.- Stone mountain showing locations of station 4, 5, and 6 and traverse line. Mosaic of 500-mm photographs from station 2. AS16- 112-18200, 02, 17, 19, 27-32.

A block field, radial to and possibly derived from South Ray crater, covers part of the sample area at 4b (pl. 6, pan 10). Alternatively this block field and that at (pl. 6, pan 9) both may be ejecta from Cinco a crater, 65 m in diameter and about 15 m deep. However, larger blocks are present away from the rim of Cinco a rather than being concentrated on it; thus the evidence for Cinco a as a source is not overwhelming.

Indurated regolith samples (64800, 64810) from the block-free rim of the crater at 4b may be from underlying Descartes material partly derived from Cinco a

TABLE 1.-Block shape and size distribution at stations 4, 5, and 6.

	10-20 cm	20-50 cm	50 cm	Total	Shape percent
Station 4					
Rounded	41	2	0	43	27.7
Subangular	55	25	0	80	51.6
Angular	23	8	1	32	20.7
Total	119	35	1	155	
Size percent	76.8	22.6	0.6		100
Station 5					
Rounded	28	4	0	67	31.7
Subangular	101	9	1	111	52.6
Angular	26	7	0	33	15.7
Total	190	20	1	211	
Size percent	90.1	9.5	0.4		100
Station 6					
Rounded	28	2	0	30	26.5
Subangular	66	4	1	71	62.8
Angular	11	1	0	12	10.7
Total	105	7	1	113	
Size percent	92.9	6.3	0.8		100.0

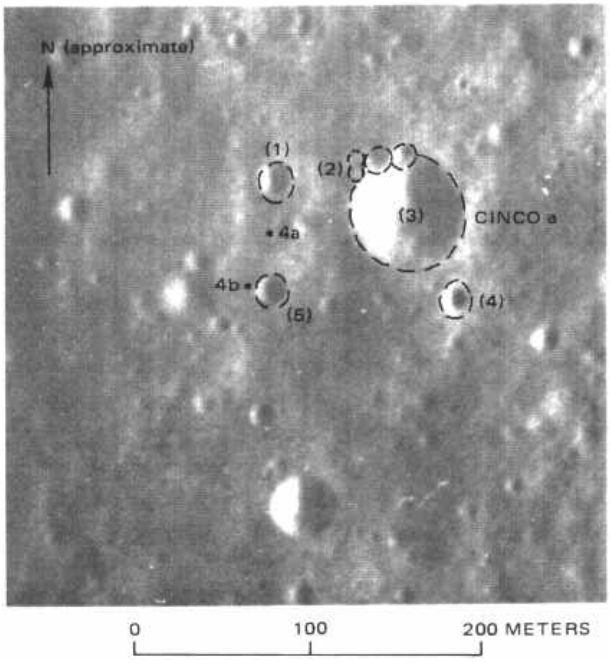

FIGURE 3.- Station 4 and vicinity. Numbers in parentheses indicate feature, correlated with plate 6, pans 9 and 10 Apollo 16 panoramic cameral frame 4618.

ejecta and reworked by local impact. The regolith surface is light gray. Near the rim of the subdued doublet crater at 4a, white material similar to that at station 1 occurs at a depth of about a centimeter; yet a trench in the floor of the crater exposed no white soil or evidence of layering.

The crew collected samples in the vicinity of the LRV at 4a but attempted to avoid sampling the large boulder field believed to be ejecta from South Ray crater. One rock, a 14-g light-matrix breccia (fig. 5; B_2 of Wilshire and others, this volume) and 0.3 kg of soil were collected from the bottom of the trench; a double-core drive-tube sample was also taken; all three of these samples should have come from below South Ray ejecta if it were present on the surface.

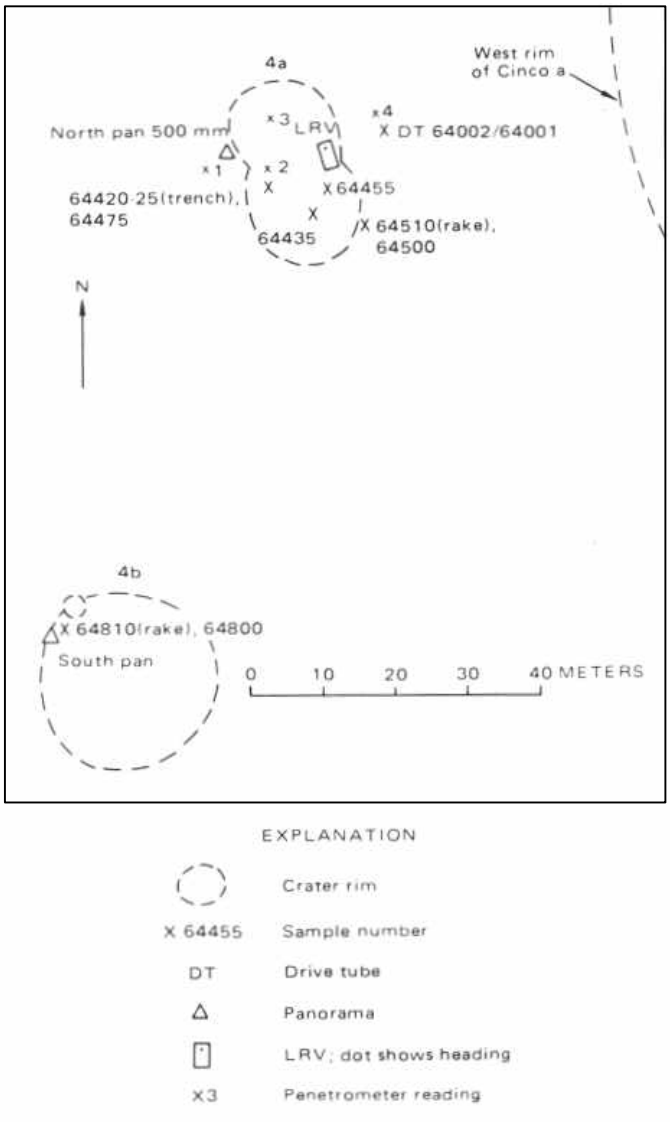

FIGURE 4.- Planimetric map of station 4 modified from Muehlberger and others (1972).

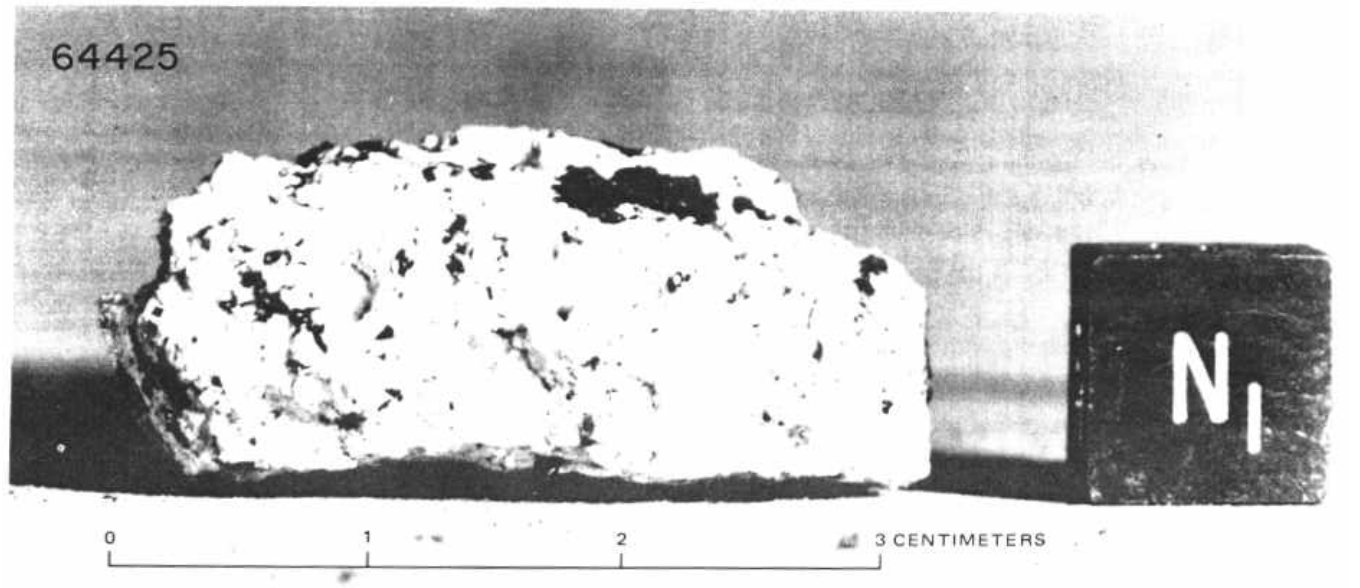

FIGURE 5.-Sample 64425; light-matrix dark-clast breccia from bottom of trench at station 4a (NASA photograph S-72-41584).

At station 4b, the blocks are mainly light colored although glass and dust coatings obscure many rock surfaces. Breccia is the predominant rock type in the area, and light clasts are visible in some of the blocks photographed (pl. 6, pan 10). Soil and rake samples consisting mainly of friable, poorly consolidated clods were collected from the northwest rim. No white soil or evidence of layering was found beneath the surface. The blocks on the northeast wall of the crater apparently are breccias containing mainly light but some dark matrices.

The most abundant rocks sampled at station 4, according to Wilshire and others (this volume), were light-matrix dark-clast breccias (B_2) and dark-matrix light-clast breccias (B_4). Their data, however, are heavily weighted by rake simples, and as they point out, many of the small fragments are probably clasts from larger rocks. Eight samples weighing 25 g or more were collected at station 4a, none at 4b. Seven of the samples from 4a are light-matrix dark-clast breccias; one is a metaclastic crystalline rock. From the location of 4a, well within the ejecta blanket of Cinco *a*, these larger fragments may be taken as characteristic of underlying rocks in the area. Sample 64435 (fig. 6*A*), the largest light-matrix (B_2) breccia collected at this station, is described as a cataclastic two-pyroxene, olivine-bearing anorthosite, partly coated with a glass rind (Wilshire and others, this volume). In thin section it appears to consist mainly of crushed feldspar invaded by dark matrix material (fig. 6*B, C*). Samples 64475, 64476, and 64535 (figs. 7-9) are additional examples of B_2 breccias collected at station 4. Probably most of, these samples were deposited as ejecta from South Ray, although the crew attempted to avoid the block field. Other samples collected at this station include a glass-coated anorthosite (64455, fig. 10) and a crushed, annealed mafic rock (64815, fig. 11), both classified as metaclastic (C_2) by Wilshire and others (this volume). A K-Ar crystallization age of 3.9+/-0.2 b.y. is reported for 64421 (Kirsten and others, (1973) and an exposure age of 210 m.y. for soil samples 64421 and 64501. These soils probably are not part of South Ray ejecta, as reliable exposure ages of 2 to 4 m.y. have been reported for rocks believed to be South Ray material collected at stations 3 and 9 (see Reed, this volume).

Within the doublet crater at station 4a, blocks are much less numerous on the southwest wall, a distribution suggesting that this side was probably shielded from South Ray ejecta. Approximately 2 percent of the surface at station 4a is covered by rocks more than 10 cm across; blocks as large as 0.8 m are scattered over the area (Muehlberger and others, (1972). Rocks less than about 5 cm across are abundant. Most of the blocks are angular, a characteristic of the ejecta believed to be from South Ray crater, but some of the smaller blocks are subround to round (table 1, fig. 12). The angular, perched appearance of the blocks near the LRV suggests derivation from South Ray crater.

At station 4b, angular blocks are concentrated on the northeast wall and rim of the crater, the rest of the rim being relatively block free. At station 4b (pl. 6, pan 10), the east wall of a 20-m crater appears to be plastered with blocks that have destroyed the raised rim of the

crater. As these blocks appear to be ejecta from South Ray, samples were collected only from the northwest interior wall of the crater, shielded from the South Ray ejecta by being on the uprange side. The strongly asymmetric distribution of these blocks, the lack of recognizable ejecta elsewhere around the crater, the partly buried rim under the block-covered area, and the relatively large size of the crater suggest that it is not of secondary origin but was formed prior to South Ray and was subsequently mantled by South Ray ejecta.

STATION 5

At station 5, the LRV was parked near the north rim of a 20-m crater (figs. 13, 14; pl. 6, pan 11). Blocks are asymmetrically distributed within the crater; their

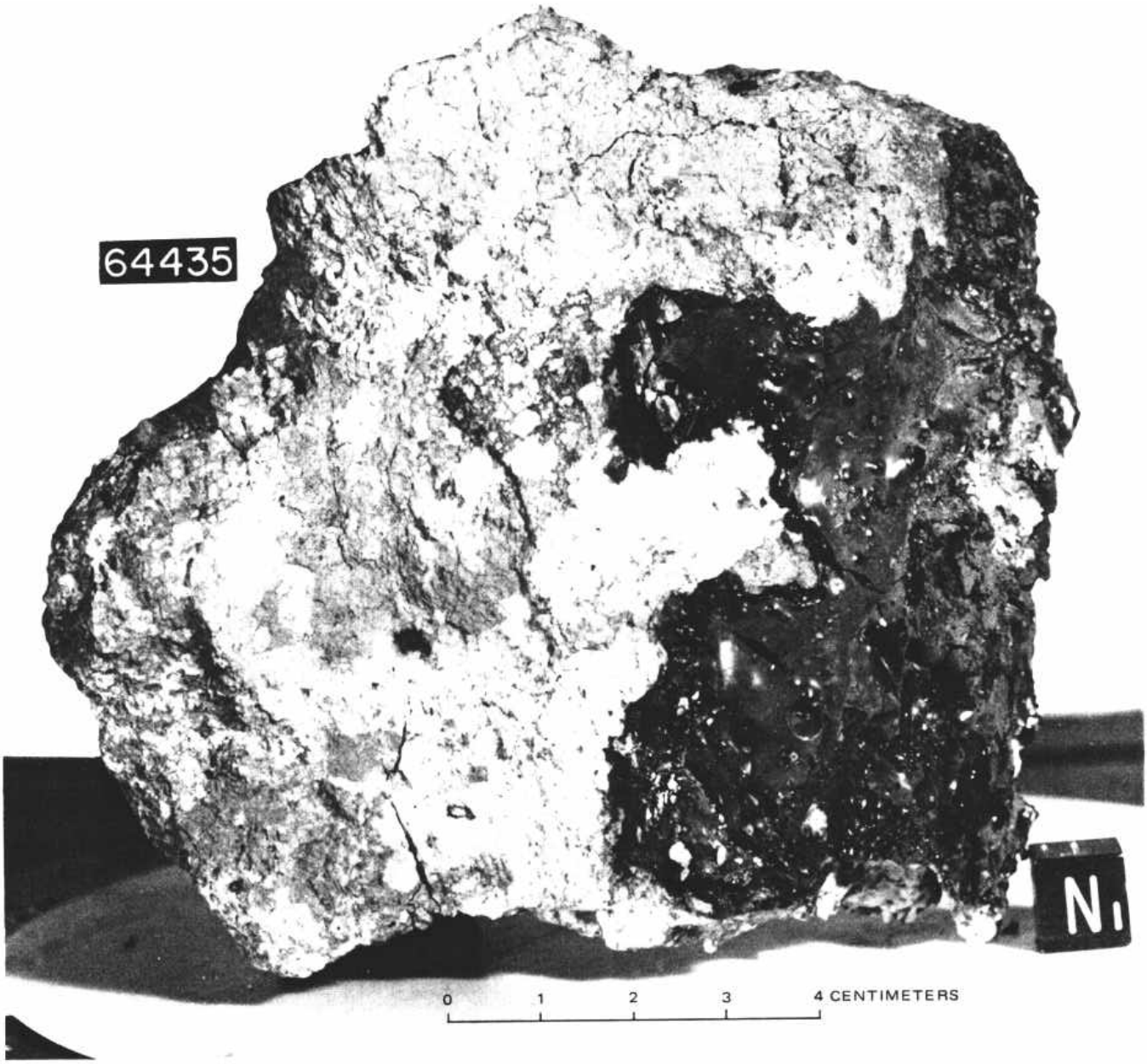

A

FIGURE 6.-Sample 64435. B_2 breccia from station 4. *A*, NASA photograph S-72-39674. *B*, Photomicrograph of 64435,73 showing glass rind dark material, right) and moderately fractured plagioclase feldspar (left). Plane-polarized light. *C*, Same as *B*, cross-polarized light.

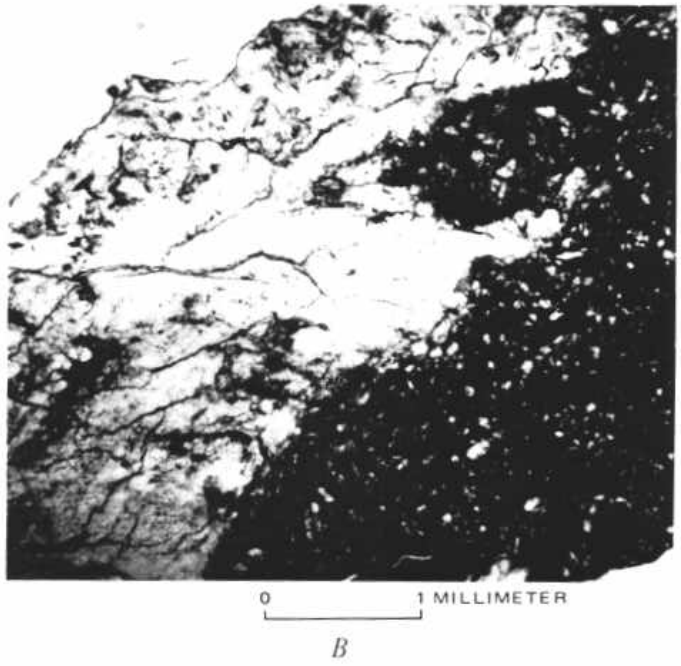

FIGURE 6.-Continued.

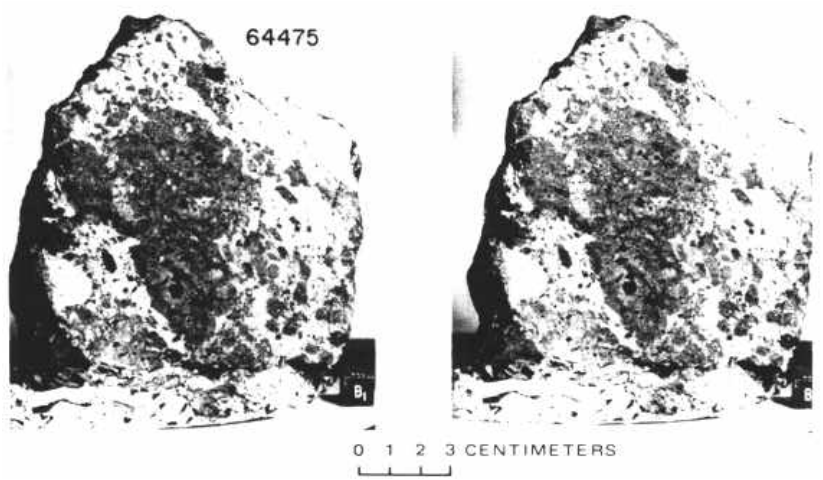

FIGURE 7-Stereopair of sample 64475, a coherent B_2 breccia from station 4 (NASA photographs S-72-43089-43089B).

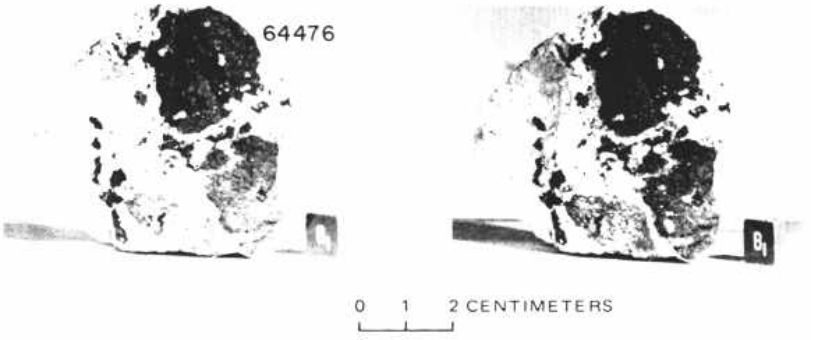

FIGURE 8.-Stereopair of sample 64476, a coherent B_2 breccia from station 4 (NASA photographs S-72-43114-43114B).

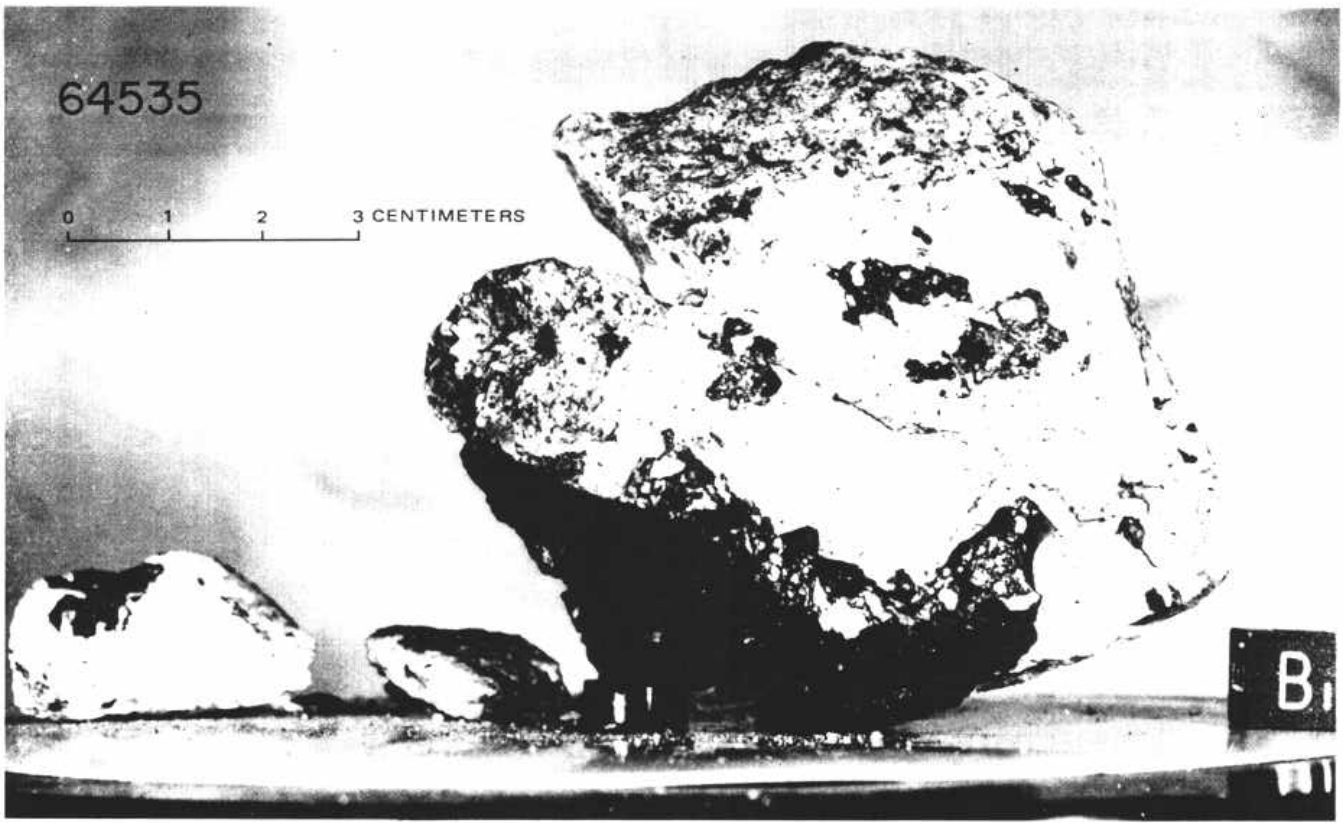

FIGURE 9.- Sample 64535, a highly fractured B_2 breccia from station 4 (NASA photograph S72--43420).

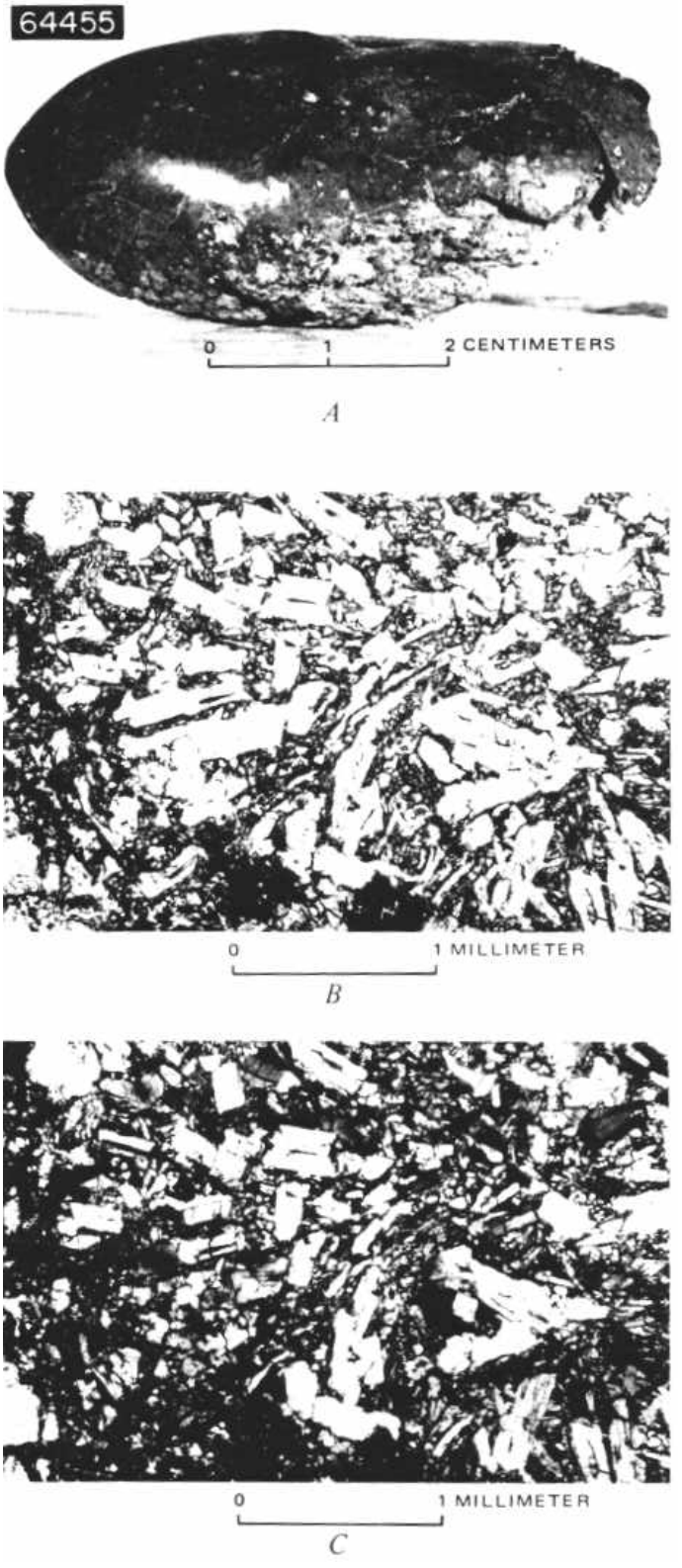

FIGURE 10.- Sample 64455, a metaclastic (C_2) glass-coated rock. *A*, NASA photograph S-72-40130. *B*, Photomicrograph showing metaclastic texture. Plane-polarized light. *C*, Same as *B*, crosspolarized light.

FIGURE 11.- Sample 64815, an unusually mafic fragment from station 4. NASA photograph S-72-42074.

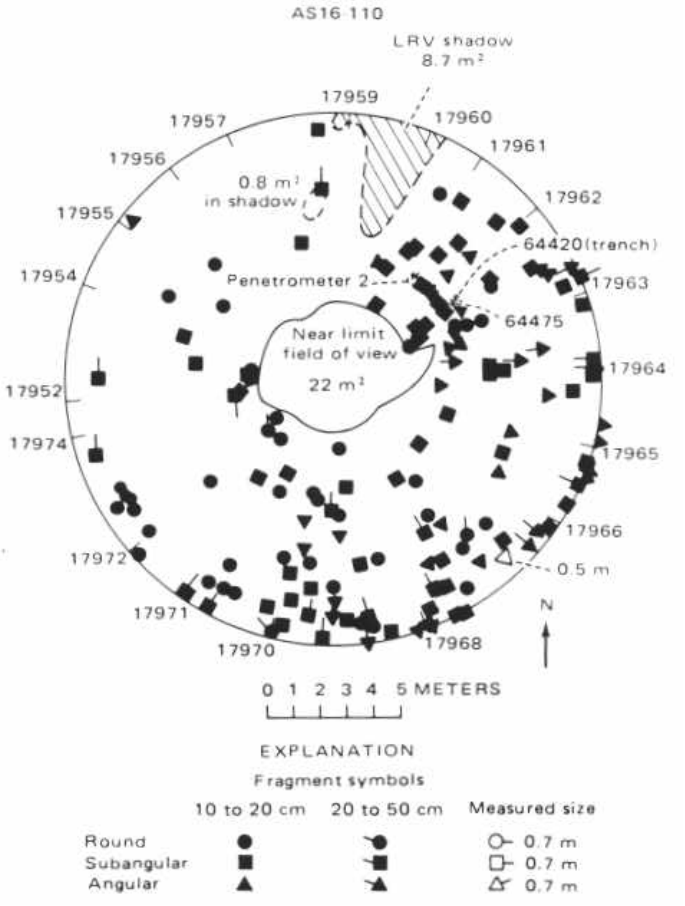

Hachures on outer circle show direction of individual photographs that constitute the panorama

FIGURE 12.-Rock distribution within 10 m of station 4a.

scarcity on the southwest wall indicates that the blocks are South Ray ejecta. Large angular blocks are sparsely scattered around the crater; 10 to 20 cm and smaller fragments are abundant (fig. 15); as observed by the crew and shown on photographs (table 1), station 5 has the highest percentage of' rounded boulders on Stone mountain. Fillets occur around some rounded cobbles; some rocks are partly buried, others perched. Soil samples are characteristically gray, although lighter soils were present beneath a gray surface at one locality.

Of the samples collected at station 5, mediumgray-matrix breccias (B_3) are the most common mainly in rake samples; glasses are also abundant. The largest samples collected are light-matrix dark-clast breccias (B_2). Of these, 65035, 65075, 65095, and 65315 (figs. 16 to 19*A*) are classified as cataclastic anorthosites (Wilshire and others, this volume). Typical matrix in B_2 breccias is shown in figure 19*B, C*. Two crystalline igneous-textured (C_1) rocks were collected; the largest is 65055 (fig. 20*A*). The subophitic texture typical of igneous rocks is shown in figure 20*B, C*. One very large (1.8 kg) metaclastic (C_2) rock, 65015 (fig. 21), is described as an anorthosite (LRL, 1972). It was collected from a small depression, possibly a secondary crater. A Rb-Sr crystallization age of 3.92 b.y. reported for this rock (Tera and others, 1973) as well as a ^{40}Ar-^{39}Ar crystallization age of 3.92±0.4 b.y. and an exposure age of 365±20 m.y. have been reported (Kirsten and others).

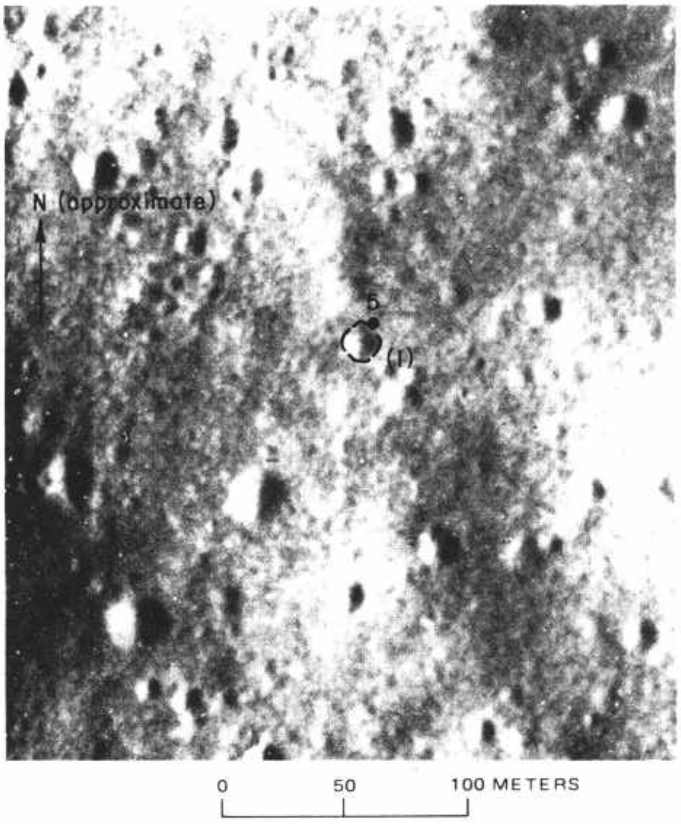

FIGURE 13.- Enlargement of orbital photograph showing station 5 and vicinity. Apollo 16 panoramic camera frame 4618.

STATION 6

Station 6 is at the foot of the lowest observable bench on Stone mountain. The LRV was parked near the northeast rim of a subdued 10-m crater (fig. 22). The northwest regional slope is somewhat less steep than at station 4 and 5 (fig. 23). Station 6 was selected before the mission for the purpose of sampling and photographing the base of Stone mountain, its mass-wasted materials, and, if observable, the contact with the Cayley plains. The primary objective was to identify compositional or textural changes between the geomorphic units.

The sampling at station 6 was on the rim and along

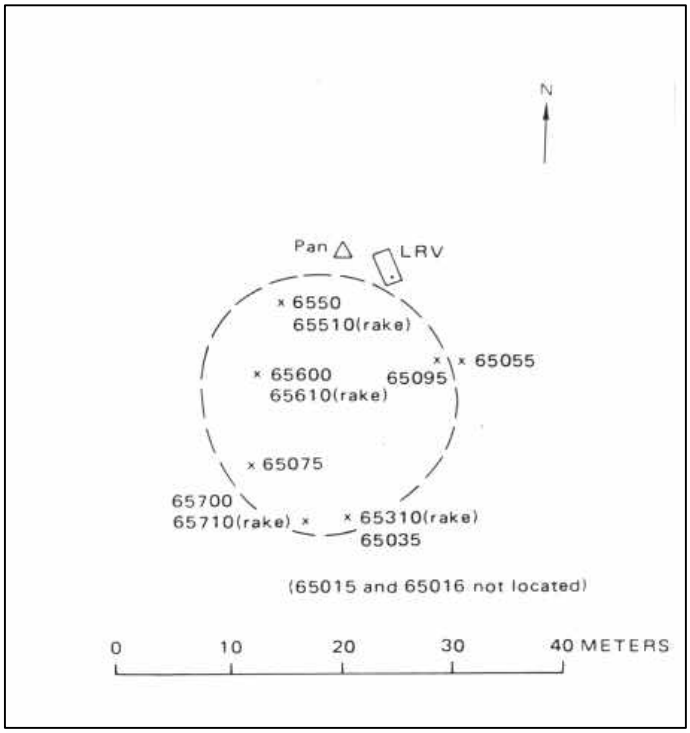

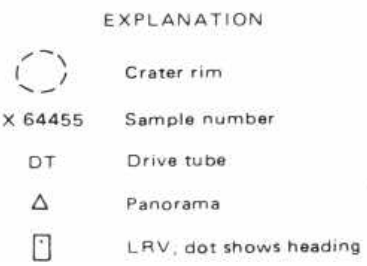

FIGURE 14.- Planimetric map of station 5.

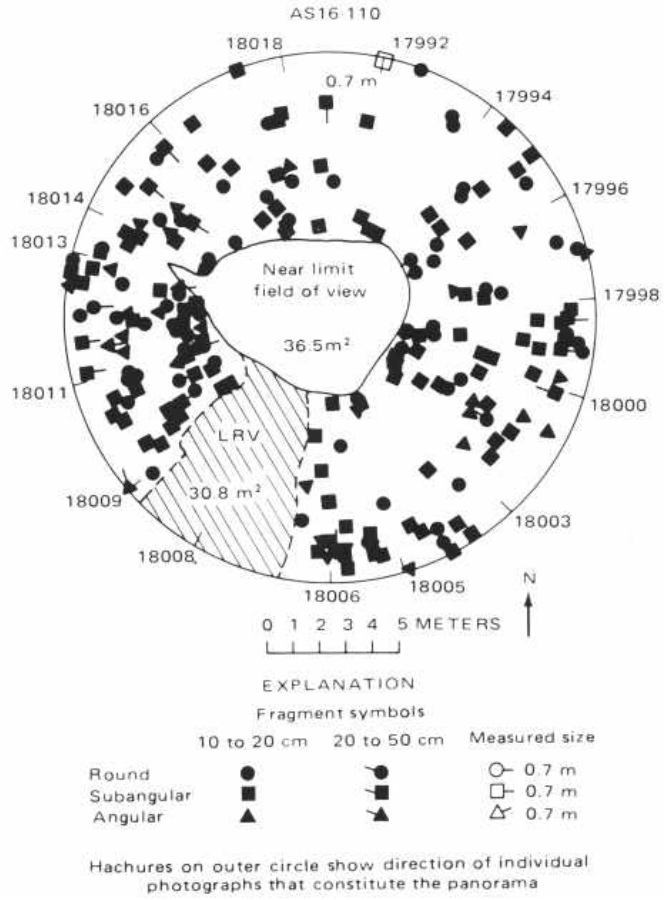

FIGURE 15.-Rock distribution within 10 m of site of station 5 panorama. See figure 12 for explanation of symbols.

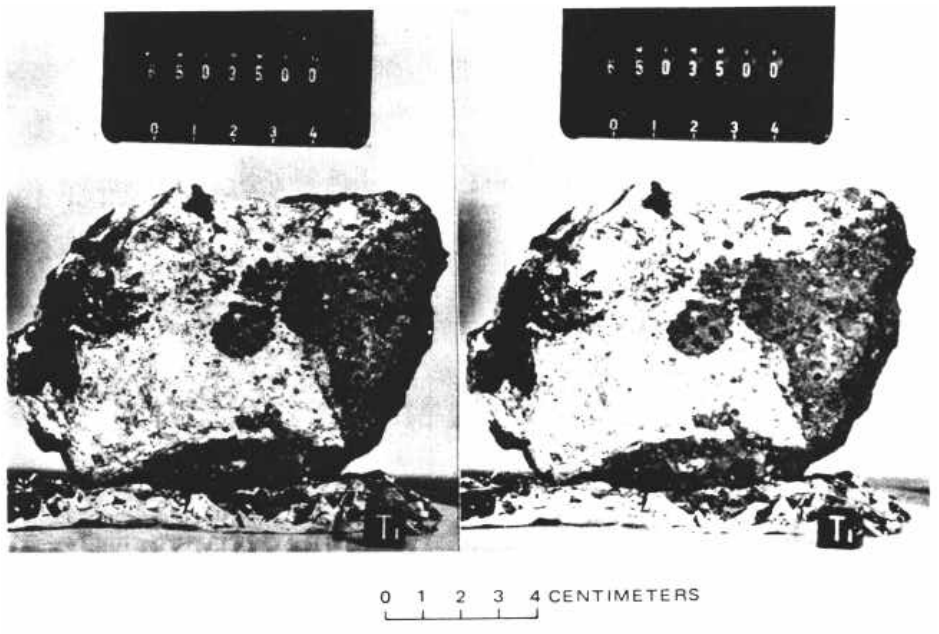

FIGURE 16.-Stereopair of sample 65035 a light-matrix dark-clast (B_2) breccia (NASA photo graphs S-72--42057-42057B).

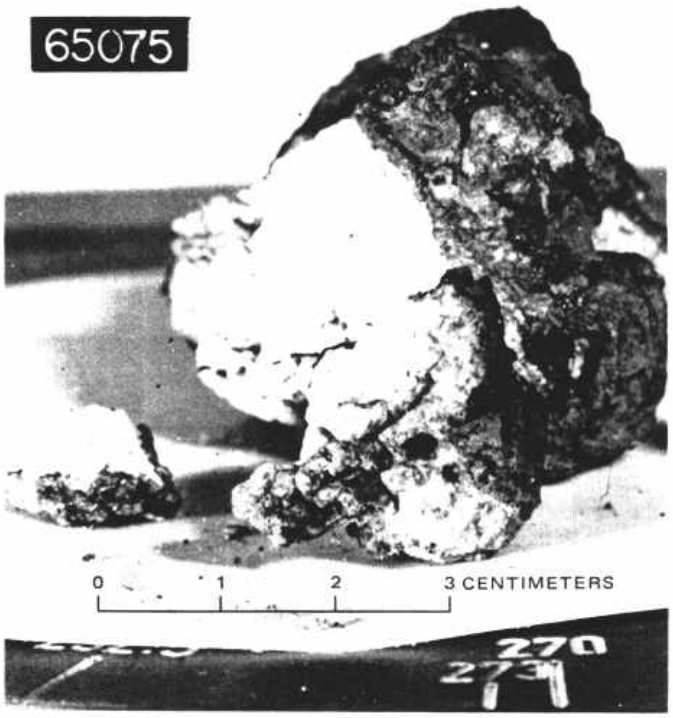

FIGURE 17.-Sample 65075, a highly fractured light-matrix darkclast (B_2) breccia (NASA photograph S-72-39412).

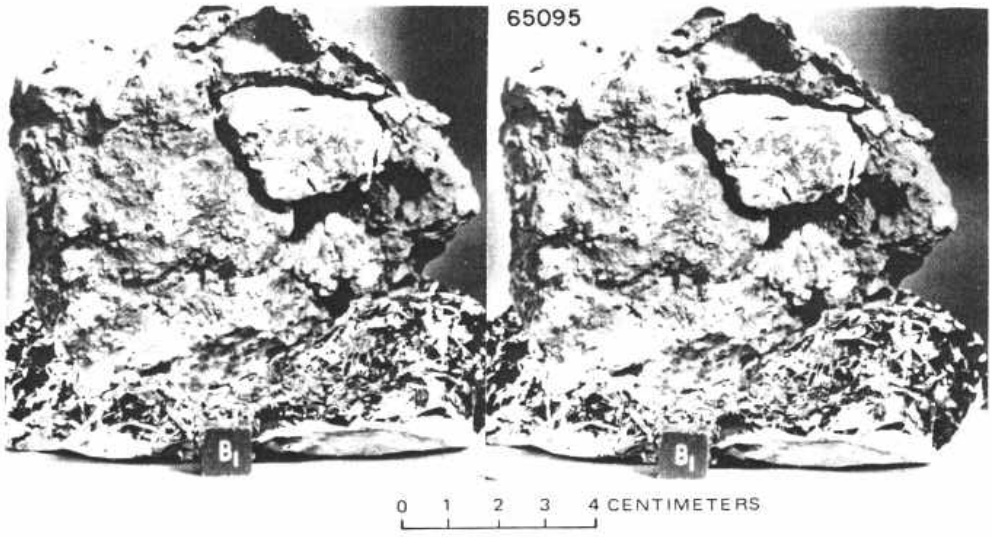

FIGURE 18. -Stereopair of sample 65095, a glass-coated light-matrix dark-clast (B_2) breccia. NASA photographs S-72- 40975-40975B.

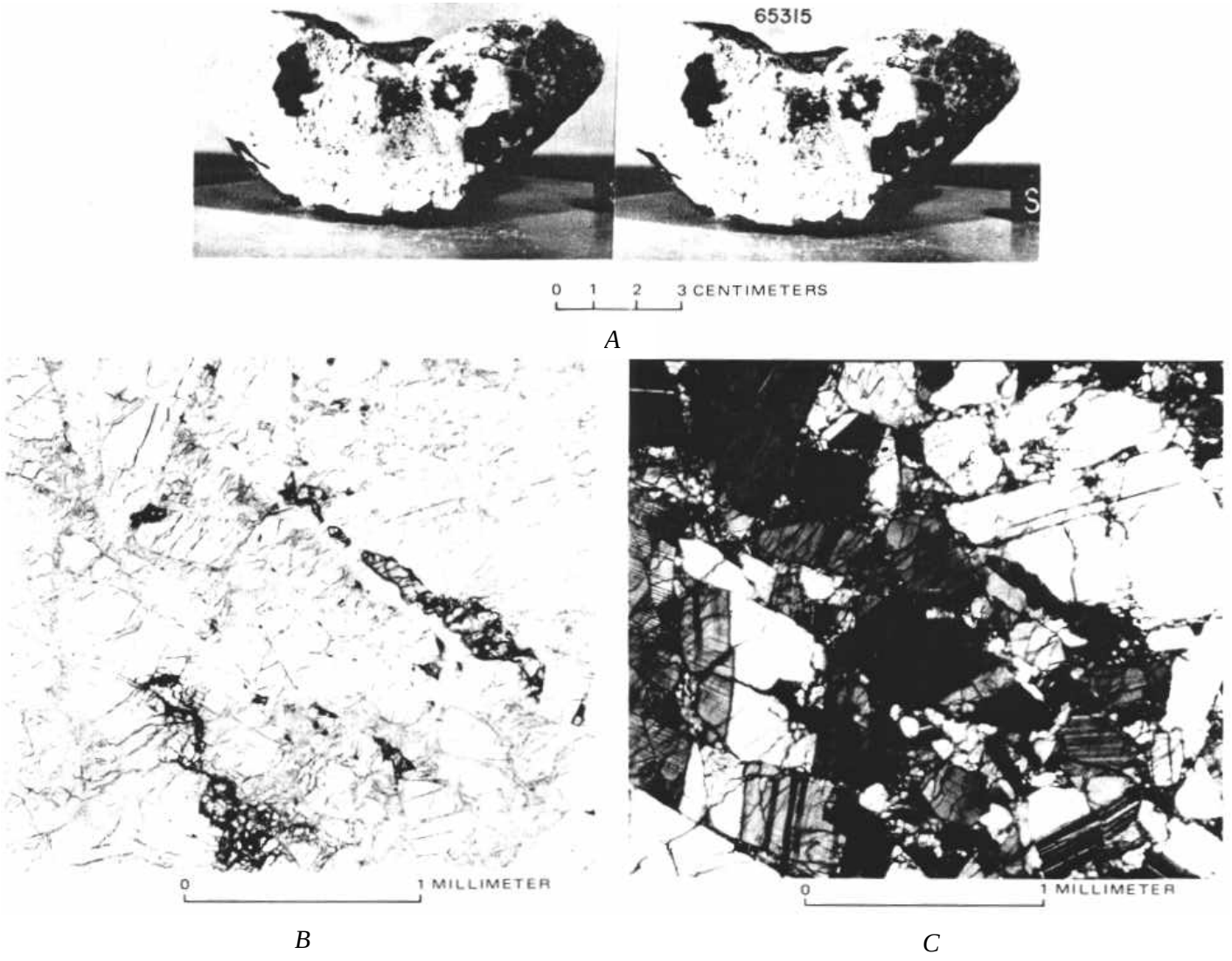

FIGURE 19.- Sample 65315, a light-matrix dark-clast (B_2) breccia displaying a partly glass-coated surface. *A*, Stereopair. NASA photographs S-72-42103-42103B. *B*, Photomicrograph of a crushed feldspar matrix in 65315, typical of cataclastic anorthosites, Plane polarized light. *C*, Same as *B*, cross-polarized light.

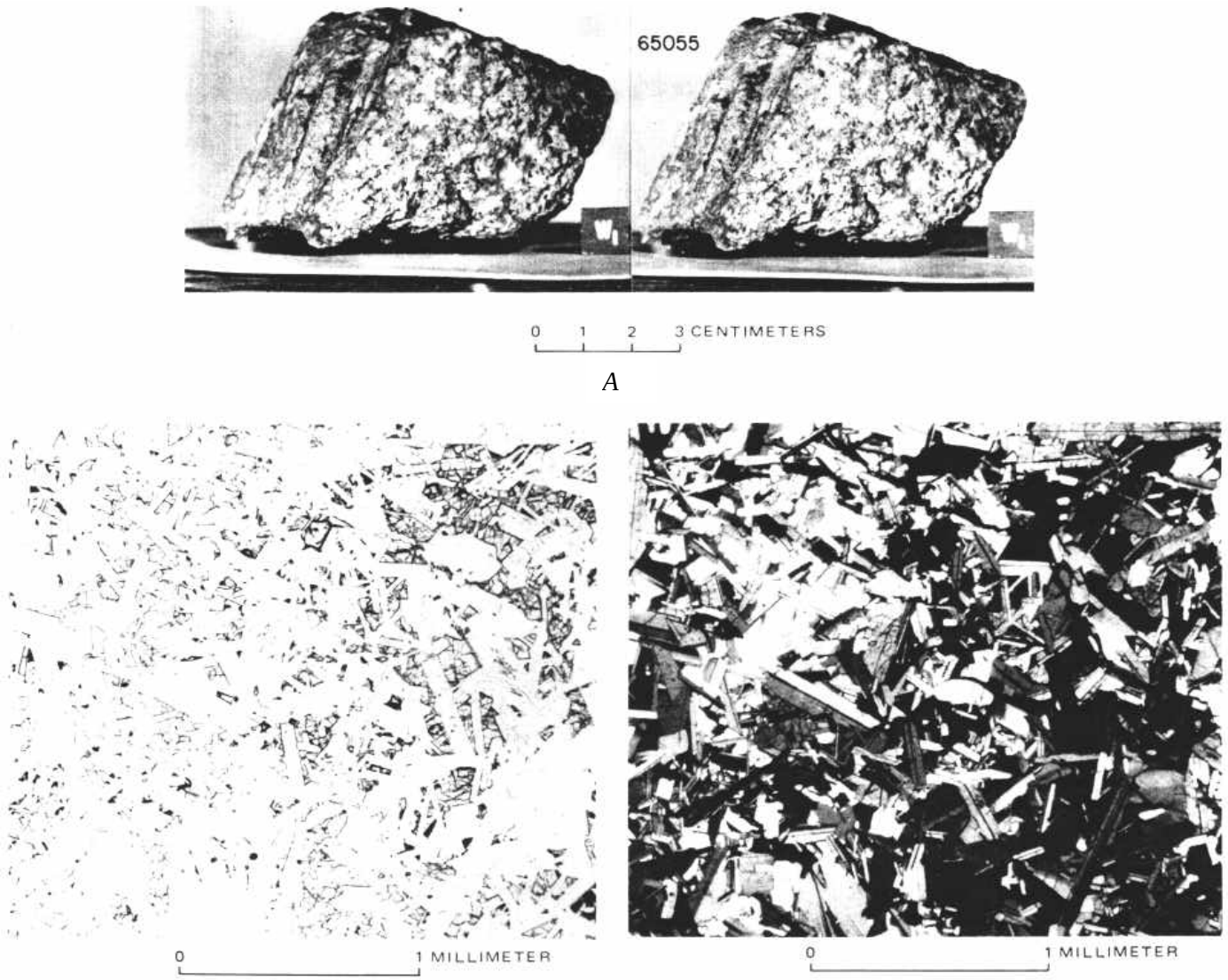

FIGURE 20.-Sample 65055, an angular igneous crystalline rock (C_1).*A*, Stereopair. NASA photographs S-72-43867 B. *B*, Photomicrograph showing subophitic texture. Plane-polarized light. *C*. Same as *B*, cross-polarized light.

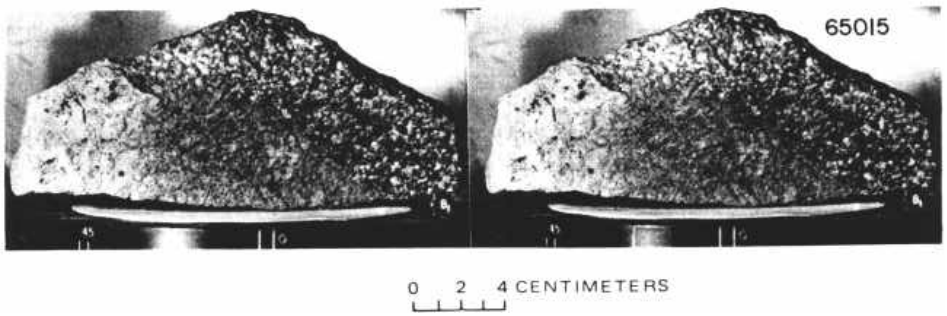

FIGURE 21.-Stereopair of sample 65015, a metaclastic rock (C_2). NASA photographs S-72-39209- 39209B.

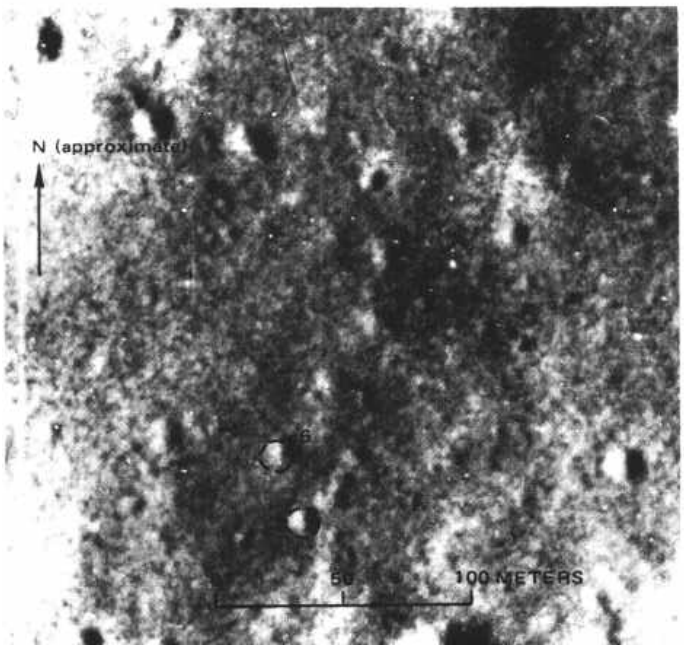

FIGURE 22.-Station 6 and vicinity. Apollo 16 panoramic camera frame 4618.

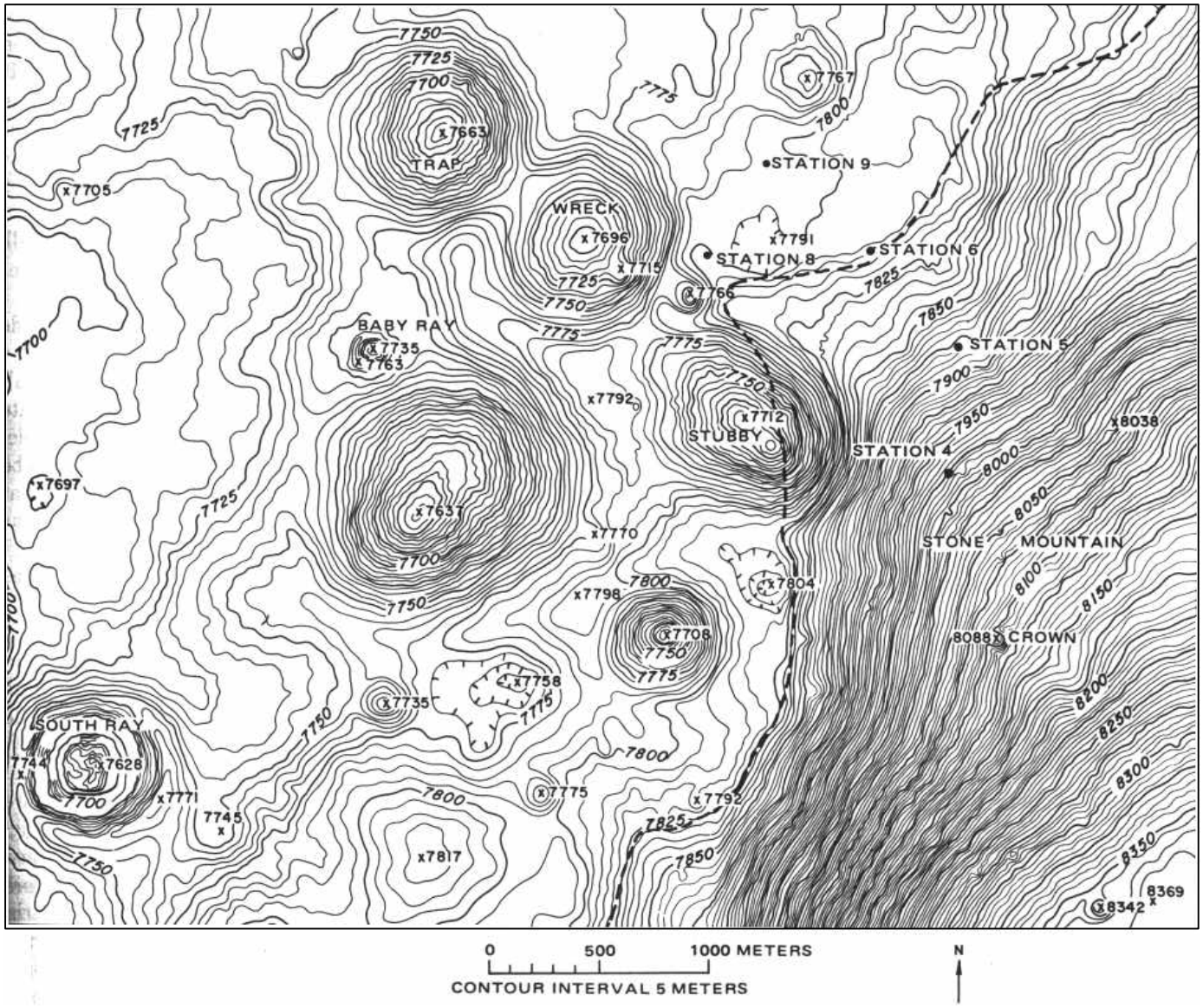

FIGURE 23.-Topographic map of the Stone mountain area showing stations 4, 5, and 6 and geologic contact from Hodges (this volume, pl. 1). Photogrammetry by G. M. Nakata.

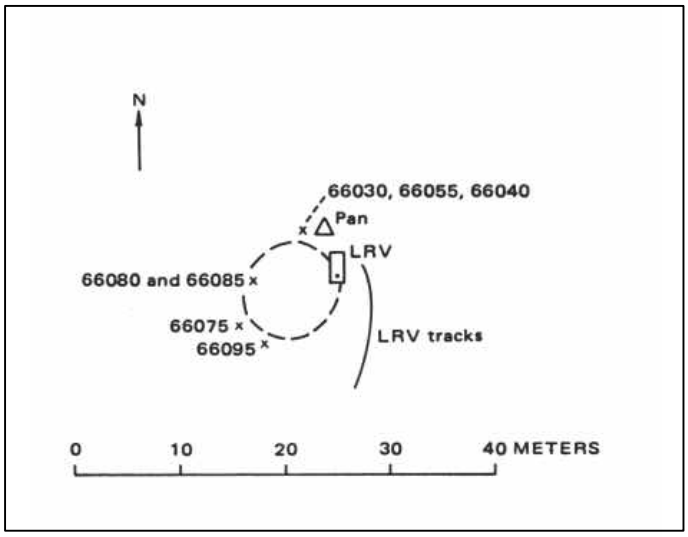

EXPLANATION

	Crater rim
X 64455	Sample number
DT	Drive tube
△	Panorama
	LRV; dot shows heading

FIGURE 24.—Planimetric map of station 6.

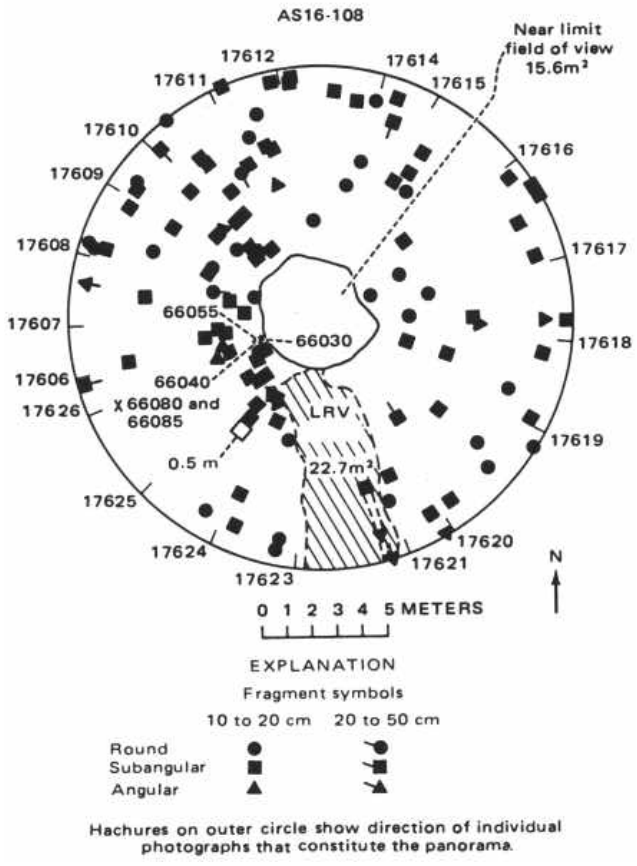

Hachures on outer circle show direction of individual photographs that constitute the panorama.

the west wall of the crater where the LRV was parked (pl. 6, pan 12; fig. 24). The surface is covered by numerous small shallow craters; only a few are as large as 10 m. Angular blocks to 0.5 m are scattered throughout the area; 10- to 20-cm fragments are most common, covering about 1 percent of the surface, (fig. 25, table 1). As shown on plate 6, pan 12, the rock distribution within the subdued 10-m crater at the LRV appears: asymmetric; rocks are sparse on the southwest wall, which was probably shielded from South Ray crater ejecta.

The rocks described and photographed exhibit a wide variety of shapes and sizes. Angular glass-coated blocks are scattered over much of the surface. Small white clasts common in many of these rocks indicate that breccias predominate. Fillets are moderately developed around some rocks. Several rocks appear to be partly buried; others appear perched, suggesting that they were transported to their present location as ejecta from South Ray crater.

One white "splotch" of indurated soil, 66080, was collected from the southwest wall of the crater; the regolith elsewhere was apparently gray throughout.

Only four large rock samples were collected at station tion 6; all have been classified as breccias by Wilshire and others (this volume). Samples 66075 and 66035 (figs. 26 and 27*A*) are classified as intermediate-gray matrix breccias (B_3), with approximately aqual amounts of dark and light clasts. As shown in figure 27*B*, 66035 has cataclastic texture. Sample 66055 (fig 28) is a light-matrix dark-clast breccia (B_2), described as a cataclastic anorthosite by Wilshire and othe (this volume). Sample 66095 (fig. 29*A*) is a dark-matri light-clast breccia (B_4). It weighs more than a kilogra and is highly fractured. The rock has been called "rusty rock" and was the first discovered to contain significant amount of hydrated iron oxide believed be of lunar origin (Nunes and Tatsumoto, 1973; Fried man and others, 1974). It can be described as an anorthositic breccia (LRL, 1972) with a locally recrystallized matrix (fig. 29*B, C*). $^{40}Ar\_^{39}Ar$ data suggest that this rock was partly recrystallized by an impact even around 3.6 b.y. ago (Turner and others, 1973, p. 1899)

DISCUSSION AND SUMMARY

Stations 4 and 5 on the north slope of Ston mountain were selected as the prime localities for Descartes mountains materials. Chemical analyses and petrographic characteristics of the samples collected on Stone mountain do not differ significantly from those of

< FIGURE 25.-Rock distribution within 10 m of site of station 6 panorama. See figure 12 for explanation of symbols.

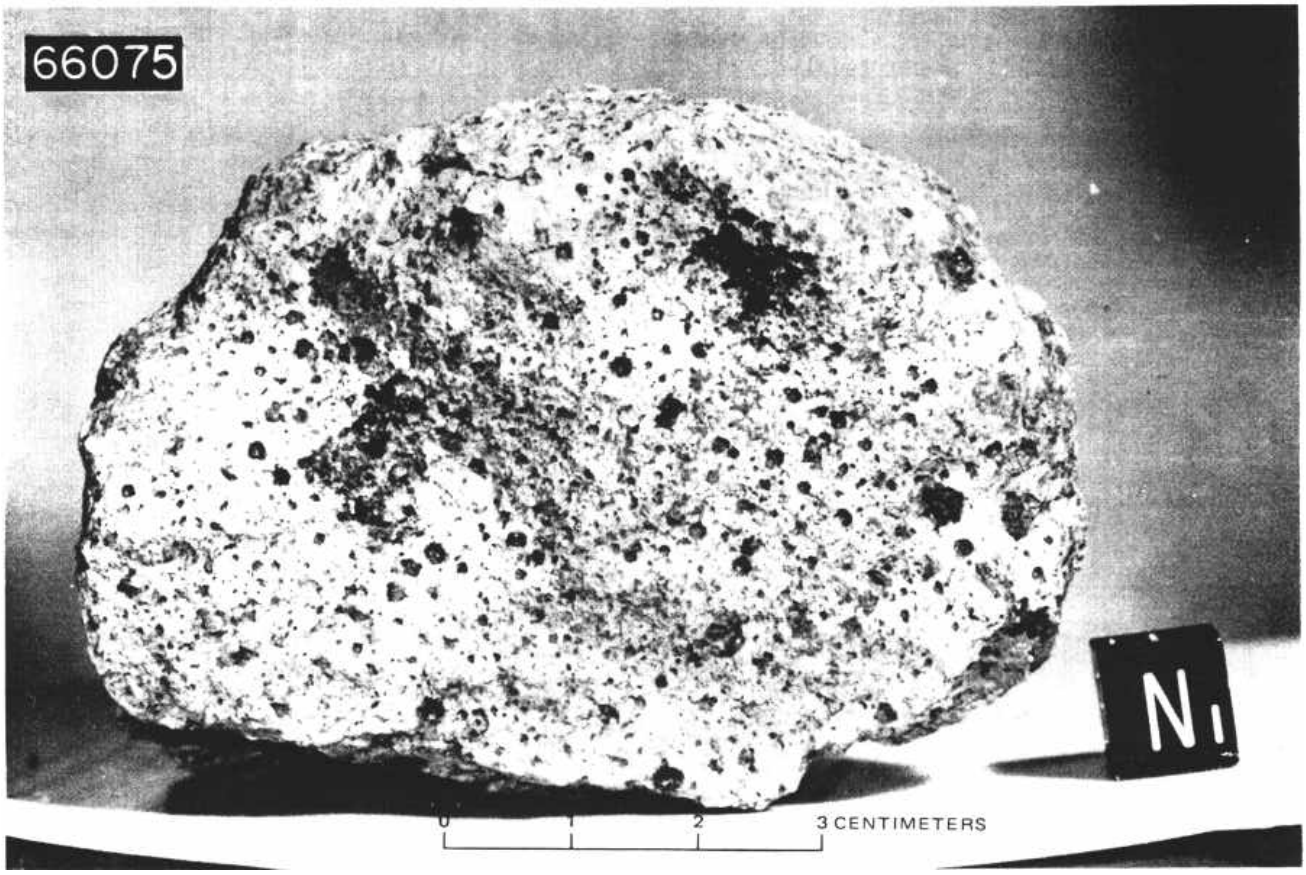

FIGURE 26.-Sample 66075, a well-indurated B_3 breccia. NASA photograph S-72-37203.

samples from the Cayley plains. As ray materials from South Ray crater occupy much of the landing site, it is possible that underlying Descartes bedrock may not have been sampled. Alternatively, both plains and highlands at this site may be accumulations of similar breccias. Detailed comparisons of soils and rocks from stations 5 and 6, which lie on opposite sides of the apparent Cayley-Descartes contact, indicate no major chemical differences between the two sample suites. If the materials that formed the Descartes mountains were indeed sampled, then whatever differences exist between the two formations must be expressed by properties other than chemical composition and petrography. The greater abundance of angular blocks of the 20- to 5-cm size fraction at station 4 can be attributed to a relatively heavy concentration of large blocks of ray material there.

From a review of surface evidence (station panorama photographs, Hasselblad 70-mm, and 16-mm photographs), it appears that station 4 may be located on the edge of a minor ray from South Ray crater. From orbit, however, no rays are visible near the station 4 location. Additional evidence for South Ray ejecta is the large asymmetric boulder field of fresh angular blocks observed at station 4. Of the three stations, station 5 has the greatest percentage of rounded boulders on the surface and appears to be contaminated by few angular blocks of South Ray ejecta. Station 6 appears to be located on the edge of a ray from South Ray crater (Freeman, this volume, fig. 1), although no large block fields are visible. As station 6 is at the base of Stone mountain, Descartes materials may have accumulated by mass wasting from the mountain and may be quite thick (see Freeman, this volume). Boulder fields possibly representing South Ray ejecta were identified on 16-mm photographs along the traverse route (fig. 30). Both stations 4 and 6 fall within boulder fields; station 5 does not, although it is near one.

Whether the materials making up the Descartes mountains were actually sampled remains undetermined. Stations 4 and 6 appear to be contaminated by Cayley materials ejected from South Ray crater, although the larger (25+ g) samples collected at station 4a are possibly Cinco *a* ejecta from beneath the regolith. Station 5, which appears to be free of South Ray ejecta, may be the most promising locality from which Stone mountain material may eventually be identified in the sample collection.

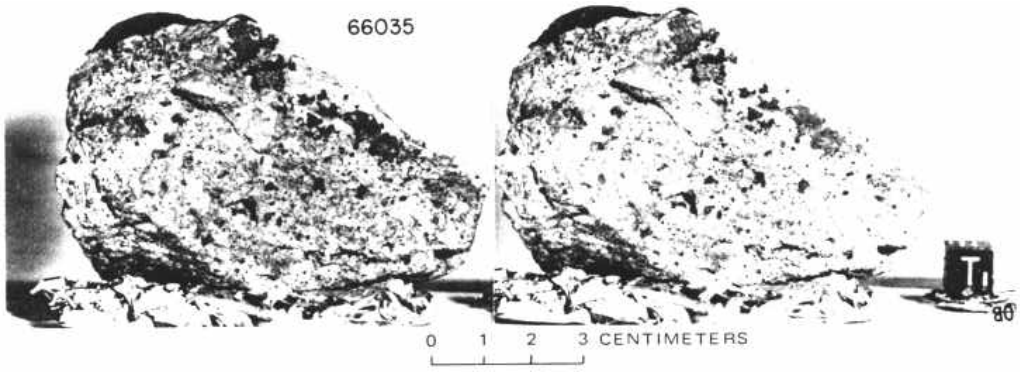

A

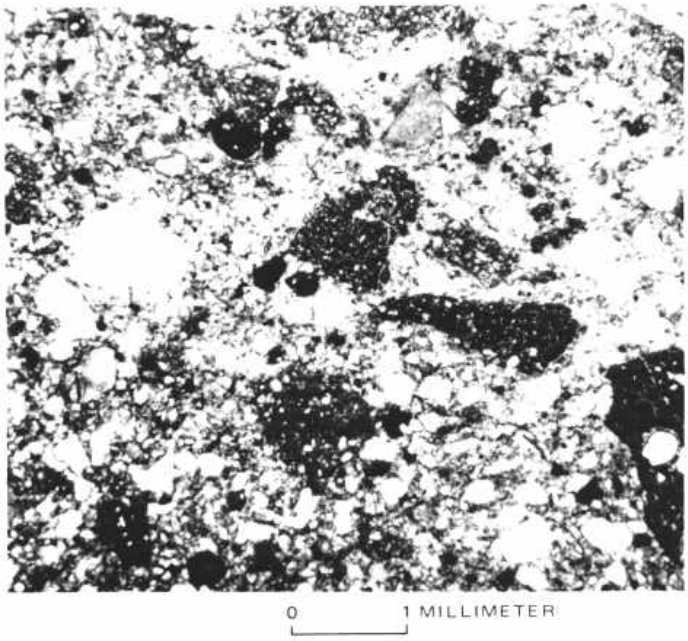

B

FIGURE 27.- Sample 66035, a coherent B_3, breccia. *A*. Stereopair NASA photographs S-72-41300-41300B. *B*, Photomicrograph showing cataclastic texture. Plane-polarized light.

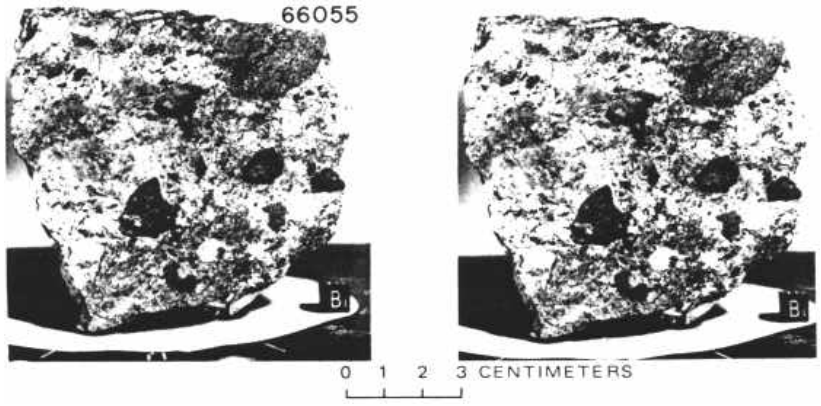

FIGURE 28.- Sample 66055 (stereopair), a light-matrix dark-clast (B_2) breccia. NASA photographs S-72-42722-42722b.

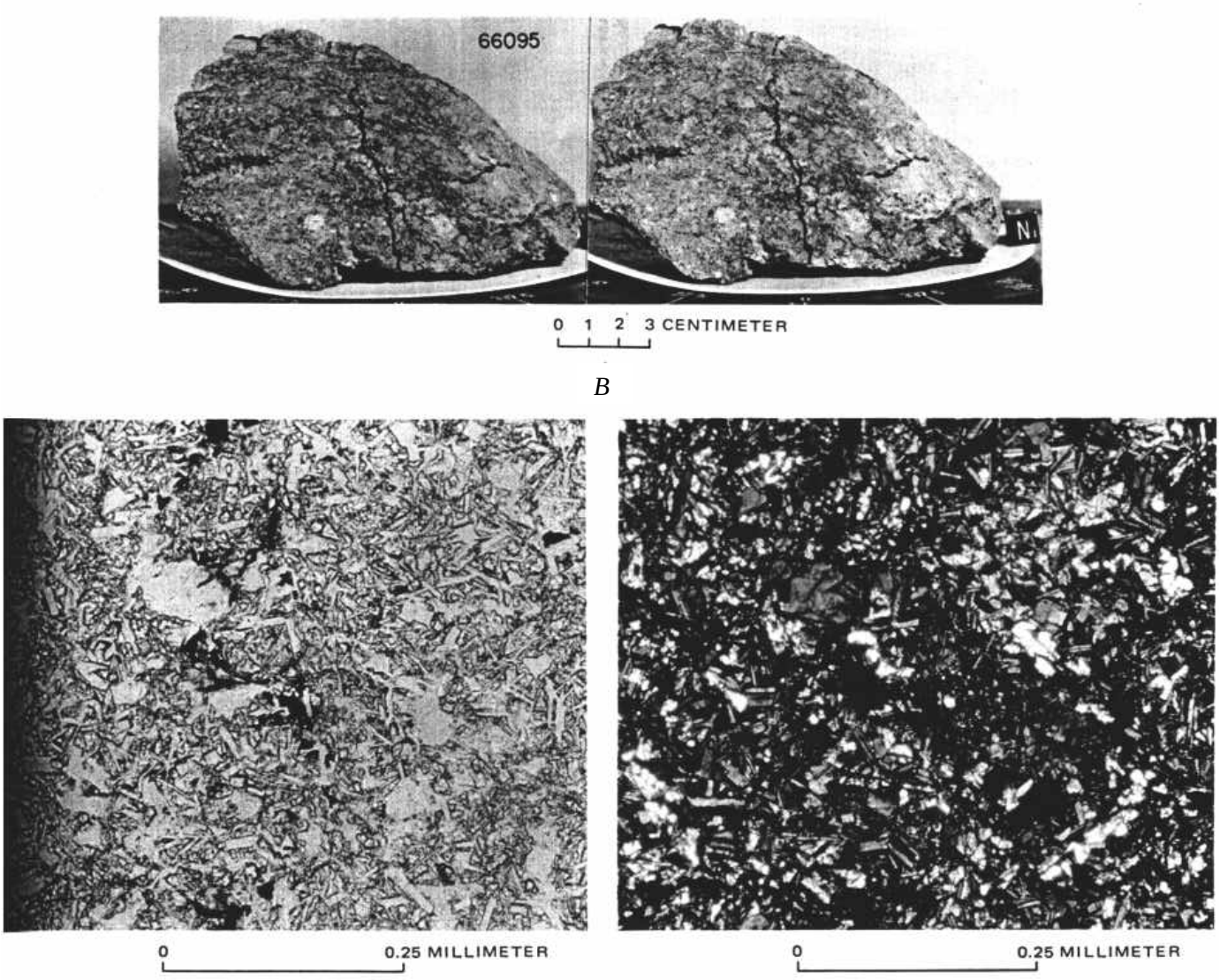

FIGURE 29.-Sample 66095, "rusty rock," a highly fractured dark-matrix light-clast B_4 breccia. *A*, Stereopair. NASA photographs S-72-41436-41436B. *B*, Photomicrograph showing ophitic matrix and interstitial opaque minerals that are partly oxidized. *C*, Same as *B*, cross-polarized light.

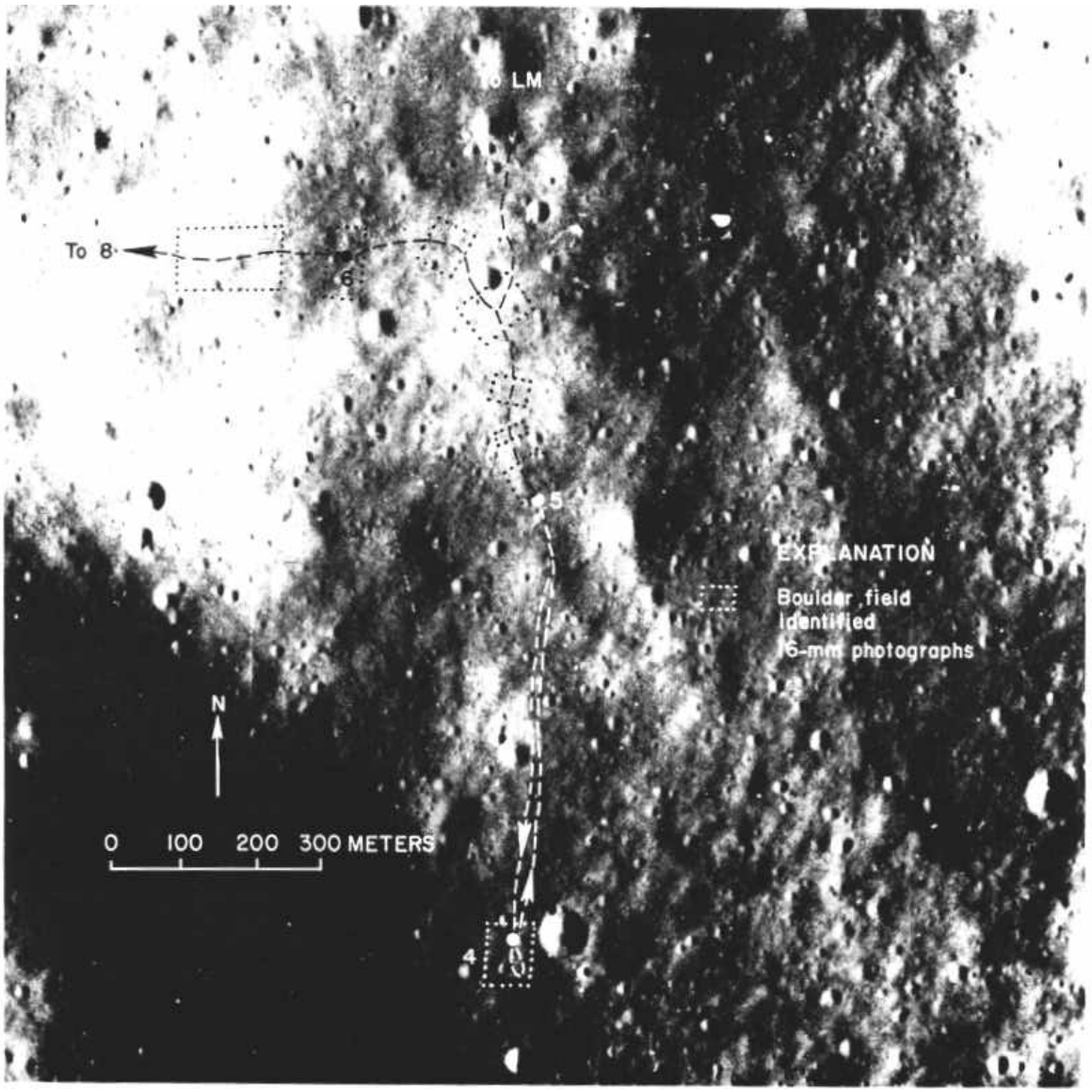

FIGURE 30.-Boulder fields, possibly South Ray ejecta, identified on 16-mm traverse photographs.